

Development of biorelevant media and dissolution tests for gastrointestinal disease states

Dissertation
zur Erlangung des Doktorgrades
der Naturwissenschaften

Vorgelegt beim Fachbereich 14
Biochemie, Chemie und Pharmazie
der Johann Wolfgang Goethe-Universität
in Frankfurt am Main

von

Domagoj Šegregur
aus Virovitica

Frankfurt (2021)

(D 30)

Vom Fachbereich für Biochemie, Chemie und Pharmazie der
Goethe-Universität als Dissertation angenommen.

Dekan: Prof. Dr. Clemens Glaubitz

1. Gutachter: Prof. Dr. Jennifer Dressman

2. Gutachter: Prof. Dr. Nikoletta Fotaki

Datum der Disputation: 14.02.2022

Slap

Teče i teče, teče jedan slap;
Što u njemu znači moja mala kap?

Gle, jedna duga u vodi se stvara,
i sja i dršće u hiljadu šara.

Taj san u slapu da bi mogo sjati,
I moja kaplja pomaže ga tkati.

Dobriša Cesarić

Waterfall

It flows and flows, flows the waterfall
Does my little drop make any difference at all?

Look, a rainbow appears in it
And in a thousand colours it appears shivering and lit!

That dream lighted up in the waterfall
And my drop helped to wave it all.

(transl. Toni Šimundža)

Wasserfall

Es fließt und fließt ein Wasserfall.
Ein kleines Tropfen bin ich in ihm, winzig, egal.

Ein Regenbogen wird im Wasser kreiert.
Er glänzt und zittert, tausendfach verziert.

Damit der Traum leuchtet aber fein
hilft auch mein Tropfen. Wenn auch klein.

(übersetz. Blago Vukadin)

Acknowledgments

This thesis was prepared under supervision of Prof. Dr. Jennifer Dressman, at the Goethe University Frankfurt, Institute of Pharmaceutical Technology, as a part of a collaboration with AstraZeneca, Macclesfield, UK, under co-supervision of Dr. James Mann.

First and foremost, I am deeply grateful to my mentor Prof. Dr. Jennifer Dressman for her guidance and constant support during this doctoral voyage. Thank you for valuing all my work (scientific and artistic alike), and encouraging my continuous development through amazing opportunities and precious insights. I am honoured to have been your doctoral student!

I would like to express my sincere gratitude to AstraZeneca and their team - Andrea Moir, Dr. Eva Karlsson, Richard Barker, and especially Dr. James Mann. Our monthly video conferences, two visits to Macclesfield and invaluable discussions enriched the project and your availability and support made it possible! I am proud to have worked on such an interesting project with such great people!

Special thank you goes to my other co-authors, in particular to Dr. Talia Flanagan for bringing great enthusiasm to our scientific work and Dr. David Turner for his support with all our questions regarding the Simcyp™ software.

Furthermore, I would like to thank my friends and colleagues accompanying me during this thesis, Dr. Mukul Ashtikar, Gerlinde Born, Dr. Tom Fiolka, Fiona Gao, Dr. Martin Hofsäss, Dr. Laura Jablonka, Dr. Fabian Jung, Ayse Kont, Dr. Edmund Kostewicz, Dr. Lukas Klumpp, Dr. Andreas Lehman, Marc-Philip Mast, Dr. Kalpa Nagersekar, Dr. Lisa Nothnagel, Chantal Wallenwein and Laurin Zöller; the visiting scientists Dr. Takao Komasa, Dr. Monica Villa-Nova and Dr. Ayahisa Watanabe and the technical and administrative staff of the Institute, Hannelore Berger, Mareike Götz, Elisabeth Herbert, Harald Kaufmann, Sylvia Niederdorf and Manuela Thurn. A very special thanks go to “the last of the Mochicans” Yaser Mansuroglu and Maximo Pettarin, the “PEARRLers” Ioannis Loisos-Konstantinidis and Dr. Rafael Leal Monteiro Paraiso, as well as to the best lab mate I could have wished for, Dr. Chara Litou! You all have

shaped my view of science and life and I cherish our shared moments. To Families Knezović, Primorac and Ursić, thank you for making me feel welcome, always! To dearest Hannah particularly, thank you for being by my side during the whole doctoral study - you made my life full and inspired me day to day.

Finally, my deepest gratitude is to my parents, for raising and guiding me to pursue the best version of myself, as well as the enormous support every step along the way, and to my four grandparents and uncle, for always believing in me and giving me courage to keep pushing; “jedan - dva!”.

I would like to acknowledge AstraZeneca for financial support of the project, Certara UK (Simcyp Division) for granting free access to the Simcyp Simulator through an academic licence, and Biorelevant.com for kindly donating the biorelevant powders used in the experiments.

Contents

| | |
|--|-----------|
| 1 Introduction | 1 |
| 1.1 <i>Physiology of the GI tract</i> | 1 |
| 1.1.1 Stomach | 2 |
| 1.1.2 Small intestine | 3 |
| 1.1.3 Large intestine | 4 |
| 1.2 <i>Biorelevant media</i> | 5 |
| 1.3 <i>Disease states linked to elevated gastric pH</i> | 6 |
| 1.3.1 Hypo- and achlorhydria | 6 |
| 1.3.2 Diseases treated with ARAs | 7 |
| 1.4 <i>Drug development and DDI predictions</i> | 8 |
| 1.5 <i>In vitro tools</i> | 10 |
| 1.5.1 Solubility measurements | 10 |
| 1.5.1.1 Shake-flask method | 10 |
| 1.5.1.2 UniPrep® method | 11 |
| 1.5.2 Permeability measurements | 12 |
| 1.5.2.1 Parallel Artificial Membrane Permeability Assay | 12 |
| 1.5.2.2 Caco-2 permeability assay | 12 |
| 1.5.3 Biorelevant dissolution measurements | 13 |
| 1.5.3.1 Simple in vitro dissolution set-ups | 14 |
| 1.5.3.1.1 One-stage dissolution | 14 |
| 1.5.3.1.2 Two-stage dissolution testing | 16 |
| 1.5.3.1.3 Transfer experiments | 17 |
| 1.5.3.2 More complex in vitro set-ups | 19 |
| 1.5.3.2.1 TNO gastrointestinal model (TIM-1) | 19 |
| 1.5.3.2.2 GastroDuo | 19 |
| 1.6 <i>In silico tools</i> | 20 |
| 1.6.1 <i>In silico</i> tools for <i>in vitro</i> dissolution parametrisation | 20 |
| 1.6.2 Physiologically based pharmacokinetic (PBPK) models | 22 |
| 1.6.2.1 Simcyp™ Simulator | 23 |
| 1.6.2.1.1 Dissolution rate model (DRM) and diffusion layer model (DLM) | 23 |
| 1.6.2.1.2 Minimal and Full PBPK model | 24 |
| 2 Structure of the thesis and thesis goals | 25 |
| 3 Results and Discussion | 27 |
| 3.1 <i>Impact of ARA administration on GI physiology and the design of in vitro media reflecting these changes</i> | 27 |
| 3.1.1 Impact of ARAs on GI physiology | 27 |
| 3.1.1.1 Antacids | 27 |
| 3.1.1.2 H2RAs | 28 |
| 3.1.1.3 PPIs | 28 |
| 3.1.2 Design of <i>in vitro</i> media reflecting ARA co-administration | 29 |
| 3.2 <i>Implementation of the ARA media in in vitro dissolution models</i> | 31 |
| 3.2.1 One-stage testing | 32 |
| 3.2.1.1 Case example PSWB 001 | 32 |
| 3.2.1.2 Case example dipyrindamole | 33 |
| 3.2.1.3 Case example raltegravir potassium | 34 |

| | |
|--|-----------|
| 3.2.2 Two-stage dissolution | 36 |
| 3.2.2.1 Case example PSWB 001 | 37 |
| 3.2.2.2 Case example dipyridamole | 38 |
| 3.2.2.3 Case example raltegravir potassium | 39 |
| 3.2.3 Transfer experiments | 41 |
| 3.2.4 TIM-1 model | 42 |
| 3.3 <i>Combining in vitro methods assessing ARA co-administration with various in silico models</i> | 43 |
| 3.3.1 Scenario one: Use of minimal PBPK model and DRM | 44 |
| 3.3.2 Scenario two: Use of a full PBPK model with DLM input | 46 |
| 3.3.3 Scenario three: Use of full PBPK model with a mathematical approach to DRM | 49 |
| 3.4 <i>Evaluating the ability of the methods developed to predict the pH effect of ARA co-administration</i> | 50 |
| 4 Summary and Outlook | 52 |
| 5 Deutsche Zusammenfassung (German summary) | 55 |
| 6 References | 60 |
| 7 Appendix | 70 |
| 7.1 <i>Publications</i> | 70 |
| 7.2 <i>Curriculum vitae</i> | 134 |
| 7.3 <i>Eidesstattliche Erklärung (Statutory declaration)</i> | 136 |

1 Introduction

1.1 Physiology of the GI tract

The gastrointestinal (GI) tract is a complex organ system primarily involved in food digestion and absorption¹; however, it also plays important roles in immunology, metabolism, and excretion. It is also the most common, and likely the oldest path to administering compounds with healing or therapeutic properties. Understanding the physiology of the GI tract is essential to understanding drug behaviour after oral administration. Changes in the GI physiology (due to a disease or co-administration of drugs) often have an impact on drug therapy. Thus, this section presents a short summary of the GI physiology in the healthy state.

Anatomically, the GI tract (GIT) can be divided into the upper and lower GIT². Upper GIT starts with the mouth and includes the esophagus, stomach and duodenum. The lower GIT is defined as the small intestine below the duodenum (including the jejunum and ileum) and the large intestine (including the caecum, appendix, ascending, transverse, descending and sigmoid colon, as well as rectum) which ends with the anus. Furthermore, GIT is the central part of the digestive system (Figure 1), incorporating other organs, such as secretory glands, the liver, pancreas, and gall bladder, and is connected to the lymphatic and cardio-vascular system.

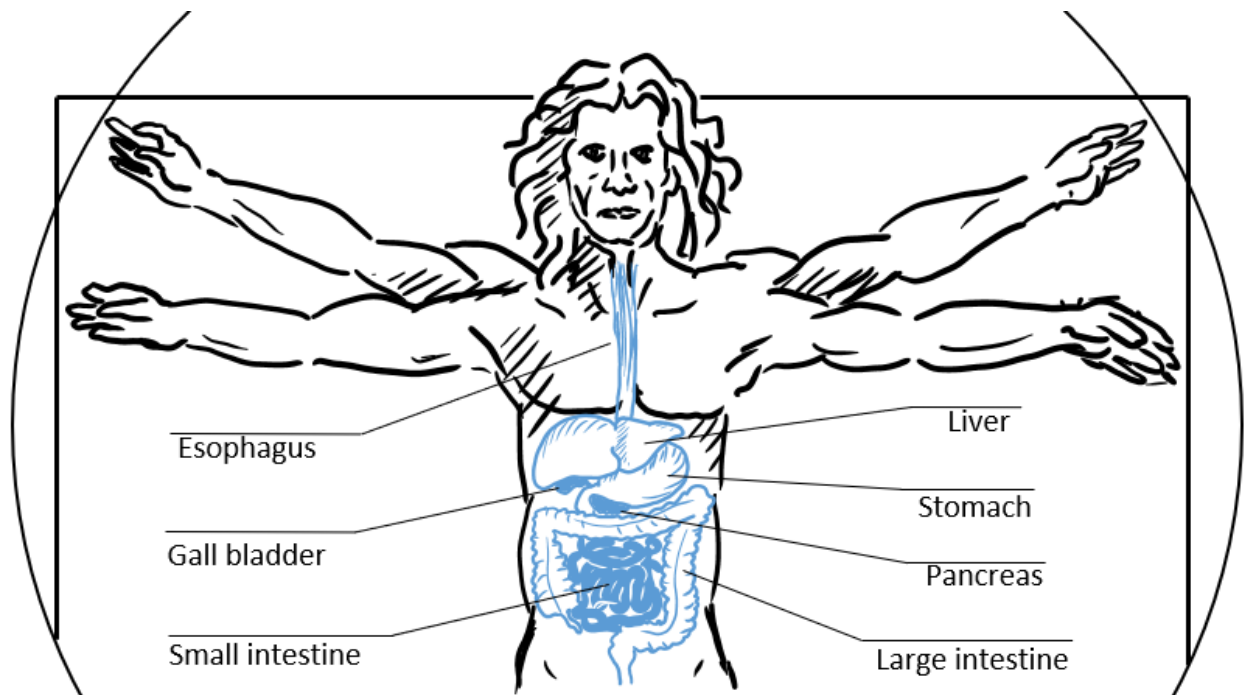


Figure 1. *Vitruvian man* and the digestive system.

1.1.1 Stomach

The main functions of the gastric compartment are to mix and reduce the size of the ingested food and to protect the lower GI segments from exogenous microorganisms, as well as to initiate the digestion of proteins.

In the fasted state, the gastric fluids have a low resting volume. The commonly accepted value of the average fasted state gastric fluid volume is 25 to 50 ml³⁻⁶. Thus, the gastric media volume in the fasted state after a glass of water (200 – 240 ml) is approximated to an average value of 250 ml. In the fed state, the gastric volume depends on the amount of the ingested food and liquid, active gastric secretion and the speed of the gastric emptying and may reach values of several hundred ml⁵.

The main component of the gastric medium is hydrochloric acid, which is secreted from parietal cell and dictates the gastric pH. The pH of the gastric medium in the healthy, fasted state has a low value, usually between pH 1 and 3⁷⁻⁹. In the fed state, the pH value rises to an extent which is dependent on the pH and buffer capacity of the meal. Thus, gastric pH in the fed state generally ranges from pH 3 to 7⁷⁻¹⁰.

The surface tension of the medium in the fasted state (30 – 45 mN/m^{8,11,12}) originates from a low concentration of surface-active components, thought to be generated by modest bile acid reflux from the duodenum into the stomach (achieving concentrations far less than 1 mM). In the fed state, the surface tension sinks to 30 mN/m¹³, on the one hand due to lipolysis of fatty components of the meal and on the other hand potentially due to higher bile reflux.

The gastric motility in the fasted state can be divided into three phases. Phase 1 shows minimal motility and lasts for on average 50 minutes. In Phase 2, the gastric contractions become more frequent and intense (period of 30 – 45 min), culminating in Phase 3 with strong contractions inducing emptying of the gastric medium (gastric emptying, GE). This pattern is repeated on average every 2 hours^{14,15}. In the fed state, a different motility pattern can be observed. The gastric contents, now a composite of gastric acid, food, liquid and secretions, is mixed by alternating contractions of the gastric muscles, and emptied over a period depending on the caloric value of the meal, with a general emptying rate of 2-4 kcal/min¹⁶.

Pepsin is an important enzyme active in the stomach. Its purpose is the digestion of proteins and as such, it cannot be secreted in an active form from the gastric chief cells. Thus, gastric chief cells secrete an inactive pro-enzyme, pepsinogen, which is transformed into the active form¹⁷, pepsin, only after secretion into the gastric fluids

and under low pH conditions (under pH 4), reaching an average concentration of 0.1 mg/ml in the fasted state^{13,18,19}. Peptic activity is not only important for food digestion, but also for the disintegration of some drug formulations, like gelatine capsules. The gastric mucosa secretes mucus and bicarbonate to protect itself from the corrosive effects of hydrochloric acid and pepsin. The bicarbonate secretion into the gastric fluids is, however, minimal²⁰: it only serves to neutralize hydrochloric acid on the mucosal surface.

The stomach was at first assumed to be sterile in the fasted state, as one of the purposes of the low gastric pH is to denature microorganisms. Nevertheless, after the discovery of *Helicobacter pylori* in the stomach, more research showed the existence of approximately 1000 bacterial colony forming units (CFU)/g in the gastric compartment^{21,22}.

1.1.2 Small intestine

The main function of the small intestine is the absorption of nutrients. This is also the main place of drug absorption for medicines administered orally. The small intestine is highly efficient in this regard due to its physiology. Due to the circular folds (Kerckring's rings), the small, finger-like formations called villi on the mucosal surface and the microvilli on the apical side of the enterocytes²³, which make up around 85 to 90 % of the cells on the mucosal surface, the surface area of the 3 - 8 meter long small intestinal tube^{1,24} increases dramatically to around 30 - 200 square meters^{25,26}, depending on the calculation.

The volume of fluids in the small intestine was reported to range from 30 to 300 ml in the fasted state and 40 to 400 ml in the fed state^{5,7}. Depending on the methodology used to define the intestinal volume (volume calculation, chymus contents, mucosal water or only water pockets), the numbers vary among authors^{4,5,7,27}.

The pH of the small intestinal compartment is mainly regulated in the fasted state by the high bicarbonate secretion (10-fold of the gastric bicarbonate secretion²⁰) into the duodenum. The function of the bicarbonate, which is secreted mainly from the pancreas, is to neutralize the acidic medium entering from the stomach and thus protect the intestinal mucosa^{7,20}. At the proximal end, the average pH value in both the fasted and fed state is around pH 5 – 6.5, whereas in the distal part of the small intestine, an average pH value of 7.5 is reported^{7,28}.

In order to further digest the food entering from the stomach, lipases, amylases, and proteases are secreted from the pancreas. Additionally, secretion of the bile components (bile salts and lecithin) promotes the “wetting” and emulsification of the chyme, due to the bile’s surface-active properties, thus promoting interaction of the chyme with the enzymes and (incidentally) higher solubility of lipophilic drugs. The basal secretion of bile components from the gall bladder into the duodenum induces an intestinal bile component concentration of 3 mM in the fasted state^{13,29,30}. In the fed state, maximal release of the bile stored in the gallbladder is triggered, raising the average bile salt concentration to 10-15 mM^{8,31}.

The contractions throughout the small intestine ensure mixing of the intestinal medium and contact with the absorptive cells (enterocytes) of the intestinal mucosa.

Regarding the microbiotic composition of the intestinal medium, the small intestine is a transition zone between the gastric conditions, where only few bacteria survive, and the large intestine, where the peak concentration of intestinal microbiota is found. Thus, the proximal part of the small intestine houses a very low bacterial count, 10^4 CFU/g, whereas the distal intestine contains up to 10^7 CFU/g²², still far lower than the microbiota-rich large intestine.

1.1.3 Large intestine

Although the great majority of nutrient absorption is complete in the proximal small intestine, certain nutrients can be absorbed from the large intestine. The thriving microflora decomposes e.g. some polysaccharides that are non-digestible by human enzymes. However, the main function of the large intestine is water and electrolyte (re)absorption¹. Drug absorption in this region is limited due to the lower surface area/volume ratio.

The pH in the large intestine is largely influenced by the fermentation processes of the colonic bacteria, which decompose polysaccharides to short-chain fatty acids¹¹, resulting in a pH of around 5 - 6.5 in the proximal colon. Aboard the pH in the large intestine rises gradually back to approximately pH 7²⁸.

The concentration of bile components in the large intestine is low, due to an almost complete re-absorption by active uptake processes in the ileum.

The residence time in the large intestine is longer than in the small intestine³². This assures enough time to absorb a large amount of water during the transit of the

residual chyme. Interestingly, the proximal colon serves as a mixing segment, such that materials can move in both the oral and aboral direction in this segment. Over time, peristalsis guides the content to the sigmoid colon, while final, strong contractions empty the content¹⁶.

The large intestine offers anaerobic surroundings, where up to 10 trillion CFU/ml, with over 500 bacterial species are identified^{22,33,34}.

1.2 Biorelevant media

Biorelevant media are dissolution media which are designed to mimic the gastric and intestinal conditions *in vitro*³⁵. They evolved from the compendial media, which are buffered aqueous solutions reflecting the pH of the GI environment. In addition to reflecting the pH, biorelevant media take other parameters of the *in vivo* media into account, like buffer capacity, osmolality and concentration of bile components³⁶. Thus, drug dissolution experiments using biorelevant media can provide a more accurate representation of drug dissolution *in vivo*³⁵ compared to compendial media.

Biorelevant media have received broad attention and are accepted in academic research, the pharmaceutical industry and regulatory authorities alike due to the fact that they indeed show important advantages over compendial media, especially for poorly soluble drugs. In recent years the procedure for making the media manufacturing have become simpler: while initially the bile components had to be introduced into the biorelevant medium via an organic solvent (which later had to be evaporated using a rotary evaporator³⁷), nowadays, a commercially available, lyophilized mixture of bile components³⁸, suitable for direct addition into an aqueous medium, is commercially available (biorelevant.com).

The first biorelevant media were defined by Dressman et al. and applied by Galia et al^{11,39}. Their research generated the first two widely used biorelevant media; which reflect the fasted state intestinal fluid (FaSSIF) and the fed state intestinal fluid (FeSSIF). FaSSIF includes a phosphate buffer with a buffer capacity of 12 mEq//ΔpH and a pH of 6.5, with sodium chloride added to adjust the osmolality to 270 mOsmol and sodium taurocholate and lecithin present in concentrations reflecting the bile component concentration in the fasted intestinal fluid (3 mM). FeSSIF includes an acetate buffer with a buffer capacity of 76 mEq//ΔpH and a pH of 5, with (initially) potassium chloride used to adjust the osmolality to 635 mOsmol and taurocholate and

lecithin concentrations adjusted to reflect the fed state intestine medium (15 mM)³⁶. In years following the publication of FaSSIF and FeSSIF, a fasted and a fed state simulated gastric fluid were developed (FaSSGF and FeSSGF)^{40,41}. FaSSGF has a pH of 1.6 and consists of hydrochloric acid, sodium chloride (121 mOsmol) and a small concentration of bile components (80 µM) reflecting the composition of the gastric fluids *in vivo*. FeSSGF is defined by “snapshot” media, corresponding to the changes in the gastric fluids after a meal over time. FeSSGF initially used milk as the basis^{39,41}, but now uses Lipofundin, a standardized oil emulsion, to introduce a lipophilic component into an *in vitro* medium³⁶.

Furthermore, by updating the osmolality and bile component ratio for the intestinal fluid as well as exchanging the phosphate buffer for a maleate buffer with a lower buffer capacity (10 mEq/l/ΔpH), a second version of FaSSIF was composed (FaSSIF V2)⁴¹. A second version of FeSSIF, i.e. FeSSIF V2, has been developed as well. In addition to updating the osmolality and buffer capacity of the maleate buffer, glyceryl monooleate and sodium oleate were introduced^{36,41} to reflect digestion products.

Fasted state simulated colonic fluid (FaSSCoF) and fed state simulated colonic fluid (FeSSCoF) have also been developed⁴², completing the set of *in vitro* biorelevant media reflecting all parts of the GI tract. These biorelevant media, as well as newer developments, such as FaSSIF V3⁴³ or FEDGAS⁴⁴, can all play an important role in predicting the drug behaviour *in vivo*. Since these media represent the average GI physiology in healthy adults, further work is needed to identify suitable media for children and various disease states and dosing conditions in which the gastrointestinal physiology is altered^{45–47}.

1.3 Disease states linked to elevated gastric pH

1.3.1. Hypo- and achlorhydria

The low pH of the gastric fluids is an essential characteristic of the gastric physiology. In the healthy state, the natural processes which can elevate the gastric pH are the intake of water or food. Due to re-acidification of the gastric compartment via basal and active acid secretion, as well as emptying of the content from the stomach, the elevation in pH is temporary.

Hypochlorhydria is a disease state in which an individual possesses a low level of gastric acid in the fasted state and thus continuously elevated gastric pH. Achlorhydria,

similarly, is a disease state, in which levels of gastric acid secretion are negligible⁴⁸, either in the fasted state or in response to a meal. Elevated gastric pH^{49,50} has been defined as a pH above 3.5. In hypo- and achlorhydria, the gastric pH value ranges from pH 3.5 (and for achlorhydria from pH 5.09⁴⁸) to as high as pH 7, depending on the degree of the acid secretion impairment.

The causes for hypo- and achlorhydria are diverse. Hypochlorhydria has been identified as the main potential physiological change in the gastric compartment due to aging⁵¹ and is more frequent in elderly populations⁵¹⁻⁵³. Impairment of gastric acid secretion can be caused by bacterial infections (*Helicobacter pylori*) or as a side-effect of surgical operations, such as partial gastrectomies - a famous example being the Billroth II surgery⁵⁴. Aside from *Helicobacter* infections, achlorhydria is very rare in young healthy adults, whereas the incidence in the elderly is thought to be around 10 %. Some populations, such as the Japanese^{55,56}, have a higher incidence of hypochlorhydria than others, although the incidence appears to be decreasing over time⁵⁶. Hypochlorhydria has also been linked to chronic stress⁵⁷.

1.3.2 Diseases treated with ARAs

Furthermore, elevated gastric pH occurs during the therapy of dyspeptic diseases. Heartburn, GastroEsophageal Reflux Disease (GERD), gastritis, Barrett's esophagus, Zollinger Ellison syndrome, as well as gastric and duodenal ulcers are all treated using acid-reducing agents (ARAs). ARAs are locally or systemic acting drugs, which aim to inhibit or reduce acid secretion or directly reduce the gastric acid quantity. ARAs include several drug families, of which the antacids, H₂-receptor antagonists (H₂RAs) and proton pump inhibitors (PPIs) are the three most prominent and well-researched groups⁵⁸.

In addition to the treatment of dyspeptic diseases, ARAs are often used during polymedication of other disease states as a preventive measure against ulceration of the stomach (e.g. in elderly patients, during chronic use of non-steroidal anti-inflammatory drugs (NSAIDs), cancer treatment or treatment of human immunodeficiency virus (HIV) infection).

Antacids are the oldest drugs used to reduce gastric acid and are still in broad use, most frequently in self-treatment of heartburn⁵⁹. Antacids are a diverse group of basic minerals and constitute the only ARA group that impacts the pH of the gastric fluid

directly, via a neutralisation of hydrochloric acid. The main sub-groups of antacids include sodium salts (e.g. sodium bicarbonate), calcium salts (e.g. calcium carbonate), magnesium and aluminium compounds (simple oxides and hydroxides, as well as basic composites and complexes including both cations).

H2RAs competitively inhibit the histamine H₂ receptors responsible for the transmission pathway of parietal cells, thus inhibiting hydrochloric acid secretion into the gastric compartment⁶⁰. Commonly used H2RAs are cimetidine, ranitidine and famotidine⁶¹. With the introduction of PPIs, H2RAs were replaced as the first-line therapy of dyspepsia and GI ulcers. Nevertheless, due to their relatively fast onset of action, they are still used e.g. in the pre-treatment of urgent surgeries, during which gastric acid aspiration must be prevented in a timely fashion.

PPIs are one of the most prescribed classes of drugs worldwide⁶². PPIs are acid-labile compounds, which irreversibly bind to proton pumps of the parietal cells, directly inhibiting acid secretion at the end of the parietal cell acid secretion pathway⁶³. Currently, a number of PPIs are approved and on the market, the most commonly used being omeprazole, esomeprazole, pantoprazole and lansoprazole. Rabeprazole is the most potent PPI, whereas pantoprazole is the least potent. Pantoprazole however has the advantage of being the PPI with the least metabolic interactions with other drugs.

1.4 Drug development and DDI predictions

The process of developing medicines has several aspects. While drug discovery, preclinical development and clinical development focus on the drug itself⁶⁴, formulation development runs in parallel to the drug development and is responsible for ensuring delivery of the drug to the site of action⁶⁵.

Drug discovery starts with identifying compounds (“hits”), which potentially interact with the target receptors or enzymes. At this stage, vast libraries of compounds are assayed using the high throughput screening (HTS) method. While this approach facilitates the assessment of thousands of potential compounds for their affinity to the target in a short period of time, it also brings some essential disadvantages. For example, the assay uses organic solvents for the stock solutions of the compounds to investigate the compound potency, thus often identifying highly lipophilic compounds as hits. While this indeed often leads to compounds showing high potency, it also

frequently leads to compounds with poor aqueous solubility being selected for development.

In addition, ionisable compounds (weak bases or acids) are more likely to be selected for further examination since precipitation and salt formation are easy ways of extracting a compound during the synthesis process. Thus, a great amount of today's approved drugs or compounds in the development pipeline are poorly soluble, ionizable compounds.

In early development, the most promising compounds are evaluated further for their pharmacodynamics, pharmacokinetics and toxicity and a "lead" compound (sometimes along with one or two back-up compounds) is subjected to further preclinical studies and optimized for clinical development.

During clinical trials, drugs pass through three phases. The size of clinical trials increases from Phase 1 to 3, so in addition to the ethical considerations around human clinical studies, they become increasingly expensive and time-consuming. This forces formulation development to quickly provide "fit for purpose" dosage forms, with the aim of identifying the finished product by Phase 3.

In Phase 1, the safety of the compound is assessed in humans in dose escalation studies. Phase 2 focuses on identifying the appropriate dose for achieving a therapeutic effect, whereas Phase 3 serves to evaluate the efficacy and safety of the drug product⁶⁴.

As a part of the efficacy and safety evaluation, drugs and their formulations are tested for drug-drug interactions (DDIs) which could potentially appear during therapy with multiple drugs, as well as the drug's efficacy in the diseased state. Co-administration of certain substances is known to alter the extent of the metabolism of a drug, possibly having a significant impact on the drug exposure^{66,67}. Inhibition of the drug metabolism may lead to toxicity, whereas induction of the enzyme activity may lead to a lack of drug efficacy. The evaluation of such DDIs early in the development process enables optimization prior to the more extensive clinical trials, thus streamlining the development timeline.

While the evaluation of such DDIs has become an essential part of the industry guidelines^{68,69}, in recent years the focus of industry and regulatory bodies has extended to DDIs affecting drug dissolution, mainly pH-dependent DDIs⁷⁰. As many of the drugs are poorly soluble ionizable compounds, their dissolution is pH-dependent.

Acid reducing agents (ARAs), compounds elevating the gastric pH, as well as hypo- and achlorhydria, can have a negative impact on the efficacy of poorly soluble, weakly basic compounds, since their availability for absorption often depends on extensive dissolution in the acidic environment of a healthy stomach. Furthermore, ARAs may have an impact on the safety of poorly soluble acidic compounds, as the amount of drug available for absorption can increase due to faster dissolution at elevated gastric pH, which could potentially lead to toxicity^{70,71}, especially if the drug has a narrow therapeutic index⁷².

As with the metabolism-dependent DDIs, an early characterisation and assessment of pH-dependent DDIs would be highly advantageous. Standardized *in vitro* methods estimating the possible extent of these DDIs prior to conducting the clinical studies are thus of great interest.

1.5 *In vitro* tools

Biorelevant *in vitro* tools are experimental set-ups aiming to reflect specific properties of the physiology or biological processes in the laboratory rather than the “real” biological surroundings. In connection to biopharmaceutics, *in vitro* tools are used to investigate solubility, permeability and dissolution behaviour of drugs. *In vitro* tools can in some cases provide data and conclusions directly connected to the drug behaviour *in vivo*, building a base for the *in vitro* - *in vivo* correlation (IVIVC) approach⁷³. Furthermore, in the last decade or so, *in vitro* tools are often being combined with *in silico* methods to develop a more robust picture of the drug behaviour *in vivo*⁷⁴. In the following sub-chapters, several *in vitro* tools relevant to the research of this thesis are described.

1.5.1 Solubility measurements

1.5.1.1 Shake-flask method

Aqueous thermodynamic solubility is defined as the concentration of a compound in a saturated solution at a certain temperature and a defined pH, provided that an equilibrium between the dissolved compound and the compound in the solid state exists^{75,76}. The most famous *in vitro* method for assessing thermodynamic drug solubility⁷⁷ is the shake-flask method. Intriguingly, in literature, the original source for the method protocol is rarely revealed, but rather waived by calling it “the classical

shake-flask method”. This contradicts the fact that there is no accepted standard procedure for carrying out the method⁷⁸. In general, an excess of the drug substance is added to a closable vessel or a flask, then a specific volume of a medium is added, the vessel closed and stirred for a period of time at 37 °C on an orbital shaker with maximum velocity, in order to reach an equilibrium between the compound in dissolved and solid state. After this period, the samples are taken, filtered or centrifuged, and quantified. Nevertheless, the details on how much drug excess should be added, which volumes are used or what stirring time should generally be used, differ between sources. Furthermore, the type of investigated solid form or the final media pH, which are also essential for interpretation of the solubility data, are often not taken into account. An assessment of the most important parameters was conducted to update the method⁷⁹, and in 2018 World Health Organisation (WHO) has published a draft for the use of a standardised shake-flask method⁸⁰. WHO suggests conducting two types of experiments. In the preliminary solubility assessment experiments an excess of 30 – 40 % of the dose necessary for the saturation of 5 ml of the medium is added, the flasks are shaken over 72 h and the concentration repeatedly measured during this period to identify the equilibration time. Then, taking the preliminary solubility data into account, in the pivotal experiments only 10 % excess of the drug is added to an appropriate amount of the medium, the flasks are shaken for a period of time previously identified to be sufficient for equilibration, and samples finally filtered or centrifuged, diluted and quantified.

1.5.1.2 UniPrep® method

A miniaturized version of the shake-flask method was introduced by Glomme et al. The UniPrep® method has the advantage of using a smaller amount of the solvent and the compound than is required for the shake-flask method, and it simplifies the solubility measurement process by including a built-in filtration mechanism within the UniPrep® housing⁸¹. For this method, an excess amount of the drug (in the original publication reported as the amount two times higher than necessary for the calculated solubility⁸¹, however nowadays 150 % of the dose expected to dissolve in 3 ml of a medium) is weighed into the UniPrep® tube, 3 ml of the medium is added and the housing closed. Similar to the shake-flask method, the UniPrep® tube is then shaken at 37 °C on an orbital shaker, operated at maximum speed per the original publication for 24 hours. After 24 hours, the built-in filter is pushed through the suspension and the clear supernatant sampled and quantified. It is important to note, that after the step

of irreversibly pushing the built-in filter through the housing, undissolved drug has minimal contact with the solution, so any further dissolution of the drug after that point is unlikely even if the equilibrium has not been reached. The shaking time of 24 hours was chosen as this equilibration time is sufficient for the majority of compounds⁸², however, some preliminary experiments with sampling times at different shaking times may be conducted to ensure that the equilibrium is reached by the 24th hour.

1.5.2 Permeability measurements

Permeability is the second important factor necessary to define when interpreting drug behaviour *in vivo*. In regard to oral drug administration, the permeability of a compound can be defined as the ability to pass through the gut wall⁸³ and thus be available for systemic distribution.

1.5.2.1 Parallel Artificial Membrane Permeability Assay

One of the popular *in vitro* permeability assessment methods is the Parallel Artificial Membrane Permeability Assay (PAMPA). This assay consists of two buffered, isotonic aqueous compartments divided by a lipid-infused artificial membrane. At the beginning of the experiment, a certain amount of drug is added to one compartment (donor compartment), and the drug is allowed to permeate through the membrane into the other compartment (acceptor compartment). At certain times, the concentration of the drug in both compartments is quantified, thus enabling the permeability to be calculated⁸⁴.

The advantages of the model are its straightforward preparation and use of readily available materials. By using 96 well-microtiter plates the speed, cost and efficacy of permeability measurement can be facilitated.

A drawback of this method is that it identifies only the permeability of a drug originating from the passive transcellular diffusion and cannot assess paracellular diffusion or active transport of a drug through the membrane. Despite this drawback, PAMPA is widely used because a majority of the drugs are absorbed *in vivo* via passive absorption, and, furthermore, the paracellular diffusion often plays only a minor role⁸⁵.

1.5.2.2 Caco-2 permeability assay

The Caco-2 permeability assay is the most widely accepted cell-based method.

Caco-2 permeability assay utilizes an adenoCarconoma Colorectal (Caco) cell monolayer. In this method, after culturing the Caco-2 cells, the cell monolayer is grown

on a porous polymer substrate, which separates a donor and an acceptor compartment⁸⁶. The composition of the fluids in both compartments can be adjusted to represent the apical (outside) and basolateral (inside) environment of the intestinal epithelial layer. With this set-up, a permeability in both directions (apical to basolateral and basolateral to apical) can be determined, depending on which compartment the drug solution is added. Thus, the apparent permeability (P_{app}) can be determined. The Caco-2 cell monolayer has the advantage over the PAMPA assay of being able to facilitate both passive trans- and paracellular transport, as well as active absorption and efflux processes⁸⁷, which are all observed in the human intestinal cells *in vivo*. Although Caco-2 cell monolayers show a good correlation to permeability *in vivo*, this method also has drawbacks. Cell-based methods demand a longer and more complicated preparation^{8,88}, as the cells have to be cultivated and held under optimal conditions. Thus, the cost of the Caco-2 permeability assay is higher than the PAMPA. The Caco-2 cells also show a higher activity of the efflux transporters, as well as narrower tight junctions between the cells⁸⁹, possibly reflecting the carcinoma cell tendency to “protect” itself from xenobiotics, thus underestimating intestinal absorption in some cases. A common problem is also a large inter- and intra-laboratory variability, which can, nevertheless, be relativized by conducting control runs with standard drugs of known permeability in parallel to the experimental measurements⁹⁰. Nevertheless, the Caco-2 permeability assay remains a valuable tool to estimating drug permeability early on in the development process and the data acquired from such assay is often used as input in *in silico* tools, as the availability of *in vivo* permeability data acquired by an intestinal perfusion double-balloon system in humans is extremely limited.

1.5.3 Biorelevant dissolution measurements

Next to the identification of the solubility and permeability, an accurate description of the drug dissolution is the third essential parameter assessed by the biopharmaceutic *in vitro* tools.

According to the USP, dissolution is the process in which a substance forms a solution. Dissolution testing thus measures the extent and rate of solution formation from the solid drug substance or a dosage form⁹¹. Dissolution testing was initially employed for quality control of pharmaceutical products, where simple aqueous buffers of high

buffer capacity (compendial media) and high solvent volumes inducing “sink” conditions was used to produce robust methods, which however do not closely resemble the GI physiology. Later, with the introduction of biorelevant media, dissolution testing started to play an important role in drug development, as here dissolution testing has been designed to reflect the physiological conditions more closely⁹² in order to simulate and predict possible dissolution behaviour *in vivo*. Biorelevant dissolution testing has thus become a standard method in drug research and development, encompassing various *in vitro* set-ups, all aiming to reflect some key aspects of dissolution behaviour *in vivo*⁹³.

1.5.3.1 Simple *in vitro* dissolution set-ups

Simple *in vitro* biorelevant dissolution set-ups are built on the concept of broadly used, standardized set-ups, like USP apparatus. Of the four main types of USP apparatus (Apparatus 1 – rotating basket, Apparatus 2 – rotating paddle, Apparatus 3 – reciprocating cylinder and Apparatus 4 – flow-through cell)⁹⁴, the paddle apparatus has served as the basis for most of the biorelevant dissolution set-ups. Its major advantage is the broad availability in dissolution laboratories, as well as its simplicity.

1.5.3.1.1 One-stage dissolution

The simplest biorelevant dissolution set-up, one-stage dissolution set-up, uses the USP paddle apparatus with a 1 l vessel and a single biorelevant medium, reflecting either gastric or intestinal and fasted or fed conditions. The experiments are usually conducted at 37 °C, the paddle rotation speed is set to 50, 75 or 100 rpm and, for IR formulations the experiment typically lasts for 2 hours (gastric) or up to 4 hours (intestinal). An example of a sampling schedule intended to characterize the dissolution profile is 5, 10, 15, 20, 30, 45, 60, 90 and 120 min after the addition of the formulation to the dissolution medium. For floating formulations (capsules), sinkers can be used to hold the formulation at the bottom of the medium⁹⁵.

One-stage biorelevant dissolution testing offers a quick and easy method to assess drug dissolution under various conditions and can serve as the basis of IVIVC or as input into *in silico* models. Nevertheless, one-stage experiments only show the dissolution of the drug under one condition, rather than dissolution as the drug / dosage form moves through the GI tract. This leads to the possibility that e.g. drug supersaturation and precipitation might be overlooked if one-stage dissolution is used exclusively.

There are some variations of the one-stage biorelevant dissolution regarding the design of the vessel. The sampling during the experiments under fasted gastric conditions may be difficult due to the low volume of the dissolution medium (typically 250 ml) because the standard paddle in the standard 1 l vessel set-up is barely immersed in the medium at this volume⁹⁶. The Erweka mini-paddle set-up aims to handle such situations by scaling down the design of the standard 1 l vessel to a 500 ml vessel⁹⁷. In the Erweka miniaturized design, the geometry and thus the hydrodynamics are properly scaled, but in other miniaturized designs this is not the case.

Another common issue during dissolution testing is formation of a mound (“cone”) of the undissolved material at the bottom of a vessel, below the paddle, which hinders the dissolution of drug from the formulation. Coning can be avoided by elevating the stirring rate or use of the apex (“peak”) vessels^{98,99}. The apex vessels differ from the standard 1 l vessels by having an indentation in the bottom of the vessel, thus reducing the occurrence of coning. Although apex vessels offer a great solution for avoiding an artefact occurring only in the *in vitro* method, the use of apex vessels is not yet broadly accepted since different manufacturers have slightly different designs for the indentation. In response, a publication on the topic of apex vessel standardization is currently under review for USP pharmacopeial forum and is expected to be published soon.

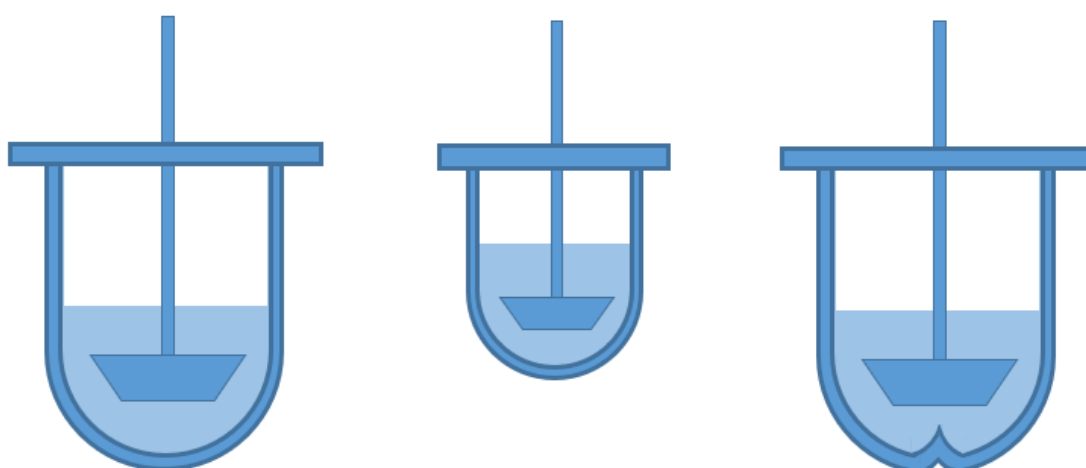


Figure 2. Graphical representation of the one-stage dissolution set-up, with (from left to right) a standard 1 l vessel, 500 ml Erweka mini-vessel, as well as a 1 l apex vessel.

1.5.3.1.2 Two-stage dissolution testing

Two-stage dissolution is an *in vitro* method which can be used to identify drug supersaturation and precipitation after a pH shift between the gastric and intestinal compartments¹⁰⁰.

There are several variations of the two-stage dissolution testing. The earliest version, which was referred to as a “dumping experiment”, adds a solution of pre-dissolved drug in the gastric medium into an intestinal medium over a very short period of time¹⁰¹ (“dumping”). The currently most broadly accepted method, described by Mann et al., was evolved in the OrBiTo project¹⁰²: In this method, dissolution is tested in a standard 1 l vessel in a paddle apparatus under gastric conditions (250 ml of FaSSGF pH 1.6) for 30 minutes at 37 °C and 50, 75 or 100 rpm. After taking the 30-minute sample, a double concentrate (containing a double amount of all components) of FaSSIF V1 with the pH of 7.5 and the volume equivalent to the volume already in the dissolution vessel (250 ml), pre-heated to 37 °C, is added via a bolus addition. The 500 ml of the resulting mixture has a composition comparable to one of FaSSIF V1 medium. The dissolution experiment is run for additional 1.5 hours in the intestinal medium and the concentration of dissolved drug is monitored. The two-stage dissolution set-up thus incorporates the pH and composition shift between the gastric and intestinal segments. This is a significant advantage over one-stage experiments, especially when assessing the drug behaviour of poorly soluble ionizable compounds. Poorly soluble weak bases dissolve more readily in the acidic, gastric environment, so a pH shift of a concentrated drug solution to a more basic, intestinal environment may result in one of three scenarios: 1) the drug solution could retain its high concentration despite the less “favourable” intestinal pH for an extended period of time (supersaturation), 2) the drug could immediately precipitate to the equilibrium solubility at the intestinal pH (immediate precipitation), or 3) the drug could slowly precipitate over time (slow precipitation), approaching the solubility of the precipitated material in the intestinal medium¹⁰³. As only the dissolved portion of the drug can be absorbed, the presence of supersaturation / precipitation *in vivo* can have a significant impact on the amount of the weakly basic drug available for absorption after the gastric emptying. *In vitro* assessment of the drug behaviour after a pH shift can also play an important role for poorly soluble weakly acidic compounds. Although the solubility of the acidic compounds is higher in the less acidic intestinal environment, a pre-exposure of the drug (formulation) to the acidic, gastric medium may alter the way it dissolves in the

intestinal compartment, e.g. due to a transition from salt into a free acid¹⁰⁴ or from an amorphous to a crystalline form prior to reaching the intestine.

Although the two-stage set-up aims to simulate the transit of the drug between two GI compartments, the *in vitro* shift between the two media happens abruptly, inducing a rapid change in the composition and the pH of the surroundings. This underpredicts the period over which the change in pH occurs during the drug transit *in vivo*, and thus frequently overestimates precipitation. As a result, biorelevant two-stage dissolution testing should be used as a qualitative tool to assess the possibility of supersaturation and precipitation, and is not suitable for quantitatively translating the observed *in vitro* behaviour to the average *in vivo* situation.

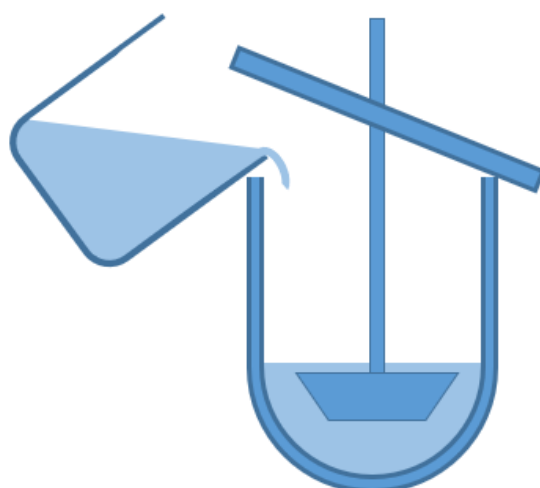


Figure 3. Graphical representation of the two-stage dissolution set-up.

1.5.3.1.3 Transfer experiments

The transfer model was introduced by Kostewicz et al. in 2004 to reflect the transition of the drug from the gastric into the intestinal compartment¹⁰⁵ and pre-dates the two-stage test. The current version of the transfer model set-up consists of a USP 2 paddle apparatus (commonly used stirring rate of 75 rpm) with 250 ml FaSSGF in a mini-vessel to represent the gastric compartment and (after transfer) 600 ml FaSSIF in a standard 1 l vessel to represent the intestinal compartment, with a peristaltic pump connecting the two compartments. The function of the programmable peristaltic pump

is to gradually transfer dissolved and disintegrated drug from the gastric (donor) compartment into the intestinal (acceptor) compartment. This is achieved by programming the pump to transfer the gastric medium over to the intestinal compartment. Frequently a first order transfer with a half-emptying time of 9 minutes is used to reflect average gastric emptying kinetics observed *in vivo*^{4,105,106}. As a result, the times over which supersaturation and precipitation occur in the transfer model are often longer than in two-stage experiments.

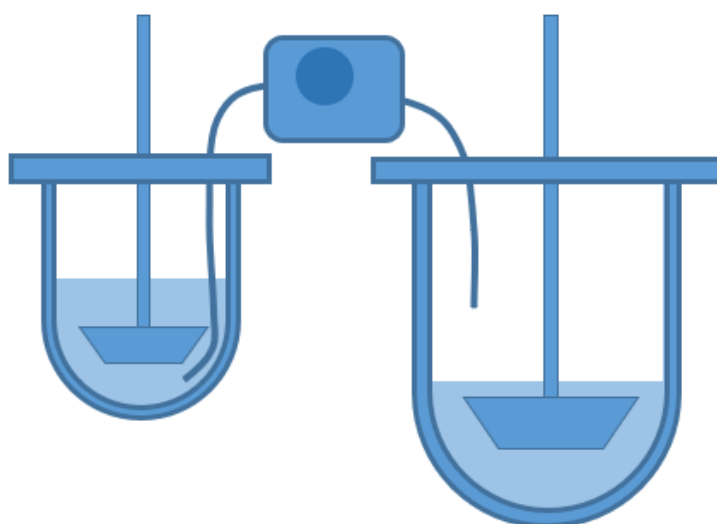


Figure 4. Graphical representation of the transfer test dissolution set-up.

Several variations on the transfer set-up have been generated to take further physiological processes into consideration. For example, the Biorelevant-GastroIntestinal-Transfer system (BioGIT)^{107,108} uses additional pumps to empty the dissolved drug from the acceptor compartment and to replenish the emptied intestinal medium using transfer of a fresh intestinal medium from another reservoir. Introducing an open set-up for the intestinal compartment mimics the absorptive process for highly permeable drugs and leads to less precipitation than the transfer model, which is a closed system.

The artificial stomach-duodenum model (ASD model)¹⁰⁹ takes a set-up comparable to BioGIT a step further by introducing a pump from a reservoir with the fresh gastric

medium to the gastric compartment in order to hold the gastric phase volume constant, in an attempt to simulate the physiological gastric acid secretion.

1.5.3.2 More complex *in vitro* set-ups

In addition to the simple biorelevant dissolution methods, which combine standard dissolution set-ups and biorelevant media to reflect the physiological conditions, while staying relatively simple, low cost, robust and reproducible, more complex *in vitro* dissolution set-ups have been evolved to simulate the physiological processes. These aim to more closely mimic the processes observed *in vivo*. A great advantage of such set-ups is that the closer the set-up is to the “real thing”, that is, to the simulation of human physiology, the fewer *in vitro* artefacts can be expected and the higher assurance that drug behaviour *in vivo* will be simulated. Nevertheless, the more complex *in vitro* set-ups come with a higher cost, the need to track a multitude of additional parameters which interact with and influencing dissolution, as well as the fact that they are (for now) not widely accessible and that the data generated is currently not compatible with input into *in silico* tools.

1.5.3.2.1 TNO gastrointestinal model (TIM-1)

TNO gastrointestinal model (TIM-1) consists of four tubing compartments representing stomach, duodenum, jejunum and ileum, enclosed by cylindrical vessels filled with water simulating peristalsis at body temperature, as well as various secretion and absorption compartments and parameter monitoring sensors^{110–112}. This set-up is able to simulate complex physiological processes, like re-acidification of the gastric compartment, mixing of “chyme” and gastric emptying and attempts to simulate drug absorption in the intestine via a polymer membrane reminiscent of the PAMPA method.

Data acquired via the set-up suggests the percentage of the dose available for absorption at a given point in time following oral administration of a formulation. The TIM-1 set-up, furthermore, allows for sampling of the simulated GI fluid *in situ*, potentially enabling insight into supersaturation and precipitation of the drug in the simulated intestine.

1.5.3.2.2 GastroDuo

GastroDuo is a biorelevant *in vitro* dissolution test consisting of a gastric and a duodenal compartment connected by a peristaltic pump, as well as additional vessels employed to simulate re-acidification of the gastric compartment^{113,114}. The gastric

compartment consists of a cell holding the drug formulation in 50 ml of a medium, and a balloon mechanism, which is able to accurately reproduce the movement and pressure exercised on the formulation in the stomach, reflecting results of the *in vivo* studies with pressure- and pH-monitoring capsules. Consequently, the GastroDuo set-up simulates the behaviour of the drug formulation in the gastric compartment and, by simulating realistic gastric emptying kinetics, can give a more physiologically relevant profile of drug dissolution.

1.6 *In silico* tools

Scientists have always aspired to explain natural processes in simple terms¹¹⁵, while the most accurate explanations have been achieved using mathematical equations. Biopharmaceutical *in silico* tools use computational power and mathematical equations to define important biopharmaceutical processes in order to simulate drug behaviour. A biopharmaceutical parameter, which can be directly linked to the drug effect *in vivo*, is the blood plasma concentration of the drug at a given timepoint after drug administration. After oral administration, the drug formulation must disintegrate and release the drug, enabling drug dissolution. Only dissolved drug can be absorbed quantitatively via the intestine and reach the systemic circulation¹. The physicochemical parameters of the drug play an important role in defining the distribution of the drug from the systemic circulation to other organs and tissues in the body. Together with drug metabolism and elimination, absorption and distribution dictate the drug's plasma concentration profile. *In silico* tools need to reflect all processes i.e. Liberation (disintegration and release/dissolution), Absorption, Distribution, Metabolism and Elimination (L-ADME) processes in order to simulate the drug plasma profile after oral administration of a drug formulation.

In the following sub-sections, several *in silico* tools relevant to this thesis are addressed.

1.6.1 *In silico* tools for *in vitro* dissolution parametrisation

The simplest way to define drug dissolution is by fitting the dissolution profile to a Weibull equation.

The Weibull equation is derived from the Weibull distribution theory defining a continuous probability distribution¹¹⁶, however the equation itself, depending on the

parameters, can define curves of various forms. The most general expression of the Weibull distribution equation is shown below;

$$f(X) = \frac{\beta}{\eta} * \left(\frac{X - \gamma}{\eta}\right)^{\beta-1} * e^{-\left(\frac{X - \gamma}{\eta}\right)^\beta}$$

where β is the shape parameter (Weibull slope), η is the scale parameter and γ the location parameter.

In relation to dissolution profile parametrisation, this equation can be simplified, where the location parameter γ does not play a significant role (set to 0), the scale parameter η is re-named “B”, the shape parameter β is re-named “C”, and the part of the equation in front of the Euler number (e) can be merged into a single parameter “A”;

$$f(t) = A * e^{-\left(\frac{t}{B}\right)^C}$$

where t is the dissolution time and $f(t)$ the percentage of the drug dissolved at a certain time point.

In case of a dissolution profile, the value A defines the maximum value of the profile, so if the complete dissolution is reached, value A can be exchanged for 100 (%) in the equation.

By estimating the best fit for the parameters (A), B and C to available data acquired in *in vitro* dissolution experiments, an equation simulating the drug dissolution behaviour at any given time point can be generated. The best fit for the parameters can be determined using the *solver* function of the Excel program.

Thus, Excel software is the simplest *in silico* tool for *in vitro* dissolution parametrisation.

A much more complex and specialized program for *in vitro* dissolution parametrisation is the Simcyp™ In Vitro Data Analysis (SIVA) Toolkit. SIVA bases its parametrisation of the drug dissolution on a modified version of the Wang and Flanagan equation^{117,118}:

$$f(t) = -N * S * \frac{D_{eff} * 4\pi a(t) * (a(t) + h_{eff}(t)) * (S_{surface}(t) - c_{bulk}(t))}{h_{eff}(t)}$$

The dissolution rate ($f(t)$) is hereby defined by the number of drug particles N , the effective diffusion coefficient D_{eff} , effective diffusion layer thickness at time t $h_{eff}(t)$, a radius of an individual drug particle at time t $a(t)$, drug solubility at the particle surface and concentration of drug in bulk solution at time t $S_{surface}(t)$ and $c_{bulk}(t)$. An

empirical scalar S , commonly referred to as the “DLM scalar”, defines a set of (unknown) parameters which are not considered in the main equation but important for an accurate simulation of drug dissolution or, on other hand, compensates for differences resulting from using default values for parameters defined in the equation but not considered in the *in silico* model input.

This equation, together with the input of other physicochemical drug and formulation properties builds a basis of the diffusion layer model (DLM)¹¹⁸. When parameterising the drug dissolution using the DLM in SIVA, the DLM scalar must be estimated in order to fit the dissolution simulation to the *in vitro* dissolution data. In *in silico* PBPK models (see section PBPK models), the dissolution behaviour can be defined by the use of the DLM scalar value, so estimation of this parameter using SIVA is an important step in simulating drug plasma profiles *in silico*.

Regarding the *in vitro* data parametrisation, SIVA offers several pre-defined models, including solubility, one-stage, two-stage and transfer dissolution behaviour parametrisation. Precipitation in two-stage and transfer set-ups can be captured as well, by defining and estimating additional parameters such as critical supersaturation ratio (CSR, a ratio between the maximum permitted kinetic solubility and the intrinsic solubility) and the precipitation rate constant (PRC, a value defining the velocity of the precipitation)¹¹⁸. These parameters can be used as input in PBPK models as well.

1.6.2 Physiologically based pharmacokinetic (PBPK) models

While previously mentioned *in silico* tools focus on describing drug dissolution via equations, Physiologically Based Pharmacokinetic (PBPK) models aim to describe all the L-ADME processes in the human body via a set of equations in order to simulate drug plasma profiles¹.

A palette of commercial softwares for developing PBPK models is available¹¹⁹. Softwares like Stella Architect or Matlab offer the ability for the user to develop a complete mathematical interface from scratch and modify it as desired, while softwares like Simcyp™ Simulator or GastroPlus offer a pre-designed interface describing the ADME parameters via ready-to-use calculation models. Stella and

¹ When a PBPK program calculates the drug plasma value over time, it follows a set of equations simulating every step of the L-ADME process. In theory, such calculations generate a single, long equation encompassing all the processes defined for the human body by the program. Like the Master equation; „equation of everything“, which combines the theory of strong and weak universal forces and quantum mechanics in order to describe the universe, PBPK models describe the microcosmos of the human body - only a droplet in the waterfall of the universe – however, for the egocentric Human, likely the most important droplet!

similar softwares have the advantage of allowing the user to define processes and approaches, which can be important for novel formulations. The disadvantage of such softwares is that they are *ab definitio* not standardized, nor are they broadly used in the pharmaceutical industry. On the other hand, softwares with pre-defined algorithms have invested in creating a standardized and validated set of models and data compilations, thus assuring a reproducible interface and building a path to becoming a standard tool accepted by regulatory bodies.

In the next sub-section, the Simcyp™ Simulator is described in more detail, as it is the main *in silico* tool used in the research described in this thesis.

1.6.2.1 Simcyp™ Simulator

The model set-up of the Simcyp™ Simulator is based on the compartmental interpretation of the human body. Advanced Dissolution, Absorption, Metabolism Model (ADAM) defines the human GI tract as a tube divided into a gastric, a duodenal, two jejunal, four ileal and one colonic segment, each with various characteristic parameters¹¹⁹. For each compartment, the absorption, metabolism and degradation input is processed and the calculated amount absorbed is directed further into drug distribution and elimination models.

An advantage of the Simcyp™ Simulator is that the pre-programmed model can assess both the administration of a drug in a single representative of a population (PopRep), as well as in a group of subjects, all with slightly different physiology. In the latter case, the software aims to simulate the variability on the pharmacokinetic response of a population likely to be observed in clinical studies. Furthermore, the Simcyp™ Simulator includes data compilations on different populations, such as the geriatric or infant population and populations of different ethnicities.

1.6.2.1.1 Dissolution rate model (DRM) and diffusion layer model (DLM)

Within the ADAM model, an important input parameter is the drug dissolution, as it dictates the amount of the drug available for absorption in each GI segment. The input of the dissolution data can be done using two approaches – the dissolution rate model (DRM) and the diffusion layer model (DLM)¹²⁰. When using DRM, the % of the drug dissolved over time, acquired from *in vitro* experiments, can be entered directly into the absorption part of the model. This approach is fast and often gives a good approximation for an individual subject having all physiological parameters equal to the average values of the population (PopRep) and for a dose of the drug equal to the

one tested *in vitro*. This approach, however, is not suitable for simulating administration of a dose higher or lower than the one tested *in vitro* and cannot be used to simulate full populations. The reason is that applying the absolute value for the % of the drug dose dissolved at a certain time point into the system forces the program to always use this value, even if the dose strength or physiology of the subject changes, either of which in turn would influence the drug dissolution.

A more mechanistic approach to dissolution data input is the diffusion layer model (DLM), explained in the section “*In silico* tools for *in vitro* dissolution parametrisation”. The input of DLM dissolution parameters allows for a characterisation of the drug dissolution independent of the dose or condition used in *in vitro* tests. Thus, using the DLM approach, exploration of different dosing regimens and populations is possible.

1.6.2.1.2 Minimal and Full PBPK model

Under the drug distribution interface, the Simcyp™ Simulator offers two options for drug distribution modelling, either a minimal PBPK model or a full PBPK model. The full PBPK model differentiates between multiple organs, tissues, venous and arterial blood as individual compartments, in which the drug can be distributed, whereas in a minimal PBPK model, the software defines only three main compartments, one of which is a generalized group of organs, the “Systemic Compartment”¹²⁰. Furthermore, to reflect a two-compartmental distribution model, the minimal PBPK model allows for an additional “Single Adjusting Compartment”.

2 Structure of the thesis and thesis goals

The thesis follows a publication-based approach and was based on four peer-reviewed publications. Although each publication can stand as an independent unit (see Appendix), in this thesis the published results and conclusions are combined and discussed together in order to present the integrated scientific contribution of the doctoral project.

The overall goal of the project was to develop biorelevant dissolution media and tools reflecting GI physiology under conditions of elevated gastric pH induced by ARAs. Several steps were set to achieve this goal, and are listed below:

The first step was to identify physiological changes in the human GI tract during ARA administration and to design *in vitro* media reflecting these changes.

Following a review of physiological parameters that affect drug release and absorption from the GI tract, a thorough literature review of changes in these parameters after ARA administration was conducted. A head-to-head comparison of parameters between healthy volunteers and those during ARA therapy was used to identify biopharmaceutically relevant physiological changes and guided all decisions when designing *in vitro* media reflecting gastric physiology during ARA therapy. A review of the changes in GI physiology during ARA therapy, along with media to reflect the compositional changes was published in Publication 1.

The second step was to design *in vitro* tests implementing developed ARA media.

Commonly used one-stage dissolution tests were the first to be conducted with ARA media in Publication 2, using a weakly basic drug in development at AstraZeneca, designated "PSWB 001". Two-stage dissolution test and transfer experiment settings reflecting ARA co-administration were developed and tested in Publication 3 using dipyridamole as the case example. In Publication 3, the concept of the ARA media was also explored using an evolved *in vitro* model, TIM-1. Extension of application of these *in vitro* tests to weak acids is the focus of Publication 4, where potassium raltegravir was studied. In every case, the drug dissolution was compared with the dissolution under standard *in vitro* conditions (without ARA co-administration).

In the third step, the compatibility of the *in vitro* tools (reflecting ARA co-administration) with various *in silico* models was evaluated (Publications 2-4).

To evaluate the compatibility of the *in vitro* tools with *in silico* models, *in silico* models of increasing complexity were implemented. First, a minimal PBPK model environment in Simcyp™, using a simple dissolution rate model as data input was investigated. Then, a full PBPK Simcyp™ model was evaluated using input via the diffusion layer model. In this case, parameters were acquired using SIVA. Furthermore, in the context of this thesis different options under the diffusion layer model (static vs. dynamic intestinal pH model) and a variation of the dissolution rate model input for modified-release tablets were also explored.

A minimal PBPK model was explored in Publication 2. Publication 3 focused on the full PBPK model and DLM with static or dynamic intestinal pH model, while a more complex, mathematical approach to DRM data input into a full PBPK model was the focus of Publication 4.

In the fourth step, the ability of the developed methods to predict the effect of ARAs on drug co-administration was assessed.

The *in silico* predictions, acquired in the third step, were compared with the available *in vivo* data for the drug administration without and during ARA therapy. The ability to predict pH-dependent DDIs was evaluated using drugs and formulations with diverse properties. The first drug, PSWB 001, was a poorly soluble weakly basic compound, formulated as an IR capsule and showed no precipitation after a pH shift. The second drug was dipyridamole, a poorly soluble weakly basic compound with a known precipitation behaviour *in vitro*. The explored formulation was an IR tablet. The third compound was raltegravir, a poorly soluble weakly acidic compound, formulated as a slowly eroding tablet.

Prediction of plasma profiles for PSWB 001 was reported in Publication 2. Evaluation of the impact of ARAs on dipyridamole absorption was published in Publication 3, whereas pH-dependent DDIs with raltegravir were the focus of Publication 4.

3 Results and Discussion

3.1 Impact of ARA administration on GI physiology and the design of *in vitro* media reflecting these changes

3.1.1 Impact of ARAs on GI physiology

Due to significant differences in the acid-reducing mechanism, the impact of the main three groups of ARAs on the GI physiology was assessed for each group individually. The analysis focused on changes in the GI pH and buffer capacity, volume, and motility, as well as additional components of the fluids and the microflora.

3.1.1.1 Antacids

After ingestion, antacids neutralize gastric acid rapidly and elevation of the pH occurs in as few as 6 minutes¹²¹. Unsurprisingly, liquid antacids raise the gastric pH faster than solid formulations, such as chewable tablets¹²². Although the extent of the pH elevation in the fasted state depends on the dose of the administered antacid, the gastric pH *in vivo* was shown to rise on average to pH 3.5 - 5 and higher^{123,124}. Due to gastric emptying of the antacid, as well as re-acidification of the gastric compartment by acid secretion, the antacid pH effect has a short duration of on average 30 – 60 minutes before returning to a low, acidic pH value^{122,123,125,126}. Interestingly, antacids show an ability to adsorb bile acids^{127–129} and pepsin^{129–132} onto the surface of their undissolved matrix. Thus, in addition to bringing metal ions into the gastric medium, antacids may alter the concentration of bile components and pepsin in the gastric fluids.

Little research has been conducted on the impact of antacids on intestinal physiology. In the small intestine, antacids likely do not affect the average pH of the intestinal fluids, however in the duodenum bulb, the part of the duodenum closest to the stomach, a carry-over effect of the raised gastric pH can be observed¹³³. Antacids appear to have a significant impact on intestinal motility and volume. While aluminium-based antacids show an adstringent effect, possibly lowering the intestinal volume, magnesium-based antacids elevate the osmotic pressure in the intestinal lumen, thus drawing more fluid into the intestine and raising the intestinal volume. Furthermore - or perhaps because of - the osmotic effect, a high concentration of magnesium ions has a laxative effect and may shorten the intestinal residence time. By contrast, a high concentration of aluminium ions may cause constipation, since aluminium ions induce

relaxation of the intestinal smooth muscles¹³⁴. In some antacid products, magnesium and aluminium salts are combined, presumably to balance out the effects on intestinal motility

3.1.1.2 H2RAs

H2RAs show a longer lag time (60-90 min) before the onset of the pH effect^{121,125} compared to antacids. The H2RAs also show a significantly longer duration of the pH effect, lasting for at least 7 h¹³⁵. Like the antacids, the H2RA pH effect is dose-dependent, with an average rise in gastric pH to values between pH 4 and 6¹³⁶⁻¹³⁸. The buffer capacity of a gastric medium sample, acquired via aspiration after administration of an H2RA, was 6.3 – 12.4 mEq/L/ Δ pH^{139,140}. Since H2RAs inhibit the histamine signalling pathway, which is responsible for gastric secretion, some researchers have reported lower gastric volume *in vivo* after administration of H2RAs^{136,141}. An effect on the activity of pepsin in the gastric medium after H2RA administration is expected if the pH of the medium shifts to above pH 5, as at that point the pepsin is no longer active. In contrast to antacids, the gastric pH after H2RA administration stays elevated over a longer period of time, rendering the impact on pepsin activity more relevant. The elevated pH over a longer period also facilitates the survival of microorganisms. Thus, several studies have linked intragastric bacterial proliferation to chronic H2RA use³³.

With regard to the impact of H2RAs on intestinal physiology, only a decrease in microbial diversity and an increased risk of *Clostridium difficile* infection could be linked to H2RA administration¹⁴²⁻¹⁴⁶. This is likely a consequence of the intragastric proliferation and trespassing of non-intestinal bacterial species into the small intestine.

3.1.1.3 PPIs

The largest body of research on the impact of ARAs on GI physiology has been reported for PPIs. PPIs are the most potent inhibitors of gastric acid. Due to the mechanism of action, PPIs influence the gastric media composition only via the inhibition of the acid secretion^{33,147}. Thus it is reasonable to assume that changes in GI physiology during PPI administration are similar to those resulting from hypo- and achlorhydria.

An extensive review by Kirchheiner et al. reported that PPI therapy elevates the gastric pH to an average value of pH 3 after a single dose, and to values generally between pH 4 and 6 after daily administration¹⁴⁸. Indeed, for a PPI to reach its full acid-reducing

effect, it has to be administered for 3 to 5 days. Up to 70 % of the active proton pumps are inhibited by one dose and the inhibition is irreversible¹⁴⁹. Thus, in contrast to antacids and H2RAs, the pH effect of PPIs has a longer duration. Of course, new proton pumps are continuously generated, so subsequent doses are needed to inhibit both the remaining proton pumps and the new ones being produced.

Due to the inhibition of gastric secretion, PPIs lower the gastric volume^{150,151}. Similar to H2RAs, PPIs consistently raise the gastric pH to values above pH 5 and thus pepsinogen is not activated. Furthermore, the buffer capacity of an aspirated gastric sample during PPI therapy was 0.7 – 1.3 mEq/L/ Δ pH¹³⁹.

The surface tension of the gastric fluids after PPI treatment was found to be lower than with no PPI therapy^{7,139}, suggesting a higher concentration of bile components in the gastric medium after PPI administration. This effect may be due to a smaller gastric volume combined with the same reflux of bile components from the small intestine. An alternative hypothesis is that weaker contractile power of the pylorus after PPI administration enables more bile component reflux from the duodenum into the stomach¹³⁹. There have also been several reports of delayed gastric emptying during PPI therapy, but due to differences in experimental methods, it is not possible to draw a firm conclusion about the effect of PPIs on gastric motility and emptying^{152–154}.

In the intestine, slight changes in the distal small intestinal pH observed during PPI therapy may be due to a change in the microbiome of the small intestine. As with H2RAs, PPIs have also been linked to changes in the microbiome, reporting a rise in the bacterial count, occurrence of new species in different gut segments, and/or a decrease in the bacterial diversity^{155–163}.

3.1.2 Design of *in vitro* media reflecting ARA co-administration

Based on the literature review (Publication 1), it is safe to say that the ARAs influence gastric physiology significantly, whereas the impact on intestinal physiology is either not significant or not pharmaceutically relevant. It is also worth noting that the gastric fluid composition after antacid administration differs significantly from the composition after the administration of other ARAs. These differences are tied to the mechanism of action: whereas the H2RAs exert their effect systemically via a decrease in gastric acid secretion, the antacids exert a local, physical effect on the gastric pH.

A medium reflecting the *in vivo* gastric physiology after the administration of an antacid should therefore incorporate metal ions originating from the chosen antacid, in order to simulate possible interactions, e.g. in case the drug builds a complex with polyvalent cations. As each antacid type has a different composition and amount of the acid-neutralizing substance(s), the optimal medium should incorporate marketed antacids into its composition, rather than be designed “from scratch” to reflect an antacid administration. Furthermore, due to the short-lived effect of antacids on the pH in the stomach, a dissolution medium with an elevated pH alone is not sufficient to predict the overall impact of antacid co-administration. Rather, a medium with a dynamic pH, simulated by an *in vitro* set-up re-acidifying the gastric medium (like the ASD model or GastroDuo), is necessary.

By contrast, the other two ARA groups, H2RAs and PPIs, seem to have a comparable effect on gastric physiology. A weak effect of an ARA, e.g. a lower dose of ARA or PPI co-administration at the beginning of the therapy, would best be reflected by a medium with pH 4. A strong effect of an ARA, e.g. after a high H2RA dose or during PPI therapy, might be better reflected by a gastric medium with pH 6. Thus, a set of biorelevant media was developed to assess the impact on the dissolution behaviour of drug product in the stomach when they are co-administered with H2RAs and PPIs of different potencies and at different doses.

To design media reflecting H2RA and PPI administration (henceforth referred to as “ARA media”), an existing biorelevant medium, FaSSGF, was modified to reflect the identified physiological changes (Table 1). While the concentration of bile components was not changed, the buffer capacity and osmolality of the ARA media were adjusted according to the physiological changes observed. For example, the ARA pH 4 medium uses an acetate buffer at pH 4 with the buffer capacity of 7.5 mEq/l/ Δ pH, to reflect the buffer capacity of the gastric fluids after a dose of H2RA, while the ARA pH 6 medium uses a maleate buffer at pH 6, with a buffer capacity of just 1 mEq/l/ Δ pH, accounting for the almost complete inhibition of gastric acid secretion by a potent or highly dosed PPI. Since pepsin activity is completely inhibited above pH 5, pepsin was removed from the composition of the ARA pH 6 medium.

In addition to these two ARA media, back-up media were developed to offer alternative buffer systems at the same two pH values, in case of an interaction between the drug

being studied and the buffer species in the ARA medium occurs. The buffers used for these alternative compositions were citrate buffer and Mcllvaine buffer (phosphate/citrate buffer). All other parameters in the media were held the same. The composition of all the ARA media can be found in Table 1.

Table 1. Overview of ARA media, including a comparison to the standard gastric biorelevant medium, FaSSGF

| Component/Parameter | FaSSGF ³ ₆ | ARA pH 4 acetate | ARA pH 6 maleate | ARA pH 4 citrate | ARA pH 6 citrate | ARA pH 4 Mcllvaine | ARA pH 6 Mcllvaine |
|----------------------------|----------------------------------|------------------|------------------|------------------|------------------|--------------------|--------------------|
| Pepsin (mg/mL) | 0.1 | 0.1 | / | 0.1 | / | 0.1 | / |
| Sodium taurocholate (mM) | 0.08 | 0.08 | 0.08 | 0.08 | 0.08 | 0.08 | 0.08 |
| Phosphatidylcholine (mM) | 0.02 | 0.02 | 0.02 | 0.02 | 0.02 | 0.02 | 0.02 |
| Sodium chloride (mM) | 34.2 | - | 22.7 | 7.7 | 22.8 | 17.5 | 21.2 |
| Sodium acetate (mM) | - | 33.3 | - | - | - | - | - |
| Maleic acid (mM) | - | - | 2.31 | - | - | - | - |
| Tri-Sodium citrate (mM) | - | - | - | 11.2 | 1.5 | - | - |
| Citric acid (mM) | - | - | - | - | - | 9.00 | 0.86 |
| Di-Sodium phosphate (mM) | - | - | - | - | - | 11.29 | 2.94 |
| pH | 1.6 | 4 | 6 | 4 | 6 | 4 | 6 |
| Buffer capacity (mEq/pH/L) | / | 7.5 | 1 | 7.5 | 1 | 7.5 | 1 |
| Osmolality (mOsmol/kg) | 121 | 91 | 50 | 75 | 50 | 75 | 50 |
| Surface tension (mN/m) | 42.6 | 64.49 | 67.21 | 63.32 | 67.86 | 63.20 | 67.58 |

3.2 Implementation of the ARA media in *in vitro* dissolution models

In order to test the behaviour of drugs in *in vitro* set-ups reflecting the ARA co-administration, three model drugs with different physicochemical properties were used:

The first model drug, PSWB 001, is a poorly soluble, weakly basic small molecule (<

500 g/mol) with pKa values of 3.5 and 5.8. In clinical trials it showed a pronounced drug-drug interaction with PPIs. The formulation studied was an immediate release (IR) gelatine capsule. Dipyridamole, the second model drug, is a poorly soluble weak base with a pKa of 6.2, a well-established clinical DDI with ARAs and a tendency to precipitate from a supersaturated solution *in vitro*. Dipyridamole was available as a 100 mg IR tablet. Raltegravir, the third model drug, is a poorly soluble weak acid with a pKa of 6.3 and is available as the potassium salt in erodible tablets (raltegravir 400 mg). Extensive descriptions of the methodologies used for dissolution experiments and quantitative analysis of the model drugs can be found in their respective publications (Appendix).

3.2.1 One-stage testing

To reflect the ARA co-administration in a one-stage set-up, apparatus parameters as well as the media choices had to be defined. Neither gastric volume nor motility are influenced by the H2RAs and PPIs to such extent, that they would significantly impact the drug behaviour. When simulating dissolution of an oral formulation *in vitro*, the gastric dissolution volume was thus set to 250 ml and stirring speed set to 50 or 75 rpm. This set-up also ensured good comparability between the standard one-stage dissolution set-up reflecting usual gastric conditions in healthy subjects and the set-up reflecting ARA co-administration.

3.2.1.1 Case example PSWB 001

One-stage dissolution of PSWB 001 capsules was explored in the standard FaSSGF medium (reflecting the gastric medium in the absence of ARAs therapy) as well as in the ARA pH 4 and pH 6 media and deionised water (Figure 5). PSWB 001 showed rapid and complete dissolution in the biorelevant medium at low pH (FaSSGF pH 1.6), whereas in pure deionised water, in which the starting pH was 5.6 and the final pH was 6.3, the dissolution was slower and less complete. In the ARA media representing a lesser ARA effect (pH 4), 20 % less drug was dissolved on average compared to the dissolution in FaSSGF, whereas dissolution of PSWB 001 in the ARA media representing a strong ARA effect (pH 6) was limited to 20 % of the drug dose. The results in deionised water, which is recommended by the Japanese Pharmacopeia as a medium representing an achlorhydric stomach¹⁶⁴, were in this case comparable to the dissolution in ARA pH 6 media.

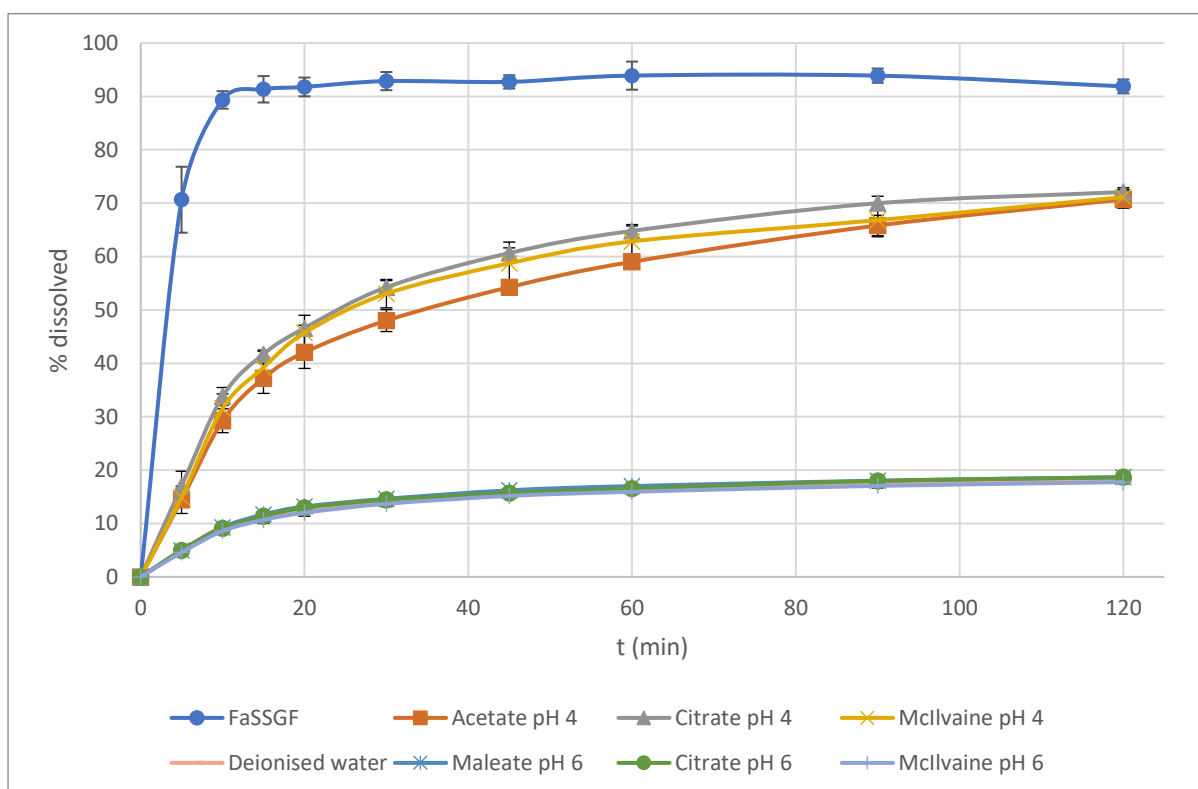


Figure 5. One-stage dissolution of PSWB 001 capsules in FaSSGF pH 1.6, ARA pH 4 and pH 6 media and deionised water. The results in deionized water are obscured by the results in ARA pH 6 media on this graph.

Reproduced with permission from a publication in Eu.J.Pharm.Sci. by Segregur et al.¹⁶⁵

3.2.1.2 Case example dipyridamole

Similar to PSWB 001, the dissolution of dipyridamole in FaSSGF was rapid and complete, whereas in ARA media dipyridamole showed slower and more limited dissolution. While the final percentage dissolved in ARA pH 4 media was approximately 20 % less than in FaSSGF, dissolution in media representing a strong ARA effect (ARA pH 6 media) was limited to only 2.5 % dissolved after two hours of dissolution.

One-stage dissolution of dipyridamole in 500 ml of the standard biorelevant intestinal media, FaSSIF V1 and FaSSIF V2 (pH 6.5), reached approximately 15 % dissolved after two hours of dissolution, which is significantly higher than during dissolution in

ARA pH 6 media. This is not only due to a two times higher volume of the medium, but also due to a higher concentration of bile components in the intestinal biorelevant medium, which elevates the solubility of dipyridamole.

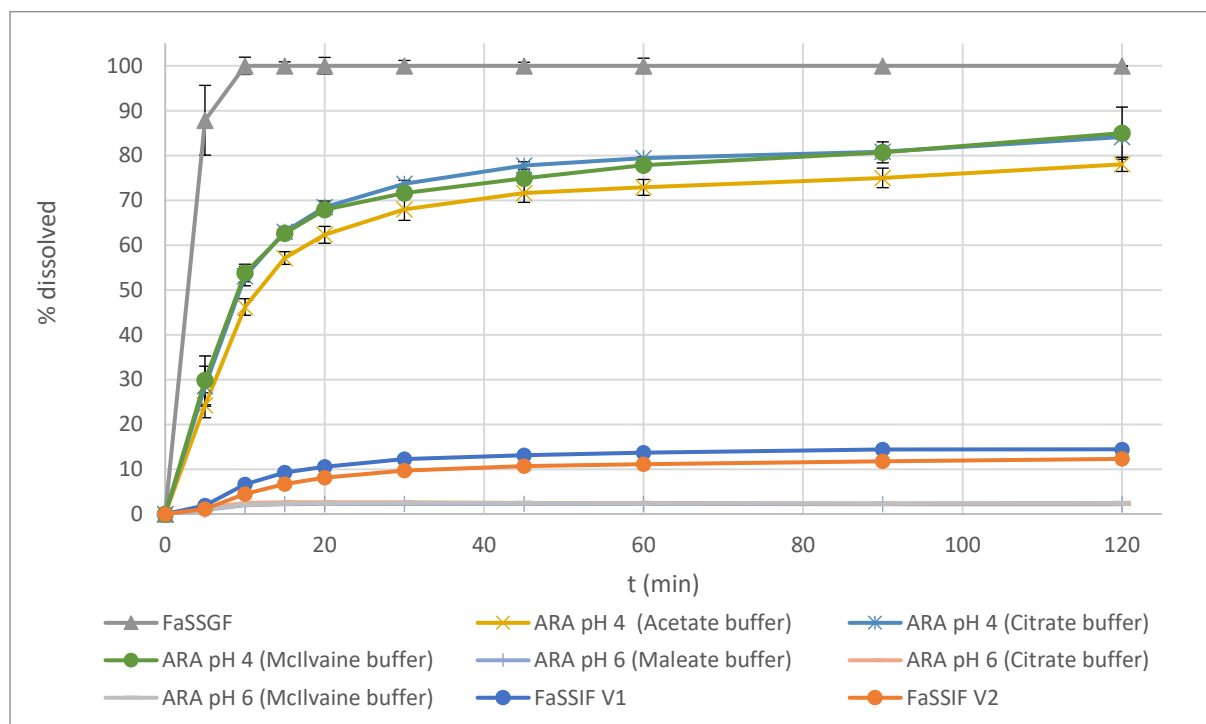


Figure 6. One-stage dissolution of dipyridamole tablets in FaSSGF pH 1.6, ARA pH 4 and pH 6, as well as FaSSIF V1 and V2 pH 6.5 (dissolution profiles in the ARA pH 6 media overlap and reach only 2.5 % dissolution after two hours)

Adapted from a publication in Eu.J.Pharm.Sci. by Segregur et al.¹⁶⁶

3.2.1.3 Case example raltegravir potassium

One-stage dissolution of raltegravir potassium is characterized by several essential differences from the other two model drugs. While the other two drugs are weak bases, raltegravir potassium is the salt of a weak acid. As an acid, raltegravir is expected to dissolve more readily in less acidic media. In addition, raltegravir potassium is formulated as an erodible tablet, whereas the other two model drugs are formulated as immediate-release formulations. Thus, the third case example, raltegravir potassium, rounds out the research on the assessment of drug behaviour in a one-stage dissolution set-up under elevated gastric pH conditions.

As raltegravir potassium was formulated in such a way that the drug is released slowly¹⁶⁷, the duration of one-stage dissolution experiments was extended from the usual 2 hours of dissolution to 7 hours.

In the standard gastric biorelevant medium, FaSSGF pH 1.6, the dissolution was slow and reached 15 % after two hours of dissolution. This concentration is, however, already significantly higher than raltegravir solubility at pH 1.6, as the salt of raltegravir dissolves more readily than the free acid form of the drug, thus generating a supersaturated solution. After reaching 20 % dissolved at 4 hours, raltegravir started to slowly precipitate from its supersaturated state.

In the ARA media, raltegravir dissolved to a greater extent. In ARA pH 4 medium, it reached 40 % dissolved in the first one hour and then started precipitating, whereas in ARA pH 6 medium the salt formulation was able to shift the pH of the medium to 7.69, enabling complete dissolution of the tablet within the first two hours. These results confirm the importance of considering a physiological buffer capacity when designing biorelevant medium. In ARA media, a high dose of the drug or large amounts of pH-active excipients in the formulation may have an impact on the overall pH of the medium. By contrast, if the buffer capacity selected is inappropriately high (which is the case when compendial media are used to represent elevated pH in the stomach), the drug / excipients will no longer be able to influence the pH of the medium and the dissolution behaviour may be quite different. In this scenario, the impact of the medicine on the surrounding medium will be overlooked. On the other hand, using a medium with negligible buffer capacity, like purified water, however, may impact the interlaboratory repeatability, and is thus also not desirable.

Raltegravir potassium dissolution in the intestinal media FaSSIF V1 and FaSSIF V2 is slow, which is expected for an erodible formulation, and complete, which is also expected for a weakly acidic compound.

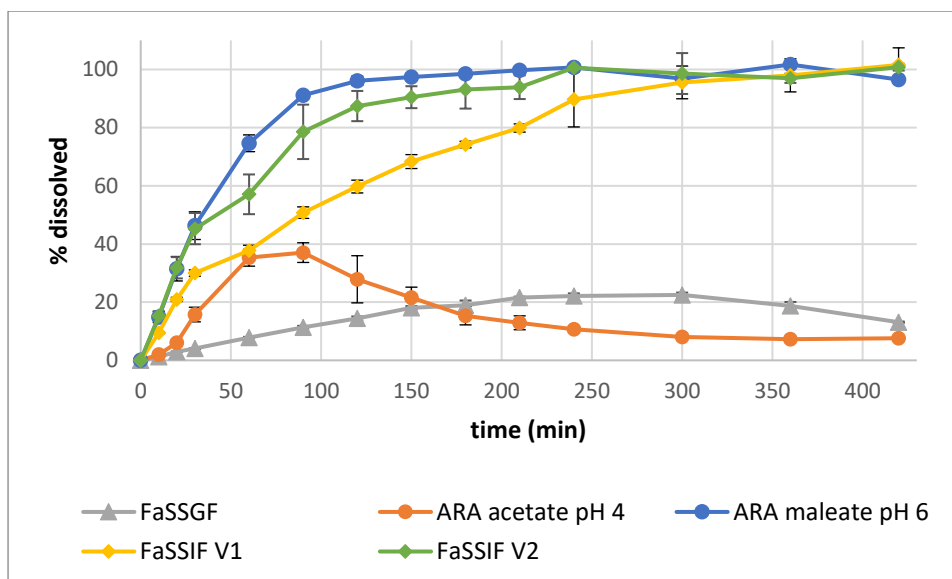


Figure 7. One-stage dissolution of raltegravir potassium erodible tablets in FaSSGF pH 1.6, ARA pH 4 and pH 6, as well as FaSSIF V1 and V2 pH 6.5.

Adapted from a publication in J.Pharm.Sci. by Segregur et al.¹⁶⁸

3.2.2 Two-stage dissolution

The dissolution set-up in the first stage of the two-stage experiment is comparable to the dissolution set-up of the one-stage test with a gastric medium. In the second stage, however, a double concentrate of the intestinal medium is added, with the intention to shift the composition and properties of the mixture to those of the intestinal biorelevant medium. A standard two-stage dissolution set-up involves FaSSGF pH 1.6 and a double concentrate of FaSSIF V1 with a pH of 7.5. Such a concept has been extended in the context of this research to the use of the FaSSIF V2 as well. Furthermore, in order to implement ARA media in two-stage set-ups, separate FaSSIF double concentrates had to be adjusted to take the properties of the ARA into consideration. An overview of the standard and developed two-stage set-ups can be seen in Table 2.

Table 2. An overview of the double concentrate intestinal media used in two-stage experiments

| Gastric medium | FaSSGF pH 1.6 / pH 2* | | ARA pH 4 acetate | | ARA pH 6 maleate | |
|--|--------------------------|-----------|------------------|-----------|------------------|-----------|
| Intestinal 2xc medium | FaSSIF V1 ¹⁰² | FaSSIF V2 | FaSSIF V1 | FaSSIF V2 | FaSSIF V1 | FaSSIF V2 |
| Sodium taurocholate (mM) | 6 | 6 | 6 | 6 | 6 | 6 |
| Phosphatidylcholine (mM) | 1.5 | 0.4 | 1.5 | 0.4 | 1.5 | 0.4 |
| Sodium chloride (mM) | 221.7 | 137.2 | 221.7 | 137.2 | 221.7 | 137.2 |
| Potassium dihydrogen phosphate (mM) | 57.4 | - | 57.4 | - | 57.4 | - |
| Maleic acid (mM) | - | 38.2 | - | 38.2 | - | 38.2 |
| pH | 7.5 | 10.8 | 7.4 | 12.13 | 6.43 | 6.46 |

*In the case of two-stage experiments with FaSSIF V1 2xc, FaSSGF pH 1.6 is used, whereas for experiments with FaSSIF V2 2xc, FaSSGF pH 2 must be used to avoid an extreme pH in the double concentrate.

3.2.2.1 Case example PSWB 001

Two-stage testing with PSWB 001 was initially conducted using low pH gastric media and the two FaSSIF versions. These experiments showed that after the shift into the second stage, the fully dissolved drug stayed supersaturated in the intestinal medium for the duration of the experiment and no precipitation was observed. This led to the assumption that no precipitation would occur during a pH shift from the ARA media with elevated gastric pH into either intestinal medium due to the lower supersaturation ratio.

It was also concluded that, in the case of the weakly basic drug which does not show precipitation during a two-stage test with a low pH gastric medium, the one-stage dissolution set-up with ARA media is sufficient to assess the drug behaviour under ARA therapy.

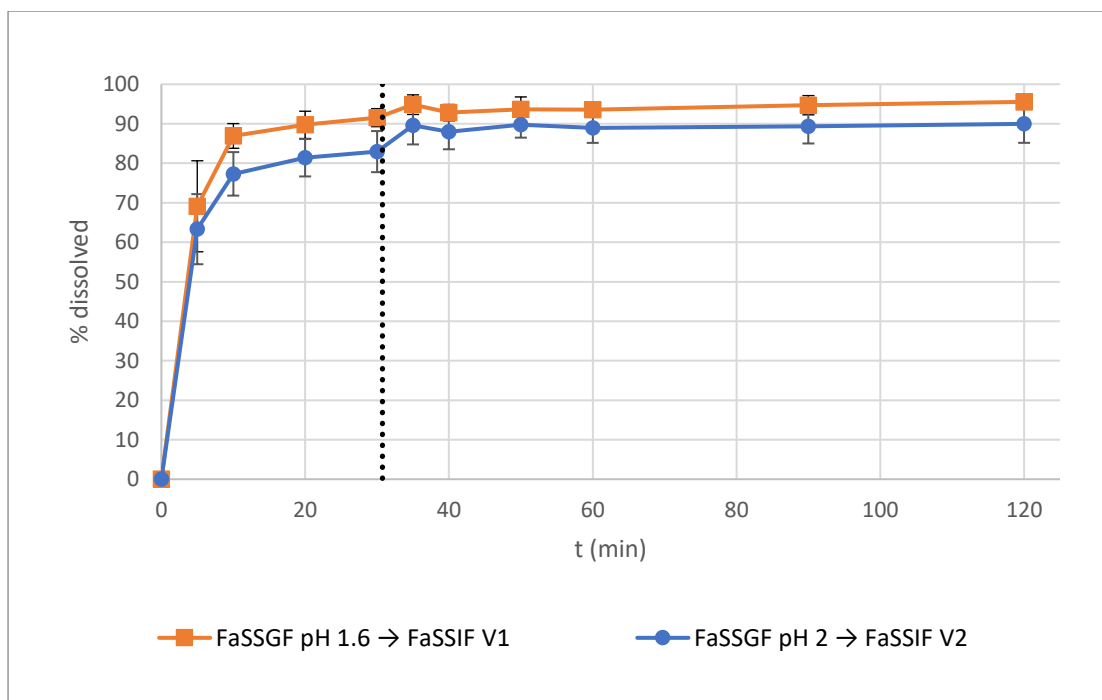


Figure 8. Two-stage dissolution of PSWB 001 using FaSSGF pH 1.6 or pH 2 and FaSSIF V1 or V2 double concentrate.

Adapted from a publication in Eu.J.Pharm.Sci. by Segregur et al.¹⁶⁵

3.2.2.2 Case example dipyridamole

Two-stage experiments with dipyridamole were conducted with FaSSGF, ARA pH 4 and ARA pH 6 media in the first stage, using FaSSIF V2 double concentrates to switch to the second stage of the experiment. Fast precipitation was observed immediately after the pH shift in experiments with the acidic gastric media (FaSSGF pH 2 and ARA pH 4), whereas for the two-stage experiment with ARA pH 6, the dissolution in the first stage did not achieve a concentration which would lead to supersaturation in the second state and therefore no precipitation could occur.

Although dipyridamole showed precipitation in two-stage experiments, little to no precipitation is reported for the compound *in vivo*¹⁶⁹. Thus, it was concluded that the two-stage set-up overestimates the precipitation of dipyridamole. This is partly due to the sudden shift into the intestinal medium, which reflects Phase 3 gastric emptying rather than the statistically more often observed Phase 1 or Phase 2 gastric emptying.

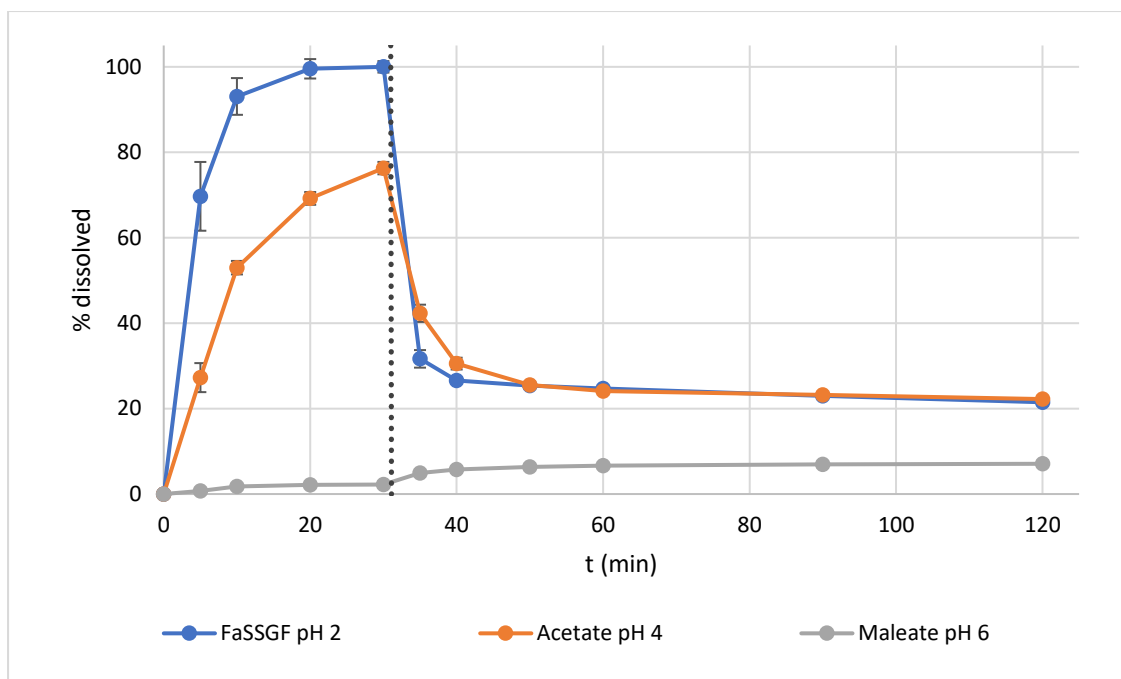


Figure 9. Two-stage dissolution of dipyrindamole in FaSSGF pH 2, ARA pH 4 or ARA pH 6 and the respective FaSSIF V2 double concentrate.

Adapted from a publication in Eu.J.Pharm.Sci. by Segregur et al.¹⁶⁶

3.2.2.3 Case example raltegravir potassium

The erodible tablet of raltegravir potassium disintegrates only slowly and behaves in the gastric compartment like a monolithic formulation. Thus, it will usually be emptied from the stomach with the housekeeper wave i.e. Phase 3 of the gastric motility pattern. Two-stage testing simulates an abrupt switch to the intestinal medium, likely reflecting the housekeeper wave *in vitro* most accurately. Due to the variability in the intake of a monolithic tablet in relation to the timing of the next housekeeper wave, different pH-shift times in the two-stage test, reflecting this variability, were explored. Two-stage tests with raltegravir potassium tablets were conducted using ARA pH 4 and pH 6 media in the first stage and FaSSIF V1 double concentrates to switch to the second stage of the experiment.

Figure 10 shows the dissolution behaviour in two-stage experiments with ARA media and pH-shift times of 30, 60 and 120 minutes. In experiments with the ARA pH 4 medium, it was found that the precipitation in the first stage has an impact on the amount of the drug dissolved in the second stage. In experiments with the ARA pH 6

medium, the increase in the pH of the gastric medium in the first stage (due to the influence of the formulation) resulted in the drug reaching complete dissolution earlier.

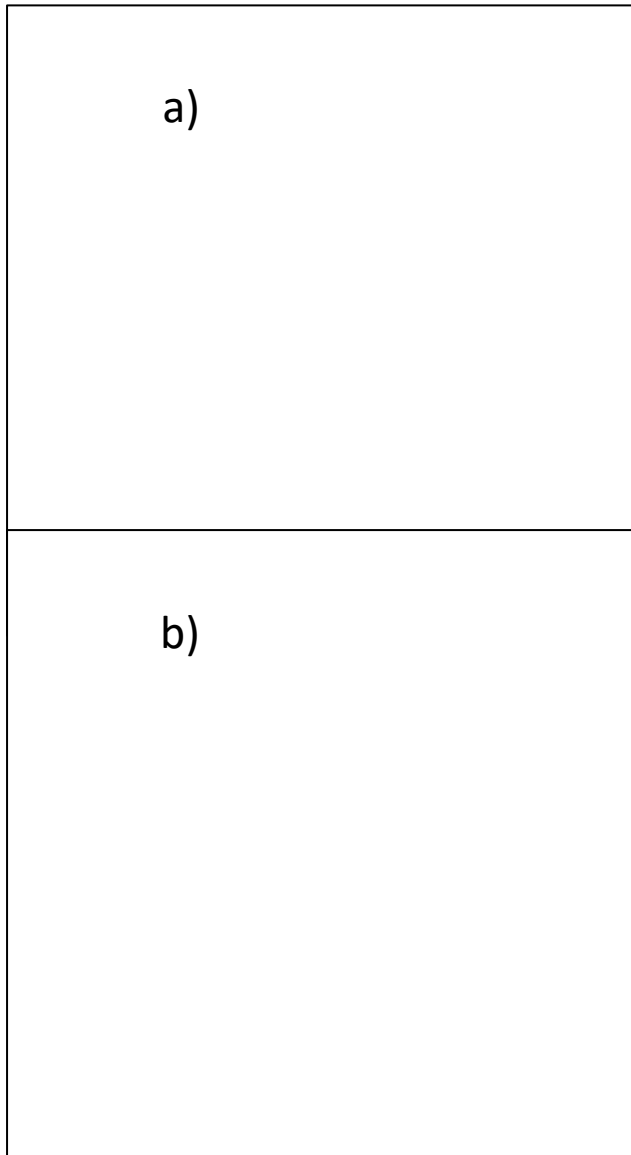


Figure 10. Two-stage dissolution of raltegravir potassium tablets using a) ARA pH 4 and b) ARA pH 6 media and a respective FaSSIF V1 double concentrate, with pH shift times of 0.5, 1 and 2 h.

Adapted from a publication in J.Pharm.Sci. by Segregur et al.¹⁶⁸

3.2.3 Transfer experiments

Transfer experiments were conducted using dipyridamole as the model drug. The transfer set-up consisted of FaSSGF, ARA pH 4 medium or ARA pH 6 medium in the gastric compartment and the respective FaSSIF V2 double concentrate in the intestinal compartment. The use of the double concentrate of the intestinal medium allowed for a direct comparison between the two-stage and transfer model set-up with respect to the influence of the transfer rate from the gastric into the intestinal medium. In contrast to the two-stage model, the transfer model introduces the dissolved drug to the intestinal surroundings more gradually. This is reflected in the slower precipitation of the drug in the intestinal compartment of the transfer model experiments (Figure 11). Thus, the transfer model simulates the average gastric emptying process more accurately, enabling a more accurate simulation of the drug precipitation *in vitro*. Nevertheless, the transfer model still overestimated the *in vivo* dipyridamole precipitation, as a substantial amount of the drug precipitated in the experiment. This is likely due to the absence of an absorptive compartment in the transfer model set-up, which would hinder the precipitation of the drug in the intestine via creation of an absorptive sink. Thus, for drugs with high permeability, precipitation behaviour achieved *in vitro* should be implemented with caution and the use of simple one-stage dissolution, assuming no precipitation, should be considered as an alternative approach.

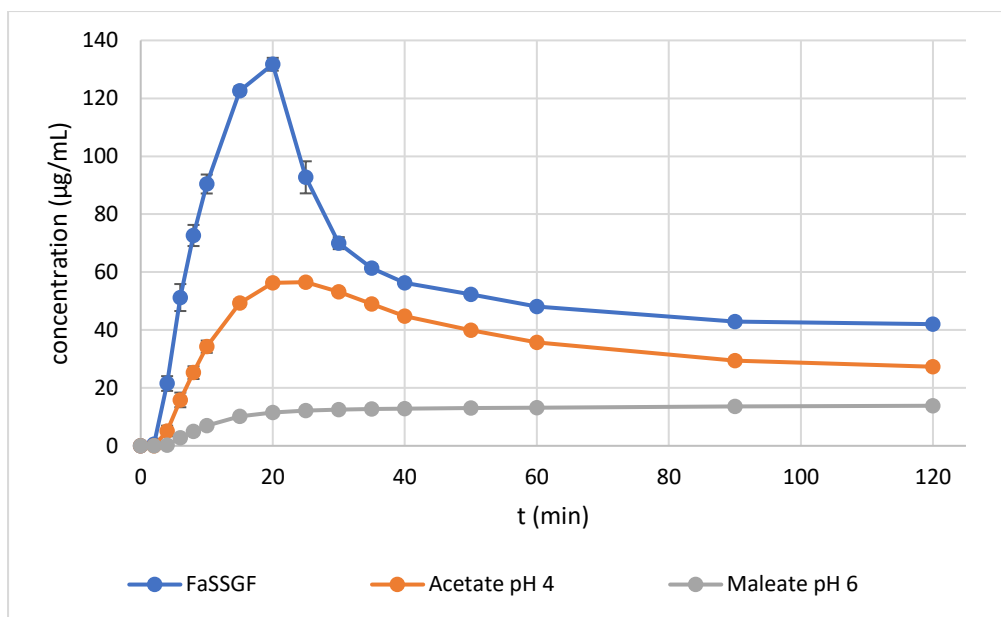


Figure 11. Dissolution of dipyrindamole in transfer experiments using FaSSGF pH 2, ARA pH 4 or ARA pH 6 medium in the gastric compartment and the respective FaSSIF V2 double concentrate in the intestinal compartment.

Adapted from a publication in Eu.J.Pharm.Sci. by Segregur et al.¹⁶⁶

3.2.4 TIM-1 model

The concept of the ARA media was explored using dipyrindamole in the TIM-1 model as well. Here, the adjustment of the pH of the gastric compartment to pH 4 or pH 6 served to assess the effect of ARAs on the percentage of the drug dose available for absorption. The final (after 5 hours) percentage of the dose available for absorption using a gastric pH of 4 was 20 % lower compared to an experiment with a gastric pH 2. The experiment with gastric pH 6 predicted 30 % of the drug dose to be available for absorption after 5 hours of the experiment. TIM-1 experiments share similarities with the two-stage and transfer experiments, however TIM-1 has the ability to simulate the absorption of the drug, leading to more accurate predictions of precipitation behaviour *in vivo*. Some limitations of the TIM-1 experiment are its long duration and the complicated set-up. Additionally, it is currently not possible to combine TIM results with an *in silico* model to predict the influence of changes in the experimental design (e.g. low vs. elevated gastric pH) on plasma profiles.

3.3 Combining *in vitro* methods assessing ARA co-administration with various *in silico* models

The Simcyp™ Simulator offers multiple models to predict the plasma profile of a drug *in vivo*. In order to evaluate whether data acquired from the *in vitro* experiments using ARA media is appropriate for input into the Simcyp™ Simulator, several Simcyp™ models were explored.

In scenario one, dissolution data from one-stage experiments with PSWB 001 was implemented directly into a minimal PBPK model, using the DRM) To develop a minimal PBPK model, clearance of the drug had to be estimated in advance, which was achieved in the case of PSWB 001 using plasma profiles after intravenous administration.

In scenario two, dissolution data from experiments with dipyridamole was implemented into a full PBPK model. Data input was achieved via the DLM, which attempts a more mechanistic approach to dissolution and can thus be used to explore variations on the dissolution conditions. The parameters needed for input into DLM were acquired using SIVA. Furthermore, in addition to the standard Simcyp™ Simulator set-up for the DLM model, which uses a static model of intestinal pH, a sub-variant using a dynamic model of intestinal pH was explored.

Scenario three focused on the input of dissolution data from experiments with raltegravir potassium into a full PBPK model. Due to the dependency of the behaviour of the formulation on the gastric emptying time, a special approach to the input of dissolution data via a DRM model was followed. The method used mathematical parametrisation of the dissolution profiles in Excel prior to input into Simcyp™ and was based on the strategy reported by Komasa et al. for acidic gastric conditions¹⁰⁴. For the raltegravir potassium studies reported here, the Komasa approach was extended to input reflecting GI physiology during ARA therapy.

Detailed summaries of the input parameters for the respective *in silico* models can be seen in Publications 2, 3 and 4, in the Appendix.

3.3.1 Scenario one: Use of minimal PBPK model and DRM

The minimal PBPK model for PSWB 001 was developed using available data for the physicochemical and pharmacokinetic properties of the compound. An *in vivo* plasma profile after an intravenous administration of the compound, which is independent of liberation or absorption parameters of the drug, was used to estimate the clearance of the drug by fitting the distribution and elimination data to a two-compartmental model. In order to validate the model, the one-stage dissolution data reflecting low gastric pH (FaSSGF) was then introduced to the model via direct input of the percentage of the drug dose dissolved over time (DRM) and the *in silico* simulation was compared to *in vivo* data for oral administration in healthy volunteers. As the simulations achieved an excellent fit to the *in vivo* data in each case example, the next step was to input the dissolution data from one-stage experiments with ARA pH 4 and ARA pH 6 media in exchange for the dissolution data from one-stage experiments with FaSSGF. The simulations using input from ARA media appropriately bracketed the available *in vivo* data for PSWB 001 administration during PPI therapy and estimated an overall decrease in plasma concentrations for PSWB 001 after ARA co-administration.

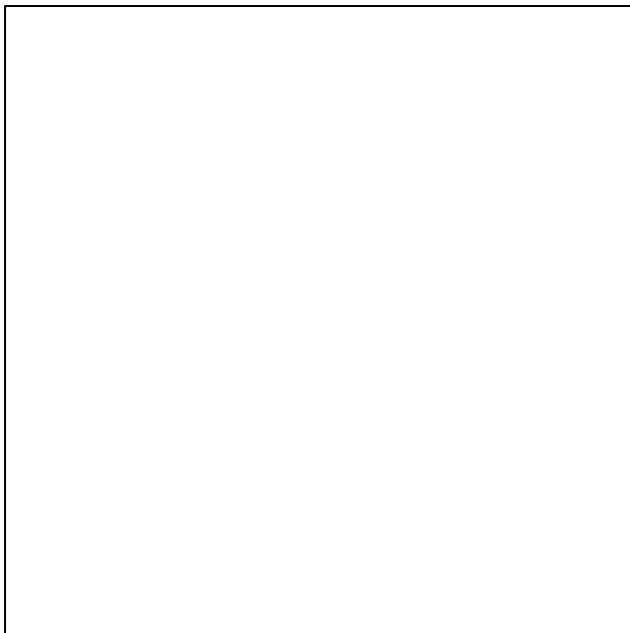
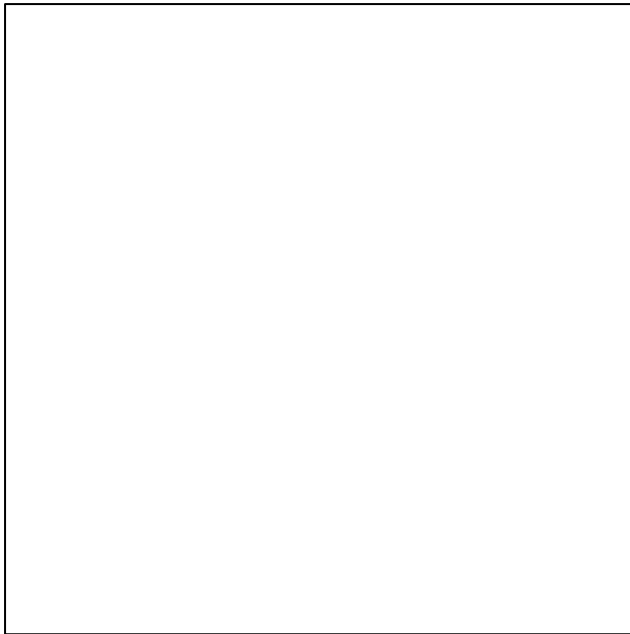


Figure 12. Simulation of plasma profiles for PSWB 001 using minimal PBPK model and dissolution data from experiments with ARA pH 4 and pH 6 media (lines), compared to the *in vivo* data for PSWB 001 administration during PPI therapy from two available studies (dots and squares)

Adapted from a publication in Eu.J.Pharm.Sci. by Segregur et al.¹⁶⁵

3.3.2 Scenario two: Use of a full PBPK model with DLM input

A full PBPK model of dipyridamole was available in the literature^{170,171}, which was updated and used to simulate dipyridamole plasma concentrations after oral administration. In order to input dissolution of the drug into Simcyp™ Simulator using DLM, the dissolution behaviour *in vitro* had to be parameterised using SIVA.

In the first step, dissolution behaviour from one-stage, two-stage and transfer experiments reflecting low gastric pH (using FaSSGF) was parameterised using the DLM scalar, as well as the precipitation parameters PRC and sPRC, where applicable. These DLM parameters were introduced into the full PBPK model, the plasma concentration profiles were simulated, and the predictions were compared to the *in vivo* data for dipyridamole administration without ARA co-administration¹⁷². The simulations using data from two-stage and transfer experiments underpredicted the plasma profiles *in vivo*, while the simulation using one-stage dissolution data showed a very good fit. This is due to the fact that two-stage and transfer experiments introduce strong precipitation into the *in silico* model, thus limiting the amount of the drug available for absorption in the intestine. The dipyridamole precipitation *in vivo*, however, seems to be very low¹⁶⁹, likely due to the high permeability of dipyridamole. Thus, one-stage dissolution data was chosen for input into the *in silico* model reflecting ARA co-administration (second step).

In the second step, the dissolution in ARA pH 4 and pH 6 media was parameterised using SIVA and the DLM parameters of the Simcyp™ model reflecting low gastric pH exchanged for the DLM parameters describing dissolution in ARA media. Furthermore, the gastric pH under the Simcyp™ population parameters was adjusted from the default pH 2 to pH 4 or pH 6, depending on which scenario was being simulated; lesser or stronger impact of ARAs. The two predictions successfully bracketed the *in vivo* plasma profiles after dipyridamole administration during PPI and H2RA therapy^{173,174}.

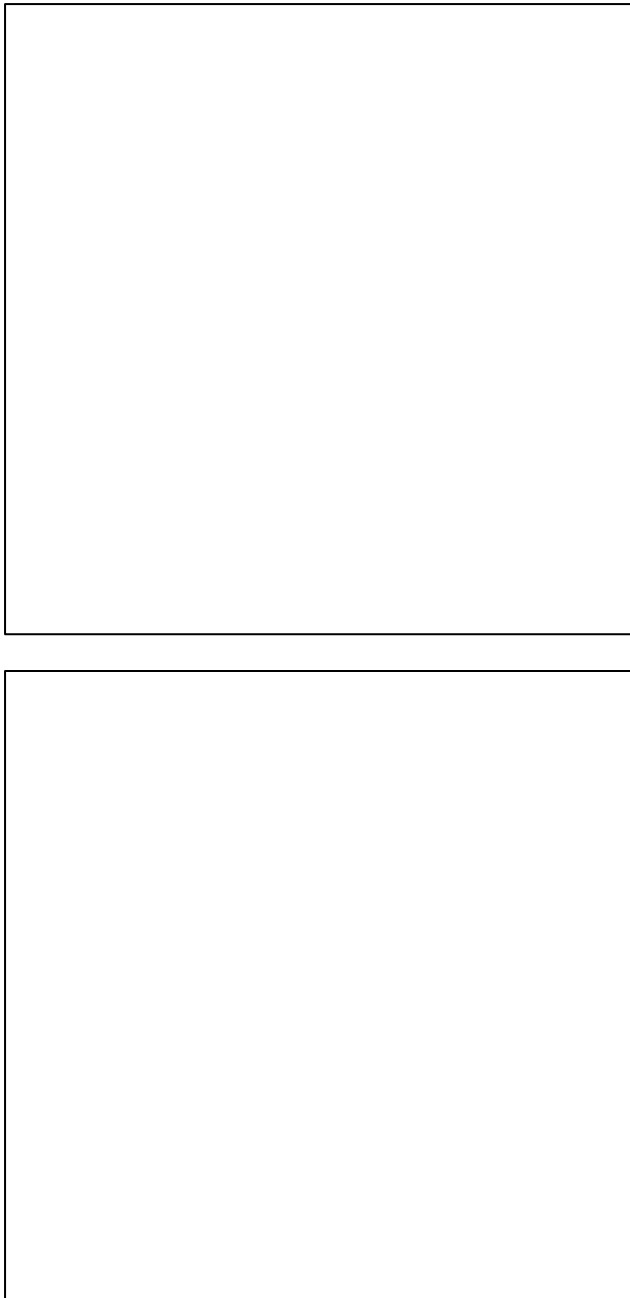


Figure 13. Simulation of dipyridamole plasma profiles using full PBPK model with default DLM set-up and dissolution data from experiments with ARA pH 4 and pH 6 media (lines), compared to the *in vivo* data for dipyridamole administration during PPI (dots) and H2RA (squares) therapy.

Reproduced with permission from a publication in Eu.J.Pharm.Sci. by Segregur et al¹⁶⁶

The third step focused on the development of the method simulating ARA co-administration, when the dynamic intestinal pH model within the Simcyp™ Simulator

is activated. In contrast to the static intestinal pH model, which defines the intestinal pH within each intestinal compartment using a static pH value (e.g. pH 6.4 for the whole of the duodenum), the dynamic intestinal pH model aims to simulate rapid changes of the pH, which the drug may experience due to heterogeneous mixing of the acidic gastric medium with the more basic intestinal medium. This could prove to be a valuable tool when simulating precipitation behaviour of drugs, as the dynamic intestinal pH model may offer a more physiologically accurate representation of pH change in the intestine. While the static intestinal pH model is used as a part of the default set-up within DLM (and was used in the second step), the dynamic intestinal pH model is an option that has to be activated by the user. The simulation of the dipyridamole plasma profile using the dynamic intestinal pH model and dissolution input from the experiments with FaSSGF (low gastric pH) were slightly higher than the one using the static intestinal pH model. Nevertheless, both simulations accurately predicted the *in vivo* plasma profile for dipyridamole administration without co-administration of ARAs.

For simulations using ARA dissolution input and the default set-up for the dynamic intestinal pH model, however, both ARA pH 4 and ARA pH 6 simulation initially overpredicted the *in vivo* data during ARA therapy. This was due to the fact, that the default dynamic intestinal pH model always assumes an acidic gastric pH and its carryover effect on the pH in the small intestine. To correct this assumption for the administration of drugs in the presence of an elevated gastric pH, the input parameters of the dynamic intestinal pH model which define the variation intensity and mean value of the simulated intestinal pH were adjusted to values simulating carryover effects from a less acidic stomach. Simulations using the modified dynamic intestinal pH model and dissolution input from the one-stage experiments with ARA media generated predictions comparable to ones using the static intestinal pH model. Despite the equivalence of the static and dynamic intestinal pH approaches observed in this case example, the dynamic intestinal pH model may be the way forward to obtaining a more accurate prediction of the drug plasma profile *in vivo* for drugs that are more prone to precipitation than dipyridamole.

3.3.3 Scenario three: Use of full PBPK model with a mathematical approach to DRM

In the case of raltegravir potassium, a complex approach to dissolution data input was taken, because a simulation using a single, average gastric emptying time was not able to predict the mean plasma profiles after administration of raltegravir potassium tablets in healthy volunteers with low gastric pH. Rather, a series of *in vitro* two-stage experiments with the pH 4 and pH 6 ARA media in the first stage and a changing pH shift time were defined using mathematical equations (Weibull equations for dissolution and exponential function for precipitation). These mathematical equations were then used in Excel to simulate theoretical dissolution profiles for two-stage experiments with ARA media at any given pH shift time from 0 to 2 hours. The theoretical two-stage dissolution profiles were then implemented as the dissolution input using the DRM approach into the full PBPK model for raltegravir. Individual plasma simulations, which used dissolution profiles with pH shift times equivalent to the GETs¹⁷⁵ of the virtual individuals were generated and the PK for the virtual population was created using a weighted average (according to the frequency at which different gastric emptying times are encountered) of these plasma profiles. This process was repeated for several virtual populations and the mean average plasma concentrations in the virtual populations were then compared with available *in vivo* data¹⁷⁶. The plasma profiles generated using dissolution in the ARA media bracket the data for raltegravir administration during PPI therapy *in vivo*. Interestingly, the simulation using ARA pH 4 dissolution data predicted the *in vivo* data very closely. This confirms the suitability of the ARA pH 4 media to reflect a lesser pH-effect of the ARA therapy (e.g. for a lower dose of an ARA), as in the *in vivo* study a low dose of PPI (20 mg omeprazole) was administered¹⁷⁶.

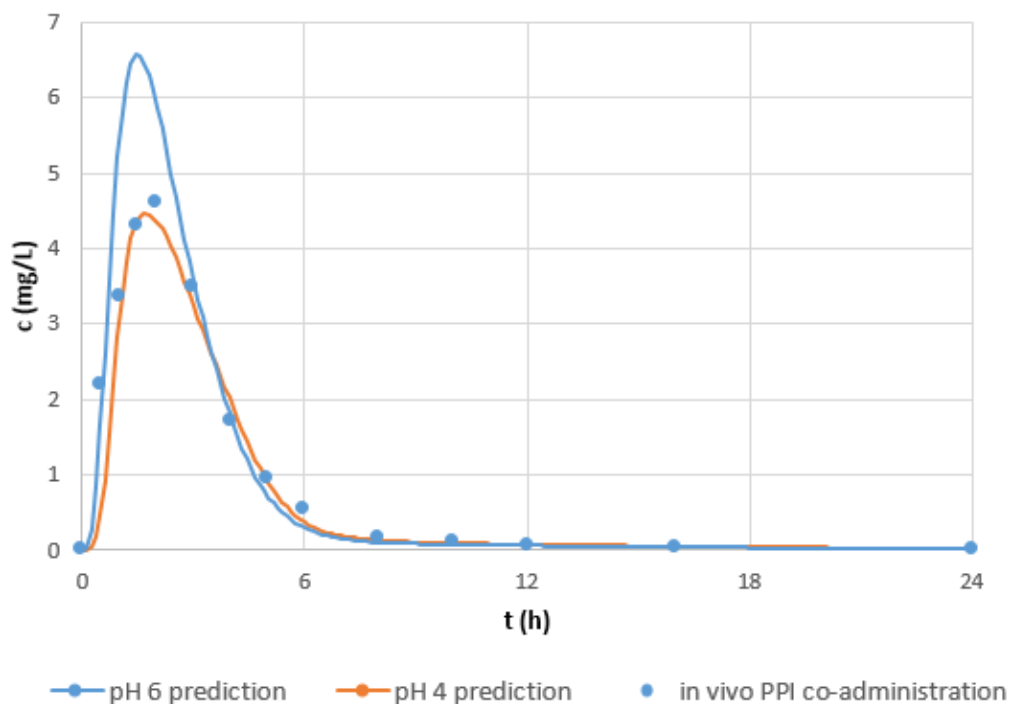


Figure 14. Simulation of average raltegravir plasma profiles for a virtual population using dissolution data input from experiments with ARA pH 4 and pH 6 media (lines), compared to the *in vivo* data during PPI therapy (dots)

Adapted from a publication in J.Pharm.Sci. by Segregur et al.¹⁶⁸

3.4 Evaluating the ability of the methods developed to predict the pH effect of ARA co-administration

In the context of this thesis, various tools aiming to predict the effect of ARAs on GI physiology were developed and implemented. These tools include biorelevant media, *in vitro* methods and *in silico* tools. A set of biorelevant media reflecting the gastric physiology under ARA therapy, in conjunction with double concentrates of biorelevant intestinal media in the case of two-stage and transfer model dissolution testing, was developed. Regarding the *in vitro* methods, one-stage, two-stage, and transfer set-ups suitable for implementation of the aforementioned media were designed. Regarding the *in silico* tools, standard models (minimal, full PBPK model, DRM and DLM) were explored using input reflecting developed *in vitro* ARA methodology. Furthermore, *in silico* add-ons specific to simulating high gastric pH, such as a dynamic model for intestinal pH under ARA therapy, were designed and tested.

The model drugs used to test the ability of the ARA methods to predict plasma profiles during co-therapy with ARAs were drugs for which *in vivo* data for both administration without and during ARA therapy is available. Drugs with different physicochemical properties and various formulations were explored, adding to the certainty that the methods developed would be applicable to a wide range of drugs.

During the development of the biorelevant media reflecting the gastric physiology under ARA therapy (ARA media), the most important parameters were taken under consideration: pH, buffer capacity, osmolality and surface tension. Every decision regarding the design of the media reflecting ARA co-administration was supported by literature data on physiological changes under ARA therapy.

When essential parameters were considered and appropriate *in vitro* and *in silico* methods implemented, the use of ARA media and tests resulted in plasma profile predictions which were able to bracket the ARA effect on drug pharmacokinetics (Figures 12, 13 and 14). This was demonstrated for both weakly basic drugs (PSWB 001 and dipyrindamole) and the salt of a weak acid (raltegravir potassium).

It was shown that the bracketing approach can encompass ARA effects after administration of both H2RAs and PPIs, as well as assess the extent of the pH effect for different doses of ARAs. Using *in vitro* set-ups and ARA media it was possible to analyse drug dissolution behaviour for both immediate release and non-dispersing formulations.

Finally, the DRM and DLM input of dissolution data in minimal and full PBPK models was validated by *in vivo* data of volunteers with low gastric pH. Subsequent application of the dissolution data from the ARA media was demonstrated to predict the *in vivo* plasma profiles for volunteers under ARA therapy (elevated gastric pH) appropriately. This, it is safe to conclude that the methods developed are able to accurately predict the pH effect of ARA co-administration across a wide range of compound and formulation properties.

4 Summary and Outlook

Standard biorelevant media reflect the average gastrointestinal (GI) physiology in healthy volunteers. The use of biorelevant media in *in vitro* experiments has become an important strategy to predict drug behaviour *in vivo* and is often combined with *in silico* tools in order to simulate drug plasma profiles over time. In addition to the healthy population, the effects of disease state or co-administration of other drugs on plasma profiles must be considered to assure drug efficacy and safety. Thus, there is a need for a more accurate representation of the human GI physiology when it is altered by disease or co-administered drugs in *in vitro* dissolution experiments.

This thesis focused on the development of biorelevant media and dissolution tests reflecting GI physiology in circumstances where the gastric pH is elevated. Diseases linked to an elevated gastric pH are hypochlorhydria and achlorhydria, but these days treatment with acid-reducing agents (ARAs) is the single greatest cause of elevation in gastric pH. pH-dependent drug-drug interactions (DDIs) with ARAs are frequent, as the ARAs are used in a number of diseases using a variety of drugs. As the drugs currently on the market are often poorly soluble and ionisable, their dissolution is highly dependent on the pH of the GI tract, especially the gastric pH.

The thesis research consisted of several steps. In the first step, physiological changes in the human GI tract during the therapy with ARAs were identified. Parameters of the standard biorelevant gastric medium FaSSGF were adjusted to the identified changes to reflect the impact of ARA co-administration on the gastric physiology. The media aim to assess the potential extent of the ARA impact on gastric physiology by introducing biorelevant media pairs, ARA pH 4 and pH 6 media, of which one reflects a lesser, and the other a stronger impact of ARAs.

In the second step these ARA media were implemented in *in vitro* dissolution set-ups. The dissolution of poorly soluble ionisable drugs was assessed using one-stage, two-stage and transfer model set-ups, as well as using a more evolved *in vitro* system TIM-1. Comparison of results from dissolution set-ups using the standard, low pH, gastric biorelevant medium FaSSGF (pH 1.6 or 2), and the same set-ups using ARA pH 4 and pH 6 media, shows a decrease in dissolution rate and extent for weakly basic compounds PSWB 001 and dipyridamole, and an increase in rate and extent of dissolution for the weakly acidic compound raltegravir potassium, when the gastric pH is elevated. Due to different physicochemical properties, the extent of the impact of

physiological changes during ARA therapy (when either ARA pH 4 or pH 6 medium is selected) on dissolution varied among the model drugs. Thus, the bracketing approach, which considers a range of the possible ARA co-administration impact on drug dissolution, was confirmed to be best practice in assessing the impact of ARAs.

In the third step, dissolution data from *in vitro* experiments with ARA media was implemented into *in silico* models. The predictions using various *in silico* model approaches in Simcyp™ Simulator (minimal and full PBPK model, dissolution input using DRM and DLM) successfully bracketed *in vivo* data on drug administration during ARA therapy and correctly predicted an overall decrease in plasma concentration for the two model weakly basic compounds and an increase in plasma concentration for the model weakly acidic compound.

In all assessed scenarios, the ARA methods proved to be an essential part of evaluating and predicting the impact of ARAs on drug pharmacokinetics, and appropriately predicted the extent of a possible impact of ARAs on the drug plasma profiles. Thus, the ARA biorelevant media and dissolution tests were demonstrated to be valuable tools reflecting administration of drugs when the gastric pH is elevated and able to predict the impact of ARA therapy on drug administration.

The ability to evaluate the impact of human (patho) physiology on drug behaviour in the gastrointestinal tract is of great importance, as the GI conditions play a significant role in drug release and absorption. Thus, there is great interest on the part of the pharmaceutical industry and regulatory agencies to develop best practices in this field, especially for pH-dependent DDIs. The media and dissolution tests developed in this thesis are biorelevant methods appropriate for evaluation of the impact of elevated gastric pH on drug efficacy and safety. Such methods, used as a risk assessment tool, in connection with evaluation of the efficacy window and potential toxicity, may help to increase confidence about decisions as to whether a pH-effect will occur and whether it is relevant or not, prior to conducting clinical studies. They may also enable changes in inclusion/exclusion criteria during recruiting for large-scale efficacy trials. In fact, the biopharmaceutic approach to drug development is becoming standard practice on a number of fronts, including metabolic DDIs, renal and hepatic insufficiency, powering decision-making process and possibly even waiving certain types of clinical studies.

The ARA media created and studied in this doctoral project reflect gastric physiology during co-administration of PPIs and H2RAs, and thus cover the majority of the scenarios where pH-dependent DDIs occur. Due to the significant differences in gastric media composition and behaviour after antacid administration, a biorelevant medium and dissolution test reflecting antacid co-administration still has to be developed and validated. Nevertheless, the approach described in this thesis can be applied to development of biorelevant media and dissolution tests for both antacid use and other situations in which the GI physiology is altered through drug administration or disease. Diseases for which a number of medications are prescribed are at especially high risk of DDIs and the assessment of the impact of other disease states and co-administered drugs will likely become a standard procedure during new drug development as well as re-assessment of the efficiency and safety of drugs which are already on the market.

Overall, as the pharmaceutical industry and regulatory bodies continue to invest in predicting the drug behaviour *in vivo* prior to running clinical studies, with the aim of assessing impact of disease state and pH-dependent DDIs early in the development process. Biorelevant *in vitro* and *in silico* tools, like those developed in this project, will surely play an essential role and become a reliable and essential tool in pharmaceutical drug development.

5 Deutsche Zusammenfassung (German summary)

Das Verständnis über die Physiologie des gastrointestinalen (GI) Traktes ist essenziell, um das Verhalten des Arzneimittels nach peroraler Gabe zu verstehen. Die Änderungen im GI Trakt, die während einer Krankheit oder bei der Gabe anderer Medikamente vorkommen, können einen Einfluss auf die Therapie mit bestimmten Arzneistoffen haben.

Die sogenannten biorelevanten Medien sind künstlich hergestellte Flüssigkeiten, die die Eigenschaften der Medien des Magen-Darmtrakts wiedergeben (pH, Pufferkapazität, Gallensalzkonzentration, Osmolalität) und in *in vitro* Freisetzungsexperimenten benutzt werden. Sie wurden auf Basis der Forschung von Dressman et al. entwickelt und beinhalten Medien wie FaSSGF und FeSSGF (Künstlicher nüchterner und prandialer Magensaft), FaSSIF V1 und FeSSIF V1 (Künstlicher nüchterner und prandialer Dünndarmsaft), FaSSIF V2 und FeSSIF V2 (die zweite Version der künstlichen Dünndarmsäfte), sowie FaSSCoF und FeSSCoF (Künstlicher nüchterner und prandialer Dickdarmsaft).

Diese Medien stellen jedoch nur die physiologischen Bedingungen der Magen-Darmtrakt-Flüssigkeiten im gesunden Zustand dar. Um ein akkurates Bild über das Verhalten eines Arzneimittels in den Patienten (der eigentlichen Zielgruppe) zu erhalten, sollte man jedoch zusätzlich die relevanten Änderungen in der Physiologie im erkrankten Zustand berücksichtigen. Dies umfasst, unter anderem, pH, Pufferkapazität, Osmolalität und die Zusammensetzung der GI Flüssigkeiten, die Permeabilität des Darms, und die Motilität des GI Traktes. Die meisten kleinmolekularen Wirkstoffe, die sich zurzeit auf dem Markt oder in der Entwicklung befinden, sind schwer lösliche ionisierbare Stoffe. Deren Auflösung und folglich die Bioverfügbarkeit sind nach peroraler Gabe dementsprechend vom pH des Auflösungsmediums abhängig. Die Krankheiten, die durch ein erhöhtes pH der Magenflüssigkeit charakterisiert sind, sind Hypo- und Achlorhydrie, sowie die Krankheiten und Zustände, die zur Behandlung der magensäureassoziierten Symptomatik mit Wirkstoffen wie Antazida, H₂-Antihistaminika (H₂RAs), und Protonenpumpenhemmer (PPIs), therapiert werden. Während dem Magen selbst bei der Hypo- und Achlorhydrie die Säuresekreptionsfähigkeit fehlt, erhöhen die Antazida, H₂RAs und PPIs den pH der Magenflüssigkeit durch die Neutralisierung der Magensäure oder die Hemmung der Säuresekretion und werden deswegen säuresenkende Mittel (engl. acid-reducing agents, ARAs) genannt. Hypo- und

Achlorhydrie sind prävalenter in geriatrischen Patienten sowie in japanischer Bevölkerung, während die ARAs in einer Reihe der Krankheiten eingesetzt werden, wie z.B. Gastritis, Refluxkrankheiten, Magen-Duodenalulzera, aber auch zur Vorbeugung der Ulzeration des Magens bei chronischer Gabe nichtsteroidaler Antirheumatika oder bei polymedizierten Patienten.

Das Ziel dieser Arbeit war es, biorelevante Medien und Freisetzungstests zu entwickeln, die den physiologischen Zustand unter GI Krankheiten wiedergebenden. Die Forschung fokussierte auf die Physiologie des GI Traktes bei den Krankheiten, die durch ein erhöhtes pH der Magenflüssigkeit charakterisiert sind, d.h. während der Therapie mit ARAs. Um das Ziel der Arbeit zu verwirklichen, wurden mehrere Schritte festgelegt. Dies diente der Entwicklung eines wissenschaftlich begründeten und schrittweise validierten Werkzeugs. Außerdem wurden drei Wirkstoffe mit unterschiedlichen physikochemischen Eigenschaften (PSWB 001 und Dipyridamol als schwache Basen und Raltegravir als schwache Säure) untersucht, um damit die Robustheit des Werkzeugs zu bestätigen. Mithilfe gründlicher Literaturrecherche wurden im ersten Schritt die relevanten Änderungen in der Physiologie des Magen-Darm-Traktes während der Therapie mit ARAs identifiziert. Des Weiteren wurde auf Basis dieser Befunde das Standardmedium FaSSGF modifiziert, um diese Änderungen zu enthalten. Die so entstandenen ARA Medien wurden im zweiten Schritt in *in vitro* Freisetzungsexperimenten eingesetzt und untersucht. Es wurden die Einstufen- und Zweistufen-Freisetzungsmodelle, das Transfer Modell sowie ein komplexes *in vitro* Modell TIM-1 untersucht und die Vergleiche zwischen Experimenten unter dem Standardzustand (saurer Magen) und den Experimenten, die den Einfluss der ARAs wiedergeben gestellt. Im dritten Schritt wurde die Kompatibilität der entwickelten Freisetzungstests mit den Computerprogrammen (*in silico* Modelling) ausgewertet. Die erworbenen Freisetzungsdaten wurden dabei in allmählich komplexere *in silico* Modelle eingesetzt: zuerst wurde ein minimales Physiologie-basiertes pharmakokinetisches (PBPK) Modell untersucht und die direkte Eingabe des prozentualen Anteils der freigesetzten Dosis (Auflösungsrate-Modell, DRM) benutzt. Danach wurde ein volles PBPK Modell mit einer Eingabe der Freisetzung, die die grundlegenden Auflösungsprozesse in *in vitro* Experimenten berücksichtigt (Diffusionsschicht-Modell, DLM), eingesetzt. Außerdem wurden im Zusammenhang mit den entwickelten Freisetzungstests ein komplexerer, mathematischer Ansatz des

DRM sowie die Varianten der intestinalen pH Darstellung im DLM untersucht. Im letzten Schritt wurden die im vorherigen Schritt generierten Simulationen der Plasmaprofile für die drei Testwirkstoffen im Zustand während der ARA Therapie mit den Literaturdaten der Wirkstoffgabe *in vivo* während der ARA Therapie verglichen. Während der Literaturrecherche über den Einfluss der ARAs auf die GI Physiologie wurde deutlich, dass die wichtigsten Änderungen im Magen stattfinden und die Änderung des biorelevanten Mediums für den Magenkompartiment notwendig ist. Weiterhin wurde entschieden die Einflüsse unterschiedlicher ARA Familien (Antazida, H2RAs und PPIs) separat zusammenzufassen, da sich die Wirkmechanismen teils stark unterscheiden. Die Antazida wirken rasch und erhöhen den Magen pH dosisabhängig auf einen Wert über pH 3.5 für eine kurze Zeit (30 – 60 Minuten). Aufgrund der physikalischen Anwesenheit im Magen können Antazida die Konzentration und die Wirkung der Gallensalze und des Pepsins durch Adsorption sinken. Außerdem bringen die Antazida mehrwertige Metallionen in die Magenflüssigkeit ein, was zur Gefahr der Chelatbildung mit komplexierbaren Wirkstoffen führt. Andererseits wirken die H2RAs und PPIs über einen Antagonismus der Magensäuresekretion. Die H2RAs wirken nach einer Zeitverzögerung von 60 bis 90 min, erhöhen den Magen pH dosisabhängig (pH 4 – 6) und die Wirkung hält deutlich länger an, als bei Antazida (über 7 Stunden). Die PPIs sind die effektivsten ARAs, sie hemmen die Protonenpumpen irreversibel, entfalten jedoch die volle Wirkung erst nach mehrfacher Dosierung. Nach peroraler Gabe der PPI Standarddosen wird der pH des Magens zu durchschnittlich pH 5 (Bereich pH 4 – 6) erhöht. Der lange pH Effekt während der Gabe der H2RAs und PPIs kann die protektive Wirkung des Magenkompartiments hindern und deren chronische Gabe wird deswegen oft in Zusammenhang mit den Veränderungen der Darmflora gebracht.

Da die H2RAs und PPIs für einen längeren pH Effekt im Magen verantwortlich sind, und als ARAs bei der Mehrheit der Krankheiten eingesetzt werden, wurden die biorelevanten Medien auf der Basis der Befunde dieser zwei ARA Gruppen entwickelt. Eine Darstellung des pH Bereiches, eher als (nur) eines einzelnen, durchschnittlich erhöhten pH, ermöglichte die Widerspiegelung einer Spanne des variablen ARA Effektes. Beim Standardmedium FaSSGF wurden die pH, Osmolalität, Pufferkapazität und Medienzusammensetzung so eingestellt, dass zwei Szenarien dargestellt werden konnten: Im ersten Fall stellte das ARA pH 4 medium einen schwächeren ARA Effekt dar (eine geringere Dosis von ARA). Dieses Medium hatte den pH Wert 4, einen

dazugehörigen Puffer mit höherer Pufferkapazität, sowie die verbliebene Pepsinaktivität. Das zweite Medium, ARA pH 6, stellte einen stärkeren ARA Effekt dar (höhere ARA Dosis, chronische Gabe), und hatte pH 6, einen Puffer mit niedriger Pufferkapazität, sowie kein Pepsin, da die Pepsinaktivität über pH 5 irrelevant ist. Es wurden drei Paare (pH 4 und pH 6) der ARA Medien mit verschiedenen Puffersalzen entwickelt, um die möglichen Wechselwirkungen zwischen den Wirk- und/oder Hilfsstoffen und der Puffersubstanz durch den Umtausch der Paare vermeiden zu können. Die Zusammensetzung der ARA Medien ist in der Tabelle 1. des Dissertationshauptteils wiedergegeben.

Die entwickelten ARA Medien wurden mit drei Testwirkstoffen in Einstufen-Freisetzungsversuchen untersucht. Im Vergleich zur Auflösung im biorelevanten Medium FaSSGF (pH 1.6) zeigten die basischen Arzneistoffe eine langsamere und eingeschränkte Freisetzung in den ARA Medien. Die Formulierung des aziden Wirkstoffs (Raltegravir) zeigte eine signifikant verbesserte Wirkstoffauflösung in den ARA Medien.

Zusätzlich zur Freisetzung der Wirkstoffe in nur einem Medium, vermittelten die Zweistufen-Freisetzungsversuche zusätzliche Daten über das Verhalten der Wirkstoffe nach einem Übergang aus der Umgebung des Magens in den Dünndarm. Aufgrund einer auftretenden Übersättigung der Lösung der schwach basischen Wirkstoffen PSWB 001 und Dipyridamol in der zweiten Stufe des Experiments, konnten die Unterschiede im Präzipitationsverhalten zweier Wirkstoffe identifiziert werden. Während PSWB 001 im Dünndarmmedium in der Lösung (übersättigt) blieb, präzipitierte Dipyridamol rasch, wenn das Magenmedium saurer war als das Dünndarmmedium. In den Versuchen mit Raltegravir wurde festgestellt, dass die Präexposition zum Magenmedium einen Einfluss auf die Freisetzung im Dünndarmmedium haben kann. Dennoch simuliert der Zweistufen-Freisetzungsmodell eine sehr rasche, abrupte Änderung des Freisetzungsmediums, und stellt physiologisch höchstens eine schnelle Magenentleerung dar. Das Transfer Modell, welches eine peristaltische Pumpe zum graduellen Transport des gelösten Stoffes aus dem Magenkompartiment in das Dünndarmkompartiment nutzt, scheint dem physiologischen Prozess der Magenentleerung näher zu sein. Die Präzipitation von Dipyridamol in den Transfer-Modell Experimenten war dementsprechend langsamer. Die Präzipitation eines Wirkstoffs im Darm ist auch von der Absorption abhängig, und da diese in der Standardkonfiguration des Transfer-Modells nicht

darstellbar ist, wurde ein TIM-1 Modell, der die Absorptionvorgänge im Darm simuliert, eingesetzt. Sowohl beim Transfer-Modell, als auch bei TIM-1 wurde bewiesen, dass die Freisetzung von Dipyridamol in Experimenten, die einen Magensaft mit erhöhtem pH nutzen, geringer ist als in Experimenten mit einem Magensaft mit niedrigem pH.

Die Freisetzungsdaten aus den Versuchen mit den Testwirkstoffen wurden erfolgreich sowohl im minimalen als auch in zwei vollen PBPK *in silico* Modellen eingesetzt. Die Eingabe dieser Daten konnte sowohl durch DRM, als auch durch unterschiedliche Varianten des DLM erfolgen. Die mithilfe dieser *in silico* Modellen erhobenen Vorhersagen der Plasmaspiegel für PSWB 001, Dipyridamol und Raltegravir beim aziden Magen stimmten mit den *in vivo* Daten für die Gabe dieser Testwirkstoffe ohne ARA Co-Therapie überein. Die Vorhersagen, die mithilfe der ARA Medien und Freisetzungstests erhoben worden sind (und einen schwächeren und einen stärkeren Effekt der ARA darstellen), rahmen die *in vivo* Plasmaprofile für drei Wirkstoffe während der ARA Therapie ein.

Das Verhalten der erforschten Arzneistoffe und dazugehöriger Arzneiformen im Zustand mit erhöhtem Magen pH wurde mithilfe entwickelter Medien und Tests erfolgreich simuliert und hat sich als eine essenzielle Eingabe in den *in silico* Modellen zur Vorhersage des pH Effektes auf die Wirkstoff-Pharmakokinetik erwiesen. Die Versuchsreihen mit schwach basischen Wirkstoffen PSWB 001 und Dipyridamol haben deren schlechtere Auflösung in der Magenflüssigkeit mit erhöhtem pH widerspiegeln sowie Schlussfolgerungen über das Präzipitationsverhalten von Wirkstoffen ermöglichen können. Die entwickelten Medien und Tests haben auch die umfangreichere Auflösung des schwach sauren Wirkstoffs Raltegravir unter erhöhtem Magen pH widerspiegeln können und waren dabei zur Untersuchung einer Formulierung mit modifizierter Freisetzung eingesetzt. Die *in silico* Simulationen von Plasmaprofilen der untersuchten Wirkstoffe nach ARA Gabe haben akkurat das wahrscheinliche Ausmaß des pH Effektes eingeschätzt.

Die entwickelte biorelevanten Medien und Freisetzungstests, die den physiologischen Zustand unter GI Krankheiten wiedergeben, sind ein wertvolles Werkzeug zur Beurteilung der pH-abhängigen Wechselwirkungen und können sich als eine Ergänzung zur aktuellen Strategie der Wirkstoffentwicklung sowie der Sicherstellung der Wirksamkeit und Unbedenklichkeit der Medizin erweisen.

6 References

- 1 Dressman JB, Reppas C. *Oral Drug Absorption*: CRC Press; 2016.
- 2 Ivančević Ž, Rumboldt Z, Bergovec M, Silobrčić V. *MSD - priručnik diagnostike i terapije: The Merck Manual of diagnosis and therapy*. Split: Placebo d.o.o; 2014.
- 3 Frankel M. The Biochemists' Handbook, Edited by Cyril Long, M.A., B. Sc., D. Phil, F. R. S. E. Publishers E. & F.N. Spon Ltd., London, 1961. pp. 1092, Price 168 s. *Isr. J. Chem.* 1963;1(1):43-44. doi:10.1002/ijch.196300012.
- 4 Mudie DM, Murray K, Hoad CL, et al. Quantification of gastrointestinal liquid volumes and distribution following a 240 mL dose of water in the fasted state. *Mol Pharm.* 2014;11(9):3039-3047. doi:10.1021/mp500210c.
- 5 Schiller C, Fröhlich C-P, Giessmann T, et al. Intestinal fluid volumes and transit of dosage forms as assessed by magnetic resonance imaging. *Aliment Pharmacol Ther.* 2005;22(10):971-979. doi:10.1111/j.1365-2036.2005.02683.x.
- 6 Steingoetter A, Fox M, Treier R, et al. Effects of posture on the physiology of gastric emptying: a magnetic resonance imaging study. *Scand J Gastroenterol.* 2006;41(10):1155-1164. doi:10.1080/00365520600610451.
- 7 Mudie DM, Amidon GL, Amidon GE. Physiological parameters for oral delivery and in vitro testing. *Mol Pharm.* 2010;7(5):1388-1405. doi:10.1021/mp100149j.
- 8 Bergström CAS, Holm R, Jørgensen SA, et al. Early pharmaceutical profiling to predict oral drug absorption: current status and unmet needs. *Eur J Pharm Sci.* 2014;57:173-199. doi:10.1016/j.ejps.2013.10.015.
- 9 Abuhelwa AY, Foster DJR, Upton RN. A Quantitative Review and Meta-models of the Variability and Factors Affecting Oral Drug Absorption-Part II: Gastrointestinal Transit Time. *AAPS J.* 2016;18(5):1322-1333. doi:10.1208/s12248-016-9953-7.
- 10 Baxevanis F, Kuiper J, Fotaki N. Fed-state gastric media and drug analysis techniques: Current status and points to consider. *Eur J Pharm Biopharm.* 2016;107:234-248. doi:10.1016/j.ejpb.2016.07.013.
- 11 Dressman JB, Amidon GL, Reppas C, Shah VP. Dissolution testing as a prognostic tool for oral drug absorption: immediate release dosage forms. *Pharm Res.* 1998;15(1):11-22. doi:10.1023/a:1011984216775.
- 12 Kurita Y, Nakazawa S, Segawa K, Tsukamoto Y. Clinical significance of gastric juice viscosity in peptic ulcer patients. *Dig Dis Sci.* 1988;33(9):1070-1076. doi:10.1007/BF01535780.
- 13 Kalantzi L, Goumas K, Kalioras V, Abrahamsson B, Dressman JB, Reppas C. Characterization of the human upper gastrointestinal contents under conditions simulating bioavailability/bioequivalence studies. *Pharm Res.* 2006;23(1):165-176. doi:10.1007/s11095-005-8476-1.
- 14 Takahashi T. Mechanism of interdigestive migrating motor complex. *J Neurogastroenterol Motil.* 2012;18(3):246-257. doi:10.5056/jnm.2012.18.3.246.
- 15 Dooley CP, Di Lorenzo C, Valenzuela JE. Variability of migrating motor complex in humans. *Dig Dis Sci.* 1992;37(5):723-728. doi:10.1007/BF01296429.
- 16 Scratcherd T, Grundy D. The physiology of intestinal motility and secretion. *Br J Anaesth.* 1984;56(1):3-18. doi:10.1093/bja/56.1.3.
- 17 Sanny CG, Hartsuck JA, Tang J. Conversion of pepsinogen to pepsin. Further evidence for intramolecular and pepsin-catalyzed activation. *Journal of Biological Chemistry.* 1975;250(7):2635-2639. doi:10.1016/S0021-9258(19)41649-9.
- 18 Lambert R, Martin F, Vagne M. Relationship between hydrogen ion and pepsin concentration in human gastric secretion. *Digestion.* 1968;1(2):65-77. doi:10.1159/000196835.

- 19 Schmidt HA, Fritzl G, Dölle W, Goebell H. Vergleichende Untersuchungen der histamin- und insulin-stimulierten Säure-Pepsin-Sekretion bei Patienten mit Ulcus duodeni und Kontrollpersonen. *Dtsch Med Wochenschr.* 1970;95(40):2011-2016. doi:10.1055/s-0028-1108771.
- 20 Seidler U, Sjöblom M. Gastroduodenal Bicarbonate Secretion. In: *Physiology of the Gastrointestinal Tract.* Vol. 3: Elsevier; 2012:1311-1339.
- 21 Bik EM, Eckburg PB, Gill SR, et al. Molecular analysis of the bacterial microbiota in the human stomach. *Proc Natl Acad Sci U S A.* 2006;103(3):732-737. doi:10.1073/pnas.0506655103.
- 22 Sousa T, Paterson R, Moore V, Carlsson A, Abrahamsson B, Basit AW. The gastrointestinal microbiota as a site for the biotransformation of drugs. *Int J Pharm.* 2008;363(1-2):1-25. doi:10.1016/j.ijpharm.2008.07.009.
- 23 Moog F. The lining of the small intestine. *Sci Am.* 1981;245(5):154-8, 160, 162 et passiom. doi:10.1038/scientificamerican1181-154.
- 24 Standring S, Gray H. *Gray's anatomy: The anatomical basis of clinical practice / editor-in-chief, Susan Standring.* Forty first edition. Oxford: Elsevier; 2016.
- 25 Niess JH, Reinecker H-C. Dendritic cells in the recognition of intestinal microbiota. *Cell Microbiol.* 2006;8(4):558-564. doi:10.1111/j.1462-5822.2006.00694.x.
- 26 Helander HF, Fändriks L. Surface area of the digestive tract - revisited. *Scand J Gastroenterol.* 2014;49(6):681-689. doi:10.3109/00365521.2014.898326.
- 27 Fordtran JS, Locklear TW. Ionic constituents and osmolality of gastric and small-intestinal fluids after eating. *Am J Dig Dis.* 1966;11(7):503-521. doi:10.1007/BF02233563.
- 28 Evans DF, Pye G, Bramley R, Clark AG, Dyson TJ, Hardcastle JD. Measurement of gastrointestinal pH profiles in normal ambulant human subjects. *Gut.* 1988;29(8):1035-1041. doi:10.1136/gut.29.8.1035.
- 29 Fuchs A, Dressman JB. Composition and physicochemical properties of fasted-state human duodenal and jejunal fluid: a critical evaluation of the available data. *J Pharm Sci.* 2014;103(11):3398-3411. doi:10.1002/jps.24183.
- 30 Lindahl A, Ungell AL, Knutson L, Lennernäs H. Characterization of fluids from the stomach and proximal jejunum in men and women. *Pharm Res.* 1997;14(4):497-502. doi:10.1023/a:1012107801889.
- 31 Riethorst D, Mols R, Duchateau G, Tack J, Brouwers J, Augustijns P. Characterization of Human Duodenal Fluids in Fasted and Fed State Conditions. *J Pharm Sci.* 2016;105(2):673-681. doi:10.1002/jps.24603.
- 32 Hirano I, Brenner D. Gastrointestinal motility. In: Reinus JF, Simon D, eds. *Gastrointestinal Anatomy and Physiology.* Vol. 334. Oxford: John Wiley & Sons, Ltd; 2014:33-45.
- 33 Simon GL, Gorbach SL. Intestinal flora in health and disease. *Gastroenterology.* 1984;86(1):174-193. doi:10.1016/0016-5085(84)90606-1.
- 34 Eckburg PB, Bik EM, Bernstein CN, et al. Diversity of the human intestinal microbial flora. *Science.* 2005;308(5728):1635-1638. doi:10.1126/science.1110591.
- 35 biorelevant.com. What are biorelevant media? https://biorelevant.com/learning_center/what-are-biorelevant-media/. Accessed May 24, 2021.
- 36 Markopoulos C, Andreas CJ, Vertzoni M, Dressman J, Reppas C. In-vitro simulation of luminal conditions for evaluation of performance of oral drug products: Choosing the appropriate test media. *Eur J Pharm Biopharm.* 2015;93:173-182. doi:10.1016/j.ejpb.2015.03.009.
- 37 Marques M. Dissolution Media Simulating Fasted and Fed States. *Dissolution Technol.* 2004;11(2):16. doi:10.14227/DT110204P16.
- 38 Boni JE, Brickl RS, Dressman J, Pfefferle ML. Instant FaSSIF and FeSSIF—Biorelevance Meets Practicality. *Dissolution Technol.* 2009;16(3):41-45. doi:10.14227/DT160309P41.

- 39 Galia E, Nicolaides E, Hörter D, Löbenberg R, Reppas C, Dressman JB. Evaluation of various dissolution media for predicting in vivo performance of class I and II drugs. *Pharm Res.* 1998;15(5):698-705. doi:10.1023/a:1011910801212.
- 40 Vertzoni M, Dressman J, Butler J, Hempenstall J, Reppas C. Simulation of fasting gastric conditions and its importance for the in vivo dissolution of lipophilic compounds. *Eur J Pharm Biopharm.* 2005;60(3):413-417. doi:10.1016/j.ejpb.2005.03.002.
- 41 Jantratid E, Janssen N, Reppas C, Dressman JB. Dissolution media simulating conditions in the proximal human gastrointestinal tract: an update. *Pharm Res.* 2008;25(7):1663-1676. doi:10.1007/s11095-008-9569-4.
- 42 Vertzoni M, Diakidou A, Chatziliadis M, et al. Biorelevant media to simulate fluids in the ascending colon of humans and their usefulness in predicting intracolonic drug solubility. *Pharm Res.* 2010;27(10):2187-2196. doi:10.1007/s11095-010-0223-6.
- 43 Fuchs A, Leigh M, Kloefer B, Dressman JB. Advances in the design of fasted state simulating intestinal fluids: FaSSiF-V3. *Eur J Pharm Biopharm.* 2015;94:229-240. doi:10.1016/j.ejpb.2015.05.015.
- 44 biorelevant.com. FeSSGF vs FEDGAS: a comparison. https://biorelevant.com/learning_center/fed-gastric-dissolution-media-fessgf-vs-fedgas/. Accessed 24.0.2021.
- 45 Kaye JL. Review of paediatric gastrointestinal physiology data relevant to oral drug delivery. *Int J Clin Pharm.* 2011;33(1):20-24. doi:10.1007/s11096-010-9455-0.
- 46 Effinger A, O'Driscoll CM, McAllister M, Fotaki N. Impact of gastrointestinal disease states on oral drug absorption - implications for formulation design - a PEARL review. *J Pharm Pharmacol.* 2019;71(4):674-698. doi:10.1111/jphp.12928.
- 47 Bhutto A, Morley JE. The clinical significance of gastrointestinal changes with aging. *Curr Opin Clin Nutr Metab Care.* 2008;11(5):651-660. doi:10.1097/MCO.0b013e32830b5d37.
- 48 Kohli D. R. Achlorhydria. <https://emedicine.medscape.com/article/170066-overview>. Updated May 30, 2021.
- 49 Morgan M. Control of intragastric pH and volume. *Br J Anaesth.* 1984;56(1):47-57. doi:10.1093/bja/56.1.47.
- 50 *The United States pharmacopeia.* 20th revision. Rockville, Md: United States Pharmacopeial Convention; 1979.
- 51 Britton E, McLaughlin JT. Ageing and the gut. *Proc Nutr Soc.* 2013;72(1):173-177. doi:10.1017/S0029665112002807.
- 52 Christiansen PM. The incidence of achlorhydria and hypochlorhydria in healthy subjects and patients with gastrointestinal diseases. *Scand J Gastroenterol.* 1968;3(5):497-508. doi:10.3109/00365526809179909.
- 53 Segal HL, Samloff IM. Gastric cancer--increased frequency in patients with achlorhydria. *Am J Dig Dis.* 1973;18(4):295-299. doi:10.1007/BF01070990.
- 54 Overbey DM, Jones EL. Acid Peptic Ulcer Disease. In: *Abernathy's Surgical Secrets.* Vol. 28: Elsevier; 2018:209-214.
- 55 Grinspoon L., Dunn J. E. A Study of the Frequency of Achlorhydria Among Japanese in Los Angeles. *JNCI: Journal of the National Cancer Institute.* 1959. doi:10.1093/jnci/22.3.617.
- 56 Morihara M, Aoyagi N, Kaniwa N, Kojima S, Ogata H. Assessment of gastric acidity of Japanese subjects over the last 15 years. *Biol Pharm Bull.* 2001;24(3):313-315. doi:10.1248/bpb.24.313.
- 57 Leonard J. What is hypochlorhydria? <https://www.medicalnewstoday.com/articles/322491>. Updated May 30, 2021.

- 58 Segregur D, Flanagan T, Mann J, et al. Impact of Acid-Reducing Agents on Gastrointestinal Physiology and Design of Biorelevant Dissolution Tests to Reflect These Changes. *J Pharm Sci.* 2019;108(11):3461-3477. doi:10.1016/j.xphs.2019.06.021.
- 59 Thorburn J, Moir DD. Antacid therapy for emergency caesarean section. *Anaesthesia.* 1987;42(4):352-355. doi:10.1111/j.1365-2044.1987.tb03973.x.
- 60 Troy DB. *Remington: The science and practice of pharmacy / David B. Troy, editor.* 21st ed. Philadelphia, PA, London: Lippincott; 2006.
- 61 *Remington: The science and practice of pharmacy.* 21st ed. London: Pharmaceutical Press, UK distributor: Stationery Office; 2011.
- 62 Chubineh S, Birk J. Proton pump inhibitors: the good, the bad, and the unwanted. *South Med J.* 2012;105(11):613-618. doi:10.1097/SMJ.0b013e31826efbea.
- 63 Brunton LL, Chabner B, Knollman BC, Goodman LS. *Goodman & Gilman's The pharmacological basis of therapeutics.* 12th ed. / editor, Laurence L. Brunton associate editors, Bruce A. Chabner, Bjorn C. Knollmann. New York, N.Y., London: McGraw-Hill; 2011.
- 64 Food and Drug Administration. The Drug Development Process. <https://www.fda.gov/patients/learn-about-drug-and-device-approvals/drug-development-process>. Accessed July 3, 2021.
- 65 Bruschi ML. *Strategies to modify the drug release from pharmaceutical systems: 2 - Modification of drug release.* 1st edition. Waltham MA: Elsevier; 2015.
- 66 Manikandan P, Nagini S. Cytochrome P450 Structure, Function and Clinical Significance: A Review. *Curr Drug Targets.* 2018;19(1):38-54. doi:10.2174/1389450118666170125144557.
- 67 Zanger UM, Schwab M. Cytochrome P450 enzymes in drug metabolism: regulation of gene expression, enzyme activities, and impact of genetic variation. *Pharmacol Ther.* 2013;138(1):103-141. doi:10.1016/j.pharmthera.2012.12.007.
- 68 European Medicines Agency. Investigation of drug interactions. <https://www.ema.europa.eu/en/investigation-drug-interactions>. Updated June 4, 2021.
- 69 Food and Drug Administration. In Vitro Drug Interaction Studies — Cytochrome P450 Enzyme- and Transporter-Mediated Drug Interactions: Guidance for Industry. <https://www.fda.gov/media/134582/download>. Accessed June 4, 2021.
- 70 Food and Drug Administration. Evaluation of Gastric pH-Dependent Drug Interactions With Acid-Reducing Agents: Study Design, Data Analysis, and Clinical Implications Guidance for Industry: Draft Guidance for Industry. <https://www.fda.gov/media/144026/download>. Accessed June 4, 2021.
- 71 European Medicines Agency. Guideline on the investigation of drug interactions. https://www.ema.europa.eu/en/documents/scientific-guideline/guideline-investigation-drug-interactions-revision-1_en.pdf. Accessed June 4, 2021.
- 72 European Medicines Agency. Guideline on the investigation of bioequivalence. https://www.ema.europa.eu/en/documents/scientific-guideline/guideline-investigation-bioequivalence-rev1_en.pdf. Accessed July 3, 2021.
- 73 Kaur P, Jiang X, Duan J, Stier E. Applications of In Vitro-In Vivo Correlations in Generic Drug Development: Case Studies. *AAPS J.* 2015;17(4):1035-1039. doi:10.1208/s12248-015-9765-1.
- 74 Jones HM, Chen Y, Gibson C, et al. Physiologically based pharmacokinetic modeling in drug discovery and development: a pharmaceutical industry perspective. *Clin Pharmacol Ther.* 2015;97(3):247-262. doi:10.1002/cpt.37.
- 75 Gamsjäger H, Lorimer JW, Scharlin P, Shaw DG. Glossary of terms related to solubility (IUPAC Recommendations 2008). *Pure and Applied Chemistry.* 2008;80(2):233-276. doi:10.1351/pac200880020233.

- 76 Atkins PW, Paula J de. *Atkins' Physical chemistry*. 7th ed. Oxford, New York: Oxford University Press; 2002.
- 77 Yalkowsky SH, Banerjee S. *Aqueous solubility: Methods of estimation for organic compounds / Samuel H. Yalkowsky, Sujit Banerjee*. New York: Marcel Dekker; 1992.
- 78 Box KJ, Völgyi G, Baka E, Stuart M, Takács-Novák K, Comer JEA. Equilibrium versus kinetic measurements of aqueous solubility, and the ability of compounds to supersaturate in solution—a validation study. *J Pharm Sci*. 2006;95(6):1298-1307. doi:10.1002/jps.20613.
- 79 Baka E, Comer JEA, Takács-Novák K. Study of equilibrium solubility measurement by saturation shake-flask method using hydrochlorothiazide as model compound. *J Pharm Biomed Anal*. 2008;46(2):335-341. doi:10.1016/j.jpba.2007.10.030.
- 80 World Health Organisation. Protocol to conduct equilibrium solubility experiments for the purpose of pharmaceuticals classification system-based classification of active pharmaceutical ingredients for biowaiver: Revised draft for discussion. https://www.who.int/medicines/areas/quality_safety/quality_assurance/03_07_18_qas_17_69_9_rev_2_protocol_equilibrium_solubility_experiments.pdf?ua=1. Accessed June 19, 2021.
- 81 Glomme A, März J, Dressman JB. Comparison of a miniaturized shake-flask solubility method with automated potentiometric acid/base titrations and calculated solubilities. *J Pharm Sci*. 2005;94(1):1-16. doi:10.1002/jps.20212.
- 82 Plöger GF, Hofsäss MA, Dressman JB. Solubility Determination of Active Pharmaceutical Ingredients Which Have Been Recently Added to the List of Essential Medicines in the Context of the Biopharmaceutics Classification System-Biowaiver. *J Pharm Sci*. 2018;107(6):1478-1488. doi:10.1016/j.xphs.2018.01.025.
- 83 Johnson LR, Ghishan FK, Kaunitz JD, Merchant JL, Said HM, Wood JD. *Physiology of the Gastrointestinal Tract, Two Volume Set*. 5th ed. Burlington: Elsevier Science; 2012.
- 84 Kansy M, Senner F, Gubernator K. Physicochemical high throughput screening: parallel artificial membrane permeation assay in the description of passive absorption processes. *J Med Chem*. 1998;41(7):1007-1010. doi:10.1021/jm970530e.
- 85 Nagahara N, Tavelin S, Artursson P. Contribution of the paracellular route to the pH-dependent epithelial permeability to cationic drugs. *J Pharm Sci*. 2004;93(12):2972-2984. doi:10.1002/jps.20206.
- 86 van Breemen RB, Li Y. Caco-2 cell permeability assays to measure drug absorption. *Expert Opin Drug Metab Toxicol*. 2005;1(2):175-185. doi:10.1517/17425255.1.2.175.
- 87 Hidalgo IJ, Raub TJ, Borchardt RT. Characterization of the human colon carcinoma cell line (Caco-2) as a model system for intestinal epithelial permeability. *Gastroenterology*. 1989;96(3):736-749.
- 88 Mariadason JM, Rickard KL, Barkla DH, Augenlicht LH, Gibson PR. Divergent phenotypic patterns and commitment to apoptosis of Caco-2 cells during spontaneous and butyrate-induced differentiation. *J. Cell. Physiol*. 2000;183(3):347-354. doi:10.1002/(SICI)1097-4652(200006)183:3<347:AID-JCP7>3.0.CO;2-W.
- 89 Pham-The H, Cabrera-Pérez MÁ, Nam N-H, et al. In Silico Assessment of ADME Properties: Advances in Caco-2 Cell Monolayer Permeability Modeling. *Curr Top Med Chem*. 2018;18(26):2209-2229. doi:10.2174/1568026619666181130140350.
- 90 Angelis ID, Turco L. Caco-2 cells as a model for intestinal absorption. *Curr Protoc Toxicol*. 2011;Chapter 20:Unit20.6. doi:10.1002/0471140856.tx2006s47.
- 91 United States Pharmacopeial. Dissolution and Drug Release Tests. <https://www.usp.org/chemical-medicines/dissolution>. Accessed June 15, 2021.
- 92 Klein S. The use of biorelevant dissolution media to forecast the in vivo performance of a drug. *AAPS J*. 2010;12(3):397-406. doi:10.1208/s12248-010-9203-3.

- 93 Butler J, Hens B, Vertzoni M, et al. In vitro models for the prediction of in vivo performance of oral dosage forms: Recent progress from partnership through the IMI OrBiTo collaboration. *Eur J Pharm Biopharm.* 2019;136:70-83. doi:10.1016/j.ejpb.2018.12.010.
- 94 *USP 42 - NF 37 The United States Pharmacopeia and National Formulary 2019: Main edition plus Supplements 1 and 2.* 1. Auflage. Stuttgart: Deutscher Apotheker Verlag; 2018.
- 95 Mansuroglu Y, Dressman J. Investigation of Dissolution Performance of Hard Gelatin Capsule Products Using Various Sinkers. *Dissolution Technol.* 2020;27(3):21-32. doi:10.14227/DT270320P21.
- 96 Fiolka T, van den Abeele J, Augustijns P, Arora S, Dressman J. Biorelevant Two-Stage In Vitro Testing for rDCS Classification and in PBPK Modeling-Case Example Ritonavir. *J Pharm Sci.* 2020;109(8):2512-2526. doi:10.1016/j.xphs.2020.04.023.
- 97 Klein S, Shah VP. A standardized mini paddle apparatus as an alternative to the standard paddle. *AAPS PharmSciTech.* 2008;9(4):1179-1184. doi:10.1208/s12249-008-9161-6.
- 98 Mirza T, Joshi Y, Liu Q, Vivilecchia R. Evaluation of Dissolution Hydrodynamics in the USP, Peak™ and Flat-Bottom Vessels Using Different Solubility Drugs. *Dissolution Technol.* 2005;1(1):11-16. doi:10.14227/DT120105P11.
- 99 Beckett A, Quach TT. Improved Hydrodynamics for USP Apparatus 2. *Dissolution Technol.* 1996;3:7-18.
- 100 Fiolka T, Dressman J. Development, current applications and future roles of biorelevant two-stage in vitro testing in drug development. *J Pharm Pharmacol.* 2018;70(3):335-348. doi:10.1111/jphp.12875.
- 101 Berlin M. *Predicting Oral Absorption of Poorly Soluble Weakly Basic Drugs.* Göttingen: Cuvillier Verlag; 2015.
- 102 Mann J, Dressman J, Rosenblatt K, et al. Validation of Dissolution Testing with Biorelevant Media: An OrBiTo Study. *Mol Pharm.* 2017;14(12):4192-4201. doi:10.1021/acs.molpharmaceut.7b00198.
- 103 Fiolka T. *Biorelevant two-stage in vitro tools to evaluate supersaturation and precipitation of weakly basic drugs.* Frankfurt am Main. 2020.
- 104 Komasa T, Dressman J. Simulation of oral absorption from non-bioequivalent dosage forms of the salt of raltegravir, a poorly soluble acidic drug, using a physiologically based biopharmaceutical modeling (PBBM) approach. *Eur J Pharm Sci.* 2021;157:105630. doi:10.1016/j.ejps.2020.105630.
- 105 Kostewicz ES, Wunderlich M, Brauns U, Becker R, Bock T, Dressman JB. Predicting the precipitation of poorly soluble weak bases upon entry in the small intestine. *J Pharm Pharmacol.* 2004;56(1):43-51. doi:10.1211/0022357022511.
- 106 Grimm M, Koziol M, Kühn J-P, Weitschies W. Interindividual and intraindividual variability of fasted state gastric fluid volume and gastric emptying of water. *Eur J Pharm Biopharm.* 2018;127:309-317. doi:10.1016/j.ejpb.2018.03.002.
- 107 Kourentas A, Vertzoni M, Barmapsalou V, et al. The BioGIT System: a Valuable In Vitro Tool to Assess the Impact of Dose and Formulation on Early Exposure to Low Solubility Drugs After Oral Administration. *AAPS J.* 2018;20(4):71. doi:10.1208/s12248-018-0231-8.
- 108 Kourentas A, Vertzoni M, Symillides M, et al. In vitro evaluation of the impact of gastrointestinal transfer on luminal performance of commercially available products of posaconazole and itraconazole using BioGIT. *Int J Pharm.* 2016;515(1-2):352-358. doi:10.1016/j.ijpharm.2016.10.018.
- 109 Carino SR, Sperry DC, Hawley M. Relative bioavailability estimation of carbamazepine crystal forms using an artificial stomach-duodenum model. *J Pharm Sci.* 2006;95(1):116-125. doi:10.1002/jps.20495.

- 110** Barker R, Abrahamsson B, Kruusmägi M. Application and validation of an advanced gastrointestinal in vitro model for the evaluation of drug product performance in pharmaceutical development. *J Pharm Sci.* 2014;103(11):3704-3712. doi:10.1002/jps.24177.
- 111** Hopgood M, Reynolds G, Barker R. Using Computational Fluid Dynamics to Compare Shear Rate and Turbulence in the TIM-Automated Gastric Compartment With USP Apparatus II. *J Pharm Sci.* 2018;107(7):1911-1919. doi:10.1016/j.xphs.2018.03.019.
- 112** Kostewicz ES, Abrahamsson B, Brewster M, et al. In vitro models for the prediction of in vivo performance of oral dosage forms. *Eur J Pharm Sci.* 2014;57:342-366. doi:10.1016/j.ejps.2013.08.024.
- 113** Schick P, Sager M, Voelker M, Weitschies W, Koziolok M. Application of the GastroDuo to study the interplay of drug release and gastric emptying in case of immediate release Aspirin formulations. *Eur J Pharm Biopharm.* 2020;151:9-17. doi:10.1016/j.ejpb.2020.03.013.
- 114** Schick P, Sager M, Wegner F, et al. Application of the GastroDuo as an in Vitro Dissolution Tool To Simulate the Gastric Emptying of the Postprandial Stomach. *Mol Pharm.* 2019;16(11):4651-4660. doi:10.1021/acs.molpharmaceut.9b00799.
- 115** Weinberg S. *Dreams of a final theory.* 1st Vintage books ed. New York: Vintage Books; 1994.
- 116** Papoulis A, Pillai SU. *Probability, random variables, and stochastic processes.* 4th ed. Dubuque, Iowa: McGraw-Hill; 2002.
- 117** Wang J, Flanagan DR. General solution for diffusion-controlled dissolution of spherical particles. 1. Theory. *J Pharm Sci.* 1999;88(7):731-738. doi:10.1021/js980236p.
- 118** *The Simcyp™ In Vitro Data Analysis (SIVA) Toolkit.*
- 119** Kostewicz ES, Aarons L, Bergstrand M, et al. PBPK models for the prediction of in vivo performance of oral dosage forms. *Eur J Pharm Sci.* 2014;57:300-321. doi:10.1016/j.ejps.2013.09.008.
- 120** *Simcyp™ PBPK Simulator.*
- 121** Netzer P, Brabetz-Höfliger A, Bründler R, Flogerzi B, Hüsler J, Halter F. Comparison of the effect of the antacid Rennie versus low-dose H₂-receptor antagonists (ranitidine, famotidine) on intragastric acidity. *Aliment Pharmacol Ther.* 1998;12(4):337-342. doi:10.1046/j.1365-2036.1998.00316.x.
- 122** Sulz MC, Manz M, Grob P, Meier R, Drewe J, Beglinger C. Comparison of two antacid preparations on intragastric acidity--a two-centre open randomised cross-over placebo-controlled trial. *Digestion.* 2007;75(2-3):69-73. doi:10.1159/000102627.
- 123** Powell RL, Westlake WJ, Longaker ED, Greene LC. A clinical evaluation of a new concentrated antacid. I. Effects on gastric pH. *J Clin Pharmacol New Drugs.* 1971;11(4):288-295.
- 124** Lin MS, Sun P, Yu HY. Evaluation of buffering capacity and acid neutralizing-pH time profile of antacids. *J Formos Med Assoc.* 1998;97(10):704-710.
- 125** Feldman M. Comparison of the effects of over-the-counter famotidine and calcium carbonate antacid on postprandial gastric acid. A randomized controlled trial. *JAMA.* 1996;275(18):1428-1431.
- 126** O'Sullivan GM, Bullingham RE. The assessment of gastric acidity and antacid effect in pregnant women by a non-invasive radiotelemetry technique. *Br J Obstet Gynaecol.* 1984;91(10):973-978. doi:10.1111/j.1471-0528.1984.tb03673.x.
- 127** Begemann F, Schumpelick V, Bandomer G. Adsorption of bile acids and lysolecithin by antacids. *Scand J Gastroenterol Suppl.* 1981;67:191-193.
- 128** Guthäuser UJ, Häcki WH. Bindung von Gallensalzen und Lysolecithin in physiologischen Medien durch verschiedene Antazida. *Schweiz Med Wochenschr.* 1987;117(9):322-327.
- 129** Weberg R, Berstad A. Symptomatic effect of a low-dose antacid regimen in reflux oesophagitis. *Scand J Gastroenterol.* 1989;24(4):401-406. doi:10.3109/00365528909093066.

- 130** Caspary WF, Kausch H. Effects of bile acids, antacids, and cholestyramine on transmural electrical potential difference in man. *Acta Hepatogastroenterol (Stuttg)*. 1978;25(5):369-375.
- 131** PIPER DW, FENTON B. The adsorption of pepsin. *Am J Dig Dis*. 1961;6:134-141. doi:10.1007/BF02231799.
- 132** Sepelyak RJ, Feldkamp JR, Regnier FE, White JL, Hem SL. Adsorption of pepsin by aluminum hydroxide II: Pepsin inactivation. *J Pharm Sci*. 1984;73(11):1517-1522. doi:10.1002/jps.2600731105.
- 133** Bendsten F, Rune SJ. Effect of a single dose of antacid on gastric and duodenal bulb pH in duodenal ulcer patients. *Scand J Gastroenterol*. 1988;23(8):935-940. doi:10.3109/00365528809090150.
- 134** Wisher D. Martindale: The Complete Drug Reference. 37th ed. *J Med Libr Assoc*. 2012;100(1):75-76. doi:10.3163/1536-5050.100.1.018.
- 135** Richardson CT, Walsh JH, Hicks MI. The effect of cimetidine, a new histamine H₂-receptor antagonist, on meal-stimulated acid secretion, serum gastrin, and gastric emptying in patients with duodenal ulcer. *Gastroenterology*. 1976;71(1):19-23.
- 136** Dubin SA, Silverstein PI, Wakefield ML, Jense HG. Comparison of the effects of oral famotidine and ranitidine on gastric volume and pH. *Anesth Analg*. 1989;69(5):680-683.
- 137** Narchi P, Edouard D, Bourget P, Otz J, Cattaneo I. Gastric fluid pH and volume in gynaecologic out-patients. Influences of cimetidine and cimetidine-sodium citrate combination. *Eur J Anaesthesiol*. 1993;10(5):357-361.
- 138** Seraj MA, El-Nakeeb MM, Estafan MY, et al. The preoperative use of cimetidine in reducing acidity of gastric secretion. *Middle East J Anaesthesiol*. 1980;5(7):445-455.
- 139** Litou C, Vertzoni M, Goumas C, et al. Characteristics of the Human Upper Gastrointestinal Contents in the Fasted State Under Hypo- and A-chlorhydric Gastric Conditions Under Conditions of Typical Drug - Drug Interaction Studies. *Pharm Res*. 2016;33(6):1399-1412. doi:10.1007/s11095-016-1882-8.
- 140** Litou C, Psachoulas D, Vertzoni M, Dressman J, Reppas C. Measuring pH and Buffer Capacity in Fluids Aspirated from the Fasted Upper Gastrointestinal Tract of Healthy Adults. *Pharm Res*. 2020;37(3):42. doi:10.1007/s11095-019-2731-3.
- 141** Domschke W, Lux G, Domschke S. Furan H₂-antagonist ranitidine inhibits pentagastrin-stimulated gastric secretion stronger than cimetidine. *Gastroenterology*. 1980;79(6):1267-1271.
- 142** Gupta RW, Tran L, Norori J, et al. Histamine-2 receptor blockers alter the fecal microbiota in premature infants. *J Pediatr Gastroenterol Nutr*. 2013;56(4):397-400. doi:10.1097/MPG.0b013e318282a8c2.
- 143** Shah R, Richardson P, Yu H, Kramer J, Hou JK. Gastric Acid Suppression Is Associated with an Increased Risk of Adverse Outcomes in Inflammatory Bowel Disease. *Digestion*. 2017;95(3):188-193. doi:10.1159/000455008.
- 144** Brown KE, Knoderer CA, Nichols KR, Crumby AS. Acid-Suppressing Agents and Risk for *Clostridium difficile* Infection in Pediatric Patients. *Clin Pediatr (Phila)*. 2015;54(11):1102-1106. doi:10.1177/0009922815569201.
- 145** Nylund CM, Eide M, Gorman GH. Association of *Clostridium difficile* infections with acid suppression medications in children. *J Pediatr*. 2014;165(5):979-84.e1. doi:10.1016/j.jpeds.2014.06.062.
- 146** Tleyjeh IM, Abdulhak AB, Abdulhak AAB, et al. The association between histamine 2 receptor antagonist use and *Clostridium difficile* infection: a systematic review and meta-analysis. *PLoS One*. 2013;8(3):e56498. doi:10.1371/journal.pone.0056498.

- 147** Brunton LL, Hilal-Dandan R, Knollmann BC, Goodman LS. *Goodman & Gilman's the pharmacological basis of therapeutics*. Thirteenth edition / editor-in-chief, Laurence L. Brunton editors, Randa Hilal-Dandan, Björn C. Knollman. New York: McGraw-Hill Education; 2018.
- 148** Kirchheiner J, Glatt S, Fuhr U, et al. Relative potency of proton-pump inhibitors-comparison of effects on intragastric pH. *Eur J Clin Pharmacol*. 2009;65(1):19-31. doi:10.1007/s00228-008-0576-5.
- 149** Shin JM, Sachs G. Pharmacology of proton pump inhibitors. *Curr Gastroenterol Rep*. 2008;10(6):528-534. doi:10.1007/s11894-008-0098-4.
- 150** Babaei A, Bhargava V, Aalam S, Scadeng M, Mittal RK. Effect of proton pump inhibition on the gastric volume: assessed by magnetic resonance imaging. *Aliment Pharmacol Ther*. 2009;29(8):863-870. doi:10.1111/j.1365-2036.2009.03947.x.
- 151** Steingoetter A, Sauter M, Curcic J, et al. Volume, distribution and acidity of gastric secretion on and off proton pump inhibitor treatment: a randomized double-blind controlled study in patients with gastro-esophageal reflux disease (GERD) and healthy subjects. *BMC Gastroenterol*. 2015;15:111. doi:10.1186/s12876-015-0343-x.
- 152** Kamiya T, Shikano M, Tanaka M, et al. The effect of omeprazole on gastric myoelectrical activity and emptying. *J Smooth Muscle Res*. 2011;47(3-4):79-87. doi:10.1540/jsmr.47.79.
- 153** Michalek W, Semler JR, Kuo B. Impact of acid suppression on upper gastrointestinal pH and motility. *Dig Dis Sci*. 2011;56(6):1735-1742. doi:10.1007/s10620-010-1479-8.
- 154** Sanaka M, Yamamoto T, Kuyama Y. Effects of proton pump inhibitors on gastric emptying: a systematic review. *Dig Dis Sci*. 2010;55(9):2431-2440. doi:10.1007/s10620-009-1076-x.
- 155** Castellani C, Singer G, Kashofer K, et al. The Influence of Proton Pump Inhibitors on the Fecal Microbiome of Infants with Gastroesophageal Reflux-A Prospective Longitudinal Interventional Study. *Front Cell Infect Microbiol*. 2017;7:444. doi:10.3389/fcimb.2017.00444.
- 156** Fujimori S. What are the effects of proton pump inhibitors on the small intestine? *World J Gastroenterol*. 2015;21(22):6817-6819. doi:10.3748/wjg.v21.i22.6817.
- 157** Jackson MA, Goodrich JK, Maxan M-E, et al. Proton pump inhibitors alter the composition of the gut microbiota. *Gut*. 2016;65(5):749-756. doi:10.1136/gutjnl-2015-310861.
- 158** Imhann F, Bonder MJ, Vich Vila A, et al. Proton pump inhibitors affect the gut microbiome. *Gut*. 2016;65(5):740-748. doi:10.1136/gutjnl-2015-310376.
- 159** Le Bastard Q, Al-Ghalith GA, Grégoire M, et al. Systematic review: human gut dysbiosis induced by non-antibiotic prescription medications. *Aliment Pharmacol Ther*. 2018;47(3):332-345. doi:10.1111/apt.14451.
- 160** Minalyan A, Gabrielyan L, Scott D, Jacobs J, Piseigna JR. The Gastric and Intestinal Microbiome: Role of Proton Pump Inhibitors. *Curr Gastroenterol Rep*. 2017;19(8):42. doi:10.1007/s11894-017-0577-6.
- 161** Oshima T, Wu L, Li M, Fukui H, Watari J, Miwa H. Magnitude and direction of the association between *Clostridium difficile* infection and proton pump inhibitors in adults and pediatric patients: a systematic review and meta-analysis. *J Gastroenterol*. 2018;53(1):84-94. doi:10.1007/s00535-017-1369-3.
- 162** Takagi T, Naito Y, Inoue R, et al. The influence of long-term use of proton pump inhibitors on the gut microbiota: an age-sex-matched case-control study. *J Clin Biochem Nutr*. 2018;62(1):100-105. doi:10.3164/jcbn.17-78.
- 163** Trifan A, Stanciu C, Girleanu I, et al. Proton pump inhibitors therapy and risk of *Clostridium difficile* infection: Systematic review and meta-analysis. *World J Gastroenterol*. 2017;23(35):6500-6515. doi:10.3748/wjg.v23.i35.6500.

- 164** The Ministry of Health, Labour and Welfare. *The Japanese pharmacopoeia: Official from April 1, 2016 : English version*. 17th edition. Tokyo: Pharmaceutical and Medical Device Regulatory Science Society of Japan; Yakuji Nippo (Hatsubai); 2016.
- 165** Segregur D, Mann J, Moir A, Karlsson EM, Dressman J. Prediction of plasma profiles of a weakly basic drug after administration of omeprazole using PBPK modeling. *Eur J Pharm Sci*. 2021;158:105656. doi:10.1016/j.ejps.2020.105656.
- 166** Segregur D, Barker R, Mann J, et al. Evaluating the impact of acid-reducing agents on drug absorption using biorelevant in vitro tools and PBPK modeling - case example dipyridamole. *Eur J Pharm Sci*. 2021;160:105750. doi:10.1016/j.ejps.2021.105750.
- 167** Food and Drug Administration. Chemistry Review(s): Application Number: 22-145. https://www.accessdata.fda.gov/drugsatfda_docs/nda/2007/022145_ChemR.pdf. Accessed July 10, 2021.
- 168** Segregur D, Mann J, Moir A, Karlsson EM, Dressman J. Biorelevant in vitro tools and in silico modelling to assess pH-dependent drug-drug interactions for salts of weak acids: case example potassium raltegravir. *J Pharm Sci*. 2021. doi:10.1016/j.xphs.2021.09.037.
- 169** Psachoulas D, Vertzoni M, Goumas K, et al. Precipitation in and supersaturation of contents of the upper small intestine after administration of two weak bases to fasted adults. *Pharm Res*. 2011;28(12):3145-3158. doi:10.1007/s11095-011-0506-6.
- 170** Pathak SM, Schaefer KJ, Jamei M, Turner DB. Biopharmaceutic IVIVE-Mechanistic Modeling of Single- and Two-Phase In Vitro Experiments to Obtain Drug-Specific Parameters for Incorporation Into PBPK Models. *J Pharm Sci*. 2019;108(4):1604-1618. doi:10.1016/j.xphs.2018.11.034.
- 171** Klumpp L, Dressman J. Physiologically based pharmacokinetic model outputs depend on dissolution data and their input: Case examples glibenclamide and dipyridamole. *Eur J Pharm Sci*. 2020;151:105380. doi:10.1016/j.ejps.2020.105380.
- 172** Ricevuti G, Mazzone A, Pasotti D, et al. Pharmacokinetics of dipyridamole-beta-cyclodextrin complex in healthy volunteers after single and multiple doses. *Eur J Drug Metab Pharmacokinet*. 1991;16(3):197-201. doi:10.1007/BF03189959.
- 173** Derendorf H, VanderMaelen CP, Brickl R-S, MacGregor TR, Eisert W. Dipyridamole bioavailability in subjects with reduced gastric acidity. *J Clin Pharmacol*. 2005;45(7):845-850. doi:10.1177/0091270005276738.
- 174** Russell TL, Berardi RR, Barnett JL, O'Sullivan TL, Wagner JG, Dressman JB. pH-related changes in the absorption of dipyridamole in the elderly. *Pharm Res*. 1994;11(1):136-143. doi:10.1023/a:1018918316253.
- 175** Koziol M, Grimm M, Becker D, et al. Investigation of pH and Temperature Profiles in the GI Tract of Fasted Human Subjects Using the Intellicap[®] System. *J Pharm Sci*. 2015;104(9):2855-2863. doi:10.1002/jps.24274.
- 176** Iwamoto M, Wenning LA, Nguyen B-Y, et al. Effects of omeprazole on plasma levels of raltegravir. *Clin Infect Dis*. 2009;48(4):489-492. doi:10.1086/596503.

7 Appendix

7.1 Publications

Publications in peer-reviewed journals:

Publication 1 (page 74)

Segregur, Domagoj; Flanagan, Talia; Mann, James; Moir, Andrea; Karlsson, Eva M.; Hoch, Matthias; Carlile, David; Sayah-Jeanne, Sakina; Dressman, Jennifer: Impact of Acid-Reducing Agents on Gastrointestinal Physiology and Design of Biorelevant Dissolution Tests to Reflect These Changes. *J Pharm Sci.* 2019;108(11):3461-3477. doi:10.1016/j.xphs.2019.06.021

Publication 2 (page 94)

Segregur, Domagoj; Mann, James; Moir, Andrea; Karlsson, Eva M.; Dressman, Jennifer: Prediction of plasma profiles of a weakly basic drug after administration of omeprazole using PBPK modeling. *Eur J Pharm Sci.* 2021;158:105656. doi:10.1016/j.ejps.2020.105656

Publication 3 (page 103)

Segregur, Domagoj; Barker, Richard; Mann, James; Moir, Andrea; Karlsson, Eva M.; Turner, David: Evaluating the impact of acid-reducing agents on drug absorption using biorelevant in vitro tools and PBPK modeling - case example dipyridamole. *Eur J Pharm Sci.* 2021;160:105750. doi:10.1016/j.ejps.2021.105750

Publication 4 (page 120)

Segregur, Domagoj; Mann, James; Moir, Andrea; Karlsson, Eva M.; Dressman, Jennifer: Biorelevant *in vitro* tools and *in silico* modelling to assess pH-dependent drug-drug interactions for salts of weak acids: case example potassium raltegravir. *J Pharm Sci.* 2021; doi:10.1016/j.xphs.2021.09.037

Posters:

Segregur D., Flanagan T., Mann J., Dressman J., “Impact of antacids on simulated gastric fluid properties” at APV 3rd European Conference on Pharmaceutics 2019, Bologna, Italy

Segregur D., Flanagan T., Mann J., Moir A., Karlsson E.M., Hoch M., Carlile D., Dressman J., “*In vitro* dissolution of a weak basic drug in standard biorelevant media and media representing PPI co-administration” at AAPS 2019 PharmSci 360, San Antonio, USA

Segregur D., Flanagan T., Karlsson E.M., Hoch M., Moir A., Carlile D., Mann J., Dressman J., “Acid-reducing effect of antacids in *in vitro* experiments”, at 8th IAPC Meeting 2019, Split, Croatia

Zöller L., Segregur D., Dressman J., Kostewicz E. S., “Design of an *in vitro* model (pH-Antacid-Test-Model) to simulate the gastrointestinal pH and motility profile following antacid administration”, at vPharmSci 2021

Personal contribution to the peer-reviewed publications:

Publication 1

Personal contribution to the first publication, Impact of Acid-Reducing Agents on Gastrointestinal Physiology and Design of Biorelevant Dissolution Tests to Reflect These Changes, includes the research and review of the literature data (together with Prof. Dressman and Dr. Sayar-Jeanne of DaVolterra), planning (together with Prof. Dressman) and execution of all *in vitro* experiments, evaluation and presentation of the data, as well as creating the first manuscript draft and improving the latter based on suggestions from co-authors and reviewers. Furthermore, personal contribution includes the original drawings of Figures 1 and 2.

Publication 2

Personal contribution to the second publication, Prediction of plasma profiles of a weakly basic drug after administration of omeprazole using PBPK modeling, includes the planning (together with Prof. Dressman and the AstraZeneca colleagues), validation and execution of all *in vitro* experiments, development and use of the PBPK model for predicting the plasma levels (together with Prof. Dressman and the AstraZeneca colleagues), validation, evaluation, comparison and visual representation of the data, as well as creation of the first draft of the publication and improvement of the same based on suggestions from co-authors and reviewers.

Publication 3

Personal contribution to the third publication, Evaluating the impact of acid-reducing agents on drug absorption using biorelevant *in vitro* tools and PBPK modeling - Case example dipyridamole, includes the planning (together with Prof. Dressman and the colleagues from AstraZeneca), validation and execution of all *in vitro* experiments, with the exception of TIM-1 experiments, which were planned, validated and carried out at AstraZeneca, Macclesfield. In addition, personal contribution includes the use of PBPK models, development of parameter sets for representation of the PPI / H2RA influence in the "dynamic intestinal pH model" together with David Turner from Simcyp, as well as evaluation, comparison and visual representation of the data, with an exception of data from the TIM-1 experiments (AstraZeneca). The first draft of the manuscript and improvement of the same based on the suggestions of co-authors and reviewers is also included in the personal contribution.

Publication 4

Personal contribution to the fourth publication, Biorelevant *in vitro* tools and *in silico* modelling to assess pH-dependent drug-drug interactions for salts of weak acids: case example potassium raltegravir, includes the planning (together with Prof. Dressman), validation and execution of all *in vitro* experiments, development of the modelling strategy for raltegravir dissolution under ARA therapy, as well as evaluation, comparison and visual representation of the data. The first draft of the manuscript and

improvement of the same on the suggestions of co-authors and reviewers is also included in the personal contribution.



Review

Impact of Acid-Reducing Agents on Gastrointestinal Physiology and Design of Biorelevant Dissolution Tests to Reflect These Changes

Domagoj Segregur¹, Talia Flanagan^{2,3}, James Mann², Andrea Moir²,
Eva M. Karlsson⁴, Matthias Hoch⁵, David Carlile⁵, Sakina Sayah-Jeanne⁶,
Jennifer Dressman^{1,*}

¹ Institute of Pharmaceutical Technology, J. W. Goethe University, 9 Max von Laue Street, 60438 Frankfurt, Germany

² Pharmaceutical Technology and Development, AstraZeneca UK Limited, Charter Way, Macclesfield, UK

³ Now employed at Product Development, UCB Pharma SA, Braine-l'Alleud, Belgium

⁴ Pharmaceutical Technology and Development, AstraZeneca SE, Pepparedsleden 1, 15185 Gothenburg, Sweden

⁵ Quantitative Clinical Pharmacology, AstraZeneca UK Limited, 1 Francis Crick Avenue, Cambridge, UK

⁶ Du Voltterra, 172 Rue de Charonne, 75011 Paris, France

ARTICLE INFO

Article history:
Received 30 May 2019
Revised 25 June 2019
Accepted 25 June 2019

Keywords:
gastrointestinal tract
pH
drug effect(s)
dissolution model(s)
biopharmaceutical characterization

ABSTRACT

Background: Of the various drug therapies that influence gastrointestinal (GI) physiology, one of the most important are the acid-reducing agents (ARAs). Because changes in GI physiology often influence the pharmacokinetics of drugs given orally, there is a need to identify *in vitro* methods with which such effects can be elucidated.

Objective: Literature concerning the effects of ARAs (antacids, H₂-receptor antagonists, and proton pump inhibitors [PPIs]) on GI physiology are reviewed with the aim of identifying conditions under which drugs are released after oral administration in the fasted state. *In vitro* dissolution tests to mimic the effects in the stomach were designed for H₂-receptor antagonists and PPIs.

Conclusions: The impact of ARAs on GI physiology depends on the type, duration, and amount of ARA administered as well as the location in the GI tract, with greatest impact on gastric physiology. While ARAs have a high impact on the gastric fluid pH and composition, changes in volume, viscosity, surface tension, and gastric emptying appear to be less profound. The proposed dissolution tests enable a ready comparison between dosage form performance in healthy adults and those receiving PPIs or H₂-receptor antagonists.

© 2019 American Pharmacists Association®. Published by Elsevier Inc. All rights reserved.

Introduction

The gastrointestinal (GI) tract is a complex organ involved primarily in food and fluid digestion and absorption but with additional roles in immunology, metabolism, and excretion. Not only is there considerable intraindividual and interindividual variability in GI physiology but also external factors such as drug therapy can further influence the physiology and functionality of the GI tract. In this article, we focus on the influence of acid-reducing agents (ARAs) on GI physiology and how the key changes can be modeled *in vitro*.

Conflicts of interest: The authors declare no conflicts of interest. This article contains supplementary material available from the authors by request or via the Internet at [10.1016/j.xphs.2019.06.021](https://doi.org/10.1016/j.xphs.2019.06.021).

* Correspondence to: Jennifer Dressman (Telephone: +49 69 7982 9680).

E-mail address: Dressman@em.uni-frankfurt.de (J. Dressman).

The treatment of acid peptic diseases has a long history.¹ The first treatments implemented in modern times were nonmedicinal therapies, for example, dietary modifications and even surgeries.² The aim of the dietary modifications such as the Sippy Diet³ was to neutralize the acidic content of the stomach, whereas surgeries such as the Billroth II surgery⁴ typically aimed to reduce acid secretion by removing the sections of the stomach that are predominantly responsible for acid secretion, that is, the distal stomach. Later, locally acting physical and pharmacological interventions were identified, and these eventually replaced the earlier strategies. The locally acting physical interventions include the antacids, which aim to neutralize the stomach acid, and sucralfate, which has some neutralizing capability but also forms a viscous material that protects the stomach mucosa from further contact with acid.⁵ With time, pharmacological interventions such

<https://doi.org/10.1016/j.xphs.2019.06.021>

0022-3549/© 2019 American Pharmacists Association®. Published by Elsevier Inc. All rights reserved.

as the anticholinergics, H₂ receptor antagonists (H₂RAs) and proton pump inhibitors (PPIs) were introduced, all of which aim to decrease or prevent gastric acid secretion. The statistics show that ARAs are now one of the most frequently sold and prescribed medicines in both the United States⁶ and the rest of the world.^{7,8} Although primarily intended to reduce symptoms associated with gastric acid (heartburn, reflux esophagitis, Barrett's esophagus, ulceration of the gastric, and/or duodenal mucosa, etc.), ARAs can also have an impact on therapy with other drugs, either through a direct effect on gastric pH or through metabolic interactions.

This review focuses on understanding the impact that different classes of ARAs and their dosing regimens have on the characteristics of GI physiology and, in turn, how these may influence drug release and absorption. Furthermore, the relevant changes in physiology are used to design *in vitro* dissolution media and tests that can be used to simulate the impact of PPIs and H₂RAs on the release of drugs from dosage forms administered in the fasted state.

Gastrointestinal Physiology—A Short Summary

Volume

In the fasted state, the stomach contents have a low resting volume. For example, Schiller et al.⁹ reported a mean value of 45 ± 18 mL using a magnetic marker method, confirming older literature summarizing the average fasted state gastric volume to be 50 mL.¹⁰ Although Ulleberg et al.¹¹ reported a higher average gastric volume of 87 mL, they also noted a high interindividual variability of ± 103 mL. There may be a gender effect on gastric volumes, as earlier studies by Hirschowitz et al.¹² suggested that the male fasted gastric volume is on average 20 mL larger than in females. In the fed state, as the gastric muscles relax in response to the meal entering the stomach, the volume of the gastric contents increases greatly. The filling capacity of the stomach was measured to be in the range 1000-2000 mL,¹³ while Schiller et al.⁹ reported volumes of gastric contents of up to 859 mL using a magnetic marker method.

Schiller et al.⁹ reported a small intestinal volume of 105 ± 72 mL in the fasted state, whereas in the fed state, the volume measured was lower, with an average of 54 ± 41 mL. Mudie et al.¹⁴, however, summarized the literature data on small intestinal volume and suggested that the volume of contents in the small intestine can range from 30-300 mL in the fasted state and 40-400 mL for the fed state. By contrast, in earlier times, when phenol red was used as a marker, volumes in the small intestine as large as 1250 mL were reported by Fordtran and Locklear after subjects consumed a hyperosmotic doughnuts and milk meal.¹⁵ Thus, there appear to be considerable discrepancies in measurements of intestinal volume in the fed state, depending on the methodology as well as the time at which the measurement was made after meal ingestion.

With respect to colonic volumes, Schiller et al. reported that food intake has no significant effect on the colonic volume of free water in the colon. They reported values of 13 ± 12 mL versus 11 ± 26 mL in fasted versus fed state, respectively.⁹ While the research by Diakidou et al.¹⁶ supports these findings (22.3 ± 7.7 mL vs. 29.9 ± 10.8 mL), other researchers reported average volumes of 170 mL¹⁷ (ascending colon) and 189 mL¹⁸ (cecum, ascending, and transverse colon). However, these values may reflect total fluid volume rather than the volume of free water.

pH

The gastric pH is mainly regulated by the secretion of gastric acid from parietal cells and the emptying of acid from the stomach. The functions of gastric acid derive from the low pH that is induced and include the denaturation of proteins, inactivation of

microorganisms, conversion of pepsinogen into its active form (pepsin), and provision of optimal conditions for pepsin activity, as well as facilitation of the absorption of polyvalent cations (Fe, Mg, Ca, etc.) and vitamin B12.^{19,20} A reduction in gastric acid secretion and hence an elevation of the pH increases the risk of infections,⁶ malabsorption of cations and vitamins, and furthermore, can have a significant impact on the dissolution and bioavailability of many drugs.²¹⁻²³

According to meta-analyses, the gastric pH in the fasted state in healthy individuals is maintained consistently between pH 1 and 3.^{14,24,25} In the fed state, the meal contents initially raise the stomach pH. The degree of elevation of the gastric pH will depend on the pH, buffer capacity, and quantity of the co-ingested fluids. For example, milk has a pH of around 6, while orange juice has a pH of around 3-3.5. The combination of meal emptying with time and concurrent additional acid secretion results in a gradual return to the baseline pH value. For these reasons, gastric pH values in the fed state cover a broader range,²⁶ generally reported as ranging from pH 3 to 7.^{14,24,25}

Small intestinal pH is, on the other hand, mainly regulated by bicarbonate secreted from the pancreas into the duodenum.¹⁴ As chyme and gastric acid empty from the stomach, the secretion of bicarbonate into the duodenum protects the mucosa from acidic erosion.²⁷ In both the fasted and fed state, the pH values cluster around pH 6 at the proximal end of the small intestine and climb gradually to around pH 7.5 by the distal end of the small intestine, before entering the large intestine.^{14,28}

While in the stomach and small intestine, pH regulation is achieved primarily by a balance between gastric acid and bicarbonate secretion, in the large intestine the pH is largely influenced by the colonic bacteria. At the beginning of the colon, a sharp decline in pH to around pH 5-6.5 from the terminal ileum value of around pH 7.5 is observed. This decline can be attributed to bacterial digestion and fermentation processes, which produce very short-chain fatty acids (acetate, propionate, etc.).²⁹ As the content moves further down the large intestine, the average pH value rises back up to approximately pH 7.²⁸

Viscosity

In the fasted state, the viscosity of gastric juice is low, around 1.5 cP.³⁰ Fed state viscosity in the stomach is highly variable, as it is highly dependent on the meal composition. Measurements of gastric juice viscosity in the fed state have been variously reported as 57 to 303 cP³¹ or 10 to 2000 cP.³² Changes in the viscosity of the gastric contents may decrease the rate of gastric emptying^{33,34} and thus influence the rate of absorption of highly soluble, highly permeable drugs. High gastric viscosity can also hinder/reduce tablet disintegration and drug release.^{35,36} Owing to the digestive process, involving the breakdown of macromolecular proteins and carbohydrates into their low molecular weight monomers and dimers, the viscosity in the upper small intestine is typically low even in the fed state, usually not exceeding values of 40 cP.³⁷

Owing to the re-uptake of water as the chyme moves along the GI tract, the large intestinal content is considerably more viscous and can be described as semi-solid.³⁸

Surface Tension

Gastric fluid surface tension shows a relatively broad range of values, from approximately 30 to 45 mN/m^{24,29,30} in the fasted state. Although there is only a modest bile acid reflux from the duodenum into the stomach, with gastric concentrations typically far less than 1 mM, these concentrations are sufficient to have an impact on the surface tension. In the fed state, the surface tension is

lower (30-31 mN/m) and less variable.³⁹ Although some bile reflux could also account partly for the reduction in surface tension in the fed state, a more plausible explanation for the low and consistent values of surface tension is the lipolysis of fatty meal components in the stomach, which produces monoglycerides and free fatty acids, both of which are strong surfactants.

In the fasted state, the surface tension in duodenum is similar to that of the gastric fluid (30-45 mN/m).^{39,40} In the jejunum, the surface tension is lower,²⁴ possibly because the bile salts are not absorbed as efficiently as other components, including water, from the upper intestine. In the fed state, the surface tension in the duodenum decreases to around 28 mN/m³⁹ as a result of the higher bile output in response to the meal.

Surface tension in the colon is higher than in the small intestine, most likely due to the almost complete re-absorption of bile acids from the small intestine due to passive re-uptake in the jejunum and active transport in the ileum. Diakidou et al.¹⁶ reported a slightly higher surface tension in the ascending colon in the fasted state (42.7 mN/m) than in the fed state (39.2 mN/m).

Gastrointestinal Motility

The residence time in a given segment of the GI tract is directly influenced by the GI motility. In turn, both the residence time and strength of contractions in the small intestine impact the efficiency and rate of absorption for drugs as well as nutrients. Decreased gastric motility and thus a slower emptying time can result in a decrease in the overall absorption rate, thus altering the pharmacokinetic profile of many drugs.²¹ In the fasted state, the motility pattern can be divided into 3 (sometimes 4) phases. Although motility is minimal in Phase I, which lasts about 45-60 min, contractions become more intense and frequent over a period of 30-45 min in Phase II, and then, approximately every 2 h, a short burst of forceful contractions (Phase III) clears the stomach contents into the intestine. The gastric residence time of a dosage form in the fasted state will therefore depend on which phase of the motility cycle is occurring when the administration takes place.

In the fed state, the stomach relaxes to accommodate the meal and the motility pattern in the upper GI tract that dominates in the fasted state is disrupted,⁴¹ replaced with contractions that mix the chyme with enzymes, bringing nutrients (and drugs) in close contact with the gut surface and thus improving absorption.⁴¹ The gastric content is gradually emptied as a result of the pressure gradient between the stomach and duodenum.¹⁹ Liquids are generally emptied from the stomach faster than solids.¹⁹ Early investigation of solid particles emptying using radiolabeled, spherical nondigestible particles indicated a dependency of emptying on both particle size and density.⁴² In those studies, a mean half-emptying time of 124 min was observed for 1 mm spheres and 211 min for 2.4 mm spheres,⁴² whereas digestible particles (radiolabeled liver cubes) were emptied faster, with a half-emptying time of 50 min for 0.3 cm³ and 70 min for 1 cm³ cubes.⁴³ As the gastric emptying rate is approximately 2-4 kcal/min in the fed state, the emptying time also depends on the type and size of the meal. In the small intestine, the frequency of basal contractile waves declines distally, with Scratcherd and Grundy reporting the duodenal frequency to be 11.8 cycles/min compared with an ileal frequency of 8 cycles/min in healthy adults.⁴¹ Thus, over time, the intestinal contractions facilitate movement of the gut contents in the aboral direction.

In the colon, the frequency of contractions is slower, about 2-4 cycles/min. Three basic contraction patterns can be recognized. In the ascending colon, contractions in the aboral as well as the oral direction drive the content backward and forward, resulting in mixing of the chyme remnants with secretions and bacteria. This

leads to a residence and mucosal contact time that is often longer than observed in the small intestine.¹⁹ Over time, peristalsis propels the content to the distal colon, and strong defecation contractions evacuate the content from the large intestine.^{38,41}

Secretion

Many substances are secreted into the stomach, including hydrochloric acid, enzymes (pepsinogen and lipase), intrinsic factor, electrolytes, and mucin. The gastric mucosa also secretes mediators, including neurocrine (acetylcholine), paracrine (histamine and somatostatin), and endocrine hormones (gastrin), all of which are involved in regulating stomach acid production and secretion.^{19,26,44} Gastric acid secretion is a continuous process,⁴⁴ with a basal acid output of 10 mmol/h in men and 8 mmol/h in women.¹⁹ The volume of basal acid secretion is reported to range from 26 to 100 mL/h.⁴⁵ Gastric acid secretion after a meal is typically initiated via both mechanical (pressure on the gastric wall) and chemical (histamine, acetylcholine, gastrin) triggers.^{19,46,47} Maximal acid output is a value usually obtained using exogenous activation of acid secretion and ranges from 10 to 50 mmol/h in men and 5 to 60 mmol in women.¹⁹ The maximum volumetric output of gastric acid was found to be 135-170 mL/h when induced by histamine.⁴⁵ Individuals with ulcer disease have an elevated basal secretion rate (102 mL/h), which can be more than doubled (to 250 mL/h) by administration of histamine.

Together with mucus, bicarbonate is secreted by the gastric mucosa to protect it from hydrochloric acid, pepsin, and other corrosive components of chyme. Compared with acid secretion, however, gastric bicarbonate secretion is much lower²⁷ and is only sufficient to neutralize the gastric acid locally in the mucosa.

Another important secreted component of gastric fluid are the (pro)enzymes. One of the most significant is pepsinogen, which is activated to pepsin at the low pH of the stomach.⁴⁸ Sanny et al.⁴⁹ stated that pepsinogen is converted to pepsin in as little as 2 min in an acidic medium. The breakdown of protein in the stomach by pepsin is not only important for food digestion but can also have an impact on drug formulations, for example gelatine capsules.⁵⁰ Concentrations of pepsin in the fasted stomach of around 0.1 mg/mL have been reported by several authors, with an average increase in the pepsin concentration to 0.3-0.6 mg/mL in the fed state.^{39,51,52} Peptic activity is highly pH dependent. A pH of 2 is optimal for pepsin's proteolytic activity. An increase up to pH 4 has little or no negative effect on peptic activity, but if the pH rises above 5, the proteolytic activity falls steeply, with complete inactivation of the protease at pH 8.⁵³

Among the electrolytes in gastric juice, sodium and chloride are the most concentrated. Chloride ions are secreted from parietal cells as hydrochloric acid in a concentration of approximately 75 mEq/L to 160 mEq/L, with the concentration rising as a function of the secretion rate. Sodium ions, on the other hand, are secreted directly from the surface epithelium. Sodium secretion is influenced by histamine stimulation, and the concentration in secretions ranges from approximately 19 to 70 mEq/L.⁵⁴

In the small intestine, the majority of secretion takes place in the duodenum. The pancreas secretes bicarbonate into the duodenum at concentrations up to 10-fold higher than the concentrations that are secreted in the stomach.²⁷ Besides protecting the mucosal surface, bicarbonate secretion in the duodenum is also required to neutralize the acidic fluids entering from the stomach. One of the main factors regulating bicarbonate secretion is the contact of the mucosa with luminal acid.²⁷

While secretin stimulates excretion of fluid and bicarbonate, cholecystokinin stimulates enzyme release from the pancreas. While lipases and amylase are secreted in their active forms to

catalyze the digestion of fat and polysaccharides, respectively, the proteases are secreted as proenzymes (trypsinogen, chymotrypsinogens, and procarboxypeptidase A and B). Trypsin cleaves the amino acid sequence at lysine or arginine residues, whereas chymotrypsins hydrolyze the amino acid sequence at phenylalanine and tyrosine residues, and carboxypeptidases cleave the C-terminal amino acid of proteins/peptides. Human amylase cleaves the α -1 \rightarrow 4-glucoside bonds of polysaccharides into maltose, isomaltose, and glucose. Along with the reduction of proteins to amino acids and oligopeptides, cleavage of polysaccharides into their individual components results in a marked decrease in viscosity of the luminal contents.

Lipases hydrolyze triglycerides to diglycerides and monoglycerides as well as free fatty acids. However, owing to the lipophilicity of their substrates, lipases only have a strong effect in the presence of surfactants, such as the bile salts.⁵⁵ While the pH optimum of gastric lipase is reported to be about pH 5,⁵⁶ pancreatic lipase has an optimal activity at pH 8, similar to those for the pancreatic proteases and amylase (pH 6.9-8).^{55,57}

Pancreatic basal secretion is calculated to be approx. 1 mL/min, with concentrations of approximately 1 mg/mL chymotrypsin, 0.2 mg/mL trypsin, 0.18 mg/mL carboxypeptidase, 0.13 mg/mL amylase, and 600 IU/mL lipase. After stimulation with cholecystokinin, pancreas secretion volume rises to around 3.1 mL/min, with outputs of 3 mg/min chymotrypsin, 0.73 mg/min trypsin, 0.72 mg/min carboxypeptidase A, 0.62 mg/min amylase, and 1650 IU/min lipase.⁵⁵

Along with the pancreatic secretions, bile is also secreted into the duodenum. The bile acids and lecithin (which is quickly and almost completely cleaved to lysolecithin and fatty acid) have several important functions in digestion and drug absorption. On the one hand, they solubilize lipophilic substances present in the GI fluids, thereby enhancing the dissolution of poorly soluble, lipophilic food components and drugs. On the other hand, they improve the contact of enzymes with lipids by emulsifying them into fine droplets for larger contact area, which in turn enhances the enzymatic efficiency.⁵⁸ The lower interfacial tension generated by the bile salts also promotes "wetting" of hydrophobic solid drug particles. Therefore, bile acids not only have an important effect on food and fluid digestion but also a great impact on the availability of poorly soluble drugs for absorption.^{26,59} The basal concentration of bile acids in the human small intestine (i.e., in the fasted state) is approximately 3 mM.^{39,60,61} Although a much broader range of values (1-86 mM)^{14,39} has been reported for the fed state, values of around 10-15 mM have been most consistently reported.^{24,62}

Microflora

The number of bacteria in the human GI tract is estimated to be 100 trillion.⁶³ There is a notable interindividual variability in the types of microflora found in the gut, whereas the composition in a given individual stays relatively stable.⁶⁴ While the oral cavity has its own established microbial ecosystem, few bacteria can survive the acidic environment of the stomach, and gastric motility patterns ensure evacuation of most of those that do. By contrast, the large intestine is a region where microbiota thrive, and this region accounts for the largest bacterial population in the gut.⁶⁵ The small intestine represents a transition zone, with few bacteria at the proximal end and increasing numbers in the ileum as it approaches the large intestine. It has been suggested that the microbiota may play an important role in drug and formulation dissolution as well as metabolism in the colon, as they influence the pH of the fluids and secrete diverse enzymes impacting the biotransformation and stability of drugs.⁶³

The stomach was at one time described as a sterile compartment because its highly acidic environment is unfavorable for most bacteria. However, because it was discovered that *Helicobacter pylori* can inhabit the stomach, the existence of a microbial ecosystem in the stomach is now discussed.⁶⁶ Studies have shown the stomach to host approximately 1000 CFU/g,⁶³ although it is yet not clear if most of the bacteria are just passing through the gastric region or are permanent colonizers.⁶⁷ Of the identified bacteria, the impact of *H. pylori* has been investigated in most detail, as it is often a cause of acute and chronic gastritis and because gastric and duodenal ulcers are usually associated with *H. pylori* infection.^{6,68}

Over the length of the small intestine, the number of colony-forming units (CFUs) per gram rises from 10⁴ CFU/g in the duodenum to 10⁷ CFU/g in the distal ileum.⁶³ Small intestinal bacterial overgrowth is defined by a bacterial count exceeding 10⁵-10⁶/mL in the proximal part of the small intestine.⁶⁷

Up to 10 trillion (10¹³) CFU/mL can be found in the large intestine,^{63,64} which also has the most diverse array of microbiota. More than 400 different bacterial species had already been identified in the human colon in the 1980s.⁶⁴ In the meantime, many more species have been identified, and current estimates exceed 500 species.⁶⁹ A change in the microbiome of the GI tract can lead to dramatic effects on the GI physiology.⁶⁴ In particular, when bacteria such as *Escherichia coli*, *H. pylori*, and *Clostridium difficile* colonize the GI tract, this can lead to a series of diseases and their unpleasant accompanying symptoms.⁷⁰

Acid-reducing Agents and Their Effects on GI Physiology

Antacids

Early on, it was recognized that to treat gastric acid/peptic diseases, neutralization of acid in the stomach would be necessary,⁴⁴ and the first drugs identified for this purpose were the antacids.² In fact, antacids are still in broad use,⁷¹ remaining popular on account of their fast onset of action, competitive pricing, and overall ease of use,¹ especially because they are readily available over-the-counter (Table 1). As well as being used in self-medication, they are also prescribed as a pretreatment for some operations, for example emergency cesarean section, to guard against acid aspiration.⁷²

Gastric Acidity

Antacids are the only ARAs that impact the pH of the gastric fluid directly.⁷³ Depending on the neutralizing capacity of the respective antacid, the fasted gastric pH can be raised to values of pH 3.5 to 5 and or even higher.^{76,77} The reference benchmark for efficacy (pH 3.5) originates from the USP 20 (1980), which defined the acid-neutralizing ability of antacids through a preliminary antacid test. According to the USP test, the minimal pH of the solution after antacid addition had to be raised to at least pH 3.5, and several articles have relied on this or a similar criterion for antacid performance.⁷⁸ Although the current official USP 41 (2018) no longer describes an antacid effectiveness test as such, pH 3.5 is still listed as the criterion in the acid-neutralizing capacity test.⁷⁹ Studies have shown that while some antacids on the market are able to elevate the pH to over pH 6 (depending on dose), others failed to raise the pH to 3.5.^{76,80}

After antacid administration the elevation in pH can occur rapidly, in as few as 6 min.⁸¹ But the antacids have a short duration of effect. Following a single dose of antacids, such as calcium carbonate, basic magnesium carbonate or magnesium, and aluminum hydroxide, the elevation in gastric pH is typically maintained for a period of 30-60 min, after which the pH returns to its basal acidic level.^{77,82-84} The duration of the antacid effect is limited by the continuous gastric acid secretion, which counteracts the

Table 1
Types of Antacids Grouped According to the Main Cation^{a,73-75}

| Type | Antacid Species | Structure |
|----------------------|--|--|
| Sodium/ potassium | Sodium bicarbonate | NaHCO ₃ |
| | Sodium citrate | Na ₃ C ₆ H ₅ O ₇ |
| | Potassium bicarbonate | KHCO ₃ |
| Calcium | Calcium carbonate | CaCO ₃ |
| | Bismuth | Al ₃ BiO ₆ |
| Bismuth | Bismuth salicylate | BiOH-salicylate |
| | Bismuth subcarbonate | (BiO) ₂ CO ₃ |
| | Bismuth subnitrate | Bi ₂ O(OH) ₂ (NO ₃) ₄ |
| | Magnesium | MgCO ₃ |
| Magnesium | Magnesium carbonate | MgCO ₃ |
| | Magnesium hydroxide | Mg(OH) ₂ |
| | Magnesium oxide | MgO |
| | Magnesium trisilicate | Mg ₂ Si ₃ O ₈ |
| Aluminum | Basic magnesium carbonate | Mg(OH) ₂ , MgCO ₃ |
| | Aceglutamide aluminum | C ₂₁ H ₃₃ AlN ₆ O ₁₂ |
| | Alexitol sodium | Na.x(AlOH)CO ₃ -hexitol complex |
| | Aloglutamol | Trometamolgluconate Al |
| | Aluminum glycinate | C ₇ H ₆ AlNO ₄ |
| | Aluminum hydroxide | Al(OH) ₃ |
| | Aluminum phosphate | AlPO ₄ |
| | Aluminum sodium silicate | Sodium silicoaluminate |
| | Basic aluminum carbonate | Al(OH) ₃ , Al ₂ (CO ₃) ₃ |
| | Carbaldrate | NaCO ₃ Al(OH) ₂ |
| Combination | Sucralfate | Sucrose sulfate-Al complex |
| | Almagate | AlMg ₃ (CO ₃)(OH) ₇ ·2H ₂ O |
| | Almasilate | Al ₂ O ₃ ·MgO·2SiO ₂ ·xH ₂ O |
| | Hydrotalcite | Mg ₆ Al ₂ (OH) ₁₆ CO ₃ ·4H ₂ O |
| | Magaldrate | Al ₃ Mg ₁₀ (OH) ₃₁ (SO ₄) ₂ ·xH ₂ O |
| | Almasilat | Al, Mg silicatehydrate |
| | Aluminum hydroxide- magnesium carbonate co-dried gel | Al(OH) ₃ ·MgCO ₃ |

^a Additional substances often used in combination with the antacids—milk powder, glycine, simeticone, and alginate.

neutralizing effect of the antacid, and by gastric emptying, which empties the antacid from the stomach over time.⁷⁷ As the antacid effect is temporary, taking a single dose after a meal will not effectively counter gastric acidity between meals.⁸⁵ Thomson et al.⁸⁶ confirmed that antacid therapy only has a prolonged effect if doses are given at regular intervals.

As there are several kinds of antacids, each with different properties, their effects on gastric pH cannot be completely generalized.⁸⁰ Furthermore, data about the effect of antacids on gastric pH in the literature are mostly from early studies, with large ranges of values reported and inconsistency among reports. Moreover, studies on antacid products have often compared different types of antacids in different formulations and at different dosages, and the results can be interpreted in different ways. For example, sodium hydrogen carbonate antacid drugs were reported to be the antacids with the highest neutralizing effect.⁷⁶ However, this conclusion was based on the administered milligram dose rather than the neutralization capacity of the pure antacid substance. If the results were to be interpreted in terms of neutralization capacity, magnesium hydroxide would have the highest neutralization capacity among the common antacids (47.45 ± 0.65 mEq HCl/g), whereas sodium bicarbonate would have the lowest (12.3 ± 0.20 mEq HCl/g).⁷⁶

The formulation of the antacid can also have an effect on its onset and duration of gastric acid neutralization, with liquid antacids not surprisingly showing on average a faster onset and greater increase in pH than tablet formulations.^{74,82} Tablet preparations disintegrate and react more slowly⁸⁷ and thus may act longer.⁷⁷ Especially if the tablet (or its disintegrated fragments) is held back longer in the stomach (e.g., if the patient has a slow gastric emptying pattern or has eaten a very large meal), the antacid will

also remain longer in the stomach and exhibit its effect over a longer period.⁸³

With regard to the effect of antacids on duodenal pH, Bendsten and Rune found that a liquid antacid combination (magnesium oxide and aluminum oxide) 2 h after a meal had a more pronounced effect on intestinal than on gastric pH in patients with duodenal ulcer disease. While the gastric pH in the study rose from 1 to 2 to pH 3 and then reacidified completely within 60 min, the pH at the duodenal bulb after one dose of antacid rose from 2.5 to around pH 5-6.⁸⁸

Gastric and Intestinal Volumes

As antacids are usually taken after a meal,⁷³ data on their influence on gastric volume are mostly focused on the fed state. In the fed state, the fluid volume increases more when using antacids. This is postulated to be a "rebound" reaction of the stomach which results in additional acid secretion to counteract the antacid effect.⁸⁹ An increase in gastric volume facilitates the dissolution process, and in some cases, this could lead to a greater availability of the drug for absorption. Nader et al.⁹⁰ reported enhanced dissolution of drugs when a larger volume of water was ingested with capsules, which resulted in lower variability in C_{max} values, although there was no significant impact on the extent of absorption.

In the intestines, the effect of antacid administration is contingent on which type of antacid is administered. For example, aluminum-based antacids have an adstringent effect, which may lead to a lower volume of intestinal fluid available for drug dissolution, whereas the osmotic pressure generated by dissolution of magnesium hydroxide-based antacids in gastric acid may pull water from the surroundings into the intestine and thus raise the intestinal volume.⁷³

Viscosity

There is little information in the literature about the impact of antacids on the viscosity of the GI fluids. What information exists is usually directed at the effect of sucralfate on the viscosity of the gastric mucus because its main mechanism of action is to raise the viscosity of the mucus layer close to the ulcer to protect it against further degradation by hydrochloric acid and pepsin. Slomiany et al.^{91,92} demonstrated that at a concentration of 1 mM sucralfate in the stomach, the viscosity of the mucus was raised by 60%. Additionally, Gröbel et al.⁹³ reported that liquid antacids elevate the viscosity of the gastric mucus, while a solid antacid (pulverized tablet) lowered the mucosal viscosity.

Binding of Surfactants

Next to their acid neutralizing effect, *in vitro* studies have shown that antacids can bind natural surfactants, with both bile acids and lysolecithin being rapidly adsorbed onto antacid formulations. While lysolecithin is reported to be strongly adsorbed (85%-100%),^{94,95} regardless of the type of antacid, bile acids appear to be better adsorbed by antacids containing aluminum,⁹⁴⁻⁹⁶ from as little as 20% to as much as 75%.^{94,95} Lipsett and Gadacz reported a more detailed investigation into the dependency of bile salt binding by antacids as a function of bile salt structure. The highest percentages adsorbed onto aluminum and magnesium antacids were reported for deoxycholate and taurocholate (47.4% and 32.5%, respectively), with cholate and taurodeoxycholate (10% and 14.6%, respectively) being adsorbed the least. Interestingly, no adsorption of cholate and deoxycholate onto sucralfate was reported, whereas taurocholate and taurodeoxycholate were extensively adsorbed (47.5% and 61%, respectively) by this substance.⁹⁷ Another *in vitro* study, by Kurtz et al.⁹⁸ in 1991, suggested that the degree of adsorption for a complex layered antacid (hydrotalcite) correlates

with bile acid lipophilicity. The consequence of a high degree of adsorption of lysolecithin and bile salts onto antacids is expected to be an increase in the surface tension of the GI fluids and a reduction in wetting and micellar solubilization of poorly soluble drugs.

GI Motility and Gastric Emptying

Raising the pH of the stomach is expected to increase gastrin activity, thus increasing gastric motility.⁷⁴ This effect is, however, more likely to be of importance for therapy with other ARAs, because the effect of antacid on gastric pH is short-lived. Hurwitz et al.⁹⁹ administered multiple doses of a liquid aluminum hydroxide antacid in the fasted state and measured an increase in half emptying time from 13.1 to 48 min, while a combination of magnesium trisilicate and aluminum hydroxide antacid resulted in only a minimal increase (to 17.3 min).

In the fed state, the increase in emptying time owing to antacid administration is more difficult to evaluate because gastric emptying is slower after meal intake and ranges from approximately 3 to 4 h.⁸⁹

In addition to effects on gastric emptying, some metal ions contained in antacids can affect intestinal transit. Magnesium preparations in higher concentrations act as laxatives. The effect is for the most part caused by the osmotic effect of magnesium salts, but a possible direct effect on intestinal motility has also been discussed.^{100,101} These changes may alter the exposure of compounds with slow dissolution and/or low permeability. Aluminum compounds, on the other hand, can cause constipation owing to their ability to relax smooth muscle,^{74,102} leading to a decrease in intestinal motility and thus providing more time for water reabsorption. The opposing effects of aluminum and magnesium salts are often used to advantage in combination antacid preparations with the aim of reducing individual side-effects.

Secretions

Antacids are recommended only as a short-term medication against dyspeptic complaints because their chronic use can induce a rebound effect, stimulating secretion of more hydrochloric acid. This rebound effect is often observed after the withdrawal of long-term antacid treatment.⁷⁴ Antacids containing calcium carbonate release calcium ions into the gastric fluid, which may also stimulate additional acid secretion.⁷⁴ Antacids may also inhibit bicarbonate secretion because the bicarbonate secretion rate is dependent on the acid concentration in the stomach.

If antacids are underdosed or have a low neutralization capacity, they will increase the pH of the medium only slightly up to around pH 2, which is the optimum for peptic activity. However, if the antacid is used at a dose which raises the pH to 5 or above, pepsin activity in the stomach and hence protein digestion will be inhibited. Furthermore, like bile acids, pepsin has a tendency to adsorb onto antacids. The presence of poorly soluble antacids in the stomach provides a solid matrix onto which pepsin can be adsorbed and inactivated.^{96,103-105} Although it is not yet clear whether the main mechanism of pepsin inactivation by antacids is pH change, precipitation, or adsorption,¹⁰⁶ a comparative study concluded that antacids reduce pepsin concentrations somewhat more than H₂RAs.⁸⁵

Microflora

Although antacids can increase the gastric pH to a value at which bacteria are not inactivated and may pass intact into the small intestine,¹⁰⁷ the gastric acid neutralizing effect is brief, most likely leading to a less significant effect on the microbiota of the intestine compared with longer acting H₂RAs and PPIs. Nevertheless, studies have shown that chronic use of antacids can raise postprandial microbial titer¹⁰⁸ in the same way as H₂RAs, which, in turn could lead to the spread of different bacteria and a shift in the

intestinal microbial diversity. Some *in vitro* experiments using a model GI tract have suggested an association between translocation of *Pseudomonas aeruginosa*, *Staphylococcus aureus*, and *E. coli* through the gut and elevation of pH by antacids,¹⁰⁹ with better survival of vibrio bacteria and phages in the presence of antacids.¹¹⁰

Histamine Type 2 Receptor Antagonists

Another approach to reducing gastric acid is to inhibit the transmission pathway of parietal cells.¹¹¹ Histamine, gastrin, and acetylcholine all stimulate acid secretion.⁴⁷ Histamine, as a neurotransmitter, plays an important and complex role in the regulation of GI processes,^{20,112-114} and among other functions, it stimulates the secretion of hydrochloric acid into the stomach. Histamine type 2 receptor antagonists (H₂RAs) competitively bind to the histamine receptors on gastric parietal cells, displacing histamine and thus inhibiting acid secretion (Fig. 1).¹⁰⁰

The first compound shown to inhibit type 2 histamine receptors selectively was burimamide,¹¹¹ and in 1976, cimetidine was introduced as the first H₂RA on the prescription drug market.² Common H₂RAs are cimetidine, ranitidine, famotidine,¹⁰⁰ as well as lafutidine and nizatidine.⁷³ Of the H₂RAs, cimetidine is the least potent, but because it was the first to be introduced, it is used as the common denominator to express relative potencies in this drug class. Thus, ranitidine has a relative potency 4-8 times higher than that of cimetidine, whereas the relative potency of famotidine is 20-50 times higher than that of cimetidine.¹⁰⁰ H₂RAs were for many years the standard therapy for a number of diseases connected to dyspepsia and GI ulcers. With the introduction of PPIs, the latter replaced H₂RAs as the first-line therapy. Nevertheless, the H₂RAs are still widely used (Table 2).

Gastric Acidity

Most of the research conducted to date on the impact of H₂RAs on GI physiology has focused on changes in gastric pH and volume. H₂RAs selectively and competitively inhibit parietal cell acid secretion,¹¹¹ thus raising the pH of the gastric fluid. Similar to the research on antacids, the efficacy of an H₂RA is judged by a somewhat arbitrary increase in pH, in this case according to whether the gastric pH is raised to over 2.5.¹¹¹ In this case, the critical pH value most likely stems from the need to prevent acid aspiration during surgery and is based on the minimum elevation in pH deemed necessary prior to administering the anesthetic and performing the operation.¹¹⁸ Extrapolating from animal experiments, it was calculated that 25 mL or more of gastric fluid with a pH of 2.5 or less must be aspirated before lung damage is significant.^{111,119} Numerous studies on both animals and humans have shown conclusively that H₂RAs are consistently able to elevate the pH above pH 2.5.¹¹⁸⁻¹²³

The usual elevation of gastric pH by H₂RAs is much greater, but few studies have reported maximum pH values achieved so it is difficult to generalize, especially because the studies have often been conducted with different doses of H₂RAs (of different potencies) administered by different routes of administration. The usual mean pH values achieved have been variously reported as pH 3-4,¹²⁴ 5.25,¹²⁵ and around pH 6,^{119,126} noting that there is also high inter-individual fluctuation in the pH response, with variations during the day, whereas the mean values cited are calculated on a 24 h basis. Alternatively, it has been reported that gastric acid secretion is reduced by 42%-55%^{127,128} with a maximal inhibition of up to 94%¹²⁹ for cimetidine, 33%-90% for ranitidine,^{128,130} and 60% for famotidine.¹²⁷ A further study reported that the overall night time proton concentration was reduced by 70% to 90% after administration of several different H₂RAs at corresponding doses.¹³¹

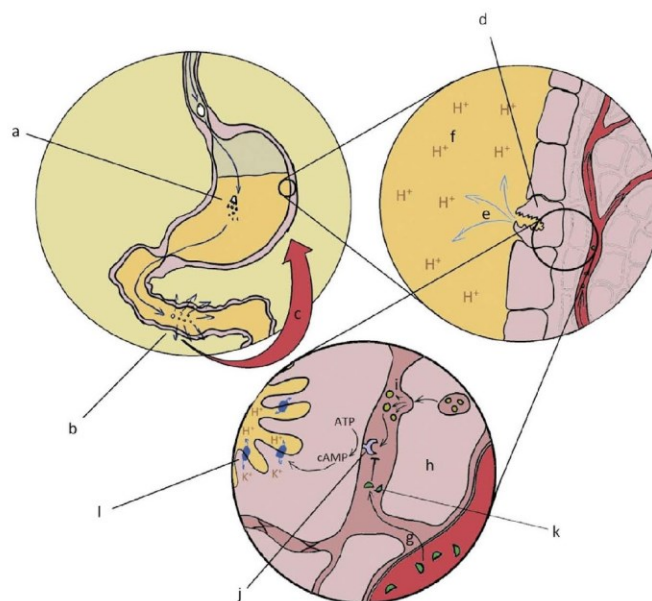


Figure 1. H₂RA mechanism of action. Dissolution of the H₂RA from the dosage form (a), followed by absorption of the H₂RA (b) and distribution via blood (c). Parietal cell (d), acid secretion (e), gastric lumen (f), absorption of the H₂RA into the epithelial intercellular space (g), enterochromaffin-like cell (h) with vesicles containing histamine, and secretion of histamine (i). Histamine activates the H₂ receptor (j), whereas H₂RA (k) competitively inhibits the receptor, stopping the activation of transmission pathway and proton pumps (l) inside the cell.

Compared with antacids, the lag time before the onset of gastric pH elevation is longer when administering oral H₂RAs (65-90 min vs. 6-30 min),^{81,84} so for example there may be some delay in relief of heartburn when H₂RAs are administered. On the other hand, the duration of acid-reducing effect is reported to be at least 7 h,¹²⁹ much longer than for antacids.^{81,132} Also when administered in the fed state, H₂RAs reduced gastric acidity significantly more than antacids, maintaining a high pH over a longer time.⁸⁵

Interestingly, Hirota et al.¹²³ found that chronic use of H₂RAs may induce tolerance, with the pH response weakening upon repeated dosing.

Gastric Volume

Although the elevation of pH by H₂RAs has consistently been confirmed in the literature, studies on the impact of H₂RAs on gastric volume have not always arrived at the same conclusion. Most studies have concluded that H₂RAs lower gastric volume, although some have found no significant impact.¹¹¹ Just as histamine stimulates gastric secretion,²⁰ H₂RAs significantly reduce it.^{118-121,126,130,131,133-135} Damman et al.¹³¹ reported a reduction in

total night time gastric volume of 40%-50%, whereas Dumin et al. demonstrated a decrease in the average resting gastric volume from 19.9 mL to 7.8 mL in the fasted state after twice daily administration of famotidine and to 11.3 mL after twice daily administration of ranitidine.¹¹⁹ Another study reported a decrease in the gastric volume of 37% in healthy individuals during H₂RA therapy.¹³⁰ But, there are also a few studies in the literature which have reported no significant effect of H₂RAs on gastric volume.^{122,125}

It is possible that the extent of H₂RA impact on secretion volume differs between healthy and diseased subjects. Meeroff et al. showed that histamine stimulates gastric volume basal secretion, raising secretion rate of healthy individuals from approximately 26-100 mL/h to 135-170 mL/h. In patients with ulcers, the basal volume secretion was raised even higher, from 102 mL/h to 250 mL/h.⁴⁵

Whether or not the decrease in gastric volume is maintained over chronic dosing has not been conclusively studied. One study suggested that gastric volume is initially decreased but then returns to pretreatment values as a consequence of developing tolerance.¹²³

Viscosity

As H₂RAs inhibit gastric acid secretion and thereby appear to reduce the gastric volume, it seems credible that H₂RAs could raise the viscosity of the gastric juice. In connection with this hypothesis, it has been shown that nonselective antihistamines inhibit secretion of saliva, thus increasing the viscosity of the saliva.¹³⁶ On the other hand, an *in vitro* investigation reported that less mucin was secreted from the intestinal epithelial cells treated with cimetidine, which in return would lower the gut viscosity.¹³⁷ As data on the impact of H₂RAs on GI fluid viscosity are sparse, no conclusions can be reached at present concerning this parameter.

Table 2

Currently Used H₂RAs^{44,73,115-117}

| H ₂ RA Species | Usual Dosage |
|---------------------------|-----------------------|
| Cimetidine | 400 mg BD, 800 mg OAD |
| Ranitidine | 150 mg BD, 300 mg OAD |
| Famotidine | 20 mg BD, 40 mg OAD |
| Nizatidine | 150 mg BD, 300 mg OAD |
| Roxatidine | 75 mg BD, 150 mg OAD |
| Lafutidine | 10 mg BD |

OAD, once a day; BD, twice a day.

Surface Tension

Potential changes in the surface tension of the GI fluids after administration of H₂RAs have only been investigated in terms of effects on bile output. Kaminski et al. reported that histamine stimulates bile volume in dogs. Thus, a histamine receptor inhibitor could potentially decrease bile output. Indeed, when metiamide was administered concurrently with histamine, the bile volume decreased.¹¹⁴ Because bile components are secreted at concentrations generally well above the critical micelle concentration, it seems unlikely that the decrease in bile output due to H₂RA therapy would be large enough to change in surface tension of GI fluids. Indeed, other authors have noted that H₂RAs are mostly described as potent gastric antisecretory agents which have no impact on postprandial gastric pancreatic and biliary functions.¹²⁸

Motility and Gastric Emptying

Diverse effects of H₂RAs on gastric emptying and intestinal motility have been reported in the literature, with studies mostly demonstrating a decrease or no impact of H₂RAs on the gastric emptying rate in humans.^{138,139}

Parkman et al.¹³⁸ found a significant increase in the mean overall 3 h postprandial antral motility index after administration of H₂RAs. These authors also reported that ranitidine and famotidine delay gastric emptying (gastric retention for ranitidine was 46% and for famotidine 41% vs. 27% for placebo). Koskenpato et al. likewise reported that gastric emptying time in the fed state in humans is prolonged by H₂RAs (110.1 vs. 65.6 min). This group differentiated between solids, for which prolonged residence was observed, and liquids, for which gastric emptying was unchanged.¹⁴⁰ By contrast, Richardson et al.¹²⁹ found cimetidine to have no effect on gastric emptying in patients with duodenal ulcers, and this was confirmed for low doses.¹⁴¹ Other researchers have similarly reported that H₂RAs have no impact on gastric emptying rate.^{128,142} Nizatidine was shown to have a prokinetic effect, but this was attributed to its cholinergic properties.¹⁴⁰

Secretions

Histamine stimulates pepsin secretion via H₂ receptors,¹¹³ so an inhibitory effect of H₂RAs on pepsin secretion is expected. Domschke et al.¹³⁹ showed that H₂RA infusion can lower pepsin concentration to 42% of the usual gastric concentration in untreated healthy volunteers. Mohammed et al.¹⁴³ also found a reduction of pepsin concentration, with concentrations of pepsin in H₂RA-treated patients reaching only 61%-65% of the concentrations in control patients (i.e., those not receiving H₂RAs) at the beginning of therapy and only 50% when treated over a longer time-frame. The inhibition of pepsin secretion was shown to be dose-dependent,¹³⁴ with the secretion rate lowered from 200 kU/h to 83 kU/h at a 300 mg dose of cimetidine and to 74 kU/h at a dose of 5 mg famotidine.¹²⁷ Sewing et al.¹³³ likewise showed a dose-dependent decrease in pepsin secretion by ranitidine and cimetidine.

As histamine stimulates also electrolyte secretion,²⁰ histamine receptor antagonists may have an impact on ion concentrations. Although canine data have shown that gastric Na⁺ concentration is elevated and Cl⁻ concentration is reduced after application of H₂RAs,¹⁴⁴ there are no available data in humans for changes in concentration of these ions.

In humans, pancreatic enzyme output was reported to be unaltered by H₂RA administration.¹²⁸

Microflora

As H₂RAs have a strong and prolonged effect on the acidity of gastric juice, it might reasonably be expected that the microbiome would flourish in the stomach in patients receiving long-term H₂RA therapy. While most of the research on the impact of ARAs on

microbiota has been carried out on newer ARAs, that is the PPIs, there have been a few reports linking intragastric bacterial proliferation to H₂RAs.⁶⁴ Newer publications on the impact of H₂RAs report a link to decreased microbial diversity and a shift toward specific bacterial phylum in infants,¹⁴⁵ to a significantly increased risk of *C. difficile* infection in children and adults,¹⁴⁶⁻¹⁴⁸ and to an overall increased risk of inflammatory bowel disease.¹⁴⁹

Proton Pump Inhibitors

Over the past 20 years, the prescription frequency of PPIs has risen more than 22-fold.¹⁵⁰ PPIs are one of the most prescribed classes of drugs in the world.⁶ Their widespread use is also promoted by the availability of numerous generic versions on the market and the resultant decrease in price,⁶⁸ as well as their availability as over-the-counter self-medication at certain doses and pack sizes. It is thus safe to say that PPIs will continue to play a leading role in the therapy of dyspepsia, GERD, *H. pylori* positive and negative ulcers, hypersecretory conditions (e.g., Zollinger Ellison syndrome), and as prophylaxis during long-term NSAID therapy in the future.^{6,53,151}

Compared with other ARAs, PPIs are more effective and less affected by external influences, as they inhibit the hydrogen pumps in parietal cells directly at the end of the common pathway for hydrochloric acid secretion.^{44,68,144} When PPIs come into contact with the acidic medium of the parietal cell secretory canaliculi,¹⁵² they inhibit the proton pumps by producing a covalent bond to H⁺/K⁺-ATPase (Fig. 2).⁴⁴ Up to 70% of the active proton pumps can be inhibited by just one dose.⁶ Although PPIs have short half-lives in plasma (60-90 min), the acid-reducing effect may last up to 24 h because the inhibition of proton pumps is irreversible and will prevent secretion until new proton pumps are synthesized.⁶ The reduction in acid secretion is not immediate, with the onset of action taking approximately 3 to 5 days compared with within 30 min for most antacids and several hours for H₂RAs.^{81,84}

While the intensity of H₂RA-inhibition of gastric acid secretion is mostly dose-dependent, the intensity of the PPI effect is more time-dependent, that is reliant on continual intake during the first few days of therapy to ensure maximum and maintained inhibition of the proton pumps. Therefore H₂RAs are often regarded as more effective in preoperative treatment,¹⁵³ where a rapid onset of action is highly desirable.

The first PPI to enter the market was omeprazole, and for this reason, it is the PPI that has been studied most.¹⁵² By the mid-2010s, there were 6 PPIs approved by the FDA and on the market. These are omeprazole, esomeprazole, lansoprazole, dexlansoprazole, pantoprazole, and rabeprazole.¹⁵¹

As omeprazole was the first PPI introduced, it is commonly used as the standard for comparing PPI potency. Esomeprazole behaves similarly to omeprazole¹⁵⁴ except that it has a faster onset of action.¹⁵⁵ Rabeprazole is one of the most potent PPIs, not only showing a longer and greater increase in pH but also a faster onset compared with most other PPIs.¹⁵² Rabeprazole is, however, also the most acid labile PPI. Pantoprazole stands at the other end of the potency scale and also has the longest onset of action (Table 3).^{6,156}

PPIs differ in their interaction potential with CYP enzymes. In general, PPIs are mostly metabolized via CYP 2C19 and CYP 3A4.¹⁵¹ Omeprazole is most extensively metabolized by CYP2C19, thus having the strongest interaction potential with drugs metabolized by this enzyme.^{44,150,151} Pantoprazole is metabolized partly through a non-CYP-related pathway and thus has the lowest interaction potential for CYP enzymes of the PPIs.^{151,155,165}

As PPIs are rapidly inactivated in acidic environments, they are formulated as enteric-coated formulations.¹⁶⁶ PPIs have a more

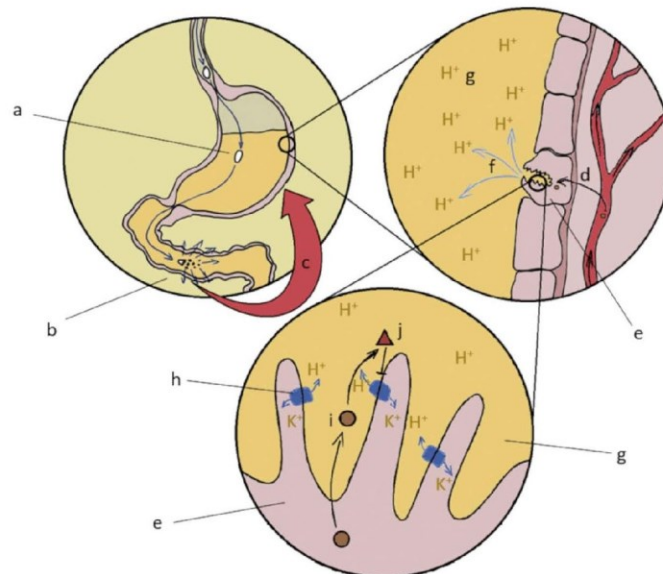


Figure 2. PPI mechanism of action. Enteric-coated formulation (a), dissolution and absorption of the PPI (b), distribution via blood (c), absorption of the PPI into the gastric epithelium (d), parietal cell (e), acid secretion (f), gastric lumen (g), proton pump (h), and PPI (i) is converted into the active form (j), which inhibits the proton pump.

complete and longer lasting effect on suppression of acid secretion than H_2 RAs, so they can be dosed once daily.^{68,167} In the Prescribers Information, it is recommended to take PPIs in the morning before breakfast.

Gastric Acidity

Of the ARAs, PPIs are the most potent inhibitors of gastric acid. As PPIs show the strongest inhibition on proton pumps that are active, the acid-reducing effect is most profound in situations where acidic secretion is stimulated, such as in the fed state or in *H. pylori* infection.¹⁵² Early studies showed that the gastric pH rises on average higher after meal ingestion during PPI therapy than in healthy individuals without PPI therapy (pH 6–7 vs. pH 5) and also remains elevated for a longer time.^{168–170}

Table 3
PPIs Currently on the Market and Their Usual Oral Daily Doses^{4,66,75,157}

| PPI Species | Dose (mg) | | | | |
|-----------------------------|--------------------|---------------------|--------------------|--------------------|-----------------------|
| | WHO ¹⁵⁸ | NICE ¹⁵⁹ | AGA ¹⁶⁰ | WGO ¹⁶¹ | Other |
| Omeprazole | 20 | 20 | 20 | 20 | – |
| Esomeprazole | 30 | 20 | 40 | 40 | – |
| Pantoprazole | 40 | 40 | 40 | 40 | – |
| Lansoprazole | 30 | 30 | 30 | 30 | – |
| Dexlansoprazole | 30 | – | – | 60 | – |
| Rabeprazole | 20 | 20 | 20 | 20 | – |
| Dexrabeprazole ^b | – | – | – | – | 10 ¹⁶² |
| Ilaprazole ^b | – | – | – | – | 10, 20 ¹⁶³ |
| S-Pantoprazole ^b | – | – | – | – | 20 ¹⁶⁴ |

Minus sign indicates the absence of component.

WHO, World Health Organization; NICE, National Institute for Health and Care Excellence; AGA, American Gastroenterological Association; WGO, World Gastroenterology Organization.

^a Higher doses may be required for the treatment of Zollinger-Ellison syndrome.
^b Only available in selected countries.

The majority of studies on PPIs, especially from more recent times, apply the time above pH 4 as the standard for efficacy of an orally dosed PPI, although a few apply the time above pH 3 as the criterion.^{151,152,171} For intravenously dosed PPIs, the standard is usually pH 6.^{171,172} In 2009, Kirchheiner et al.¹⁵⁶ published an extensive review of the effects of PPIs on intragastric pH. While the overall fasted state gastric pH after a single dose of a PPI rose to pH 3, values after multiple dose administration showed significantly higher intragastric pH values, with usual values in the area of pH 4 to 6 and a few studies recording mean values of over pH 6. A recent report underlined Kirscheiner's conclusion that the average fasted state gastric pH of patients taking PPIs is around pH 5.¹⁷³ Only in studies which applied extremely high doses of PPIs orally or applied PPIs intravenously have results deviated from those reviewed by Kirscheiner, showing a faster and more complete inhibition of proton pump activity.

According to a 2017 review, PPIs can elevate gastric pH to over pH 4 for up to 15 to 21 h.¹⁵¹ A study by Miner et al.¹⁷⁴ which directly compared different PPIs with respect to their average duration of acid suppression concluded that esomeprazole has the longest duration of 14 h, followed by rabeprazole (12.1 h), omeprazole (11.8 h), and pantoprazole with 10.1 h (Fig. 3).

Although there have been many studies of PPI effects on gastric pH, literature data are scarce with respect to the carryover effect on intestinal pH. Omeprazole was shown to result in higher rates of proximal duodenal mucosal bicarbonate secretion compared with H_2 RAs.¹⁷⁵ Combined with the higher pH of fluids entering the duodenum from the stomach, this might result in a higher pH in the upper small intestine. On the other hand, Michalek et al.¹⁷⁶ observed a shift in pH to lower values in the distal small intestine (from approximately pH 7.7 without, to pH 7.2 during PPI therapy) and discussed the possibility that a change in microbiome is responsible for this decrease.

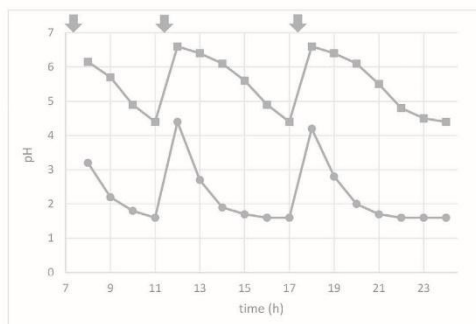


Figure 3. Typical gastric pH profile without (●) and during chronic PPI administration (■). Meal ingestion is indicated by an arrow.

Gastric Volume

Most studies of PPI effects on the volume of gastric fluids have shown a decrease in this parameter. A study by Steingoetter et al. investigated the effect of PPIs on gastric secretion and thus on gastric volume. This study determined the *maximal* secretion volume in fasted, healthy subjects and in GERD patients to be approximately 200 mL. Dosing 40 mg pantoprazole daily for 1 week reduced this maximal secretion volume by 93 ± 20 mL.¹⁷⁷ Babaei et al. reported that the postprandial gastric volume during therapy with PPIs was slightly, but statistically significantly, reduced compared with control subjects not receiving PPI therapy. These researchers compared the gastric volume of a control group before and after administration of a standard meal (85 ± 29 mL prior to a meal vs. 437 ± 41 mL 90 min after the meal) with the gastric volume in the fasted and fed state in subjects receiving 40 mg esomeprazole twice daily for 1 week (78 ± 25 mL prior to a meal vs. 398 ± 16 mL at 90 min after the meal).¹⁷⁸ It has also been shown that the average fasted state gastric fluid volume of Japanese patients was significantly lower while taking a combination of H₂RAs and PPIs (10 mg omeprazole/rabeprazole or 15 mg lansoprazole for 4 weeks plus 2 doses of 75 mg roxatidine) than when receiving a placebo.¹⁷⁹

Although the effects of common H₂RA and PPIs on the gastric volume before surgery were at first thought to be equal,¹⁸⁰ a subsequent study suggested that PPIs can further elevate the gastric pH and lower the gastric volume in the fasted state when administered to patients already on H₂RA therapy.¹⁸¹

Viscosity of Gastric Fluids

The impact of PPIs on the viscosity of gastric mucus has not been extensively investigated, and results are contradictory. While Goddard and Spiller reported that the viscosity of fasted gastric fluid falls after application of PPIs (from an average of 146 to an average of 85 cP),³¹ Foltz et al.¹⁷³ reported a far lower mean viscosity of the gastric contents (1.22cP), which then rose slightly during PPI administration to 1.73 cP.

Surface Tension

There has only been 1 study reported in the open literature that directly compared surface tension between PPI and control groups. In that study, the surface tension of samples aspirated from the stomach was measured to be considerably lower in subjects receiving PPIs (34.29 ± 0.51 mN/m) than in control subjects (43.22 ± 0.74 mN/m).^{14,182} One possible explanation for this observation is based on the observation that the concentration of bile acids in the gastric fluid is higher in individuals taking

PPIs.^{173,182} Litou et al.¹⁸² opined that the higher concentration of bile acids in the stomach might be owing to the reduction in gastric volume by the PPIs; if the amount of bile acids refluxed into the stomach stays the same but the gastric volume is lower, the concentration will be higher. Another hypothesis is that PPIs may weaken the contractile power of the pylorus,¹⁸³ leading to more reflux of bile acids from duodenum into the stomach.

Litou et al. also observed that the surface tension was slightly lower in the upper small intestine after pantoprazole administration than in the control group. The values in the fasted state averaged 32.7 ± 0.51 mN/m,^{14,182} while after PPI administration the surface tension averaged 29.8 ± 0.65 mN/m.¹⁸²

Gastric Emptying

Although several research groups have studied the effects of PPIs on gastric emptying, it is difficult to draw conclusions because different meal compositions have been used.¹⁸⁴ In a review article, Sanaka et al.¹⁸⁵ stated that the gastric emptying of solids shows a consistent delay during PPI therapy, while emptying time of liquids shows high variability. By contrast, research studies published shortly afterward reported that there is no significant delay in gastric emptying of solid/semi-solid meals under PPI administration.^{176,186}

Secretions

PPIs reduce both fasted and fed state acid secretions,¹⁸⁷ and no tolerance effect has been observed during chronic use.⁶⁸ The secretion volume was reported to be reduced from 193 mL to 100 mL in healthy individuals and from 227 mL to 94 mL in GERD patients.¹⁷⁷

When chronic therapy with PPIs is discontinued, a rebound effect on acid secretion is observed.⁶ During therapy, up to 3 times higher concentrations of gastrin are released because the feedback inhibition of gastrin release by stomach acid is suppressed.¹⁸⁸ Upon discontinuation of PPI therapy, the elevated gastrin blood concentration invokes a higher gastric acid secretion and can induce rebound dyspepsia.

PPIs have an impact on the secretion of pepsinogen and on the conversion of pepsinogen to pepsin. According to the findings of Foltz et al., the mean concentration of pepsin in stomach falls from 55.1 to 20.2 μ g/mL during PPI therapy.

PPIs appear to have no significant effect on biliary or pancreatic secretion.¹⁸⁷ Despite this, the trypsin concentration in the gastric fluid is much higher in individuals on PPI medication (5.26 μ g/mL for non-PPI vs. 29.9 μ g/mL for PPI users).¹⁷³ This might be explained by a stronger reflux of the trypsin from the duodenum or the reduction in gastric volume, as has been hypothesized for the higher bile acid concentrations in the stomach after PPI administration. Another possibility discussed by Foltz et al.¹⁷³ is that the rate of trypsin degradation, which is faster under acidic conditions, is reduced during PPI therapy due to the elevation in gastric pH.

Microflora

In recent years, there has been a growing interest in PPI-induced changes in the GI microbiota. The higher pH of the stomach can be seen as an improved opportunity for bacteria to survive the gastric environment and enter the intestinal tract. As the potency of PPIs to inhibit acid secretions exceeds that of H₂RAs, a higher prevalence of new flora during PPI therapy might be expected than during therapy with H₂RAs or antacids.¹⁸⁹

While the number of oropharyngeal and fecal bacteria found in the gut increases⁶⁷ as a result of PPI therapy, researchers generally agree that there is a concomitant fall in the diversity of the bacterial GI population. Thus, the changes reported in the literature can be assigned to 3 categories—rise in the bacterial count, occurrence of

bacterial species not specific to the respective gut segment, and fall in the bacterial diversity.

Engstrand and Lindberg opined that PPI treatment raises the possibility of bacterial overgrowth in the stomach,¹⁹⁰ while Sanduleanu et al.¹⁹¹ reported non-*H. pylori* flora colonizing the gastric mucus during long-term treatment with PPIs. While *Streptococaceae* in particular were reported to have increased relative abundance in the gastric mucosa,¹⁹² the overall microbiota in the stomach were found to be less diverse during PPI therapy.¹⁹³

Nevertheless, the gastric microbial population is not the only concern with PPI administration because viable bacteria will be emptied within a few hours into the intestines, where the residence time (particularly in the large intestine) can be considerably longer. As for the stomach, several studies show a change in the diversity of bacteria in the intestines.¹⁹⁴⁻¹⁹⁶ While introduction of non-native genera expands the diversity of microbiota *per se*, these species can also suppress other genera, thus lowering the overall diversity. One of the species not native to the gut and an indicator of the susceptibility of the GI tract to bacterial imbalance is *C. difficile*. Indeed, a significant association of PPI therapy with an increased incidence of *C. difficile* infection has been reported.^{197,198} More generally, research shows that PPIs may provoke dysbiosis, that is lower abundance of gut bacteria and higher abundance of oral and upper intestinal bacteria, as well as a shift in the microbiota and microbiological diversity in the small intestine,^{57,199,200} with a higher frequency of bacterial overgrowth.²⁰¹ Disruption of the balance among the gut flora may also be responsible for the diarrheal symptoms summarized in product information documents.

Permeability

Another impact of PPIs on GI physiology is the increase in gastric mucosa permeability for some substances. The effect was first described by Mullin et al.²⁰² as a transmucosal leak in the stomach. The increase in permeability to sucrose was reported to occur quickly, within days of taking PPIs and to be temporary, as the effect was reversed when PPI administration was terminated. Further research demonstrated a raised permeability to sucrose, mannitol, and PEG 4000 in stomach and stated that the flux of molecules was bidirectional.^{203,204} Other studies reported an increased permeability of some drugs, as bradykinin and digoxin.^{204,205} Farrel et al. confirmed that initial application of PPIs results in sucrose leak, dramatically increasing the permeability. However, the experiments were conducted in Barrett's esophagus patients, who already have a sucrose leak owing to the disease. The authors also showed that after 1 week of PPI therapy the sucrose leak decreased again.²⁰⁶ König et al.⁷⁰ offered a possible explanation for the PPI effect, suggesting that smooth muscle relaxation connected to PPIs may affect tight junctions, thus increasing the paracellular permeability.

Important to note in this discussion is that the observed effects on permeability have only been investigated for the stomach, and there are no current data suggesting that PPIs induce changes in permeability in the small intestine.

Biorelevant Media and Dissolution Test Design to Reflect the Fasted State Gastric Fluid Under Co-administration of PPIs and H₂RAs

One of the key aspects of designing *in vitro* dissolution tests to investigate the impact of reduced stomach acidity on administered drugs is the choice of the dissolution medium. It should accurately represent the fasted state gastric conditions, while staying relatively simple and easy to prepare. Further important aspects of the dissolution test design are the choice of apparatus, operating conditions, and the duration of the test. Another consideration is to be

able to compare performance of drug products under PPI/H₂RA administration with performance under nontreatment conditions that is healthy volunteers receiving no medication.

Dissolution Medium Design

The first step in the design of the dissolution media for patients on therapy with ARAs is to describe the key parameters influencing drug dissolution²⁹: pH, buffer capacity, type and concentration of surface active agents, type and concentration of enzymes and concentration of chloride ions, as well as the osmolality of gastric fluid. Using the composition of existing biorelevant media²⁰⁷ and the information resulting from the literature review as a starting point, new media to represent gastric fluid under PPI conditions were developed.

pH

The clinical literature data on fasted gastric pH under co-administration of PPIs summarized in this review show a broad span of values. For standard PPI therapy, consisting of oral once daily dosing, pH values of pH 4-6 best represent values found *in vivo*. It would, however, be inaccurate to represent the change in gastric pH after administration of PPIs with just one dissolution medium at a mean pH value, for example pH 5. Instead, the large intraindividual and interindividual variability is better accounted for using a bracketing approach, that is 2 media with pH values of pH 4 and pH 6, respectively. This approach is similar to the idea behind the snapshot media developed for FeSSGF by Jantravid et al.²⁰⁸ While the pH 4 medium reflects the elevation in gastric pH that serves as a criterion for successful PPI therapy, the pH 6 medium reflects pH conditions under therapy at higher doses and/or more potent ARAs. Additionally, the pH 6 medium represents a "worst case" value for testing the dissolution of poorly soluble weakly basic compounds.

Buffer Capacity

As the dissolution media, from the design perspective, should be reproducible with respect to pH, they should contain a small amount of buffer to counteract pH shifts that can occur if basic or acidic compounds dissolve into the medium during dissolution testing. The first step to reflecting the gastric buffer capacity in the test medium is the selection of buffer species. The buffer species should be selected according to its pK_a value, ideally deviating less than ±1 from the pH value of the medium. For media representing PPI co-administration, maleate buffer (pK_{a2} 6.07) was chosen for the pH 6 medium and acetate (pK_a 4.74) for the pH 4 medium. A weak acetate buffer had already been proposed by Wunderlich in 2004 to simulate gastric conditions under the influence of H₂-receptor antagonists.²⁰⁹ Citrate buffer with a pK_{a2} value of 4.76 and a pK_{a3} of 6.40 would also be appropriate for both the pH 4 and pH 6 media. McIlvaine buffer, a combination of citrate and phosphate buffers, represents a third option and is mentioned in the Japanese Pharmacopoeia as a dissolution fluid for pioglitazone and glimepiride tablets.²¹⁰ Maleate (pH 6) and acetate buffers (pH 4) were selected as the first-line buffer species for the 2 bracketing media, as these 2 buffers are frequently used in dissolution media and thus provide a one-to-one comparison to dissolution tests run under conditions representing healthy subjects who are not receiving ARAs. The McIlvaine and citrate buffers were chosen as backup buffers, to be used if and when interactions between the drug and maleate or acetate buffers occur.²¹¹ Additionally, they are more amenable to online UV analysis compared with maleate.

The selection of buffer concentrations in the PPI media was based on the buffer capacity of gastric fluid in volunteers under PPI and H₂RA conditions. Litou et al.¹⁸² investigated the impact of pantoprazole (PPI) and famotidine (H₂RA) on various parameters, including buffer capacity. Based on the Litou et al. data, a buffer capacity of 7.5 mEq/ΔpH/L was chosen for the pH 4 medium, while the buffer capacity of the pH 6 medium was adjusted to 1 mEq/ΔpH/L, as determined in gastric fluid recovered from healthy volunteers after administration of water.³⁹

The buffer species concentrations for the 2 pH/buffer capacity combinations were calculated using the following equation:

$$\beta = 2.303 * \left(\frac{K_w}{[H^+]} + [H^+] + \sum_i \frac{c_i * K_{a_i} * [H^+]}{(K_{a_i} + [H^+])^2} \right)$$

After calculating the amounts of buffer required to produce the desired buffer capacity and pH, the buffers were prepared, and the compositions adjusted as necessary to ensure that the correct pH/buffer capacity is achieved.

Surface Tension

Although there seems to be an impact of PPI administration on the surface tension of fasted state gastric fluid, the change is not significant enough to require a change from the quantities used in the standard FaSSGF composition described by Markopoulos et al.²¹²

Enzymes

The gastric enzyme most relevant for dissolution tests is pepsin, as it can contribute to the faster dissolution of capsule formulations if the gelatin becomes crosslinked. On account of pepsin's pH-dependent activity, the concentration in the dissolution medium was adjusted according to the pH of the medium. Although it is possible for pepsin to be activated from pepsinogen at pH values up to pH 5, above this pH there is a steep fall in pepsin activity.²¹³ As a result, the same concentration of pepsin in the pH 4 medium as in the standard FaSSGF recipe was adopted, whereas in the pH 6 medium, pepsin was omitted.

Osmolality

Jantratid et al.²⁰⁸ considered the impact of osmolality and ionic strength of a medium on the dissolution rate of drugs when revising the compositions of biorelevant media in 2008. Osmolality has been shown to have an impact on the release from some tablet coatings.²¹⁴⁻²¹⁶ Thus, the impact of PPI co-administration on the gastric secretion should be reflected in the dissolution medium. The only clinical data on the osmolality of gastric fluid under PPI administration appear in the Litou et al.¹⁸² publication. In accordance with those results, the osmolality was set to 75 mOsmol/kg for the pH 4 medium and 50 mOsmol/kg for the pH 6 medium. After the addition of buffer species in the respective amount, the osmolality of the media is adjusted with sodium chloride, as necessary.

The compositions of the media to represent fasted gastric conditions during therapy with H₂RAs and PPIs are shown in Tables 4-6.

As the potential for adsorption must also be considered in the case of antacid administration, other options are currently being developed for studying dissolution interactions with these ARAs.

Dissolution Test Design

The second step in the dissolution test design is to consider changes of gastric volume and gastric emptying time under PPI administration and choose test conditions and duration accordingly.

Table 4

The Composition of Media Recommended for Simulating Fasted State Gastric Fluid Under PPI/H₂RA Co-administration

| Component/Parameter | Acetate pH 4 Medium | Maleate pH 6 Medium |
|----------------------------|---------------------|---------------------|
| Pepsin (mg/mL) | 0.1 | – |
| Sodium taurocholate (mM) | 0.08 | 0.08 |
| Phosphatidylcholine (mM) | 0.02 | 0.02 |
| Sodium chloride (mM) | – | 22.7 |
| Maleic acid (mM) | – | 2.31 |
| Sodium acetate (mM) | 33.3 | – |
| + NaOH (1 M) (mL) | – | qs. (-3.5) |
| + HCl (1 M) (mL) | qs. (-25) | – |
| pH | 4 | 6 |
| Buffer capacity (mEq/pH/L) | 7.5 | 1 |
| Osmolality (mOsmol/kg) | 91 | 50 |
| Surface tension (mN/m) | 64.49 | 67.21 |

Minus sign indicates the absence of component.

Volume

Fasted state gastric volume is on average 28–45 mL.^{9,14} Although a decrease in gastric secretions and the volume of gastric juice during PPI co-administration has been reported, oral drugs are normally administered (at least in clinical studies) with a glass of water (200–240 mL), which is already reflected in the recommended media volume for dissolution experiments with FaSSGF (250 mL).²¹⁷ Thus, the dissolution test volume for PPI experiments was also set at 250 mL.

Duration

The *in vivo* gastric residence time should be reflected in the duration of the *in vitro* test. Because PPIs do not appear to affect gastric emptying and the H₂RAs appear to at most slightly slow gastric emptying, the duration of the dissolution test was maintained at 30–45 min for fasted state gastric conditions.

Apparatus

Although the hydrodynamics can obviously not represent all conditions in the fasted state stomach, using the USP 2 apparatus at 50 rpm ensures good comparability with testing of drug products under standard conditions (i.e., in the absence of ARA therapy). Should coning occur, an increase in rotational speed to 75 rpm or use of a peak vessel can be used to counteract the coning problem.

A summary of the test parameters for dissolution testing of drug products under fasted state gastric conditions under PPI or H₂RA administration is shown in Table 7.

Discussion

The impact of ARAs on the GI physiology is complex, dependent on the type of ARA, duration/amount of ARA administered, as well as the part of the GI tract under consideration. In July 2018, in its

Table 5

The Composition of Media Simulating Fasted State Gastric Fluid Under PPI/H₂RA Co-administration—Back-Up Media Based on Citrate Buffer

| Component/Parameter | Citrate pH 4 Medium | Citrate pH 6 Medium |
|----------------------------|---------------------|---------------------|
| Pepsin (mg/mL) | 0.1 | – |
| Sodium taurocholate (mM) | 0.08 | 0.08 |
| Phosphatidylcholine (mM) | 0.02 | 0.02 |
| Sodium chloride (mM) | 7.7 | 22.8 |
| Tri-Sodium citrate (mM) | 11.2 | 1.5 |
| + HCl (1 M) (mL) | qs. (-20) | qs. (-0.7) |
| pH | 4 | 6 |
| Buffer capacity (mEq/pH/L) | 7.5 | 1 |
| Osmolality (mOsmol/kg) | 75 | 50 |
| Surface tension (mN/m) | 63.32 | 67.86 |

Minus sign indicates the absence of component.

Table 6
The Composition of Media Simulating Fasted State Gastric Fluid Under PPI/H₂RA Co-administration—Back-Up Media Based on Mcllvaine's Buffer

| Component/Parameter | Mcllvaine pH 4 Medium | Mcllvaine pH 6 Medium |
|----------------------------|--------------------------|--------------------------|
| Pepsin (mg/mL) | 0.1 | — |
| Sodium taurocholate (mM) | 0.08 | 0.08 |
| Phosphatidylcholine (mM) | 0.02 | 0.02 |
| Sodium chloride (mM) | 17.5 | 21.2 |
| Citric acid (mM) | 9.00 | 0.86 |
| Di-Sodium phosphate (mM) | 11.29 | 2.94 |
| + HCl/NaOH (1 M) (mL) | qs. | qs. |
| pH | 4 | 6 |
| Buffer capacity (mEq/pH/L) | 7.5 | 1 |
| Osmolality (mOsmol/kg) | 75 | 50 |
| Surface tension (mN/m) | 63.20 | 67.58 |

Minus sign indicates the absence of component.

docket on pH-dependent drug-drug interactions, FDA highlighted the importance of developing a standardized policy or guidance document and asked for public input on best practices in the planning and evaluation of pH-dependent drug-drug interactions (DDIs).²¹⁸ Soon after, public comments from pharmaceutical companies and academia confirmed the need for a systematic approach to understanding the interactions with different types of ARAs, including the development of appropriate *in vitro* experiments.²¹⁹ Although there are several additional drug families used for gastric acid reduction, for example anticholinergics and (selective M1) muscarinic receptor antagonists, the 3 groups of ARAs used most frequently are antacids, H₂RAs, and PPIs.

Antacids have an immediate but short-lived effect and are usually administered on an acute basis. Interactions between ingestion of the antacid and dissolution of a co-administered drug need to consider the type of antacid compound administered, its dose, and because antacids act locally to increase the gastric pH, the possibility of direct interactions with the drug substance. For this reason, the design of the dissolution tests portrayed in this research was limited to co-administration of H₂RAs and PPIs. For the representation of GI physiology in fasted state stomach during the administration of antacids, additional media should be developed considering the additional (physical) impact antacids may have on the drugs tested directly in the medium, mainly complexation processes.

H₂RAs have a slower onset of action but a more prolonged effect on GI physiology than antacids and can be used either as an acute therapy or on a long-term basis. Thus, pH data reflecting both acute and long-term therapy with H₂RAs were taken under consideration. Because PPIs have the longest onset of action of the ARAs (up to several days to reach the full effect), they are usually used in long-term therapy. In this case, only data about the multiple dose and long-term therapy with PPIs were taken into consideration when designing the media.

Using a bracketing approach, media at both pH 4 and pH 6 were developed. The pH 4 value reflects lower doses of H₂RAs and PPIs as

Table 7
Test Apparatus, Operating Conditions, and Duration for the Simulation of Dissolution in Fasted State Gastric Fluids Under the Influence of PPI/H₂RA Co-administration

| Parameters | Simulation of PPI/H ₂ RA Co-administration |
|---------------------|---|
| Method | Paddle (USP apparatus 2) |
| Volume (mL) | 250 |
| Temperature (°C) | 37 ± 0.5 |
| Rotation rate (rpm) | 50 (75) ^a |
| Vessel | Standard (Peak [®]) Vessel, Sinkers (if needed) |
| Duration (min) | 30 |

^a It is recommended to use either 75 rpm or a peak vessel if coning occurs.

well as potential DDIs when the H₂RA is administered at a higher dose for the first time. For higher doses of H₂RAs and PPIs given chronically, the pH 6 medium may be more representative. Although there have been studies demonstrating pH values outside the 4-6 range, these can be regarded as extreme cases rather than being representative of usual therapy.

Three different buffer systems have been tested (see Tables 4-6) for reproducibility of parameters (such as pH, buffer capacity, osmolarity, etc.), enabling scientists to choose media that are compatible with the drug substance. This may be particularly important if the drug in question is susceptible to acid or base catalyzed hydrolysis.

For the pharmaceutical industry and development, the development of appropriate *in vitro* experiments to represent co-administration of ARAs may have wide benefits. During the development of a drug, these tests may increase confidence that no significant interaction due to the changes in GI physiology will occur when PPIs or H₂RAs are co-administered, thus enabling a broader population to be recruited to clinical studies. Such data might even be used to waive DDI studies with PPIs or H₂RAs, thus avoiding unnecessary exposure of healthy volunteers to the new drug.

Conclusion

As there is an increasing demand to forecast the effects of concomitant therapy of drugs on the pharmacokinetics of new compounds as well as to better understand how generic brand formulations might behave differently under different dosing circumstances, *in vitro* experiments which can reflect ARA co-administration are timely. In the dissolution tests proposed in this work, the most pronounced changes in GI physiology during ARA therapy are adequately reflected, and the test conditions enable a ready comparison with experiments under usual gastric conditions in fasted, healthy adults. It is expected that these tests will be particularly useful in understanding the dissolution behavior of poorly soluble, weakly basic compounds.

Acknowledgments

The authors wish to acknowledge funding of Mr. Domagoj Segregur by AstraZeneca UK.

References

1. Texter EC. A critical look at the clinical use of antacids in acid-peptic disease and gastric acid rebound. *Am J Gastroenterol.* 1989;84(2):97-108.
2. Warner CW, McIsaac RL. The evolution of peptic ulcer therapy. A role for temporal control of drug delivery. *Ann N Y Acad Sci.* 1991;618:504-516.
3. Sippy BW. Gastric and duodenal ulcer. Medical cure by an efficient removal of gastric juice corrosion. *JAMA.* 1915;64(20):1625-1630.
4. Overbey DM, Jones EL. Acid peptic ulcer disease. In: Harken AH, Moore EE, eds. *Abernathy's Surgical Secrets.* 7th ed. Philadelphia, PA: Elsevier; 2018:209-214.
5. Brogden RN, Heel RC, Speight TM, Avery GS. Sucralfate. A review of its pharmacodynamic properties and therapeutic use in peptic ulcer disease. *Drugs.* 1984;27(3):194-209.
6. Chubineh S, Birk J. Proton pump inhibitors: the good, the bad, and the unwanted. *South Med J.* 2012;105(11):613-618.
7. HealthPrep. The 10 most prescribed drugs in the World. Available at: <https://healthprep.com/articles/medications/the-10-most-prescribed-drugs-in-the-world/>. Accessed April 26, 2019.
8. Apotheke Adhoc. Die 20 meistverkauften Arzneimittel der Welt. Available at: <https://www.apotheke-adhoc.de/mediathek/detail/die-20-meistverkauften-arzneimittel-der-welt/>. Accessed April 26, 2019.
9. Schiller C, Frohlich C-P, Geissmann T, et al. Intestinal fluid volumes and transit of dosage forms as assessed by magnetic resonance imaging. *Aliment Pharmacol Ther.* 2005;22(10):971-979.
10. Long C. *Biochemists' Handbook.* London: Spon; 1961.
11. Ulleberg EK, Comi I, Holm H, Herud EB, Jacobsen M, Vegarud GE. Human gastrointestinal juices intended for use in *in vitro* digestion models. *Food Dig.* 2011;2(1-3):52-61.

12. Hirschowitz BL. A critical analysis, with appropriate controls, of gastric acid and pepsin secretion in clinical esophagitis. *Gastroenterology*. 1991;101(5):1149-1158.
13. Snyder WS, Cook MJ, Nasset ES, Karhausen LR, Parry Howells G, Tipton IH. *Report of the Task Group on Reference Man*. Oxford: The International Commission on Radiological Protection, Pergamon Press; 1975.
14. Mudie DM, Amidon GL, Amidon GE. Physiological parameters for oral delivery and in vitro testing. *Mol Pharm*. 2010;7(5):1388-1405.
15. Fordtran JS, Locklear TW. Ionic constituents and osmolality of gastric and small-intestinal fluids after eating. *Digest Dis Sci*. 1966;11(7):503-521.
16. Diakidou A, Vertzoni M, Goumas K, et al. Characterization of the contents of ascending colon to which drugs are exposed after oral administration to healthy adults. *Pharm Res*. 2009;26(9):2141-2151.
17. Badley AD, Camilleri M, O'Connor MK. Noninvasive measurement of human ascending colon volume. *Nucl Med Commun*. 1993;14(6):485-489.
18. Cummings JH, Banwell JG, Segal I, et al. The amount and composition of large bowel contents in man. *Gastroenterology*. 1990;98:A408.
19. Hirano I, Brenner D. Gastrointestinal motility. In: Reinius JF, Simon D, eds. *Gastrointestinal Anatomy and Physiology*. Vol. 334. Oxford: John Wiley & Sons, Ltd.; 2014:33-45.
20. Farrar GE, Bower RJ. Gastric juice and secretion: physiology and variations in disease. *Annu Rev Physiol*. 1967;29:141-168.
21. Levine RR. Factors affecting gastrointestinal absorption of drugs. *Dig Dis Sci*. 1970;15(2):171-188.
22. Dressman JB, Vertzoni M, Goumas K, Reppas C. Estimating drug solubility in the gastrointestinal tract. *Adv Drug Deliv Rev*. 2007;59(7):591-602.
23. Kambayashi A, Yasuji T, Dressman JB. Prediction of the precipitation profiles of weak base drugs in the small intestine using a simplified transfer ("dumping") model coupled with in silico modeling and simulation approach. *Eur J Pharm Biopharm*. 2016;103:95-103.
24. Bergström CAS, Holm R, Jørgensen SA, et al. Early pharmaceutical profiling to predict oral drug absorption: current status and unmet needs. *Eur J Pharm Sci*. 2014;57:173-199.
25. Abulhelwa AY, Foster DJR, Upton RN. A quantitative review and meta-models of the variability and factors affecting oral drug absorption—Part I: gastrointestinal pH. *AAPS J*. 2016;18(5):1309-1321.
26. Baxevanis F, Kuiper J, Fotaki N. Fed-state gastric media and drug analysis techniques: current status and points to consider. *Eur J Pharm Biopharm*. 2016;107:234-248.
27. Seidler U, Sjöblom M. Gastrointestinal bicarbonate secretion. In: *Physiology of the Gastrointestinal Tract: Gastrointestinal Bicarbonate Secretion [Chapter 48]*. New York: Elsevier, Academic Press; 2012:1311-1339.
28. Evans DF, Pye G, Bramley R, Clark AG, Dyson TJ, Hardcastle JD. Measurement of gastrointestinal pH profiles in normal ambulant human subjects. *Gut*. 1988;29:1035-1041.
29. Dressman JB, Amidon GL, Reppas C, Shah VP. Dissolution testing as a prognostic tool for oral drug absorption: immediate release dosage forms. *Pharm Res*. 1998;15(1):11-22.
30. Kurita Y, Nakazawa S, Segawa K, Tsukamoto Y. Clinical significance of gastric juice viscosity in peptic ulcer patients. *Dig Dis Sci*. 1988;33(9):1070-1076.
31. Goddard AF, Spiller RC. The effect of omeprazole on gastric juice viscosity, pH and bacterial counts. *Aliment Pharmacol Ther*. 1996;10:105-109.
32. Abrahamsson B, Pal A, Sjöberg M, Carlsson M, Laurell E, Brasseur JG. A novel in vitro and numerical analysis of shear-induced drug release from extended-release tablets in the fed stomach. *Pharm Res*. 2005;22(8):1215-1226.
33. Marciani I, Gowland PA, Spiller RC, et al. Effect of meal viscosity and nutrients on satiety, intragastric dilution, and emptying assessed by MRI. *Am J Physiol Gastrointest Liver Physiol*. 2001;280(6):G1227-G1233.
34. Sirois PJ, Amidon GL, Meyer JH, Doty J, Dressman JB. Gastric emptying of nondigestible solids in dogs: a hydrodynamic correlation. *Am J Physiol*. 1990;258(1 Pt 1):G65-G72.
35. Reppas C, Eleftheriou G, Macheras P, Symillides M, Dressman JB. Effect of elevated viscosity in the upper gastrointestinal tract on drug absorption in dogs. *Eur J Pharm Sci*. 1998;6(2):131-139.
36. Radwan A, Amidon GL, Langguth P. Mechanistic investigation of food effect on disintegration and dissolution of BCS class III compound solid formulations: the importance of viscosity. *Biopharm Drug Dispos*. 2012;33(7):403-416.
37. Reppas C, Meyer JH, Sirois PJ, Dressman JB. Effect of hydroxypropylmethylcellulose on gastrointestinal transit and luminal viscosity in dogs. *Gastroenterology*. 1991;100(5 Pt 1):1217-1223.
38. Yang L. Biorelevant dissolution testing of colon-specific delivery systems activated by colonic microflora. *J Control Release*. 2008;125(2):77-86.
39. Kalantzi L, Goumas K, Kalioras V, Abrahamsson B, Dressman JB, Reppas C. Characterization of the human upper gastrointestinal contents under conditions simulating bioavailability/bioequivalence studies. *Pharm Res*. 2006;23(1):165-176.
40. Clarysse S, Tack J, Lammert F, Duchateau G, Reppas C, Augustijns P. Post-prandial evolution in composition and characteristics of human duodenal fluids in different nutritional states. *J Pharm Sci*. 2009;98(3):1177-1192.
41. Scratcherd T, Grundy D. The physiology of intestinal motility and secretion. *Br J Anaesth*. 1984;56(1):3-18.
42. Meyer JH, Elashoff J, Porter-Fink V, Dressman J, Amidon GL. Human post-prandial gastric emptying of 1-3-millimeter spheres. *Gastroenterology*. 1988;94(6):1315-1325.
43. Finholt P, Solvang S. Dissolution kinetics of drugs in human gastric juice—the role of surface tension. *J Pharm Sci*. 1968;57(8):1322-1326.
44. Brunton LL, Goodman LS, Gilman A, Chabner BA, eds. *Goodman & Gilman's the pharmacological basis of therapeutics: [DVD incl.]*. 12. New York, NY: McGraw-Hill Medical; 2011.
45. Meeroff JC, Rofrano JA, Meeroff M. Electrolytes of the gastric juice in health and gastroduodenal diseases. *Dig Dis Sci*. 1973;18(10):865-872.
46. Hörter D, Dressman JB. Influence of physicochemical properties on dissolution of drugs in the gastrointestinal tract. *Adv Drug Deliv Rev*. 2001;46:75-87.
47. Schubert ML. Gastric physiology. In: Reinius JF, Simon D, eds. *Gastrointestinal Anatomy and Physiology*. Vol. 56. Oxford: John Wiley & Sons, Ltd.; 2014:58-77.
48. Richter C, Tanaka T, Yada RY. Mechanism of activation of the gastric aspartic proteinases: pepsinogen, progastricsin and prochymosin. *Biochem J*. 1998;335(Pt 3):481-490.
49. Sanny CG, Hartsuck JA, Tang J. Conversion of pepsinogen to pepsin. Further evidence for intramolecular and pepsin-catalyzed activation. *J Biol Chem*. 1975;250(7):2635-2639.
50. Guzman ML, Marques MR, Olivera Me ME, Stippler ES. Enzymatic activity in the presence of surfactants commonly used in dissolution media. Part 1: pepsin. *Results Pharma Sci*. 2016;6:15-19.
51. Schmidt HA, Fritzljar G, Dölle W, Goebell H. Vergleichende Untersuchungen der histamin- und insulin-stimulierten Säure-Pepsin-Sekretion bei Patienten mit Ulcus duodeni und Kontrollpersonen. *Dtsch Med Wochenschr*. 1970;95:2011-2016.
52. Lambert R, Matin F, Vagne M. Relationship between hydrogen ion and pepsin concentration in human gastric secretion. *Digestion*. 1968;1:65-77.
53. Roberts NB. Review article: human pepsins - their multiplicity, function and role in reflux disease. *Aliment Pharmacol Ther*. 2006;24(Suppl 2):2-9.
54. Diem K, Lentner C, eds. *Documenta Geigy, Scientific Tables*. 7th ed. Basel: Geigy Pharmaceuticals, J.R. Geigy A.G., Pharma; 1975.
55. Rick W. *Zur Physiologie und Pathologie der Enzymsekretion des Pankreas: Habilitation thesis*. Gießen: Gießen, University of Gießen; 1963.
56. Willstätter R, Waldschmidt-Leitz E, Memmen F. Bestimmung der pankreatischen Fettsäure. *Hoppe Seyler's Z Physiol Chem*. 1923;125(1-4):93-131.
57. Harrow B. *Textbook of Biochemistry*. 4th ed. Philadelphia: W. B. Saunders Company, W.B. Saunders Company; 1946.
58. Guncheva M, Stippler E. Effect of four commonly used dissolution media surfactants on pancreatic proteolytic activity. *AAPS PharmSciTech*. 2017;18(4):1402-1407.
59. Zhou Z, Dunn C, Khadra I, Wilson CG, Halbert GW. Statistical investigation of simulated fed intestinal media composition on the equilibrium solubility of oral drugs. *Eur J Pharm Sci*. 2017;99:95-104.
60. Fuchs A, Dressman JB. Composition and physicochemical properties of fasted-state human duodenal and jejunal fluid: a critical evaluation of the available data. *J Pharm Sci*. 2014;103(11):3398-3411.
61. Lindahl A, Ungell A-L, Knutson L, Lennerås H. Characterization of fluids from the stomach and proximal jejunum in men and women. *Pharm Res*. 1997;14(4):497-502.
62. Riethorst D, Mols R, Duchateau G, Tack J, Brouwers J, Augustijns P. Characterization of human duodenal fluids in fasted and fed state conditions. *J Pharm Sci*. 2016;105(2):673-681.
63. Sousa T, Paterson R, Moore V, Carlsson A, Abrahamsson B, Basit AW. The gastrointestinal microbiota as a site for the biotransformation of drugs. *Int J Pharm*. 2008;363(1-2):1-25.
64. Simon GL, Gorbach SL. Intestinal flora in health and disease. *Gastroenterology*. 1984;86(1):174-193.
65. Canny GO, McCormick BA. Bacteria in the intestine, helpful residents or enemies from within? *Infect Immun*. 2008;76(8):3360-3373.
66. Bik EM, Eckburg PB, Gill SR, et al. Molecular analysis of the bacterial microbiota in the human stomach. *Proc Natl Acad Sci U S A*. 2006;103(3):732-737.
67. Minalyan A, Gabrielyan L, Scott D, Jacobs J, Pisegna JR. The gastric and intestinal microbiome: role of proton pump inhibitors. *Curr Gastroenterol Rep*. 2017;19(8):42.
68. Savarino V, Dulbecco P, Bortoli N de, Ottonello A, Savarino E. The appropriate use of proton pump inhibitors (PPIs): need for a reappraisal. *Eur J Intern Med*. 2017;37:19-24.
69. Eckburg PB. Diversity of the human intestinal microbial flora. *Science*. 2005;308(5728):1635-1638.
70. König J, Wells J, Cani PD, et al. Human intestinal barrier function in health and disease. *Clin Transl Gastroenterol*. 2016;7(10):e196.
71. **Leading antacid tablet brands in the United States in 2017, based on sales. Available at:** <https://www.statista.com/>. Accessed July 3, 2018.
72. Thorburn J, Moir DD. Antacid therapy for emergency caesarean section. *Anaesthesia*. 1987;42(4):352-355.
73. Wisher D. Martindale: the complete drug reference. 37th ed. *J Med Libr Assoc*. 2012;100(1):75-76.
74. Goodman LS, Gilman A, Gilman AG. *Goodman and Gilman's The Pharmacological Basis of Therapeutics*. 8th ed. New York: Pergamon Press; 1990.
75. Rote Liste® Service GmbH. *Rote Liste 2016*. Frankfurt am Main: Rote Liste® Service GmbH; 2016:56.
76. Lin MS, Sun P, Yu HY. Evaluation of buffering capacity and acid neutralizing-pH time profile of antacids. *J Formos Med Assoc*. 1998;97(10):704-710.
77. Powell RL, Westlake WJ, Longaker ED, Greene LC. A clinical evaluation of a new concentrated antacid. I. Effects on gastric pH. *J Clin Pharmacol New Drugs*. 1971;11(4):288-295.

78. Rockville MD, Easton PA. *The United States pharmacopeia, 20th revision: the National formulary, 15th ed.* Rockville, MD: The Convention; Distributed by Mack Pub. Co., United States Pharmacopeial Convention, Inc.; 1979.
79. *The United States Pharmacopeia, 41st Revision: the National Formulary, 36th ed.: Main edition plus Supplements 1 and 2.* Rockville, MD: United States Pharmacopeial Convention; 2017.
80. Peterson CI, Perry DL, Masood H, et al. Characterization of antacid compounds containing both aluminum and magnesium. I. Crystalline powders. *Pharm Res.* 1993;10(7):998-1004.
81. Netzer P, Brabetz-Höfliger A, Bründler R, Flogerzi B, Hüster J, Halter F. Comparison of the effect of the antacid Rennie versus low-dose H2-receptor antagonists (ranitidine, famotidine) on intragastric acidity. *Aliment Pharmacol Ther.* 1998;12(4):337-342.
82. Sulz MC, Manz M, Grob P, Meier R, Drewe J, Beglinger C. Comparison of two antacid preparations on intragastric acidity—a two-centre open randomised cross-over placebo-controlled trial. *Digestion.* 2007;75(2-3):69-73.
83. O'Sullivan GM, Bullingham RE. The assessment of gastric acidity and antacid effect in pregnant women by a non-invasive radiotelemetry technique. *Br J Obstet Gynaecol.* 1984;91(10):973-978.
84. Feldman M. Comparison of the effects of over-the-counter famotidine and calcium carbonate antacid on postprandial gastric acid. A randomized controlled trial. *JAMA.* 1996;275(18):1428-1431.
85. Berstad A, Rydning A, Kolstad B, Frislid K. Reduction of postprandial gastric acidity and pepsin concentration by ranitidine and antacids in healthy volunteers. *Scand J Gastroenterol Suppl.* 1981;69:67-73.
86. Thomson AB, Kirdeikis P, Zuk L. Comparison of 200 mg cimetidine with multiple doses of antacid on extent and duration of rise in gastric pH in volunteers. *Dig Dis Sci.* 1999;44(10):2051-2055.
87. Barnett CC, Richardson CT. In vivo and in vitro evaluation of magnesium-aluminum hydroxide antacid tablets and liquid. *Dig Dis Sci.* 1985;30(11):1049-1052.
88. Bendtsen F, Rune SJ. Effect of a single dose of antacid on gastric and duodenal bulb pH in duodenal ulcer patients. *Scand J Gastroenterol.* 1988;23(8):935-940.
89. Deering TB, Carlson GL, Malagelada JR, Duenes JA, McCall JT. Fate of oral neutralizing antacid and its effect on postprandial gastric secretion and emptying. *Gastroenterology.* 1979;77(5):986-990.
90. Nader AM, Quinney SK, Fadda HM, Foster DR. Effect of gastric fluid volume on the in vitro dissolution and in vivo absorption of BCS class II drugs: a case study with Nifedipine. *AAPS J.* 2016;18(4):981-988.
91. Slomiany BL, Laszewicz W, Murty VL, Kosmala M, Slomiany A. Effect of sucrallose on the viscosity and retardation of hydrogen ion diffusion by gastric mucus glycoprotein. *Comp Biochem Physiol C.* 1985;82(2):311-314.
92. Slomiany BL, Laszewicz W, Slomiany A. Effect of sucrallose on the viscosity of gastric mucus and the permeability to hydrogen ion. *Digestion.* 1986;33(3):146-151.
93. Grübel P, Bhaskar KR, Cave DR, Garik P, Stanley HE, Lamont JT. Interaction of an aluminum-magnesium containing antacid and gastric mucus: possible contribution to the cytoprotective function of antacids. *Aliment Pharmacol Ther.* 1997;11(1):139-145.
94. Guthauser UJ, Häcki WH. Bindung von Gallensalzen und lysocleithin in physiologischen Medien durch verschiedene Antazida. *Schweiz Med Wochenschr.* 1987;117(9):322-327.
95. Begemann F, Schumpelick V, Bandomer G. Adsorption of bile acids and lysocleithin by antacids. *Scand J Gastroenterol Suppl.* 1981;67:191-193.
96. Weberg R, Berstad A. Symptomatic effect of a low-dose antacid regimen in reflux oesophagitis. *Scand J Gastroenterol.* 1989;24(4):401-406.
97. Lipsett P, Gadacz TR. Bile salt binding by maalox, sucrallose, and meciadanol: in vitro and clinical comparisons. *J Surg Res.* 1989;47(5):403-406.
98. Kurtz W, Guldütuna S, Leuschner U. Einfluss von pH und Antazidummenge auf die Gallensäurenbindung in quasinatürlichem Refluxmilieu. *Z Gastroenterol.* 1991;29(5):237-241.
99. Hurwitz A, Robinson RG, Vats TS, Whittier FC, Herrin WF. Effects of antacids on gastric emptying. *Gastroenterology.* 1976;71(2):268-273.
100. Troy DB, ed. *Remington: The science and practice of pharmacy.* Philadelphia: Lippincott Williams & Wilkins; 2005:21.
101. Harvey RF, Read AE. Mode of action of the saline purgatives. *Am Heart J.* 1975;89(6):810-813.
102. Hava M, Hurwitz A. The relaxing effect of aluminum and lanthanum on rat and human gastric smooth muscle in vitro. *Eur J Pharmacol.* 1973;22(2):156-161.
103. Sepelyak RJ, Feldkamp JR, Regnier FE, White JL, Hem SL. Adsorption of pepsin by aluminum hydroxide II: pepsin inactivation. *J Pharm Sci.* 1984;73(11):1517-1522.
104. Piper DW, Fenton B. The adsorption of pepsin. *Dig Dis Sci.* 1961;6:134-141.
105. Liebman WM. Effect of antacids and cholestyramine on pepsin activity in vitro. *IRCS J Med Sci.* 1980;8(2):114.
106. Sepelyak RJ, Feldkamp JR, Moody TE, White JL, Hem SL. Adsorption of pepsin by aluminum hydroxide I: adsorption mechanism. *J Pharm Sci.* 1984;73(11):1514-1517.
107. Smith JL. The role of gastric acid in preventing foodborne disease and how bacteria overcome acid conditions. *J Food Prot.* 2003;66(7):1292-1303.
108. Snepar R, Poporad GA, Romano JM, Kobasa WD, Kaye D. Effect of cimetidine and antacid on gastric microbial flora. *Infect Immun.* 1982;36(2):518-524.
109. Goeger MP, Dupuis GK, Herndon DN, Robson MC, Heggors JP. Antacid, sucrallose, and prostaglandin E2 effects on the growth and potential for translocation of *Pseudomonas aeruginosa*, *Escherichia coli*, and *Staphylococcus aureus* in an in vitro gastric simulation. *J Burn Care Rehabil.* 1991;12(1):7-12.
110. Koo J, Marshall DL, DePaola A. Antacid increases survival of *Vibrio vulnificus* and *Vibrio vulnificus* phage in a gastrointestinal model. *Appl Environ Microbiol.* 2001;67(7):2895-2902.
111. Morgan M. Control of intragastric pH and volume. *Br J Anaesth.* 1984;56(1):47-57.
112. Hirschowitz BI, Rentz J, Molina E. Histamine H-2 receptor stimulation and inhibition of pepsin secretion in the dog. *J Pharmacol Exp Ther.* 1981;218(3):676-680.
113. Haggstrom GD, Hirschowitz BI. Histamine H1 and H2 effects on gastric acid and pepsin, heart rate and blood pressure in humans. *J Pharmacol Exp Ther.* 1984;231(1):120-123.
114. Kaminski DL, Ruwart MJ, Jellinek M. Effect of the histamine (H2) inhibitor metiamide on histamine-stimulated bile flow in dogs. *Am J Physiol.* 1976;231(2):516-521.
115. Tripathi K d. *Essentials of Medical Pharmacology.* New Delhi: Jaypee Brothers Medical Publishers (P) Ltd.; 2013.
116. Heidelbaugh JJ, Nostrand TT, Kim C, van Harrison R. Management of gastroesophageal reflux disease. *Am Fam Physician.* 2003;68(7):1311-1318.
117. UCB Japan Co. L. **Stogar® Tablet 5. Stogar® Tablet 10: label.** Available at: [https://www.ucb.com/_up/ucb.com_products/documents/STOGAR-April2005\(050414\).tcm62-3741.tcm81-8593.pdf](https://www.ucb.com/_up/ucb.com_products/documents/STOGAR-April2005(050414).tcm62-3741.tcm81-8593.pdf). Accessed April 1, 2019.
118. Abe K, Shibata M, Demizu A, et al. Effect of oral and intramuscular famotidine on pH and volume of gastric contents. *Anesth Analg.* 1989;68(4):541-544.
119. Dubin SA, Silverstein PL, Wakefield ML, Jense HG. Comparison of the effects of oral famotidine and ranitidine on gastric volume and pH. *Anesth Analg.* 1989;69(5):680-683.
120. Mikawa K, Nishina K, Maekawa N, Asano M, Obara H. Gastric fluid volume and pH after nizatidine in adults undergoing elective surgery: influence of timing and dose. *Can J Anaesth.* 1995;42(8):730-734.
121. Escolano F, Castaño J, Pares N, Bisbe E, Monterde J. Comparison of the effects of famotidine and ranitidine on gastric secretion in patients undergoing elective surgery. *Anaesthesia.* 1989;44(3):212-215.
122. Oikkonen M, Erkola O, Collan R. Ranitidine suspension or famotidine re-sorbable and gastric fluid volume and pH. *Can J Anaesth.* 1995;42(9):793-796.
123. Hirota K, Kudo M, Kushikata T, Hashimoto H, Matsuki A. Regular use of H2 blockers reduces the efficacy of roxatidine to control gastric pH and volume. *Can J Anaesth.* 2005;52(2):166-171.
124. Narchi P, Edouard D, Bourget P, Oltz J, Cattaneo I. Gastric fluid pH and volume in gynaecologic out-patients. Influences of cimetidine and cimetidine-sodium citrate combination. *Eur J Anaesthesiol.* 1993;10(5):357-361.
125. Tripathi A, Somwanshi M, Singh B, Bajaj P. A comparison of intravenous ranitidine and omeprazole on gastric volume and pH in women undergoing emergency caesarean section. *Can J Anaesth.* 1995;42(9):797-800.
126. Seraj MA, El-Nakeeb MM, Estafan MY, et al. The preoperative use of cimetidine in reducing acidity of gastric secretion. *Middle East J Anaesthesiol.* 1980;5(7):445-455.
127. Smith JL, Gamal MA, Chremos AN, Graham DY. Famotidine, a new H2-receptor antagonist. Effect on parietal, nonparietal, and pepsin secretion in man. *Dig Dis Sci.* 1985;30(4):308-312.
128. Longstreth GF, Go VL, Malagelada JR. Postprandial gastric, pancreatic, and biliary response to histamine H2-receptor antagonists active duodenal ulcer. *Gastroenterology.* 1977;72(1):9-13.
129. Richardson CT, Walsh JH, Hicks MI. The effect of cimetidine, a new histamine H2-receptor antagonist, on meal-stimulated acid secretion, serum gastrin, and gastric emptying in patients with duodenal ulcer. *Gastroenterology.* 1976;71(1):19-23.
130. Domschke W, Lux G, Domschke S. Furan H2-antagonist ranitidine inhibits pentagastrin-stimulated gastric secretion stronger than cimetidine. *Gastroenterology.* 1980;79(6):1267-1271.
131. Dammann HG, Gottlieb WR, Walter TA, Müller P, Simon B, Keohane P. The 24-hour acid suppression profile of nizatidine. *Scand J Gastroenterol Suppl.* 1987;136:56-60.
132. Konturek JW, Beneke M, Koppermann R, Petersen-Braun M, Weingärtner U. The efficacy of hydrotalcite compared with OTC famotidine in the on-demand treatment of gastroesophageal reflux disease: a non-inferiority trial. *Med Sci Monit.* 2007;13(1):CR44-CR49.
133. Sewing KF, Billian A, Malchow H. Comparative study with ranitidine and cimetidine on gastric secretion in normal volunteers. *Gut.* 1980;21(9):750-752.
134. Palacios B, Montero MJ, Sevilla MA, Román LS. JB-9322, a new selective histamine H2-receptor antagonist with potent gastric mucosal protective properties. *Br J Pharmacol.* 1995;115(1):57-66.
135. Jan M, Mughal MA, Tanwani RK, Aamir K, Ali M. Evaluation of combined effect of verapamil and ranitidine on the volume and acidity of carbachol induced gastric secretion. *J Ayub Med Coll Abbottabad.* 2004;16(2):34-37.
136. McDonald RE. The effect of antihistaminic drugs on salivary flow and viscosity. *J Dent Res.* 1953;32(2):224-226.
137. Diebel LN, Liberati DM, Hall-Zimmerman L. H2 blockers decrease gut mucus production and lead to barrier dysfunction in vitro. *Surgery.* 2011;150(4):736-743.

138. Parkman HP, Urbain JL, Knight LC, et al. Effect of gastric acid suppressants on human gastric motility. *Gut*. 1998;42(2):243-250.
139. Tomita T, Miwa H. Do histamine-2 receptor antagonists and proton pump inhibitors really have no effect on the gastric emptying rate? *J Neurogastroenterol Motil*. 2011;17(4):434. author reply 435.
140. Koskenpato J, Punkkinen JM, Kairemo K, Färkkilä M. Nizatidine and gastric emptying in functional dyspepsia. *Dig Dis Sci*. 2008;53(2):352-357.
141. Scarpignato C, Bertaccini G. Different effects of cimetidine and ranitidine on gastric emptying in rats and man. *Agents Actions*. 1982;12(1-2):172-173.
142. Takahashi Y, Amano Y, Yuki T, et al. Influence of acid suppressants on gastric emptying: cross-over analysis in healthy volunteers. *J Gastroenterol Hepatol*. 2006;21(11):1664-1668.
143. Mohammed R, Holden RJ, Hearn JB, McKibben BM, Buchanan KD, Crean GP. Effects of eight weeks' continuous treatment with oral ranitidine and cimetidine on gastric acid secretion, pepsin secretion, and fasting serum gastrin. *Gut*. 1983;24(1):61-66.
144. Hirschowitz BI, Molina E. Effect of cimetidine on histamine-stimulated gastric acid and electrolytes in dogs. *Am J Physiol*. 1983;244(4):G416-G420.
145. Gupta RW, Tran L, Norori J, et al. Histamine-2 receptor blockers alter the fecal microbiota in premature infants. *J Pediatr Gastroenterol Nutr*. 2013;56(4):397-400.
146. Brown KE, Knoderer CA, Nichols KR, Crumby AS. Acid-suppressing agents and risk for Clostridium difficile infection in pediatric patients. *Clin Pediatr (Phila)*. 2015;54(11):1102-1106.
147. Nylund CM, Eide M, Gorman GH. Association of Clostridium difficile infections with acid suppression medications in children. *J Pediatr*. 2014;165(5):979-984.e1.
148. Tleyjeh IM, Abdulhak AB, Abdulhak AAB, et al. The association between histamine 2 receptor antagonist use and Clostridium difficile infection: a systematic review and meta-analysis. *PLoS One*. 2013;8(3):e56498.
149. Shah R, Richardson P, Yu H, Kramer J, Hou JK. Gastric acid suppression is associated with an increased risk of adverse outcomes in inflammatory bowel disease. *Digestion*. 2017;95(3):188-193.
150. Mössner J. Magen-Darm-Mittel und Lebertherapeutika. In: Schwabe U, Paffrath D, Ludwig WD, Klauber J, eds. *Arzneiverordnungs-Report 2017*. Berlin, Heidelberg: Springer; 2017.
151. Strand DS, Kim D, Peura DA. 25 Years of proton pump inhibitors: a comprehensive review. *Gut Liver*. 2017;11(1):27-37.
152. Williams MP, Sercombe J, Hamilton ML, Pounder RE. A placebo-controlled trial to assess the effects of 8 days of dosing with rabeprazole versus omeprazole on 24-h intragastric acidity and plasma gastrin concentrations in young healthy male subjects. *Aliment Pharmacol Ther*. 1998;12(11):1079-1089.
153. Uesugi T, Mikawa K, Nishida K, Morikawa O, Takao Y, Obara H. The efficacy of lalutidine in improving preoperative gastric fluid property: a comparison with ranitidine and rabeprazole. *Anesth Analg*. 2002;95(1):144-147. table of contents.
154. Wang X, Fang J-Y, Lu R, Sun D-F. A meta-analysis: comparison of esomeprazole and other proton pump inhibitors in eradicating Helicobacter pylori. *Digestion*. 2006;73(2-3):178-186.
155. Çelebi A, Aydın D, Kocaman O, Konduk BT, Şentürk Ö, Hülagü S. Comparison of the effects of esomeprazole 40 mg, rabeprazole 20 mg, lansoprazole 30 mg, and pantoprazole 40 mg on intragastric pH in extensive metabolizer patients with gastroesophageal reflux disease. *Türk J Gastroenterol*. 2016;27(5):408-414.
156. Kirchheiner J, Glatt S, Fuhr U, et al. Relative potency of proton-pump inhibitors-comparison of effects on intragastric pH. *Eur J Clin Pharmacol*. 2009;65(1):19-31.
157. Novotny M, Klimova B, Valis M. PPI long term use: risk of neurological adverse events? *Front Neurol*. 2018;9:1142.
158. WHOCC. WHOCC - ATC/DDD index. Available at: <https://www.whooc.no/atc-ddd-index/>. Accessed May 2, 2019. Updated May 2, 2019.
159. NICE (National Institute for Health and Care Excellence). Dyspepsia gastro-oesophageal reflux disease overview. Available at: <https://pathways.nice.org.uk/pathways/dyspepsia-and-gastro-oesophageal-reflux-disease>. Accessed May 2, 2019.
160. American Gastroenterological Association. Esophageal & gastric disorders guidelines. Available at: <https://www.gastro.org/guidelines/esophageal-and-gastric-disorders>. Accessed May 2, 2019. Updated February 8, 2019.
161. World Gastroenterology Organisation. Global Perspective on Gastroesophageal Reflux Disease. Available at <http://www.worldgastroenterology.org/guidelines/global-guidelines/gastroesophageal-reflux-disease/gastroesophageal-reflux-disease-english>. Accessed May 2, 2019. Updated 10/2015.
162. CIMS. DIRAB-D dosage & drug information | CIMS India. Available at: <https://www.mims.com/india/drug/info/dirab-d/dirab-d%20cap>. Accessed May 2, 2019.
163. Actuaed Norutec tabletas, medicamento para esofagitis, Vademécum actuaed-rx. Available at: <https://www.medicamentos.com.mx/doctm/34613.htm>. Accessed May 2, 2019. Updated April 3, 2019.
164. Chiral Emcure. Research, Manufacturing of APIs, Formulations and Biotechnology. Available at: <http://www.chiralemcare.com/chiraldrugs.php>. Accessed April 1, 2019.
165. Ferreiro JL, Angiolillo DJ. Clopidogrel response variability: current status and future directions. *Thromb Haemost*. 2009;102(1):7-14.
166. Otake K, Sakurai Y, Nishida H, et al. Characteristics of the novel potassium-competitive acid blocker vonoprazan fumarate (TAK-438). *Adv Ther*. 2016;33(7):1140-1157.
167. Hatlebakk JG, Katz PO, Camacho-Lobato L, Castell DO. Proton pump inhibitors: better acid suppression when taken before a meal than without a meal. *Aliment Pharmacol Ther*. 2000;14(10):1267-1272.
168. Tolman KG, Sanders SW, Buchi KN, Karol MD, Jennings DE, Ringham GL. The effects of oral doses of lansoprazole and omeprazole on gastric pH. *J Clin Gastroenterol*. 1997;24(2):65-70.
169. Sanders SW, Tolman KG, Greski PA, Jennings DE, Hoyos PA, Page JG. The effects of lansoprazole, a new H₂K⁺-ATPase inhibitor, on gastric pH and serum gastrin. *Aliment Pharmacol Ther*. 1992;6(3):359-372.
170. Bell NJ, Hunt RH. Time to maximum effect of lansoprazole on gastric pH in normal male volunteers. *Aliment Pharmacol Ther*. 1996;10(6):897-904.
171. Lenz K, Buder R, Firlinger F, Lohr G, Voglmayr M. Effect of proton pump inhibitors on gastric pH in patients exposed to severe stress. *Wien Klin Wochenschr*. 2015;127(1-2):51-56.
172. Laine L, Shah A, Bermanian S. Intragastric pH with oral vs intravenous bolus plus infusion proton-pump inhibitor therapy in patients with bleeding ulcers. *Gastroenterology*. 2008;134(7):1836-1841.
173. Foltz E, Azad S, Everett ML, et al. An assessment of human gastric fluid composition as a function of PPI usage. *Physiol Rep*. 2015;3(1):1-13.
174. Miner P, Katz PO, Chen Y, Sostek M. Gastric acid control with esomeprazole, lansoprazole, omeprazole, pantoprazole, and rabeprazole: a five-way cross-over study. *Am J Gastroenterol*. 2003;98(12):2616-2620.
175. Mertz-Nielsen A, Hillingsjö J, Bukhave K, Rask-Madsen J. Omeprazole promotes proximal duodenal mucosal bicarbonate secretion in humans. *Gut*. 1996;38(1):6-10.
176. Michalek W, Semler JR, Kuo B. Impact of acid suppression on upper gastrointestinal pH and motility. *Dig Dis Sci*. 2011;56(6):1735-1742.
177. Steingold A, Sauter M, Curcic J, et al. Volume, distribution and acidity of gastric secretion on and off proton pump inhibitor treatment: a randomized double-blind controlled study in patients with gastro-oesophageal reflux disease (GERD) and healthy subjects. *BMC Gastroenterol*. 2015;15:111.
178. Babaei A, Bhargava V, Aalam S, Scadeng M, Mittal RK. Effect of proton pump inhibition on the gastric volume: assessed by magnetic resonance imaging. *Aliment Pharmacol Ther*. 2009;29(8):863-870.
179. Hashimoto H, Kushikata T, Kudo M, Hirota K. Does long-term medication with a proton pump inhibitor induce a tolerance to H₂ receptor antagonist? *J Gastroenterol*. 2007;42(4):275-278.
180. Gouda B, Lydon A, Badhe A, Shorten CD. Effects of ranitidine and omeprazole on residual gastric volume and pH in elective surgical patients. *Eur J Anaesthesiol*. 2000;17(Supplement 19):32.
181. Hirota K, Kudo M, Hashimoto H, Kushikata T. The efficacy of preanesthetic proton pump inhibitor treatment for patients on long-term H₂ antagonist therapy. *Anesth Analg*. 2005;101(4):1038-1041. table of contents.
182. Litou C, Vertzoni M, Goumas C, et al. Characteristics of the human upper gastrointestinal contents in the fasted state under hypo- and A-chlorhydric gastric conditions under conditions of typical drug - drug interaction studies. *Pharm Res*. 2016;33(6):1399-1412.
183. Yaşar NF, Polat E, Duman M, et al. In vitro effects of rabeprazole on human pylorus tone. *J Neurogastroenterol Motil*. 2015;21(2):217-221.
184. Rasmussen L, Qvist N, Oster-Jørgensen E, Rehfeld JF, Holst JJ, Pedersen SA. A double-blind placebo-controlled study on the effects of omeprazole on gut hormone secretion and gastric emptying rate. *Scand J Gastroenterol*. 1997;32(9):900-905.
185. Sanaka M, Yamamoto T, Kuyama Y. Effects of proton pump inhibitors on gastric emptying: a systematic review. *Dig Dis Sci*. 2010;55(9):2431-2440.
186. Kamiya T, Shikano M, Tanaka M, et al. The effect of omeprazole on gastric myoelectrical activity and emptying. *J Smooth Muscle Res*. 2011;47(3-4):79-87.
187. Vidon N, Dutreuil C, Scoule JC, Delchier JC. Does lansoprazole influence postprandial digestive function? *Aliment Pharmacol Ther*. 1993;7(6):629-634.
188. Lundell L, Vieth M, Gibson F, Nagy P, Kahrilas PJ. Systematic review: the effects of long-term proton pump inhibitor use on serum gastrin levels and gastric histology. *Aliment Pharmacol Ther*. 2015;42(6):649-663.
189. Tariq R, Singh S, Gupta A, Pardi DS, Khanna S. Association of gastric acid suppression with recurrent clostridium difficile infection: a systematic review and meta-analysis. *JAMA Intern Med*. 2017;177(6):784-791.
190. Engstrand L, Lindberg M. Helicobacter pylori and the gastric microbiota. *Best Pract Res Clin Gastroenterol*. 2013;27(1):39-45.
191. Sanduleanu S, Jonkers D, Bruine A de, Hameeteman W, Stockbrugger RW. Non-Helicobacter pylori bacterial flora during acid-suppressive therapy: differential findings in gastric juice and gastric mucosa. *Aliment Pharmacol Ther*. 2001;15(3):379-388.
192. Paroni Sterbini F, Palladini A, Masucci L, et al. Effects of proton pump inhibitors on the gastric mucosa-associated microbiota in dyspeptic patients. *Appl Environ Microbiol*. 2016;82(22):6633-6644.
193. Parsons BN, Ijaz UZ, D'Amore R, et al. Comparison of the human gastric microbiota in hypochlorhydric states arising as a result of Helicobacter pylori-induced atrophic gastritis, autoimmune atrophic gastritis and proton pump inhibitor use. *PLoS Pathog*. 2017;13(11):e1006653.
194. Castellani C, Singer G, Kashofer K, et al. The influence of proton pump inhibitors on the fecal microbiome of infants with gastroesophageal reflux-A

- prospective longitudinal interventional study. *Front Cell Infect Microbiol*. 2017;7:444.
195. Le Bastard Q, Al-Ghalith GA, Grégoire M, et al. Systematic review: human gut dysbiosis induced by non-antibiotic prescription medications. *Aliment Pharmacol Ther*. 2018;47(3):332-345.
 196. Takagi T, Naito Y, Inoue R, et al. The influence of long-term use of proton pump inhibitors on the gut microbiota: an age-sex-matched case-control study. *J Clin Biochem Nutr*. 2018;62(1):100-105.
 197. Oshima T, Wu L, Li M, Fukui H, Watari J, Miwa H. Magnitude and direction of the association between Clostridium difficile infection and proton pump inhibitors in adults and pediatric patients: a systematic review and meta-analysis. *J Gastroenterol*. 2018;53(1):84-94.
 198. Trifan A, Stanciu C, Girleanu I, et al. Proton pump inhibitors therapy and risk of Clostridium difficile infection: systematic review and meta-analysis. *World J Gastroenterol*. 2017;23(35):6500-6515.
 199. Jackson MA, Goodrich JK, Maxam M-E, et al. Proton pump inhibitors alter the composition of the gut microbiota. *Gut*. 2016;65(5):749-756.
 200. Imhann F, Bonder MJ, Vich Vila A, et al. Proton pump inhibitors affect the gut microbiome. *Gut*. 2016;65(5):740-748.
 201. Fujimori S. What are the effects of proton pump inhibitors on the small intestine? *World J Gastroenterol*. 2015;21(22):6817-6819.
 202. Mullin JM, Valenzano MC, Whitby M, et al. Esomeprazole induces upper gastrointestinal tract transmucosal permeability increase. *Aliment Pharmacol Ther*. 2008;28(11-12):1317-1325.
 203. Murray LJ, Gabello M, Rudolph DS, et al. Transmucosal gastric leak induced by proton pump inhibitors. *Dig Dis Sci*. 2009;54(7):1408-1417.
 204. Gabello M, Valenzano MC, Barr M, Zurbach P, Mullin JM. Omeprazole induces gastric permeability to digoxin. *Dig Dis Sci*. 2010;55(5):1255-1263.
 205. Gabello M, Valenzano MC, Zurbach EP, Mullin JM. Omeprazole induces gastric transmucosal permeability to the peptide bradykinin. *World J Gastroenterol*. 2010;16(9):1097-1103.
 206. Farrell C, Morgan M, Tully O, et al. Transepithelial leak in Barrett's esophagus patients: the role of proton pump inhibitors. *World J Gastroenterol*. 2012;18(22):2793-2797.
 207. Vertzoni M, Dressman J, Butler J, Hemenstall J, Reppas C. Simulation of fasting gastric conditions and its importance for the in vivo dissolution of lipophilic compounds. *Eur J Pharm Biopharm*. 2005;60(3):413-417.
 208. Jantravid E, Janssen N, Reppas C, Dressman JB. Dissolution media simulating conditions in the proximal human gastrointestinal tract: an update. *Pharm Res*. 2008;25(7):1663-1676.
 209. Wunderlich M. *Biorelevante in vitro Methoden zur Vorhersage des in vivo Verhaltens von schlecht wasserlöslichen, schwach basischen Arzneistoffen*. Dissertation zur Erlangung des Doktorgrades der Naturwissenschaften. 2004.
 210. *The Japanese Pharmacopoeia: Seventeenth Edition*. 17th ed. Tokyo: Pharmaceutical and Medical Device Regulatory Science Society of Japan; 2016.
 211. Sheng JJ, McNamara DP, Amidon GL. Toward an in vivo dissolution methodology: a comparison of phosphate and bicarbonate buffers. *Mol Pharm*. 2009;6(1):29-39.
 212. Markopoulos C, Andreas CJ, Vertzoni M, Dressman J, Reppas C. In-vitro simulation of luminal conditions for evaluation of performance of oral drug products: choosing the appropriate test media. *Eur J Pharm Biopharm*. 2015;93:173-182.
 213. Piper DW, Fenton BH. pH stability and activity curves of pepsin with special reference to their clinical importance. *Gut*. 1965;6(5):506-508.
 214. Jenquin MR, Liebowitz SM, Sarabia RE, McGinity JW. Physical and chemical factors influencing the release of drugs from acrylic resin films. *J Pharm Sci*. 1990;79(9):811-816.
 215. Bodmeier R, Guo X, RE S, Skultety PF. The influence of buffer species and strength on diltiazem HCl release from beads coated with the aqueous cationic polymer dispersions, Eudragit RS, RL 30D. *Pharm Res*. 1996;13(1):52-56.
 216. Rudolph MW, Klein S, Beckert TE, Peterleit H, Dressman JB. A new 5-aminosalicylic acid multi-unit dosage form for the therapy of ulcerative colitis. *Eur J Pharm Biopharm*. 2001;51(3):183-190.
 217. Mann J, Dressman J, Rosenblatt K, et al. Validation of dissolution testing with biorelevant media: an OrBiTo study. *Mol Pharm*. 2017;14(12):4192-4201.
 218. FDA. Framework for assessing pH-dependent drug-drug interactions; establishment of a public docket; request for comments. Available at: <https://www.regulations.gov/document?D=FDA-2018-N-1820-0001>. Accessed May 2, 2019.
 219. FDA. Framework for assessing pH-dependent drug-drug interactions; request for comments. Available at: <https://www.regulations.gov/docketBrowser?rpp=25&so=DESC&sb=commentDueDate&po=0&dt=PS&D=FDA-2018-N-1820>. Accessed May 2, 2019.

Supporting information

Table 8. Fasted state gastric fluid properties

| Parameters | Physiology | Antacids | HZRAs | PPIs | FaSSGF ²⁰⁷ |
|------------------------|--|---|--|--|------------------------|
| Volume (mL) | 28 - 45 ^{9,14} | No data | Reduction ¹¹⁸⁻¹²⁰ , biopharmaceutically insignificant | Reduction ^{177,179,181} , biopharmaceutically insignificant | 250 |
| pH | 1 - 3 ^{14,24} | 3 - 4 ^{7,82} (short elevation) Raised with surcalate formulations (dose dependent) ^{91,92} | 3 - 6 ^{119,124-126} | 4 - 6 ¹⁵⁶ | 1.6 |
| Viscosity (cP) | 1.5 ³⁰ | | No consistent data | No consistent data | No data |
| Surface tension (mN/m) | 30 - 45 ^{26,33,39} | Bile salt adsorption ⁹⁴⁻⁹⁶ in vivo significance disputed | No data | Lower ¹⁸² , biopharmaceutically insignificant | 42.6 |
| Gastric emptying (min) | 60 | Possibly prolonged ⁹⁹ | No consistent data | No data | Paddle speed 50/75 rpm |
| Pepsin (mg/mL) | 0.1 ³⁹ | 0.02 - 0.08 ^{103,105} | 0.05 - 0.07 ¹⁴³ | 0.02 ¹⁷³ | 0.1 |
| Secretion | 75 - 160 mEq/l (HCl), 19 - 70 mEq/l Na ⁺ ⁵⁴ (98 - 140 mOsmol) ¹³⁹ | Higher secretion with chronic use (rebound effect) ⁷⁴ | Inhibition of HCl production ^{121,134,135} | Inhibition of HCl production ¹⁷⁷ | 120 mOsmol (NaCl) |
| Microflora | Sterile - 1000 CFU/g ⁶³ | No significant change | Possible changes with chronic use ⁶⁴ | Possible changes with chronic use ^{190,191} | - |

Table 9. Fed state gastric fluid properties

| Parameters | Physiology | Antacids | HZRAs | PPIs | FeSSGF ⁴¹ |
|------------------------|--|--|-------------------------------------|---|------------------------|
| Volume (mL) | 859 ² | Higher ⁴² , biopharmaceutically insignificant | No significant change | Reduction ⁴³ , biopharmaceutically insignificant | 900 |
| pH | 3 - 7 ⁹⁻¹¹ | 6 - 7 (short elevation) ⁴⁴ | 6 - 7 ⁴⁴ | 6 - 7 ⁴⁵⁻⁴⁷ | 5 |
| Viscosity | 10 - 2000 ^{48,49} | No data | No consistent data | No data | No data |
| Surface tension (mN/m) | 30 - 31 ²² | No data | No significant change ⁵⁰ | No data | 52 |
| Gastric emptying (min) | Dependent of caloric value of the meal | Possibly prolonged ⁴² | No consistent data | No consistent data | Paddle speed 50/75 rpm |
| Meal content | Diverse (e.g. USP reference meal: proteins, carbohydrates and fat 800 – 1000 cal) | No significant change | No significant change | No significant change | Milk:Buffer (1:1) |
| Osmolality | Diverse | No significant change | No significant change | No significant change | 400 mOsmol (NaCl) |

Table 10. Fasted state small intestinal fluid properties

| Parameters | Physiology | Antacids | H2RAs | PPIs | FaSSIF ⁵¹ | FaSSIF (v.2) ⁴¹ |
|------------------------|---|--|---|--|------------------------|----------------------------|
| Volume (mL) | 40 - 400 ^{2,9} | Change possible ⁵² , biopharmaceutically insignificant | No data | No data | 500 | 500 |
| pH | 6 - 7 ^{9,53} | 5 - 6 ⁵⁴ | No data | Lower ⁵⁵ , biopharmaceutically insignificant | 6.5 | 6.5 |
| Viscosity | No data | Rise possible (sulfate formulations) | Change possible ⁵² , biopharmaceutically insignificant | No data | No data | No data |
| Surface tension (mN/m) | 30 - 45 ^{22,56} | Higher due to possible adsorption effects | No data | No significant change ⁵⁷ | No data | 54.3 |
| Motility (cycles/min) | 8 - 12 ⁵⁸ | Increased due to Mg ^{59,60} , decreased due to Al formulations ^{53,61} | No consistent data | No data | Paddle speed 50/75 rpm | Paddle speed 50/75 rpm |
| Secretion | 140 - 150 mM bicarbonate ⁶² | No data | No data | Higher duodenal bicarbonate secretion ⁶³ | 270 ± 10 mOsmol | 180 ± 10 mOsmol |
| Microflora | 10 ⁴ - 10 ⁷ CFU/g ³⁷ | No significant change | Increased risk of microbiome diversity change ^{64,65} | Increased risk of microbiome diversity change ⁶⁶⁻⁷⁰ | - | - |



Prediction of plasma profiles of a weakly basic drug after administration of omeprazole using PBPK modeling

Domagoj Segregur^a, James Mann^b, Andrea Moir^c, Eva M. Karlsson^d, Jennifer Dressman^{a,e,*}

^a Institute of Pharmaceutical Technology, J. W. Goethe University, 9 Max von Laue St., 60438 Frankfurt am Main, Germany

^b Oral Product Development, Pharmaceutical Technology & Development, Operations, AstraZeneca, Macclesfield, UK

^c New Modalities & Parenteral Development, Pharmaceutical Technology & Development, Operations, AstraZeneca, Macclesfield, UK

^d Oral Product Development, Pharmaceutical Technology & Development, Operations, AstraZeneca, Gothenburg, Sweden

^e Fraunhofer Institute for Translational Medicine and Pharmacology, ITMP, Theodor Stern Kai 7, 60596 Frankfurt am Main, Germany

ARTICLE INFO

Keywords:

Weak base
Drug-drug interaction(s)
Proton pump inhibitor
Acid-reducing agent
Physiologically based pharmacokinetic (PBPK) modeling
Dissolution
pH

ABSTRACT

Background: Oral medicines must release the drug appropriately in the GI tract in order to assure adequate and reproducible absorption. Disease states and co-administration of drugs may alter GI physiology and therefore the release profile of the drug. Acid-reducing agents (ARAs), especially proton pump inhibitors (PPIs), are frequently co-administered during various therapies. As orally administered drugs are frequently poorly soluble weak bases, PPI co-administration raises the risk of pH-induced drug-drug interactions (DDIs) and the potential for changes in the therapeutic outcome.

Methods: This research compared the dissolution data of a poorly soluble weakly basic drug ("PSWB 001") from capsules in standard fasted state biorelevant media (FaSSGF, FaSSIF V1 and FaSSIF V2), water and recently devised media representing gastric conditions under various levels of PPI co-administration. An *in silico* simulation model, based on Simcyp software, was developed to compare simulated plasma profiles with clinical data. **Results:** PSWB 001 capsules showed rapid and complete dissolution in acidic conditions representing gastric fluids, whereas limited dissolution was observed in deionized water, media representing PPI co-administration and in two biorelevant media representing fluids in the upper small intestine. Buffer capacity and the presence of native surfactants were shown to be important factors in the *in vitro* dissolution of PSWB 001. The data from *in vitro* experiments were used in conjunction with the *in silico* simulation model, which correctly predicted the plasma profiles of PSWB 001 when administered without PPIs, as well as bracketing the PPI effect observed *in vivo*.

Conclusions: Recently developed biorelevant media representing gastric conditions under PPI therapy, combined with PBPK modeling, were able to bracket the observed plasma profiles of PSWB 001. These media may also be useful for predicting PPI effects for other poorly soluble, weakly basic drugs.

1. Introduction

One of the important steps to successful oral drug therapy is to ensure the appropriate release of the drug in the gastrointestinal (GI) tract. Only when the drug is released and dissolved from the formulation into the GI fluids can a reproducible and adequate absorption of the drug be attained and the therapeutic aims realized.

Many factors have a significant impact on GI physiology, including food intake, disease state and drug co-administration (Dressman and Reppas, 2016; Hedaya, 2012). Since changes in the GI fluids and overall physiology may affect drug release, these factors should be taken into

consideration during the prediction and evaluation of drug performance. During development of oral products, *in vitro* dissolution experiments which are designed to represent the behavior of oral formulations *in vivo* can be applied for this purpose. When choosing the experimental design, particular attention should be given to changes in GI physiology which occur due to the influence of co-administered drugs, as well as changes that occur in the patient population due to the disease state.

An example of drugs which are often co-administered to patients are the acid-reducing agents (ARAs). As many new oral medicines are poorly soluble and weakly basic, their release in the gastrointestinal (GI) tract

* Corresponding author at: Institute of Pharmaceutical Technology, J. W. Goethe University, 9 Max von Laue St., 60438 Frankfurt am Main, Germany.
E-mail address: Dressman@em.uni-frankfurt.de (J. Dressman).

<https://doi.org/10.1016/j.ejps.2020.105656>

Received 8 July 2020; Received in revised form 24 November 2020; Accepted 24 November 2020

Available online 27 November 2020

0928-0987/© 2020 Elsevier B.V. All rights reserved.

can be strongly impacted by the elevation in gastric pH which results from co-administration of ARAs. In an earlier publication we described two sets of media designed to reflect gastric conditions after administration of proton pump inhibitors (PPIs), which are an important subclass of ARAs. Media with pH 4 were used to represent a milder PPI effect on gastric pH, while media with pH 6 were used to represent a stronger PPI effect (Segregur et al., 2019).

PSWB 001 is a poorly soluble, weakly basic compound which shows a pronounced drug-drug interaction with PPIs (see *Pharmacokinetic Studies*) and thus serves as a suitable example to determine whether the extent of the PPI impact on drug release and hence absorption from the GI tract can be predicted from *in vitro* experiments in conjunction with an *in silico* PBPK model.

2. Materials and methods

2.1. Materials

PSWB 001 100 mg capsules and active pharmaceutical ingredient (API) powder were provided by AstraZeneca. The composition of the capsules consisted of commonly used excipients including a filler, disintegrant and lubricant, which were blended with PSWB 001 and dry granulated. FaSSiF/FaSSiF/FaSSGF and FaSSiF-V2 powders were kindly donated by biorelevant.com (Surrey, UK). Acetonitrile, tri-sodium citrate dihydrate, sodium chloride, hydrochloric acid 1 M and sodium hydroxide 1 M were purchased from VWR Chemicals ProLabo (Leuven, Belgium), sodium dihydrogen phosphate dihydrate, sodium acetate, disodium hydrogen phosphate and ammonium acetate from Merck KGaA (Darmstadt, Germany), maleic acid and pepsin from porcine gastric mucosa from Sigma-Aldrich (Steinheim, Germany) and anhydrous citric acid from Caesar & Loretz GmbH (Hilden, Germany).

2.2. Solubility measurements

PSWB 001 solubility in deionized water, various buffers and biorelevant media was investigated using the UniPrep™ method (Glomme et al., 2005). An excess of PSWB 001 API powder was added into the UniPrep™ vial (GE Healthcare, Whatman Inc., New Jersey, USA), 3 ml of the respective medium was added, the vial was sealed, and then shaken at 37 °C for 24 h using a Heidolph Polymax 1040 platform shaker (Heidolph Instruments GmbH & CO., Schwabach, Germany) in a Heraeus Function Line heating oven (Thermo Fisher Scientific Inc., Waltham, USA). After 24 h, the built-in filter in the vial was plunged through the suspension and the filtrate was sampled, immediately diluted, and analyzed by HPLC (see section *Quantitative analysis of samples*). The buffers used in the solubility experiments were acetate pH 4 (corresponding to a Level 1 version (Markopoulos et al., 2015) of the PPI pH 4 acetate medium), maleate pH 6 (10 mEq/L/ΔpH), phosphate pH 6.5 (corresponding to the Level 1 version of FaSSiF V1) and maleate pH 6.5 (corresponding to the Level 1 version of FaSSiF V2). Solubility was additionally measured in the following Level 2 biorelevant media: FaSSiF V1, FaSSiF V2, PPI pH 4 acetate, citrate and McIlvaine, as well as pH 6 maleate, citrate and McIlvaine media. The pH was confirmed at the end of each solubility experiment and, with the exception of deionized water, did not deviate more than ± 0.05 from the starting pH. All solubility measurements were done in triplicate (n = 3).

2.3. Single-stage dissolution testing

The dissolution test apparatus used in the experiments was a USP 2 (Paddle) apparatus Erweka DT 700 (ERWEKA GmbH, Langen, Germany). Standard 1 liter vessels and Japanese Pharmacopeia (The Ministry of Health, Labour and Welfare 2016) sinkers (Cole-Parmer GmbH, Wertheim, Germany) were used. The temperature was set to 37 ± 0.5 °C, the paddle rotation speed to 50 rpm and samples were taken 5, 10, 15, 20, 30, 45, 60, 90 and 120 min after starting the experiment. Samples

were filtered through 0.45 µm PTFE filters (ReZist™ filter unit, GE Healthcare, Whatman Inc., New Jersey, USA) and diluted immediately thereafter to prevent precipitation. Dissolution of the capsules was studied in deionized water (measured pH was 5.6), FaSSGF (pH 1.6), PPI pH 4 media (made with acetate, citrate or McIlvaine buffers), PPI pH 6 media (made with maleate, citrate or McIlvaine buffers), as well as FaSSiF V1 (pH 6.5) and FaSSiF V2 (pH 6.5). The pH of the buffered media at the end of the dissolution experiment did not deviate from the starting value before the experiment. The number of replicates for each experiment was n = 3.

2.4. Two-stage dissolution testing

The dissolution test apparatus, vessels and sinkers used in the experiments were the same as in the single-stage dissolution experiments. The temperature was set to 37 ± 0.5 °C, the paddle rotation speed to 50 rpm. The procedure for the two-stage methodology was adapted from the OrBiTo methodology (Mann et al., 2017), using (a) FaSSGF (pH 1.6) 250 ml as the gastric compartment, with bolus addition of 250 ml FaSSiF V1 double concentrate (with a pH of 7.5) to generate FaSSiF V1 as the intestinal medium, and (b) FaSSGF (pH 2) 250 ml as the gastric compartment, with bolus addition of 250 ml FaSSiF V2 double concentrate (pH 10.8) to generate FaSSiF V2 as the intestinal medium (the buffer capacity of FaSSiF V2 is lower than that of FaSSiF V1, hence the adjustment of the gastric compartment pH in this case). Samples were taken 5, 10, 20, 30, 35, 40, 50, 60, 90 and 120 min after starting the experiment, whereby after the 30 min sample was taken from the gastric compartment, the FaSSiF V1 or V2 double concentrate was added as a bolus. The final pH and composition of the 500 ml of media after the addition of the FaSSiF double concentrates were comparable to the standard FaSSiF V1 and FaSSiF V2 media. Following two hours of dissolution, an “infinity spin” was conducted: the paddle rotation speed was set to 120 rpm and the experiment continued for additional 30 min before taking an additional sample. The infinity spin is used to facilitate dissolution of the drug particles that would otherwise, at a low rotation speed, dissolve only after a long (“infinite”) time. Samples were filtered through 0.45 µm PTFE filters (ReZist™ filter unit, GE Healthcare, Whatman Inc., New Jersey, USA) and diluted immediately thereafter to prevent any potential precipitation of PSWB 001. All two-stage experiments were conducted with n = 3.

2.5. Quantitative analysis of samples

Diluted solubility and dissolution samples were analyzed using an HPLC system consisting of a Hitachi LaChrom-L 7200 autosampler (VWR Hitachi, Darmstadt, Germany), L 7220 pump (VWR Hitachi, Darmstadt, Germany), D 7000 interface (VWR Hitachi, Darmstadt, Germany), L 7420 UV Vis detector (VWR Hitachi, Darmstadt, Germany) and L 7360 oven (VWR Hitachi, Darmstadt, Germany) with a C18, 10 cm, 4.6 mm Ultracarb™ 5 µm ODS (30) column (Phenomenex LTD, Aschaffenburg, Germany). A gradient mobile phase consisting of 10 mM ammonium acetate/acetonitrile was applied, as shown in Table 1. The column temperature was held at 40 °C and the flow rate was set at 1 ml/min. The drug substance was quantified at a detection wavelength of 285 nm. The lower limit of quantification was 3 µg/ml and the method was linear over the range of 3 to 90 µg/ml.

Table 1
The gradient method for PSWB 001 HPLC analysis.

| Time (min) | 0 | 4 | 6 | 9 | 10 |
|--|----|----|----|----|----|
| Channel A (10 mM ammonium acetate) (%) | 90 | 10 | 10 | 90 | 90 |
| Channel B (acetonitrile) (%) | 10 | 90 | 90 | 10 | 10 |

2.6. Pharmacokinetic studies

The mean plasma profile after intravenous administration was obtained from a study conducted on behalf of AstraZeneca in 8 healthy adult subjects to whom PSWB 001 was micro-dosed as an intravenous solution over 2 min. This study was conducted in accordance with the relevant US Code of Federal Regulations (21 CFR 50, 54, 56, 312 and 314) and was consistent with the Declaration of Helsinki. Mean plasma profiles after oral administration with and without PPI co-administration were obtained from two studies: "Study A" and "Study B" (data for the i.v. and both oral studies are on file at AstraZeneca). In Study A, capsules containing 100 mg of PSWB 001 presented as a blend of API with an insoluble filler, were used. The study was conducted in 24 healthy adult volunteers. In the first period, a PSWB 001 capsule was administered orally with approximately 240 ml of water after an overnight fast. In the second period the healthy volunteers were administered a 40 mg omeprazole capsule q.d. for 5 days, with the PSWB 001 capsule administered with approximately 240 ml of water after an overnight fast on day 5.

In the second oral study (Study B), capsules containing a PSWB 001 100 mg formulation with the same composition as described for use in the *in vitro* experiments (see *Materials*) were administered. The study was conducted in 12 healthy adult volunteers, who were administered a single oral dose of PSWB 001 with water on Day 1. They were then given 40 mg omeprazole q.d. from Day 4 to Day 8 before administering a single oral dose of PSWB 001 with water on Day 8. Both oral studies were run in accordance with the ethical requirements referred to in the European Union (EU) directive 2001/20/EC and the ethical principles set forth in the Declaration of Helsinki.

2.7. *In silico* modeling and prediction of plasma concentrations

A "minimal" *in silico* model, based on the physicochemical and pharmacokinetic properties of PSWB 001, was developed using the

Table 2
Summary of input parameter values used for PSWB 001 simulation in the Simcyp simulator (minimal PBPK model).

| Parameter (Unit) | Value used |
|--|------------------------|
| Phys.Chem. Properties | |
| Molecular weight (g/mol) | < 500 |
| $\log P_{ow}$ | 2 |
| Compound type | Diprotic base |
| pK_{a1} | 3.5 |
| pK_{a2} | 5.8 |
| Fraction unbound in plasma | 0.026 |
| Blood/plasma ratio | 0.787 |
| Drug absorption parameters (ADAM model) | |
| $P_{eff, man}$ (10^{-4} cm/s) | 4.6 |
| Distribution | |
| Model | Minimal PBPK model |
| SAC parameters | |
| k_{in} ($-k_{12}$) | 1.66 |
| k_{out} ($-k_{21}$) | 1.45 |
| V_{sac} | 0.33 |
| V_{ss} (L/kg) | 0.484 |
| Elimination parameters | |
| Cl_r (L/h) | 47.5 |
| Population parameters | |
| Population | Sim Healthy Volunteers |
| Oral dose (mg) | 100 |

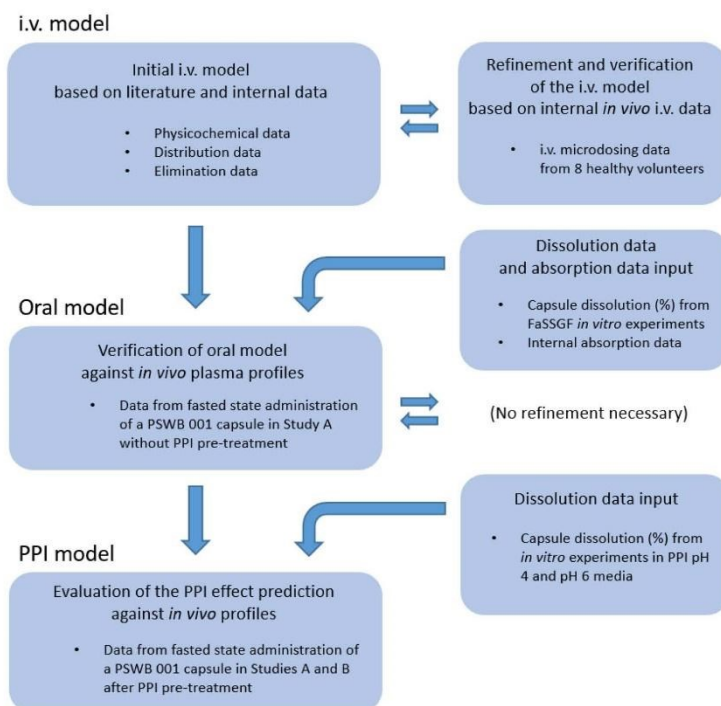


Fig. 1. Schematic of the workflow for building and verifying the PSWB 001 *in silico* model.

Simcyp Simulator 18.1 (Certara UK Limited, Simcyp, Sheffield, UK) (Fig. 1.) The parameters used to develop the model are shown in Table 2. Intravenous data were used to refine the model and determine PSWB 001's clearance by fitting the data to a two compartmental model in Simcyp. Next, the model was used to generate a simulation of the oral dose (100 mg) administered to a representative healthy volunteer (Sim-Healthy Volunteers population) with no PPI pre-treatment. The *in vitro* data for drug dissolution in 250 ml of FaSSGF (pH 1.6) was implemented in the PBPK model as a discrete profile. Predicted values were in accordance with the values observed *in vivo* and within the confidence interval of the *in vivo* values. The values of the average fold error (AFE) and the absolute average fold error (AAFE) (see section Statistics) for both the intravenous and oral plasma concentration simulations compared to the observed values were < 2.

As a next step, the dissolution data from standard biorelevant media (representing a healthy volunteer without PPI pre-treatment) were substituted with data from the dissolution experiments in media representing administration of PSWB 001 after PPI pre-treatment, also using direct input of the concentration vs. time data. Simulations were again conducted in the healthy volunteer model of Simcyp and the plasma profiles were compared against the *in vivo* PK data in healthy volunteers for the study phase in which they had received a PPI pre-treatment.

2.8. Statistics

Solubility and dissolution data are presented as arithmetic mean values and standard deviations. For comparison of the dissolution profiles the similarity factor (f_2) was used, per the FDA guidance (FDA, 1997).

To assess prediction accuracy, the average fold error (AFE) and the absolute average fold error (AAFE) (Obach et al., 1997) were calculated using the mean *in vivo* plasma concentrations and predicted concentrations corresponding to the *in vivo* sampling time points as shown below:

$$AFE = 10^{\lambda} \left(\frac{\sum \log \frac{c_p}{c_o}}{n} \right)$$

$$AAFE = 10^{\lambda} \left(\frac{\sum \left| \log \frac{c_p}{c_o} \right|}{n} \right)$$

c_p , predicted concentration at time point x ; c_o , observed concentration at time point x ; n , number of sampling points

AFE and AAFE values were determined over the time span 0 to 3 h after intravenous dosing and 0 to 6 h after oral dosing, after which respective times the plasma concentrations were negligible.

3. Results

3.1. Solubility in dissolution media

The aqueous solubility of PSWB 001, as well as its solubility in buffers, FaSSIF V1 and V2 and the PPI media are shown in Table 3.

3.2. Dissolution in gastric media simulating the fasted state with and without PPI pretreatment

PSWB 001, which has two basic moieties, dissolves quickly in FaSSGF (pH 1.6), reaching over 90% dissolved in under 30 min (Fig. 2).

If PPIs are co-administered during a therapy, or in the case of achlorhydric patients, it is anticipated that the higher gastric pH will hinder the dissolution of PSWB 001. Results for dissolution of PSWB 001 from the capsules in 250 ml of the PPI media can be viewed in Fig. 2. Three pairs of PPI media were used: acetate pH 4 / maleate pH 6, citrate

Table 3

Experimental PSWB 001 solubility in various media.

| Medium | Mean solubility (mg/ml) | Standard deviation (mg/ml) |
|--|-------------------------|----------------------------|
| FaSSGF (pH 1.6) ^a | > 100 | - |
| PPI acetate pH 4 ^b | 1.528 | 0.010 |
| PPI citrate pH 4 ^b | 1.354 | 0.002 |
| PPI McIlvaine pH 4 ^b | 1.323 | 0.038 |
| pH 4 buffer (acetate 7.5 mM) | 1.572 | 0.037 |
| PPI maleate pH 6 ^b | 0.092 | 0.002 |
| PPI citrate pH 6 ^b | 0.094 | 0.001 |
| PPI McIlvaine pH 6 ^b | 0.095 | 0.004 |
| pH 6 buffer (maleate 10 mM) | 0.099 | 0.001 |
| Deionised water (pH 5.6, final pH 6.9) | 0.082 | 0.002 |
| FaSSIF V1 Level 1 ^a | 0.084 | 0.001 |
| FaSSIF V2 Level 1 ^a | 0.087 | 0.004 |
| FaSSIF V1 Level 2 ^a | 0.100 | 0.002 |
| FaSSIF V2 Level 2 ^a | 0.094 | 0.003 |

^a Markopoulos et al. (2015).

^b Segregur et al. (2019).

pH 4 / pH 6 and McIlvaine pH 4 / pH 6. Compared to the dissolution in FaSSGF, the dissolution in the pH 4 media is slower and less complete, reaching approximately 50% dissolved by 30 min and 70% dissolved after two hours. In the pH 6 PPI media the dissolution was even slower, reaching just under 20% after two hours.

Water is recommended by the Japanese Pharmacopeia as a medium to represent the achlorhydric stomach (The Ministry of Health, Labour and Welfare 2016; Kaniwa 2002). In this study, the pH of the deionized water before the experiment was pH 5.6 and after two hours of dissolution pH had risen to 6.3. The dissolution of PSWB 001 from the capsules in 250 ml of deionized water was poor and almost identical to the results from the experiments with PPI pH 6 media (Fig. 2), in which just over 10% was dissolved after 30 min and just under 20% after two hours.

3.3. Additional experiments with novel PPI media

A possible effect of pepsin on dissolution from the capsules was investigated in an additional experiment. Dissolution results in two PPI media, both containing pepsin but adjusted to pH 4 with either acetate buffer or McIlvaine buffer, were thus compared to the results from the dissolution experiments with the same media *sine pepsin*. No significant difference in the dissolution behavior of the formulation in the media with and without pepsin was observed (data not shown).

Additionally, the impact of the vessel size/paddles was investigated. Using the PPI pH 6 medium with maleate as the buffer, dissolution behavior in standard Erweka vessels was compared to the dissolution in mini-vessels (Erweka). No significant difference was found (data not shown), in line with the efforts on the part of Erweka to scale down the paddle and the vessel proportionally, thus maintaining the hydrodynamics constant at a given rpm (Klein and Shah, 2008).

3.4. Dissolution in FaSSIF V1 and FaSSIF V2

In addition to fasted gastric biorelevant media, dissolution in fasted intestinal biorelevant media was investigated. The dissolution of PSWB 001 in FaSSIF V1 and FaSSIF V2 showed comparable profiles ($f_2 = 81.76$). As the solubility of PSWB 001 in the presence of a biorelevant concentration of surfactants was a little higher than for simple aqueous media, these dissolution experiments were conducted in both Level 1 and 2 media. A greater extent in dissolution in Level 2 than Level 1 media was observed, with 25% dissolved at 45 min and over 30% after two hours of dissolution (Fig. 3). Although these data reflect a modest influence of bile components on solubility of PSWB 001, there was a less than 10% difference in the dissolution between the Level 1 and 2 media

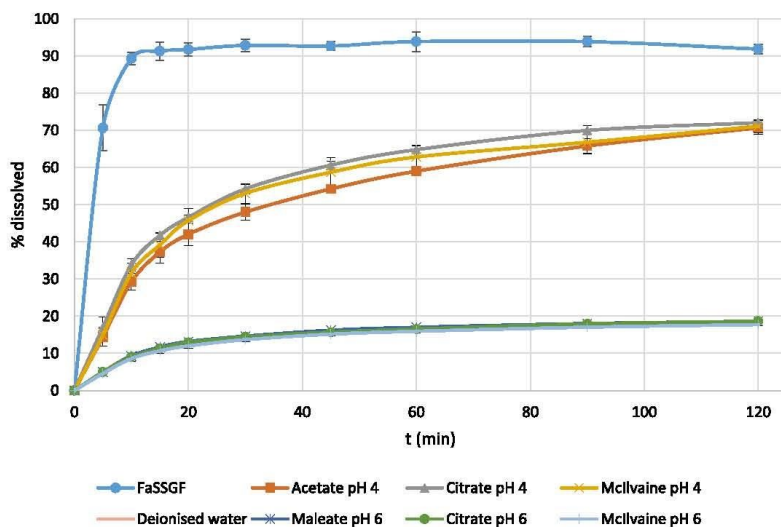


Fig. 2. Dissolution of PSWB 001 capsule in 250 ml of FaSSGF, PPI pH 4 and pH 6 media and in deionised water.

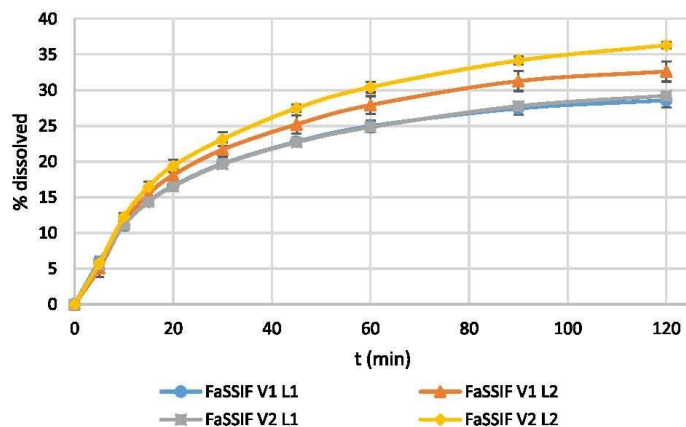


Fig. 3. A comparison of dissolution of PSWB 001 capsules in 900 ml of Level 1 and 2 FaSSIF V1 and Level 1 and 2 FaSSIF V2.

according to f_2 calculations (f_2 (FaSSIF-V1) = 78.9, f_2 (FaSSIF-V2) = 67.4).

3.5. Two-stage dissolution experiments

The dissolution behavior of PSWB 001 was also investigated in two-stage experiments to determine whether drug that dissolves under gastric conditions might subsequently precipitate after entering the intestines. For this purpose, FaSSGF pH 1.6 and FaSSIF V1 double concentrate or FaSSGF pH 2 and FaSSIF V2 double concentrate were used as the media. The final composition of the media matched the corresponding FaSSIF versions and the final pH after two hours of dissolution was pH 6.5 and 6.7, respectively (theoretical value pH 6.5 for both cases, but FaSSIF V2 has a lower buffer capacity, leading to some deviation in the final pH). No precipitation occurred during two-

stage tests (Fig. 4) and PSWB 001 remained supersaturated after the "infinity spin" (data not shown).

3.6. In silico PBPK modeling

The initial *in silico* model for the Simcyp simulation was based on literature data for the physicochemical and blood binding properties of PSWB 001. To refine and validate the model three steps were undertaken.

First, the intravenous clearance of PSWB 001 was estimated by fitting the mean plasma profile after administration of an intravenous solution to a two compartmental model in Simcyp using a single adjusting compartment (SAC) (Fig. 5). When comparing the predicted and observed data, the AfE_{0-3h} value was 0.74, whereas $AAfE_{0-3h}$ value was 1.38.

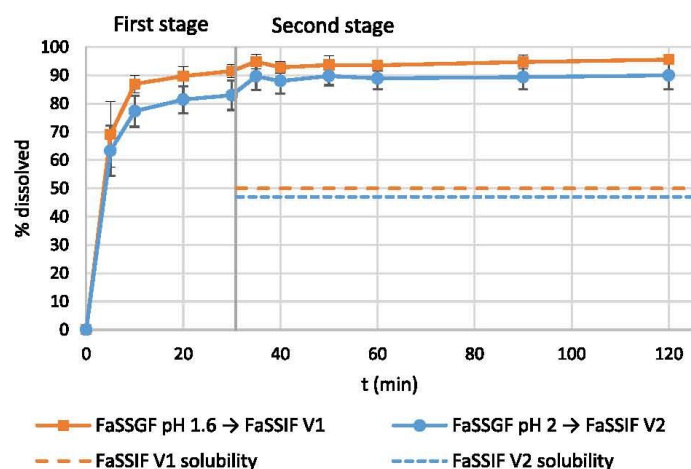


Fig. 4. Concentration profiles in the acceptor phase of two-stage experiments using FaSSGF (pH 1.6) with addition of Level 2 FaSSIF V1 double concentrate at 30 min (vertical division line, final pH 6.5). The same experimental design was repeated with FaSSGF (pH 2) and Level 2 FaSSIF V2.

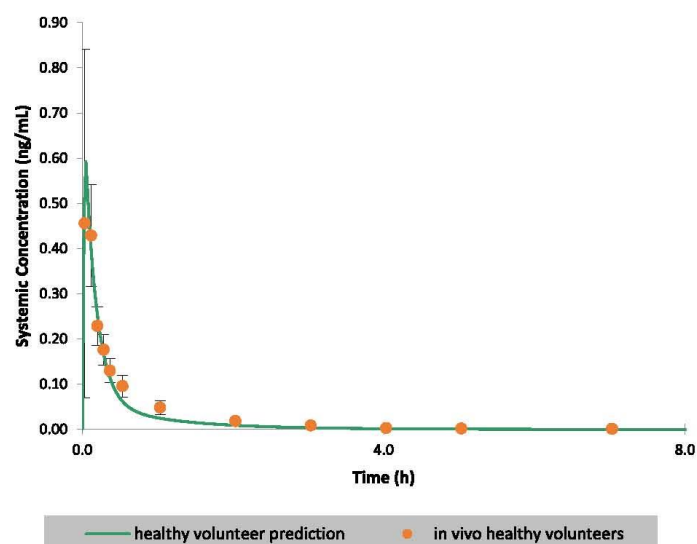


Fig. 5. Simulation of plasma concentrations for a representative healthy population subject (solid line) and *in vivo* average values in 8 healthy volunteers after intravenous administration of PSWB 001 (filled circles) along with the standard deviation (error bars).

Second, to simulate an oral administration of PSWB 001 to a representative healthy population subject, the dissolution profile acquired from the experiments with PSWB 001 capsules in FaSSGF, as well as the effective permeability (p_{eff}) were added to the existing model. The simulated profile was compared to the *in vivo* average plasma concentration values in healthy volunteers after oral administration without a PPI pre-treatment from Study A (Fig. 6.). No adjustments to the model were necessary to achieve an adequate fit ($AFE_{0-6h} = 1.25$, $AAFE_{0-6h} = 1.36$). The predicted t_{max} for healthy volunteers was 0.86 h, c_{max} 458 ng/ml and AUC 789 ng h/ml.

Third, the oral model was applied to simulate administration of PSWB 001 to the same representative population subject after PPI pre-treatment in Study A, this time applying the dissolution profiles from the experiments in PPI pH 4 (acetate buffer) or PPI pH 6 (maleate buffer) media [Fig. 7(a)] instead of the dissolution data in FaSSGF. The simulated profiles effectively bracket the PPI effect observed in both studies [Fig. 7(a) and (b)], between a lesser (pH 4) and a greater effect (pH 6) of PPI treatment.

The *in silico* prediction of the PPI effect using media with pH 4 and pH 6 thus bracket the mean *in vivo* plasma profiles for both Study A and

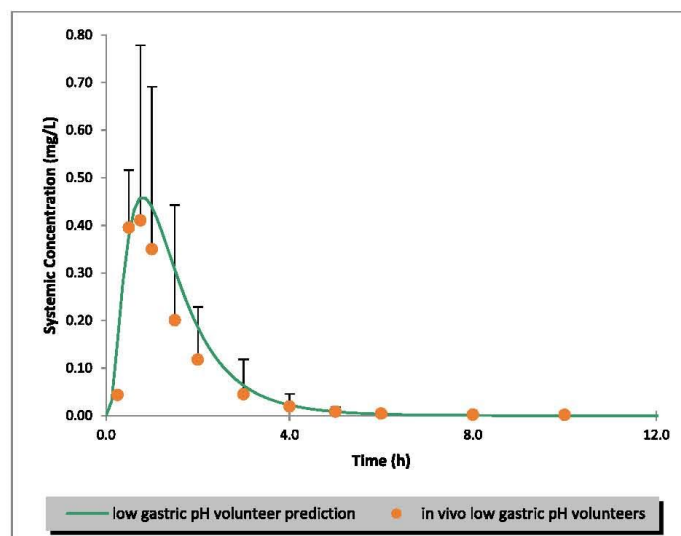


Fig. 6. Simulation of the plasma concentration profile for a representative healthy population subject (solid line) compared to the observed average values in volunteers from Study A (filled circles), along with the standard deviation (error bars), in the study phase without PPI pretreatment.

Study B, with simulations based on pH 4 *in vitro* dissolution data lying above and simulations based on pH 6 *in vitro* data lying well below the mean observed plasma profile in both cases (Tables 4 and 5).

4. Discussion

Many new oral medicines in the pipeline and entering the market contain weakly basic poorly soluble drugs (Kalepu and Nekkanti, 2015; Loftsson and Brewster, 2010). Due to their physicochemical characteristics, these drugs are particularly susceptible to DDIs with drugs that change the gastric pH, namely the ARAs. Assessment of DDIs with ARAs for poorly soluble weak bases is important, because these DDIs can have a negative impact on drug exposure/absorption thereby reducing efficacy. The ability to predict the impact of gastric pH elevation on a drug's release profile during preclinical development would be helpful to guide the decision to proceed to clinical studies as well as designing appropriate studies in healthy volunteers and patients. Thus there is an interest from the regulatory perspective, as well as on the part of the pharmaceutical industry, to develop best practices for the evaluation and de-risking of pH-dependent DDIs, including both *in vitro* and *in silico* predictions of the extent of the interaction (FDA, 2018). In response to this interest, two sets of media have been developed, one to reflect a moderate and one to reflect a strong PPI effect on gastric pH (Segregur et al., 2019).

Whereas the poorly soluble weakly basic PSWB 001 showed rapid and almost complete dissolution in the biorelevant medium representing gastric fluids in fasted healthy subjects (FaSSGF), its dissolution was slower and somewhat less complete in PPI pH 4 media and much slower and less complete in the PPI pH 6 media. These results were then combined with an *in silico* PBPK model built from intravenous data for PSWB 001 in healthy volunteers. This model was then verified for oral administration by inputting *in vitro* dissolution data for PSWB 001 capsules in FaSSGF into the model and simulating the *in vivo* data from healthy volunteers who had not been pre-treated with PPIs and were administered PSWB 001 capsules in the fasted state. The predicted t_{max} , c_{max} and AUC values were comparable with the observed data reported

for PSWB 001 in this population, providing some verification of the model.

Next, the *in vitro* dissolution data in the PPI pH 4 and PPI pH 6 media were entered into the model to simulate the change in pharmacokinetics of PSWB 001 under PPI pre-treatment. The *in silico* simulations suggest that C_{max} and AUC would be reduced in the presence of PPIs, with the effect greater for a strong PPI pre-treatment (PPI pH 6 media), and less so for a moderate PPI pre-treatment (PPI pH 4 media). The two simulations bracketed the observed *in vivo* data from Study A, with the simulation based on pH 4 data corresponding to the upper bound of the standard deviations around the observed mean plasma concentrations and the simulation based on pH 6 data well below the mean observed plasma concentrations.

Comparison of the *in silico* simulations with the data from the Study B further confirms the ability of the simulations based on results in PPI media to essentially bracket the PPI effect, although (perhaps due to the smaller number of volunteers) the standard deviations were very high in the early part of the plasma profile.

The AUC ratio (PPI co-administration vs. no pre-treatment) for both studies indicates a comparable reduction in AUC (0.52 and 0.58), which is within the range predicted by the simulations (AUC ratio of 0.76 for the pH 4 simulation vs. healthy volunteer simulation and a ratio of 0.18 for the pH 6 simulation vs. healthy volunteer simulation). The c_{max} ratio observed in two studies (0.35 and 0.33) is also bracketed well by the ratios from the simulations (0.63 for the pH 4 simulation and 0.18 for the pH 6 simulation).

Moreover, the representation of the PPI effect using a bracketing approach is appropriate because extensive literature research suggests that, after continuous PPI administration, the gastric pH typically ranges between pH 4 and pH 6 in the healthy volunteer population, when standard oral doses are considered (e.g., 40 mg omeprazole q.d.). Thus, while the PPI pH 4 media data appear to be useful for predicting mean values for a less pronounced PPI effect, such as with short-term PPI administration or administration of a less potent PPI, the pH 6 PPI media may help to predict mean values for a strong PPI effect, such as prolonged dosing with a highly potent PPI.

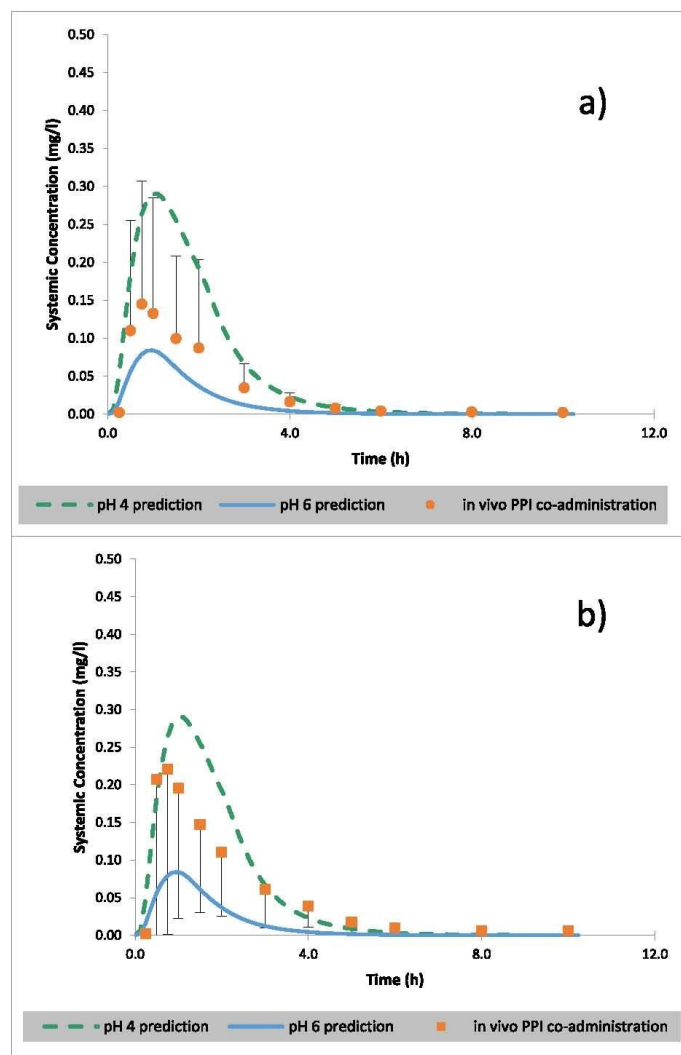


Fig. 7. Simulation of the plasma concentration profile for a representative healthy population subject showing a lesser PPI effect (pH 4) (broken line), as well as a subject showing greater PPI effect (pH 6) (solid line), along with the observed average values in volunteers who received PSWB 001 after pre-treatment with omeprazole from a) Study A (filled circles) and standard deviation (error bars) and b) Study B (filled squares) and standard deviation (error bars).

Although the dissolution of PSWB 001 in deionized water was similar to that in PPI pH 6 media, deionized water is not considered suitable for testing dissolution under elevated gastric pH conditions as the pH of the water may vary highly among sources and, having essentially no buffer capacity, is easily influenced by excipients and/or the drug itself. By contrast, the biorelevant PPI media are composed at a set pH (pH 4 or pH 6) and buffer capacity (7.5 or 1 mEq/L/ Δ pH, respectively) ensuring reproducibility of these two parameters.

Another advantage of the biorelevant PPI media is that the user has a choice among three different buffer species for each of the two PPI media. For PSWB 001, the different buffer species showed comparable

dissolution profiles at a given pH, indicating the interchangeability of the media when there are no interactions between the drug and the buffer species. But if interactions occur with one buffer system (e.g. catalysis of drug degradation, incompatibility with excipients in the formulation), one has the possibility of choosing an alternative buffer system. A further advantage of PPI media is the more accurate prediction of the solubility and dissolution of the drug in the stomach due to the physiological concentration of surface-active components present (Efentakis and Dressman, 1998). Finally, with the PPI media one can bracket the expected dissolution behavior of the drug product within the usual range of PPI administration, providing a “best case/worst case”

Table 4
Summary of the PK parameters for clinical Study A, with and without PPI pre-treatment, and the Simcyp simulations.

| Population | C_{max} (ng/ml) | AUC (ng h/ml) | t_{max} (h) | AFE_{0-6h} | $AAFE_{0-6h}$ |
|--|----------------------|------------------|------------------|--------------|---------------|
| Healthy volunteers (no pre-treatment) - observed | 410 ± 342 | 638* | 0.75* | 1.25 | 1.36 |
| Healthy volunteers (no pre-treatment) - simulation | 458 | 789 | 0.86 | | |
| PPI pH 4 simulation | 290 | 600 | 1.1 | | |
| Healthy volunteers (PPI pre-treatment) - observed | 145 ± 162 | 334* | 0.75* | | |
| PPI pH 6 simulation | 84 | 144 | 0.98 | | |

*unfortunately the standard deviation in AUC and the range of t_{max} values are not available for comparison.

Table 5
Summary of the PK parameters for clinical Study B, with and without PPI pre-treatment, and the Simcyp simulations.

| Population | C_{max} (ng/ml) | AUC (ng h/ml) | t_{max} (h) | AFE_{0-6h} | $AAFE_{0-6h}$ |
|--|----------------------|------------------|------------------|--------------|---------------|
| Healthy volunteers (no pre-treatment) - observed | 675 ± 447 | 937* | 0.75* | 1.06 | 1.61 |
| Healthy volunteers (no pre-treatment) - simulation | 458 | 789 | 0.86 | | |
| PPI pH 4 simulation | 290 | 600 | 1.1 | | |
| Healthy volunteers (PPI pre-treatment) - observed | 220 ± 219 | 546* | 0.75* | | |
| PPI pH 6 simulation | 84 | 144 | 0.98 | | |

*unfortunately the standard deviation in AUC and the range of t_{max} values are not available for comparison.

analysis as part of a risk assessment toolkit during development projects. Predictions leading to lower plasma concentrations and a wider range of PK profiles suggest a high sensitivity of the drug to gastric pH, as well as potentially high inter- and intra-subject variability, whereas for compounds with a moderate risk for PPI effects, the plasma profile predictions based on dissolution in the pH 4 and 6 PPI media are expected to be more similar and closer to the simulation of the low gastric pH state. The predictions, combined with a knowledge of the efficacy window and toxicity concentration limits, can guide decisions about the clinical relevance of the PPI effect for a given drug. Furthermore, data obtained from dissolution experiments and simulations using PPI media may be a valuable input for formulation development, as formulations can be screened for their ability to mitigate the PPI effect in these media (Segregur et al., 2019).

Of course, since these media have only recently been developed, more case examples are needed to evaluate and verify their ability to predict PPI interactions with drug products *in vivo*.

5. Conclusion

There is a need for a more accurate representation of human (patho) physiology in *in vitro* dissolution experiments, as the gastrointestinal conditions can play an important role in drug release and absorption. Dissolution experiments with PSWB 001, a weakly basic drug, showed significant changes in dissolution between a biorelevant medium developed for subjects with normal gastric pH (FaSSGF) and media recently developed to represent gastric conditions in patients co-

administered PPIs. When the results of dissolution tests of PSWB 001 in the PPI media were applied as input parameters in a Simcyp PBPK model, the model successfully bracketed the PPI effect observed *in vivo*. These data support the use of PPI media for predicting the PPI effect on the release and pharmacokinetics of poorly soluble, weakly basic drugs and further studies are warranted to determine whether they could also be used to test the robustness of different formulations of the drug to changes in gastric pH.

CRediT authorship contribution statement

Domagoj Segregur: Conceptualization, Methodology, Validation, Investigation, Writing - original draft, Visualization. **James Mann:** Conceptualization, Resources, Writing - review & editing, Project administration. **Andrea Moir:** Resources, Writing - review & editing. **Eva M. Karlsson:** Writing - review & editing. **Jennifer Dressman:** Conceptualization, Methodology, Writing - review & editing, Supervision, Project administration.

Declaration of Competing Interest

None.

Acknowledgments

Certara UK (Simcyp Division) granted free access to the Simcyp Simulators through an academic licence (subject to conditions).

References

- Dressman, J.B., Reppas, C., 2016. *Oral Drug Absorption*. CRC Press.
- Eftentakis, M., Dressman, J.B., 1998. Gastric juice as a dissolution medium: surface tension and pH. *Eur. J. Drug Metab. Pharmacokinet.* 23 (2), 97–102. <https://doi.org/10.1007/BF03189322>.
- FDA (1997): Dissolution Testing of Immediate Release Solid Oral Dosage Forms. Guidance for Industry. Available online at <https://www.fda.gov/media/70936/download>, checked on 3/22/2020.
- FDA (2018): Framework for Assessing pH-Dependent Drug-Drug Interactions; Establishment of a Public Docket. Request for Comments. Available online at <https://www.regulations.gov/document?D=FDA-2018-N-1820-0001>, checked on 3/22/2020.
- Glomme, A., März, J., Dressman, J.B., 2005. Comparison of a miniaturized shake-flask solubility method with automated potentiometric acid/base titrations and calculated solubilities. *J. Pharm. Sci.* 94 (1), 1–16. <https://doi.org/10.1002/jps.20212>.
- Hedayat, M.A., 2012. *Basic Pharmacokinetics*, second ed. CRC Press (Pharmacy Education Series), Hoboken. Available online at <http://gbv.eblib.com/patron/FullRecord.aspx?p=1446417>.
- Kalepu, S., Nekkanti, V., 2015. Insoluble drug delivery strategies: review of recent advances and business prospects. *Acta Pharm. Sin.* B 5 (5), 442–453. <https://doi.org/10.1016/j.apsb.2015.07.003>.
- Kaniwa, N., 2002. Japanese perspectives on pharmaceutical product release rate testing. *Drug Inf. J.* 36 (2), 407–415. <https://doi.org/10.1177/009286150203600220>.
- Klein, S., Shah, V.P., 2008. A standardized mini paddle apparatus as an alternative to the standard paddle. *AAPS Pharm. Sci. Tech.* 9 (4), 1179–1184. <https://doi.org/10.1208/s12249-008-9161-6>.
- Löfsson, T., Brewster, M.E., 2010. Pharmaceutical applications of cyclodextrins: basic science and product development. *J. Pharmacy Pharmacol.* 62 (11), 1607–1621. <https://doi.org/10.1111/j.2042-7158.2010.01030.x>.
- Mann, J., Dressman, J., Rosenblatt, K., Ashworth, L., Muenster, U., Frank, K., et al., 2017. Validation of dissolution testing with biorelevant media: an OrBiTo study. *Mol. Pharm.* 14 (12), 4192–4201. <https://doi.org/10.1021/acs.molpharmaceut.7b00198>.
- Markopoulos, C., Andreas, C.J., Vertzoni, M., Dressman, J., Reppas, C., 2015. In-vitro simulation of luminal conditions for evaluation of performance of oral drug products: Choosing the appropriate test media. *Eur. J. Pharm. Biopharm.* 93, 173–182. <https://doi.org/10.1016/j.ejpb.2015.03.009>.
- Obach, R.S., Baxter, J.G., Liston, T.E., Silber, B.M., Jones, B.C., MacIntyre, F., et al., 1997. The prediction of human pharmacokinetic parameters from preclinical and *in vitro* metabolism data. *J. Pharmacol. Exp. Therap.* 283 (1), 46–58.
- Segregur, D., Flanagan, T., Mann, J., Moir, A., Karlsson, E.M., Hoch, M., et al., 2019. Impact of acid-reducing agents on gastrointestinal physiology and design of biorelevant dissolution tests to reflect these changes. *J. Pharm. Sci.* 108 (11), 3461–3477. <https://doi.org/10.1016/j.xphs.2019.06.021>.
- The Ministry of Health, Labour and Welfare (2016): *Japanese Pharmacopoeia*. Seventeenth Edition: The Stationery Office.



Evaluating the impact of acid-reducing agents on drug absorption using biorelevant *in vitro* tools and PBPK modeling - case example dipyridamole

Domagoj Segregur^a, Richard Barker^b, James Mann^c, Andrea Moir^b, Eva M. Karlsson^d, David B. Turner^e, Sumit Arora^e, Jennifer Dressman^{a,f,*}

^a Institute of Pharmaceutical Technology, J. W. Goethe University, 9 Max von Laue St., 60438, Frankfurt am Main, Germany

^b New Modalities & Parenteral Development, Pharmaceutical Technology & Development, Operations, AstraZeneca, Macclesfield, United Kingdom

^c Oral Product Development, Pharmaceutical Technology & Development, Operations, AstraZeneca, Macclesfield, United Kingdom

^d Oral Product Development, Pharmaceutical Technology & Development, Operations, AstraZeneca, Gothenburg, Sweden

^e Certara UK Limited, Simcyp Division, Sheffield, United Kingdom

^f Fraunhofer Institute of Translational Medicine and Pharmacology, Theodor Stern Kai 7, 60596, Frankfurt am Main, Germany

ARTICLE INFO

Keywords:

Acid-reducing agent
Proton pump inhibitor
H₂ receptor antagonist
Physiologically based pharmacokinetic (PBPK) modeling
Dissolution
Transfer experiment
Dipyridamole

ABSTRACT

Background: *In vitro* and *in silico* methods have become an essential tool in assessing metabolic drug-drug interactions (DDI) and avoiding reduced efficacy and increased side-effects. Another important type of DDI is the impact of acid-reducing agent (ARA) co-therapy on drug pharmacokinetics due to changes in gastric pH, especially for poorly soluble weakly basic drugs.

Methods: One-stage, two-stage and transfer dissolution experiments with dipyridamole tablets using novel biorelevant media representing the ARA effect were conducted and the results were coupled with a PBPK model. Clinical pharmacokinetic data were compared with the simulations from the PBPK model and with output from TIM-1 experiments, an evolved *in vitro* system which aims to simulate the physiology in the upper GI tract.

Results: Two-stage and transfer experiments confirmed that these *in vitro* set-ups tend to overestimate the extent of dipyridamole precipitation occurring in the intestines *in vivo*. Consequently, data from one-stage dissolution testing under elevated gastric pH conditions were used as an input for PBPK modeling of the ARA/dipyridamole interaction. Using media representing the ARA effect in conjunction with the PBPK model, the ARA effect observed *in vivo* was successfully bracketed. As an alternative, the TIM-1 system with gastric pH values adjusted to simulate ARA pre-treatment can be used to forecast the ARA effect on dipyridamole pharmacokinetics.

Conclusion: Drug-drug interactions of dipyridamole with ARA were simulated well with a combination of dissolution experiments using biorelevant media representing the gastric environment after an ARA treatment together with the PBPK model. Adjustment of the TIM-1 model to reflect ARA-related changes in gastric pH was also successful in forecasting the interaction. Further testing of both approaches for predicting ARA-related DDIs using a wider range of drugs should be conducted to verify their utility for this purpose.

Introduction

Metabolic drug-drug interactions (DDIs) can have a positive or negative effect on drug exposure, boosting efficacy or (if the effect is larger than desired) even leading to toxicity if exposure is increased, but potentially leading to lack of efficacy if the exposure is decreased. In addition to metabolic interactions, DDIs also exist with regard to drug dissolution in the gastrointestinal (GI) tract. These interactions may have a negative impact on drug exposure and absorption and thus lead to reduced efficacy. Like the metabolic DDIs, these types of interactions

also need to be assessed early in the development process.

A significant proportion of orally administered drugs in development and on the market are poorly soluble and weakly basic. Drugs with such characteristics depend on a low gastric pH to achieve adequate dissolution and absorption after oral administration. Both the pharmaceutical industry and regulatory bodies are aiming to develop best practices for the evaluation and de-risking of these pH-dependent DDIs (Food and Drug Administration (FDA) 2018, 2020 a).

The aim of the current studies was to explore various physiologically based pharmacokinetic (PBPK) analyses for biopharmaceutics

* Corresponding author.

E-mail address: dressman@em.uni-frankfurt.de (J. Dressman).

<https://doi.org/10.1016/j.ejps.2021.105750>

Received 7 December 2020; Received in revised form 4 February 2021; Accepted 5 February 2021

Available online 11 February 2021

0928-0987/© 2021 Elsevier B.V. All rights reserved.

applications (Food and Drug Administration (FDA) 2020 b, Pepin et al. 2020) for their ability to simulate the interaction of poorly soluble weakly basic drugs with acid-reducing agents (ARAs). Due to its physicochemical properties and well-established DDI with ARAs, dipyridamole was chosen as the model drug for this purpose.

Dipyridamole is a phosphodiesterase inhibitor which decreases platelet aggregation and promotes vasodilatation. It is thus used in the prevention of cardioembolic complications (Food and Drug Administration (FDA)), as well as against coronary and peripheral arterial diseases (Brown et al. 2015). On the one hand, an acutely administered high dose of dipyridamole induces tachycardia and an acute drop in blood pressure, which are usually unwanted side-effects but has led to the i.v. application of dipyridamole as an alternative to exercise stress testing (Leppo 1994). However, doses that are too high may provoke dizziness (Food and Drug Administration (FDA)), leading to fainting. On the other hand, if the drug does not reach therapeutic plasma concentrations, which can occur when ARAs are co-administered (Derendorf et al. 2005; Russell et al. 1994), the therapeutic aim of cardioprotection and/or lowering of blood pressure may not be achieved.

Previously proposed biorelevant dissolution tests (Segregur et al. 2019) reflecting changes in GI physiology caused by ARAs, such as proton pump inhibitors (PPIs) and H2 receptor antagonists (H2RAs), have been applied in one-stage *in vitro* experiments with a model poorly soluble weakly basic drug (Segregur et al. 2020). In combination with a Simcyp *in silico* model, these dissolution data were able to successfully simulate pharmacokinetic changes during oral administration after PPI pre-treatment.

While one-stage methodology uses a single aqueous phase as a dissolution medium, two-stage methodology aims to simulate the pH shift from the gastric to the small intestinal compartment via a bolus addition of an intestinal medium concentrate into the medium simulating gastric surroundings (Mann et al. 2017). Alternatively, a transfer model can be used, in which first-order emptying via a pump is used to empty the gastric contents into the intestinal compartment (Ruff et al. 2017). A more evolved approach is the TNO intestinal model (TIM-1) system, a multi-compartmental system which aims to apply physiologically relevant fluid compositions and hydrodynamics and couple them with absorptive compartments. While the simpler *in vitro* set-ups (one-stage, two-stage and transfer) are usually coupled with physiologically based pharmacokinetic (PBPK) modeling to predict drug pharmacokinetics, the TIM-1 output is usually correlated directly with the fraction of a poorly soluble drug available for absorption (Barker et al. 2014). In this work, dipyridamole dissolution was studied with all of the above-mentioned methods.

Materials

Dipyridamole (Persantin®) 100 mg tablets (Boehringer Ingelheim Ltd., Bracknell, Berkshire, UK) were provided by AstraZeneca and dipyridamole powder was purchased from Sigma-Aldrich (Steinheim, Germany). FaSSiF/FaSSiF/FaSSGF and FaSSiF-V2 powders were kindly donated by biorelevant.com (Surrey, UK). Acetonitrile, tri-sodium citrate dihydrate, sodium chloride, hydrochloric acid 1 M and sodium hydroxide 1 M were purchased from VWR Chemicals Prolabo (Leuven, Belgium), sodium dihydrogen phosphate dihydrate, sodium acetate and disodium hydrogen phosphate from Merck KGaA. (Darmstadt, Germany), maleic acid and pepsin from porcine gastric mucosa from Sigma-Aldrich (Steinheim, Germany), anhydrous citric acid from Caesar & Loretz GmbH (Hilden, Germany) and formic acid from Carl Roth GmbH + Co. KG (Karlsruhe, Germany). The media used in one-stage, two-stage and transfer model experiments are summarized in the Supplementary Material (Table A).

Methods

Solubility measurements

Dipyridamole solubility was determined in deionized water, various buffers and biorelevant media. The buffers used were acetate pH 4 (corresponding to Level 1 (Markopoulos et al. 2015) of the ARA pH 4

acetate medium), maleate pH 6 (10 mEq/L/ Δ pH), phosphate pH 6.5 (corresponding to the Level 1 version of FaSSiF V1) and maleate pH 6.5 (corresponding to the Level 1 version of FaSSiF V2). Solubility was additionally measured in the following Level 2 biorelevant media: FaSSiF V1, FaSSiF V2, ARA pH 4 acetate, citrate and McIlvaine media, and ARA pH 6 maleate, citrate and McIlvaine media. The following UniPrep™-based method was used to determine dipyridamole solubility (Glomme et al. 2005): an excess of dipyridamole powder and 3 mL of the respective medium was added into each UniPrep™ vial (GE Healthcare, Whatman Inc., New Jersey, USA). The vial was sealed and shaken using a Heidolph Polymax 1040 platform shaker (Heidolph Instruments GmbH & CO., Schwabach, Germany) for 24 h in a Heraeus Function Line heating oven (Thermo Fisher Scientific Inc., Waltham, USA) at 37°C. After 24 h, the filter incorporated into the UniPrep™ vial system (0.45 μ m PTFE filter) was pushed to the floor of the vial, the filtrate was sampled, and then diluted and analyzed using HPLC with a UV-Vis detector (see section *Quantitative analysis of solubility, dissolution and transfer samples*). The pH in the vials was confirmed at the end of each solubility experiment and, with the exception of deionised water, did not deviate more than ± 0.05 from the starting pH. All solubility measurements were conducted in triplicate ($n = 3$).

One-stage dissolution

The dissolution test experiments were performed using a USP 2 (Paddle) apparatus Erweka DT 600 (ERWEKA GmbH, Langen, Germany). As coning was observed in preliminary dissolution experiments both at 50 and 75 rpm, the standard 1 litre vessels were substituted with peak vessels (Pharma Test Apparatebau, Hainburg, Germany). The temperature was set to $37 \pm 0.5^\circ\text{C}$, the paddle rotation speed to 50 rpm and samples were taken 5, 10, 15, 20, 30, 45, 60, 90 and 120 min after starting the experiment. Samples were filtered using 0.45 μ m PTFE filters (ReZist™ filter unit, GE Healthcare, Whatman Inc., New Jersey, USA) and diluted immediately thereafter using mobile phase to prevent precipitation. Dissolution of the tablets was studied in 250 mL of FaSSGF (pH 1.6), ARA pH 4 media (made with acetate, citrate or McIlvaine buffers) and ARA pH 6 media (made with maleate, citrate or McIlvaine buffers), as well as in 900 mL of FaSSiF V1 (pH 6.5) and FaSSiF V2 (pH 6.5). The pH of the buffered media at the end of the dissolution experiment did not deviate from the starting value before the experiment. The number of replicates for each experiment was $n = 3$.

Two-stage dissolution

Two-stage dissolution experiments were performed using the same dissolution test apparatus, vessels, temperature and rotation speed set-up as in the one-stage dissolution experiments. The two-stage methodology representing dissolution without an ARA effect was adapted from the study by Mann et al., conducted as part of the OrBiTo project (Mann et al. 2017): Dissolution in 250 mL of FaSSGF (pH 2) was used to represent dissolution in the gastric compartment, whereas the pH shift was induced by a bolus addition of 250 mL of FaSSiF V2 (pH 10.8) double concentrate (rather than FaSSiF V1 double concentrate at pH 7.5, which was used in the OrBiTo methodology), thus producing 500 mL of FaSSiF V2 to represent the intestinal compartment. The adjustment of the FaSSiF V2 double concentrate pH to a value higher than reported for FaSSiF V1 double concentrate was necessary due to the lower buffer capacity of FaSSiF V2.

In addition to the two-stage methodology representing dissolution without ARA co-administration, a two-stage dissolution methodology using ARA media as the gastric media was developed: dissolution in 250 mL of the ARA pH 4 medium (acetate buffer) or ARA pH 6 medium (maleate buffer) was used to represent dissolution in the gastric compartment. The pH shift was induced by a bolus addition of 250 mL of a FaSSiF V2 double concentrate with a pH of 12.13 when ARA pH 4 (acetate buffer) medium was used, and a pH of 6.46 when ARA pH 6 (maleate buffer) medium was used. The adjustment of the FaSSiF V2

double concentrate pH for experiments with the ARA pH 4 medium to a value higher than the one used for the FaSSiF V2 double concentrate in experiments with FaSSGF pH 2 was necessary due to the higher buffer capacity of the ARA pH 4 acetate buffer. In all three experimental setups, the samples were taken 5, 10, 20, 30, 35, 40, 50, 60, 90 and 120 min after starting the experiment, whereby the pH shift was induced immediately after the 30 min sample was taken from the gastric compartment. The final pH and composition of the 500 mL of media after the addition of the FaSSiF V2 double concentrate corresponded to the standard FaSSiF V2 medium.

Samples were filtered through 0.45 µm PTFE filters (ReZist™ filter unit, GE Healthcare, Whatman Inc., New Jersey, USA) and diluted immediately thereafter using mobile phase to prevent further precipitation of dipyrindamole. All two-stage experiments were conducted with $n = 3$.

Transfer experiments

Transfer experiments were performed using the same dissolution test apparatus and temperature set-up as for the one-stage and two-stage experiments. The dissolution set-up used for the donor compartment (compartment simulating the gastric environment) was a 500 mL ERWEKA® mini-vessel with a corresponding mini-paddle, whereas the dissolution set-up used for the acceptor compartment (compartment simulating intestinal environment) was a standard 1000 mL ERWEKA® vessel with a standard paddle. The paddle rotation speed was set to 75 rpm, as coning was observed during preliminary experiments performed at 50 rpm. Fluids representing the gastric and the intestinal environment, added to the mini-vessel and standard vessel, respectively, as well as their volumes, were the same as in two-stage experiments.

An ISMATEC MC-Process IP5 peristaltic pump (Cole-Parmer GmbH, Wertheim am Main, Germany) and 70–80 cm long ISMATEC® neoprene tubing (Cole-Parmer GmbH, Wertheim am Main, Germany) with an internal diameter of 2.06 mm were used to transfer the dissolution fluid from the gastric to the intestinal compartment. The pump was programmed to empty the gastric fluid into the intestinal compartment using a first-order transfer rate, with a half-emptying time of 9 min.

After adding the tablets to the gastric compartment, the pump was started and samples were taken from the intestinal compartment at 2, 4, 6, 8, 10, 15, 20, 25, 30, 35, 40, 50, 60, 90 and 120 min in order to capture the precipitation behavior. As in the two-stage dissolution experiments, the final pH and composition of the 500 mL of media in the intestinal compartment corresponded to the standard FaSSiF V2 medium. After the experiment, the contents of the donor compartment (solid particles that had sedimented during the transfer of the fluid) were dissolved using 0.1 N HCl and sampled as well.

Samples were filtered and diluted using the method described for one-stage and two-stage experiments and all transfer experiments were run in triplicate ($n = 3$).

Quantitative analysis of solubility, dissolution and transfer samples

Diluted samples were analyzed using an HPLC system consisting of a Hitachi LaChrom-L 7200 autosampler (VWR Hitachi, Darmstadt, Germany), L 7220 pump (VWR Hitachi, Darmstadt, Germany), D 7000 interface (VWR Hitachi, Darmstadt, Germany), L 7420 UV-Vis detector (VWR Hitachi, Darmstadt, Germany) and L 7360 oven (VWR Hitachi, Darmstadt, Germany) with a C18, 10 cm, 4.6 mm Ultracarb™ 5 µm ODS (30) column (Phenomenex LTD, Aschaffenburg, Germany). A gradient mobile phase consisting of 0.1% formic acid and acetonitrile was applied, as shown in Table 1. The column temperature was held at 30°C and the flow rate was set to 0.75 mL/min. The drug substance was quantified at a detection wavelength of 288 nm. The lower limit of quantification was 1 µg/mL and the method was linear over the range of 1 to 44 µg/mL.

Table 1

The gradient method for dipyrindamole HPLC analysis.

| Time (min) | 0 | 2 | 4 | 7 | 7.1 | 10 |
|-----------------------------------|----|----|----|----|-----|----|
| Channel A (0.1 % formic acid) (%) | 90 | 90 | 10 | 10 | 90 | 90 |
| Channel B (acetonitrile) (%) | 10 | 10 | 90 | 90 | 10 | 10 |

In silico modeling and prediction of plasma concentrations

A full PBPK model (Table 2), based on the model reported by Pathak et al. 2019 (Pathak et al. 2019), was adapted for use in this work. First, there was an adjustment to the logarithms of bile micelle:buffer partition coefficients ($\log K_{in:w}$) for FaSSiF V2, as suggested by Klumpp and Dressman (Klumpp und Dressman 2020). A second adjustment was to run the simulations under the assumption of no precipitation (i.e. the default settings), since luminal precipitation reported in upper small intestine aspirates from humans is minimal (< 10%) (Psachoulis et al. 2011). The software used for the simulations was the Simcyp Simulator Version 19 (Certara UK Limited, Sheffield, UK). To test the model's ability to simulate the clinical data for ARA effects, the simulated profiles were compared to the *in vivo* plasma concentration data for dipyrindamole administration with and without pre-treatment with ARAs. Several literature sources were used for this purpose: Ricevuti et al. reported plasma profiles following the administration of 75 mg dipyrindamole in volunteers with low gastric pH (Ricevuti et al. 1991) (these *in vivo* data were also used by Pathak et al. as a comparison to their simulation data); Derendorf et al. reported plasma levels following the administration of 100 mg

Table 2

Summary of input parameter values used for dipyrindamole simulation in the Simcyp Simulator (full PBPK model).

| Parameter (Unit) | Value used | | | |
|--|--|------------|-----------------------|-----------------|
| Phys. Chem. Properties | | | | |
| Molecular weight (g/mol) | 504.6 | | | |
| $\log P_{o:w}$ | 3.77 | | | |
| Compound type | Monoprotic base | | | |
| pK_a | 6.2 | | | |
| Fraction unbound in plasma | 0.002 | | | |
| Blood/plasma ratio | 0.56 | | | |
| Drug absorption parameters (ADAM model) | | | | |
| $P_{eff, man}$ (10^{-4} cm/s) | Predicted in Simcyp | | | |
| Caco-2 (10^{-6} cm/s) | 11.24 | | | |
| Ref. Cimetidine | 1.64 | | | |
| Ref. Propranolol | 21.29 | | | |
| Ref. Verapamil | 22.68 | | | |
| Formulation (Solid formulation, IR) | Simulation | DLM Scalar | DLM Scalar Intestinal | Solubility F. 1 |
| Diffusion layer model | | Gastric | | |
| | No ARA | 0.014 | 0.183 | 1000 |
| | ARA pH 4 | 0.057 | 0.183 | 71.07 |
| | ARA pH 6 | 0.053 | 0.183 | 1000 |
| | Default value (10 µm) | | | |
| Particle size | | | | |
| Intrinsic solubility S_0 (mg/mL) | 0.0043 | | | |
| $\log K_{ow}$ (N / L) | 4.44 / 3.05 | | | |
| Supersaturation and Precipitation | Model 2 | | | |
| Critical Supersaturation Ratio | 1000 | | | |
| Precipitation Rate Constant (1/h) | 4 | | | |
| Distribution | Full PBPK model | | | |
| Model V_{ss} (L/kg) | Method 3 | | | |
| Elimination parameters | | | | |
| Cl_{int} (L/h) | 12 | | | |
| Population parameters | Sim-Healthy Volunteers | | | |
| GI Tract /Luminal pH | Stomach - fasted: 1.5 (non-ARA), 4 and 6 (ARA pH 4 and pH 6) | | | |

dipyridamole after pre-treatment with lansoprazole (PPI) (Derendorf et al. 2005) and Russell et al. reported plasma levels following the administration of two tablets of 25 mg dipyridamole after pre-treatment with famotidine (H2RA) (Russell et al. 1994).

Since the doses administered in the three studies differed, it was necessary to use the diffusion layer model (DLM) in SIVA to characterize the dissolution data from the one-stage dissolution experiments with 100 mg of dipyridamole. The DLM parameters were estimated with SIVA 3.0 software (Certara UK Limited, Sheffield, UK). Using this approach, the DLM parameters could be scaled to any given dose and used as input for the Simcyp model. The particle size for the formulation was not known, so the default particle radius (10 μm) was selected and the DLM scalars, rather than particle size, were estimated. For the DLM parameterization of dipyridamole dissolution in FaSSGF, ARA pH 6 maleate buffer medium and FaSSIF V2, DLM scalar estimation provided an accurate fit. For dissolution of dipyridamole in ARA pH 4 acetate buffer medium, DLM scalar estimation was combined with an adjustment of the solubility factor, SF1, to provide a close fit of the data.

An overview of the *in silico* model development and implementation is shown in Fig. 1.

In the first step, the model was used to simulate the oral administration of 75 mg dipyridamole to a representative healthy volunteer (Sim-Healthy Volunteers population) with no ARA pre-treatment, using the DLM scalar value estimated from the dissolution experiment in FaSSGF for the gastric

compartment and the DLM scalar value estimated from the dissolution experiment in FaSSIF V2 for the small intestine. This simulation agreed well with the values observed *in vivo* (Ricevuti et al. 1991), with both the average fold error (AFE) and absolute average fold error (AAFE) well below 2.

As a second step, the DLM scalar value from the experiment with FaSSGF (representing low gastric pH in healthy volunteers) was substituted with the DLM scalar values estimated from the dissolution experiments using media representing the administration of dipyridamole after ARA pre-treatment.

When implementing PBPK models, the Simcyp simulator offers several options and sub-models to choose from to simulate human physiology. A standard set-up for the Simcyp model includes a "static" intestinal pH model, consisting of time-averaged pH values for each intestinal compartment (plus population variability) based on values reported in the literature. An alternative intestinal pH model is the "dynamic" intestinal pH model, which aims to simulate a heterogeneous neutralization of gastric acid, reflecting data obtained from measurements using a pH probe *in situ* (Koziolek et al. 2015a; Koziolek et al. 2015b). The dynamic intestinal pH model uses equations 1 and 2 to simulate the observed fluctuations in luminal pH with time throughout the intestine. The simulated fluctuations are greater in the proximal part of the small intestine than in the distal parts of small intestine, in accordance with clinical data. However, it should be noted that in the current version of the dynamic pH model, the intestinal pH and variations are not yet automatically linked to or influenced by the gastric pH values.

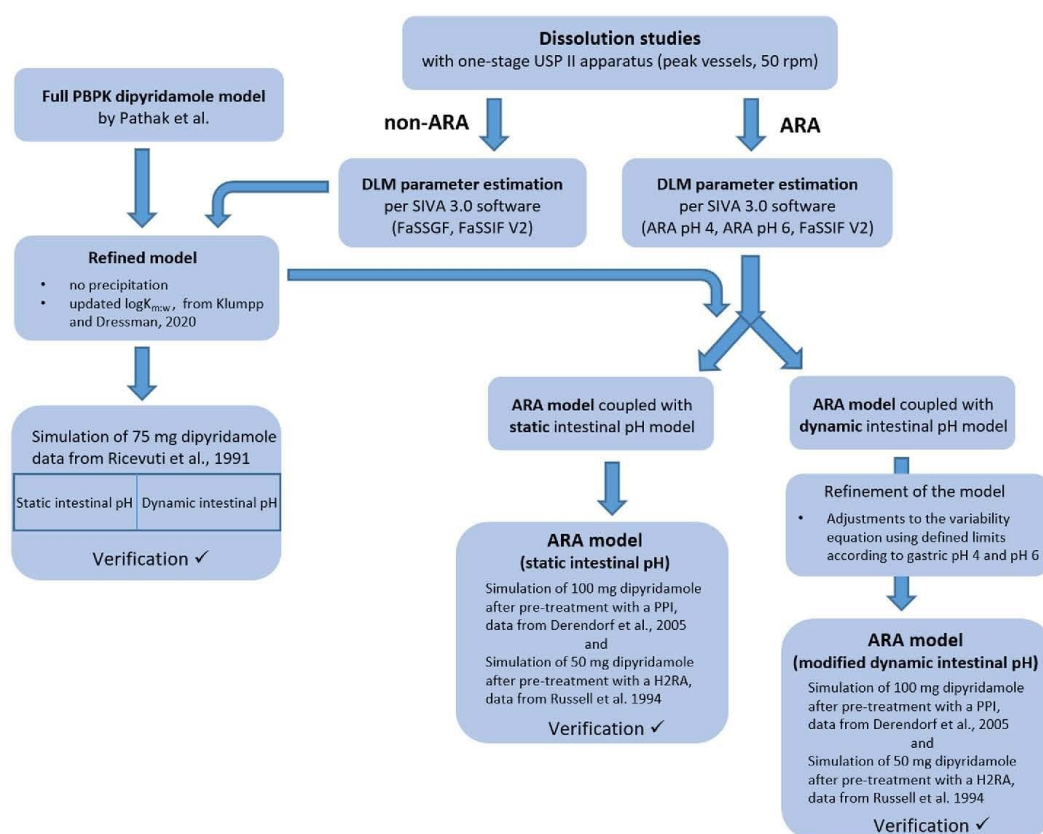


Fig. 1. Schematic of the workflow for development and verification of the dipyridamole *in silico* model.

$$pH_{mean}(t, K, A, B, C, D) = K \left(A - \frac{Bt + 1}{C e^{Bt} + D} \right) \quad (1)$$

$$var(t, a, b, c) = \frac{a e^{-bt}}{1 + c^x t} \quad (2)$$

Simulations of the administration of 100 mg dipyrindamole were conducted using the same virtual representative healthy volunteer, with the exception that the luminal pH value of the fasted stomach was changed from the default pH 1.5 to pH 4 or pH 6, respectively. The first set of simulations was run with the static intestinal pH option. The simulations were compared to the plasma profiles observed *in vivo* after administration of 100 mg dipyrindamole to volunteers pre-treated with a PPI (Derendorf et al. 2005). This set-up was also used to simulate administration of 50 mg dipyrindamole under the three gastric pH conditions and the simulations were compared to the plasma concentrations observed *in vivo* after administration of two 25 mg tablets of dipyrindamole to elderly volunteers pre-treated with an H2RA (Russell et al. 1994).

The simulations described above were then repeated using the dynamic intestinal pH model. For the simulation of dipyrindamole administration without ARA pre-treatment, the default set-up for the dynamic intestinal pH model was used. In this case, the values of the average fold error (AFE) and the absolute average fold error (AAFE) for the fit of the simulated profiles to the *in vivo* concentrations were < 2.

When simulating dipyrindamole administration after an ARA pre-treatment, to account for carryover effects on the intestinal pH during treatment with ARAs, an intestinal pH model parameter set-up reflecting these changes had to be developed (Table 3). The parameter values were selected to constrain the variation in duodenal pH within the limits expected to result from a gastric pH of 4 (corresponding to the ARA pH 4 medium) or pH 6 (corresponding to the ARA pH 6 medium).

TIM-1 experiments and quantitative analysis

An alternative approach to experimental measurement of solubility and *in vitro* dissolution testing combined with PBPK modeling is to apply an *in vitro* model that attempts to reproduce the luminal conditions in the GI tract. One such model is the TNO intestinal model (TIM-1). Experiments using TIM-1, an evolved dissolution model described by Barker et al. (Barker et al. 2014), with an advanced gastric compartment (Hopgood et al. 2018), were conducted at AstraZeneca, Macclesfield, UK. All samples were tested using a fasted state protocol with a stomach half-emptying time of 30 min and a housekeeper wave cycle set at 90 min. The jejunal and ileal "absorption" samples were collected hourly for 5 h to determine the amount of dissolved drug available for absorption. Residue and rinse samples were collected at the end of the test, in order to determine the mass balance. In addition to the standard set-up representing the administration of the dipyrindamole tablet with no ARA pre-treatment (with the gastric compartment adjusted to pH 2), experiments representing a lesser (pH 4) and a stronger (pH 6) ARA gastric pH effect were conducted. The adjustment of the pH in the gastric compartment to pH 4 or pH 6 was made to provide a comparison to the dissolution-based simulations using ARA pH 4 and ARA pH 6 media. Experiments with gastric pH 2 and 6 were run with n = 2 and the experiment

with gastric pH 4 as a single run. The samples were diluted with acetonitrile and quantified with an internal gradient HPLC-UV method, similar to one described in *Quantitative analysis of solubility, dissolution and transfer samples*. The LOQ of the method was 0.25 µg/ml.

Statistics

Solubility, dissolution and fraction absorbed values are presented as arithmetic means and standard deviations. The average fold error (AFE) and the absolute average fold error (AAFE) (Obach et al. 1997), as shown below (equations 3 and 4), were used to evaluate the accuracy of the *in silico* predictions, compared to the data observed *in vivo*.

$$AFE = 10 \left(\frac{\sum \left| \frac{c_p}{c_o} - 1 \right|}{n} \right) \quad (3)$$

$$AAFE = 10 \left(\frac{\sum \left| \frac{c_p}{c_o} \right|}{n} \right) \quad (4)$$

c_p - predicted concentration at time point x
 c_o - observed concentration at time point x
 n - number of sampling points

AFE and AAFE values were determined for a period of 12 h after administration, after which the plasma concentrations of dipyrindamole are negligible.

Results

Solubility

The solubilities of dipyrindamole in deionized water, buffers, FaSSIF V1 and V2, as well as in biorelevant media representing the administration of a drug after ARA pre-treatment, are shown in Table 4.

One stage dissolution

Dissolution results for dipyrindamole tablets in various biorelevant media representing gastric surroundings without (FaSSGF) and after ARA pre-treatment (ARA pH 4 and pH 6 media) are shown in Fig. 2. Dissolution in FaSSGF pH 1.6 is rapid and complete, with 100 % dissolved at 10 min. On the other hand, dissolution experiments with dipyrindamole tablets in ARA pH 4 and 6 media predict incomplete dissolution in the stomach after ARA pre-treatment, with about 80 % dissolved in ARA pH 4 media and only about 2.5 % dissolved in ARA pH 6 media after 2 h of dissolution.

Dissolution of dipyrindamole tablets in the intestinal biorelevant media FaSSIF V1 and FaSSIF V2 are shown in Fig. 3. In these media, dipyrindamole tablets reach about 15 % dissolved after two hours of dissolution, which is in accordance with the results of solubility

Table 3
 Summary of input parameter values used for simulation of the intestinal pH without and during ARA co-administration in the dynamic intestinal pH model of Simcyp.

| Parameter | Low gastric pH (pH 1.5) | ARA therapy, gastric pH 4 | ARA therapy, gastric pH 6 |
|---------------------------|-------------------------|---------------------------|---------------------------|
| K (pH_{mean} function) | default | default | 8.59 |
| A (pH_{mean} function) | default | default | default |
| B (pH_{mean} function) | default | default | 6 |
| C (pH_{mean} function) | default | default | 4 |
| D (pH_{mean} function) | default | default | 4 |
| a (var function) | default | 1* | 0.32* |
| b (var function) | default | default | default |
| c (var function) | default | default | default |

* Note that in the standard configuration of the Simcyp V.19 software, it is not possible to input a value below 2 for parameter "a" of the var function. The access and changes to the default program constraints, to allow a wider range of values, were provided by Simcyp.

Table 4
Experimental dipyrindamole solubility in various media.

| | Medium | Mean solubility \pm SD ($\mu\text{g/mL}$) |
|------------------------------|--|---|
| Gastric media and buffers | FaSSGF (pH 1.6) ^a | > 1000 |
| | ARA acetate pH 4 ^b | 537.4 \pm 5.8 |
| | ARA citrate pH 4 ^b | 523.6 \pm 7.0 |
| | ARA Mclvaine pH 4 ^b | 508.1 \pm 3.1 |
| | pH 4 buffer (acetate 7.5 mM) | 518.8 \pm 18.9 |
| | ARA maleate pH 6 ^b | 12.0 \pm 0.3 |
| | ARA citrate pH 6 ^b | 11.8 \pm 0.1 |
| | ARA Mclvaine pH 6 ^b | 12.2 \pm 0.5 |
| Control | pH 6 buffer (maleate 10 mM) | 12.0 \pm 0.2 |
| | Deionised water (pH 5.6, final pH 6.0) | 6.5 \pm 0.3 |
| Intestinal media and buffers | FaSSIF V1 Level 1 ^a | 7.4 \pm 0.2 |
| | FaSSIF V2 Level 1 ^a | 7.2 \pm 0.2 |
| | FaSSIF V1 Level 2 ^a | 20.3 \pm 0.1 |
| | FaSSIF V2 Level 2 ^a | 17.3 \pm 0.1 |

^a Markopoulos, Andreas et al. 2015

^b Segregur et al. 2019

experiments.

Two-stage dissolution

Fig. 4 shows the results of dipyrindamole tablet dissolution in two-stage experiments. Dissolution before the pH shift (at 30 min), is comparable with the first 30 min of dissolution in one-stage experiments with FaSSGF, ARA pH 4 acetate buffer medium and ARA pH 6 maleate buffer medium. After the bolus addition of a FaSSIF V2 double concentrate, rapid precipitation, and thus a steep decline in the percentage dissolved, is observed for experiments in which acidic media were used for the first stage (FaSSGF pH 2 and ARA pH 4 acetate buffer medium). However, the concentrations of dipyrindamole in 500 mL of the newly generated FaSSIF V2 stayed well above the values observed in solubility experiments, indicating a prolonged supersaturation. In the ARA pH 6 experiment, no precipitation occurred after addition of the FaSSIF V2 double concentrate and the percentage dissolved gradually increased to the solubility value in FaSSIF V2.

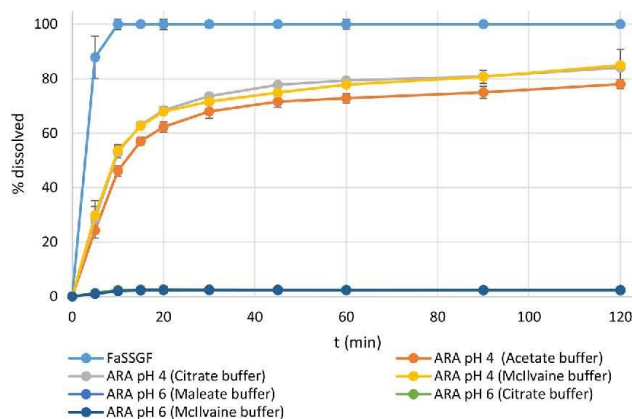


Fig. 2. Dissolution of dipyrindamole tablets in 250 mL of gastric media simulating fasted state without (FaSSGF) and with ARA pre-treatment (ARA pH 4 and ARA pH 6 media), noting that dissolution profiles in the ARA pH 6 media overlap. Symbols represent the mean values and the error bars represent the standard deviation ($n = 3$). Some error bars are occluded by the symbol for the mean.

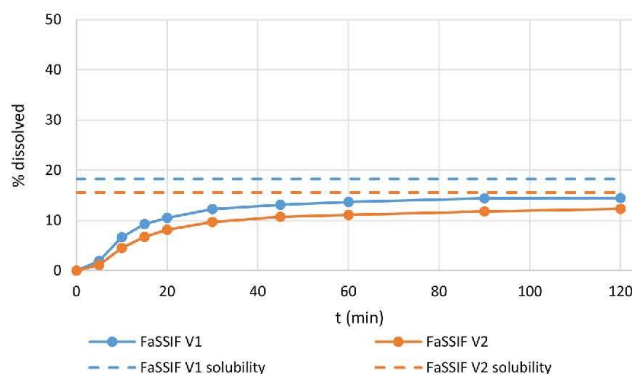


Fig. 3. Dissolution of dipyrindamole tablets in 900 mL of intestinal media simulating fasted state (FaSSIF V1 and FaSSIF V2). Symbols represent the mean values ($n = 3$). Error bars (standard deviation) are occluded by the symbol for the mean. The broken lines represent the solubility of dipyrindamole in FaSSIF V1 and V2.

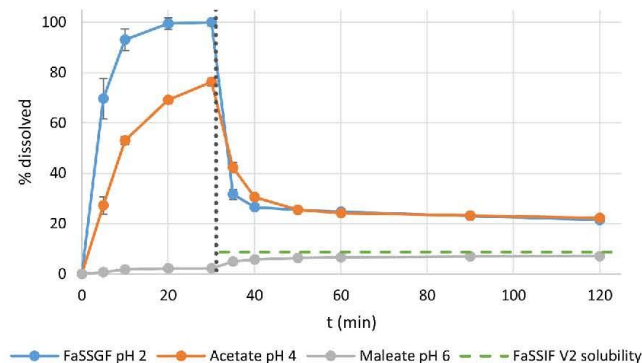


Fig. 4. Dissolution of dipyrindamole tablets during two-stage experiments using FaSSGF pH 2, ARA pH 4 (acetate buffer) or ARA pH 6 (maleate buffer), with the addition of FaSSIF V2 double concentrate at 30 min (vertical division line, final pH in all three experiments pH 6.5). Symbols represent the mean values and the error bars represent the standard deviation ($n = 3$). Some error bars are occluded by the symbol for the mean. The broken line represents the solubility of dipyrindamole in FaSSIF V2.

Transfer experiments

Concentrations observed in the acceptor ("intestinal") compartment during experiments using the transfer model for dissolution and precipitation are shown in Fig. 5. The highest concentrations of dipyrindamole were observed during experiments using FaSSGF as the gastric medium, which is in accordance with one-stage and two-stage experiments. The amount of dipyrindamole left behind in the donor compartment after transfer was less than 6%. Similar to the two-stage experiments, precipitation to a concentration above that of the solubility in FaSSIF V2 were observed in transfer experiments using FaSSGF and the ARA pH 4 acetate buffer medium. In contrast to two-stage experiments, the precipitation rate was much slower.

In the experiments with ARA pH 6 maleate buffer medium in the donor compartment, the amount of dipyrindamole left behind in the donor compartment after the transfer was on average 38.5% of the dose. No precipitation was observed and the concentration of dipyrindamole in the acceptor compartment gradually approached the solubility in FaSSIF V2.

Simulations based on solubility and *in vitro* dissolution

The *in silico* model for the Simcyp simulation was based on the model reported by Pathak et al. However, in view of the *in vivo* data (Psa-chouliás et al. 2011), which show very low precipitation of dipyrindamole in the small intestine, the "no precipitation" (default) option was

selected. Consequently, the DLM model was built using data from the one-stage dissolution experiments and the DLM parameters were used as the input to the PBPK model (Table 2).

First, the prediction of the plasma concentrations after oral administration of 75 mg dipyrindamole was compared with the *in vivo* plasma profile data reported for the administration of 75 mg dipyrindamole to healthy volunteers (Ricevuti et al. 1991), the same study that had been used by Pathak et al. to verify their model. The simulation showed a very good fit to the *in vivo* data (Fig. 6): the AFE_{0-12h} value was 1.26 and $AAFE_{0-12h}$ was 1.50.

Second, to simulate a pH effect on the oral administration of dipyrindamole caused by ARAs, the simulation was run using the DLM parameters from the one-stage dissolution experiments in ARA pH 4 and ARA pH 6 as the gastric compartment input. The simulations were initially run with the "static" intestinal pH values. The simulation of 100 mg dipyrindamole administered after the ARA pre-treatment was compared to the *in vivo* profiles reported for the administration of 100 mg dipyrindamole to volunteers pre-treated with lansoprazole (Derendorf et al. 2005) (Fig. 7a). The simulation was then repeated using 50 mg dipyrindamole and compared to *in vivo* plasma profiles reported for 50 mg dipyrindamole administration to geriatric volunteers after a pre-treatment with famotidine (Russell et al. 1994) (Fig. 7b). The resulting simulations bracketed the pH effect on C_{max} and AUC observed in the clinical studies.

As a third step, the simulations using the default, static intestinal pH model were repeated using the dynamic intestinal pH model. Simulation

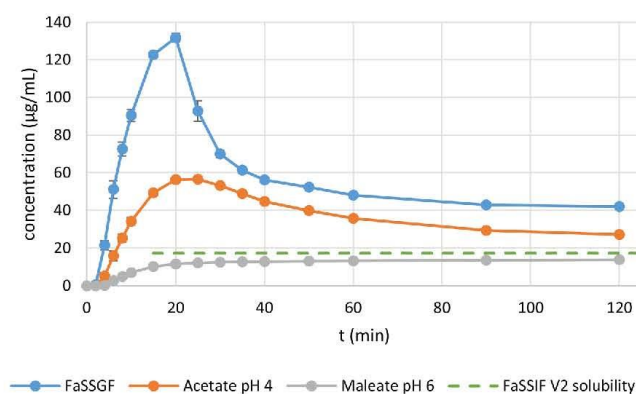


Fig. 5. Concentration profiles ($\mu\text{g/mL}$) in the acceptor phase of transfer experiments using FaSSGF pH 2, ARA pH 4 acetate buffer and ARA pH 6 maleate buffer medium in the donor compartment and the belonging FaSSIF V2 double concentrate in the acceptor compartment. Symbols represent the mean values and the error bars represent the standard deviation ($n = 3$). Some error bars are occluded by the symbol for the mean. The broken line indicates the solubility of dipyrindamole in FaSSIF V2.

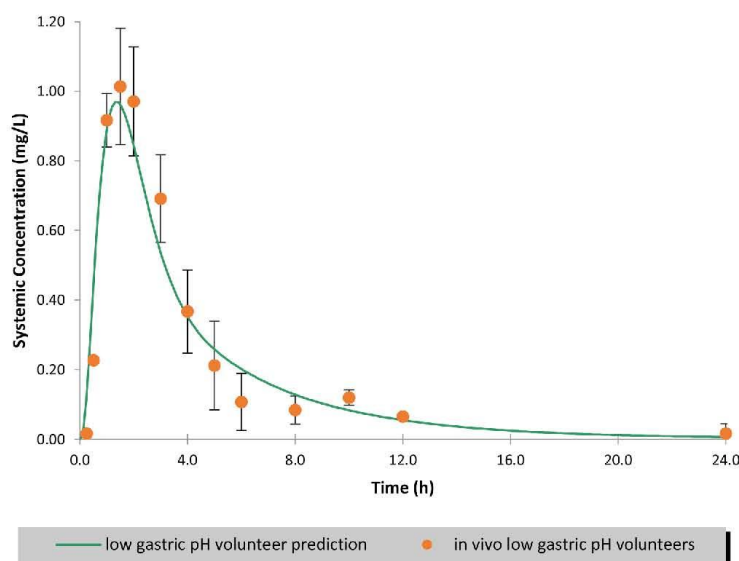


Fig. 6. Simulation of the plasma concentration profile for a representative healthy population subject (solid line) compared to the observed average values in volunteers without ARA pre-treatment (filled circles), dipyridamole dose 75 mg (Ricevuti et al. 1991).

of the plasma concentration for a representative healthy population subject using the dynamic intestinal pH model predicted slightly higher concentrations (Fig. 8), compared to the simulation using the static model. Nevertheless, the AFE_{0-12h} and $A_{AFE_{0-12h}}$ values were below 2 (1.57 and 1.65), indicating that the simulation predicted the *in vivo* data appropriately.

However, simulation of the ARA pH effect using the default dynamic intestinal pH model set-up may not be appropriate, since the default dynamic intestinal pH model set-up always assumes an acidic gastric pH and its carryover effect on the small intestinal pH (especially in the duodenum, seen in Fig. 9a). Although the resulting large fluctuation in pH, which embraces momentarily low pH values in the duodenum, is not a problem when low gastric pH conditions are to be simulated, this became an issue when trying to simulate the plasma profile of a weak base under high gastric pH conditions. In this case, the momentarily low duodenal pH provokes a momentarily high solubility, resulting in overestimation of the plasma concentrations (Supplementary Material, Figure A). Therefore, a parameter set-up reflecting the carryover effect of elevated gastric pH on the variability in small intestinal pH (Fig. 9b) had to be developed. For the simulation using pH 4 as the gastric pH, values in the modified dynamic intestinal pH model set-up were restricted (with 99.7 % probability) to values between 3 and 8.45. For the simulation using pH 6 as the gastric pH, the starting mean duodenal pH was set to 6.5 and duodenal pH values were restricted (with 95.5 % probability) to values between 5 and 8.

When the modified dynamic intestinal pH model was used, predicted plasma profiles were comparable with profiles predicted using the static intestinal pH model (Fig. 10.).

TIM experiments

The output from the experiments using the TIM-1 apparatus is shown in Fig. 11. Although precipitation was observed during the experiment, the final bioavailable fraction from the experiments using a standard set-up with gastric pH 2 was similar to the final bioavailable fraction of a BCS I drug used by AstraZeneca as a historical reference (Supplementary

Material, Figure B). The maximal jejunal concentration using the standard set-up, representing dipyridamole administration without ARA therapy, was higher than the solubility in FaSSIF V1 and V2 (93 - 99 $\mu\text{g}/\text{mL}$ vs. 20.3 and 17.3). As in the two-stage and transfer experiments, these results suggest that supersaturation occurred.

Experiments using a gastric fluid with pH 6 showed a lower bioavailable fraction compared to the standard (low gastric pH) set-up. The maximal jejunal concentrations (20 - 40 $\mu\text{g}/\text{mL}$) were closer to the values of FaSSIF solubility than those observed with the low gastric pH set-up. Significantly more drug was recovered from the rinses after the experiment, compared to the experiments with pH 2 gastric fluid, in line with the recovery of residual dipyridamole in the donor compartment after the transfer experiments with the ARA pH 6 medium.

The profile of the bioavailable fraction from the experiment using a gastric fluid with pH 4 lies between the two other profiles (gastric pH 2 and pH 6), with just under 60 % for the final bioavailable fraction.

Discussion

Solubility and *in vitro* dissolution approaches

As a BCS class II drug, dipyridamole shows poor solubility in water. Its solubility is highly dependent on the pH of the medium, with a difference of well over 1,000 fold between aqueous solubility at pH 1 and pH 6. Thus, it is important to understand its dissolution behavior across this pH range to reveal the potential extent of DDIs with ARAs. In addition to one-stage dissolution testing using FaSSGF as a surrogate for the acidic gastric fluid usually observed in a healthy individual, dissolution testing using novel ARA media to represent a lesser (gastric pH 4) and a stronger (gastric pH 6) effect of ARAs is a valuable tool for understanding this behavior and assessing the risks associated with it.

For drugs that are not prone to precipitation or for which fast permeation across the intestinal wall ensures that luminal concentrations stay below the critical precipitation concentration *in vivo*, one-stage tests can provide an accurate representation of *in vivo* drug dissolution.

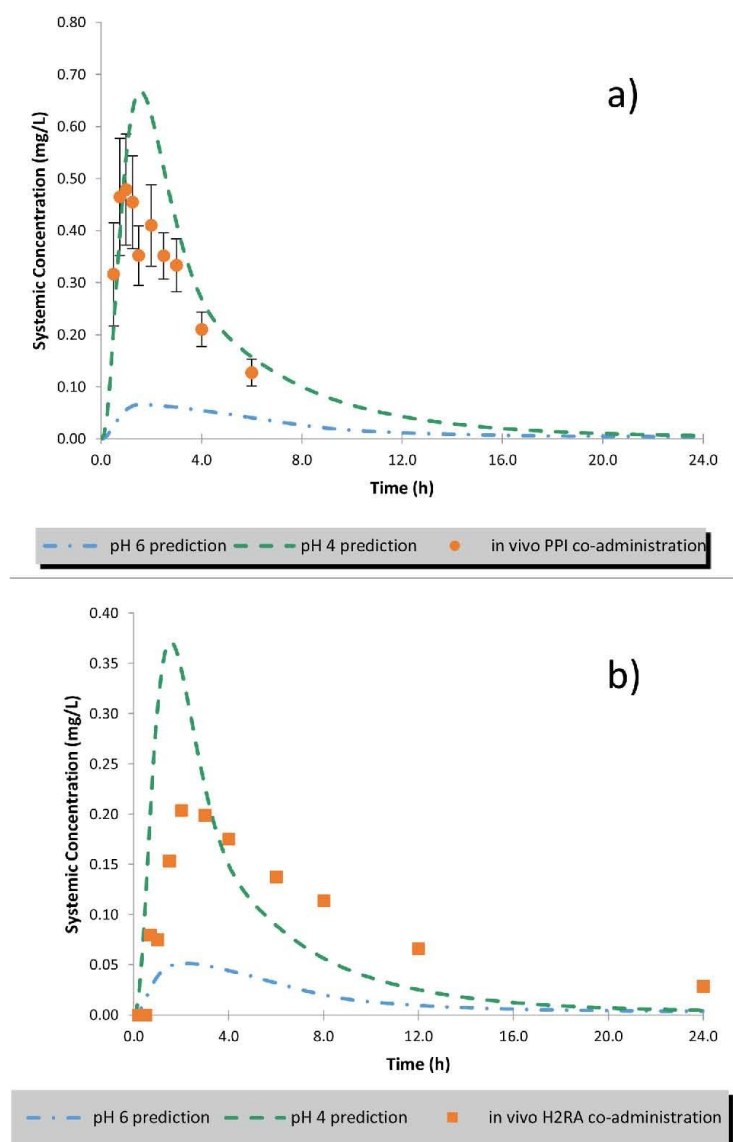


Fig. 7. Simulation of the plasma concentration profile for a representative healthy population subject showing a lesser ARA pH effect (pH 4, dashed line) and a greater ARA pH effect (pH 6, dash dot line), compared to the observed average values in: a) volunteers after PPI pre-treatment (full circles), dipyridamole dose 100 mg (Derendorf et al. 2005) and, b) elderly volunteers after H2RA pre-treatment (full squares), dipyridamole dose 50 mg (Russell et al. 1994). These simulations were run with the static intestinal pH model.

This can be confirmed by linking the dissolution data to a plasma profile prediction *in silico*: An example for the first scenario (drugs not prone to precipitation), was reported in a previous study (Segregur et al. 2020), in which it was shown in two-stage experiments that the poorly soluble weakly basic compound under study stayed supersaturated during the second stage. In this case, input of one-stage dissolution data led to an accurate prediction of plasma profiles *in vivo*. Dipyridamole likely belongs to the second scenario, where precipitation is, for the most part, circumvented by rapid absorption. This hypothesis stems from the

rapid and substantial precipitation observed in the two-stage and transfer models, with simulations using precipitation parameters estimated from these experiments severely underpredicting plasma concentrations, whereas a report in the literature indicates that there is minimal precipitation of dipyridamole *in vivo* (Psachoulas et al. 2011).

Due to the high sensitivity of its solubility to pH, dipyridamole shows a large difference in dissolution behavior when administration without pre-treatment (rapid and complete dissolution) and during treatment with ARAs (limited dissolution) are simulated. Such data are essential as

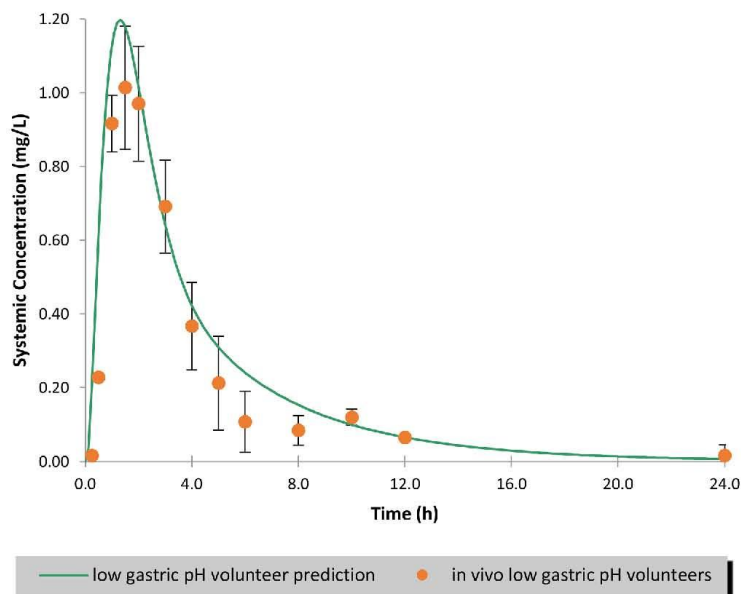


Fig. 8. Simulation of the plasma concentration profile for a representative healthy population subject using the dynamic intestinal pH model (solid line) compared to the observed average values in volunteers without ARA pre-treatment (filled circles), dipyridamole dose 75 mg (Ricevuti et al. 1991).

input to the PBPK model when predicting the clinical relevance of the ARA co-administration. Interestingly, this results not only in a large difference between the simulations based on low gastric pH and those based on elevated pH, but there are also substantial differences between the simulations based on the pH 4 and pH 6 ARA media dissolution profiles. This may suggest a high inter- and intra-subject variability, and can be investigated further *in silico*.

As described in a recent publication (Segregur et al. 2019), both the pH and buffer capacity of the ARA media reflect the values found *in vivo* after administration of ARAs. In this regard, ARA media were shown to be superior to deionized water (Segregur et al. 2020). While ARA pH 4 media possess a moderate buffer capacity (7.5 mEq/pH/L), the ARA pH 6 media possess minimal buffer capacity (1 mEq/pH/L). Nevertheless, in dissolution experiments with dipyridamole, 250 ml of both pH 4 and pH 6 ARA media managed to maintain the initial pH. While these buffer capacities appear to be sufficient for weakly basic or acidic compounds at relatively low doses, they may not be able to maintain the initial pH at very high doses, especially for salt forms or formulations containing strongly pH active excipients (e.g. solid acids). This is especially so for ARA pH 6 media. But since such a pH shift may also be expected *in vivo* in these cases, the ARA media should yield more physiologically relevant data than aqueous buffer systems with strong buffer capacities, such as those found in the pharmacopeia.

Dipyridamole solubility is increased in media containing bile components. The influence of the bile components is observed most clearly when comparing the results of solubility in intestinal biorelevant media at Level 1 (buffer only) and Level 2 (buffer plus bile components). Although solubilisation is likely to play a lesser role for the ionized than the non-ionized form of a weakly basic compound, the ionized drug may also interact with the bile components in the ARA media. However, the impact of bile components on solubility in the ARA media is likely to be greater at pH values where a higher percentage of the drug is in its non-ionized form i.e. close to or above the pKa for a weak base. Since these aspects should be addressed in the design of ARA media, they are

composed with the same bile component concentrations as in the standard gastric biorelevant medium, FaSSGF (Segregur et al. 2019).

For all the above-mentioned reasons, one-stage dissolution testing using the various biorelevant media (FaSSGF, ARA pH 4 and ARA pH 6) constitutes an informative *in vitro* set-up to be used in conjunction with PBPK models to simulate ARA effects on plasma profiles.

Two-stage dissolution experiments have the advantage of being able to detect any supersaturation and precipitation of the drug due to a shift from gastric to intestinal pH. While PSWB 001, a BCS class II weakly basic compound reported in a recent study, showed supersaturation but no precipitation after the pH shift (Segregur et al. 2020), dipyridamole showed fast precipitation in two-stage experiments using acidic gastric media (pH 2 and pH 4). Using an ARA pH 6 medium to simulate the gastric environment under a strong ARA influence, no supersaturation or precipitation was observed, as concentrations above the solubility in FaSSIF V2 were not reached before the pH shift. Thus, two-stage dissolution experiments are a fast and useful tool to screen for potential intestinal precipitation when ARAs are co-administered. However, it should be noted that two-stage experiments produce an abrupt change in pH, maximizing the potential for precipitation, and are therefore likely to over-predict the precipitation *in vivo*.

Standard transfer methodology uses 350 mL of FaSSIF (V1) as the intestinal medium (Ruff et al. 2017). In this study, however, 250 mL of a FaSSIF V2 double concentrate was used in the acceptor compartment to better compare results with those from two-stage dissolution. The transfer experiment introduces a more gradual transit of the dissolved drug into the intestinal environment, which for dipyridamole leads to a more gradual precipitation of dipyridamole when pH 2 and ARA pH 4 media are used in the gastric compartment.

Nevertheless, two-stage dissolution and transfer experiments lack an absorptive compartment and therefore are likely to underestimate the effect of absorption on precipitation kinetics in the intestine. Thus, data from one-stage, two-stage and transfer experiments should be used in connection with *in silico* modelling to predict the drug fraction absorbed

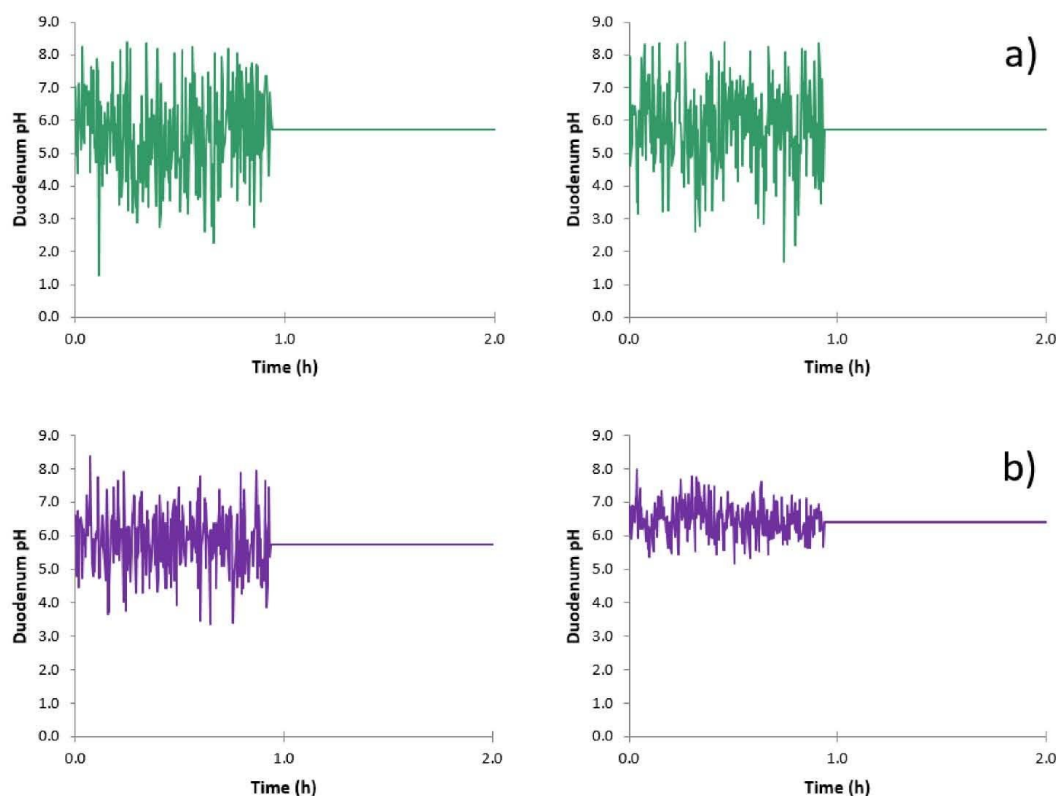


Fig. 9. Simulation of the duodenal pH for a representative healthy population subject with gastric pH 4 (left) and pH 6 (right), using a) the default dynamic intestinal pH set-up and b) modified set-ups of the dynamic intestinal pH model tailored to the respective mean gastric pH.

and concentrations of the drug in plasma.

To better account for absorption, a more complex set-up, such as the Biorelevant Gastro-Intestinal Transfer (BioGIT) can be used. The BioGIT includes a transfer system from a gastric into the intestinal compartment, as well as a transfer out of the intestinal compartment (simulating absorption) and from a reservoir into the intestinal compartment (maintaining constant volume) (Kourentas et al. 2016). With such a set-up, Kourentas et al. recorded less dipyridamole precipitation and was better able to reflect (Kourentas et al. 2016) the *in vivo* luminal data. An alternative approach to account for intestinal absorption are dissolution set-ups with an organic sink: O'Dwyer et al. recently introduced an *in vitro* biphasic pH shift set-up for dipyridamole, using biorelevant media for the aqueous phase and decanol as an organic absorptive sink (O'Dwyer et al. 2020). Likewise, Pathak et al. reported a better performance for the model including precipitation when data from a 2-phase dissolution with octanol as an absorptive organic phase was used (Pathak et al. 2019). That being said, it is important to note that approaches which attempt to address absorption *in vitro* may in some cases lead to simulations exceeding the actual plasma concentrations. Indeed, one should be careful to avoid applying an "absorptive sink" *in vitro* and then using the results for PBPK modelling, which also simulates an "absorptive sink" if a high permeability is applied.

While the TIM-1 experiment shares similarities with the two-stage and transfer experiments, it also includes absorptive compartments (filters) designed to estimate the percentage of the drug dose available

for absorption *in vivo*. Additionally, TIM-1 experiments simulate gastric emptying, housekeeper wave, and peristalsis. With these extra features, although some precipitation was observed during TIM-1 experiments with an acidic gastric pH, the final fraction bioavailable was still high and similar to a non-precipitating, readily soluble internal reference compound. A limitation of the TIM-1 experiment is that, since it is time-consuming, it is often impractical to evaluate the reproducibility of the data. Further, a new experiment must be set up and conducted to explore e.g. a change in the gastric emptying rate, whereas using a PBPK model, this can be handled *in silico*.

Combined dissolution and modelling approaches

When simulating dipyridamole administration without ARA co-administration, a slightly higher plasma concentration was predicted in the *in silico* model when the dynamic intestinal pH model was used. This model simulates the mixing of the acidic gastric fluid with buffers in the upper small intestine, leading to variability in the intestinal pH and thus allowing a greater amount of the drug to dissolve in the upper small intestine. Another feature of the dynamic intestinal pH model is that, depending on dose, luminal concentrations may fluctuate rapidly between super- and subsaturation, making precipitation events short-lived and re-dissolution of any precipitated drug more rapid. Therefore, the use of the dynamic intestinal pH model may provide a more accurate prediction of the dissolution surroundings during the transfer of the drug

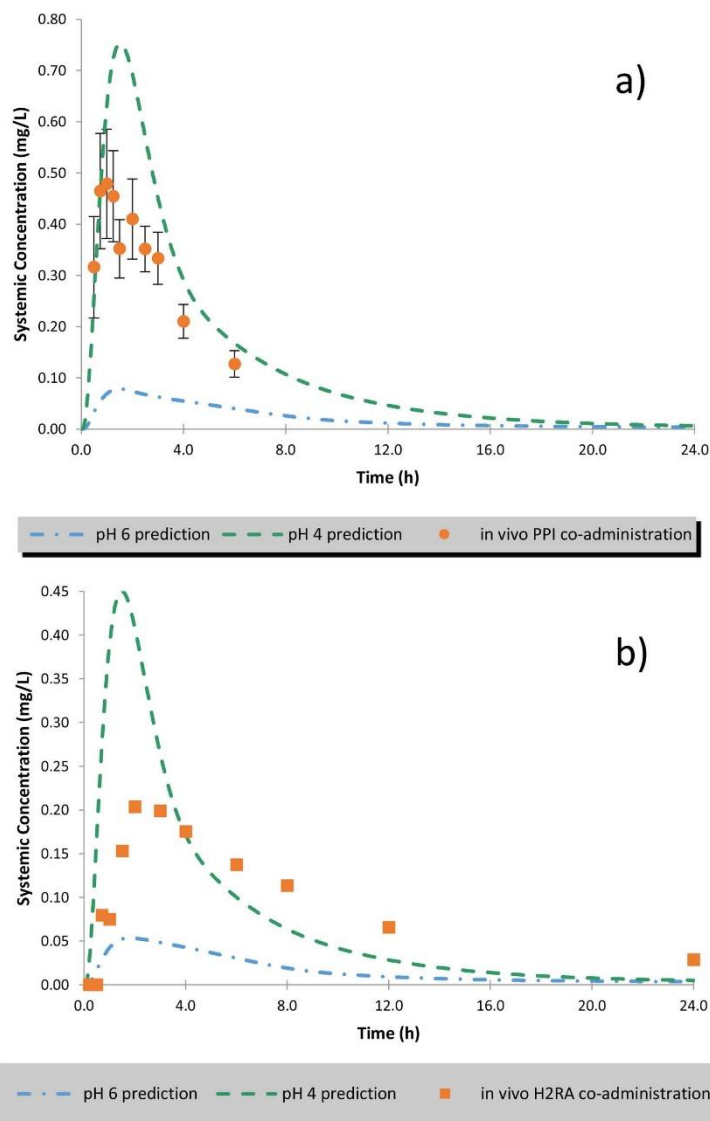


Fig. 10. Simulation of the plasma concentration profile for a representative healthy population subject showing lesser ARA pH effect (pH 4, dashed line) and a greater ARA pH effect (pH 6, dash dot line), using a modified dynamic intestinal pH model, compared to the observed average values in: a) volunteers after PPI pre-treatment (full circles), dipyrindamole dose 100 mg (Derendorf et al. 2005) and, b) elderly volunteers after H2RA pre-treatment (full squares), dipyrindamole dose 50 mg (Russell et al. 1994).

from the gastric into the intestinal compartment. It is, however, important to mention that the current default Simcyp dynamic intestinal pH model settings are only appropriate for simulation of the intestinal pH when the gastric pH is low (mean value of pH 1.5 for fasted state conditions only). When simulating the intestinal pH after a treatment with ARAs, a higher gastric pH, and the resulting carryover effects on intestinal pH have to be taken into account. The settings used to reflect the ARA effect in the intestine reported in this paper successfully simulated intestinal pH within constraints imposed by the elevated gastric pH and produced predictions in accordance with the predictions

using the default static intestinal pH model. Although the performance of both pH models proved to be similar for dipyrindamole, consideration of the dynamic pH may be important for drugs more prone to precipitation.

Overall, depending on the precipitation behavior of the drug, *in vitro* one-stage, two-stage and/or transfer experiments, combined with *in silico* modeling, may all be useful to predict plasma profiles. In our case, assuming no dipyrindamole precipitation *in vivo*, one-stage dissolution data successfully simulated the plasma profiles with or without ARA pre-treatment, when combined with a full PBPK *in silico* model. The model

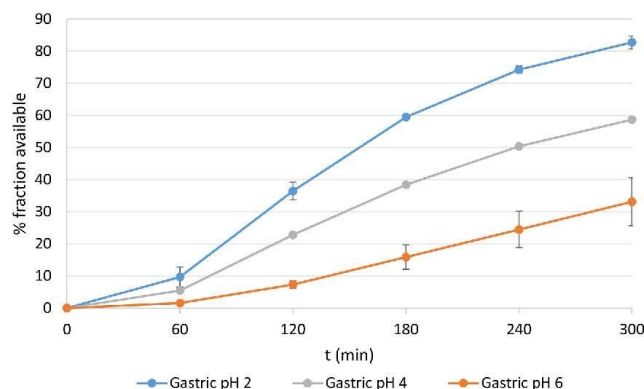


Fig. 11. Dipyrindamole fraction available for absorption with time according to TIM-1 experiments using the standard set-up (gastric pH 2, n 2)) and set-up simulating ARA co-administration (gastric pH 4 (n 1) and pH 6 (n 2)).

predicted on average a 45-90% decrease in C_{max} and a 42-88% decrease in AUC due to the interaction with ARAs, depending on whether the ARA effect on gastric pH is moderate (pH 4) or strong (pH 6).

Thus, the predictions using ARA dissolution data as input to the PBPK model represent the range of values most likely to be found in a population due to the PPI effect. In this regard, it is important to note that the bracketing approach is meant to be used as a risk assessment tool, rather than an approximation of the average ARA effect or of the mean plasma profile found *in vivo*. When the ARA co-administration model predicts a wide range of possible individual plasma profiles and a strong overall effect on PK parameters, compared to simulations based on low gastric pH, the ARA effect may well be clinically relevant. In this case, depending on the efficacy window and potential toxicity of the compound, further steps can be undertaken to minimize the ARA effect. On the other hand, if the model predictions for a drug or a given formulation for both moderate (pH 4) and strong (pH 6) ARA effect are within the efficacy window, the ARA effect may be less clinically relevant. Such predictions may help guide decisions on formulation development and increase confidence when designing clinical studies (Segregur et al. 2019).

Recently, the FDA has published a draft guidance on "Evaluation of gastric pH-dependent drug interactions with acid-reducing agents" (Food and Drug Administration (FDA) 2020 a), which proposes PBPK as an alternative to running PK trials to determine the effects of PPI co-administration on plasma profiles. The workflow proposed in this study may be an appropriate starting point for the application of PBPK analyses in the area of absorptive DDIs (Food and Drug Administration (FDA) 2020 b).

As an alternative, a more evolved *in vitro* set-up, which takes into account upper GI hydrodynamics as well as the permeation step, can be used as a stand-alone method to predict the change in bioavailable fraction due to therapy with ARAs. In our case, the TIM-1 model predicted about a 30% decrease in bioavailable fraction if the ARA increases the gastric pH to 4 and about a 60% decrease in bioavailable fraction if the ARA increases the gastric pH to 6.

Interestingly, the ratios from the experiments of the fraction available for absorption acquired from TIM-1 (0.29 and 0.60) are comparable with the ratios for final percentage dissolved from the transfer experiment (0.36 and 0.67) and the absolute values of fractions available for absorption are about two-fold of the final values of percentage dissolved

in transfer experiments (83, 59 and 33% vs. 42, 27 and 14 %).

As the interest of both industry and regulatory agencies shifts increasingly to the prediction of drug behavior *in vivo* early on in the development process, as well as waiving clinical studies while still maintaining and guaranteeing drug safety and efficacy, *in vitro* and *in silico* methods will surely become more important tools in pharmaceutical development. Thus, a comparison of the *in vitro* and *in silico* predictive methods for dipyrindamole, a well-known weakly basic BCS class II drug, should be helpful to identifying best practices for evaluating DDIs with drugs such as PPIs and H2RAs. Of course, there is a wide range of dissolution/precipitation behavior across the class of weakly basic drugs, so it will be necessary to compare results for further examples from this class before defining standard approaches.

Conclusion

It was demonstrated that novel *in vitro* tests representing the gastric environment after ARA treatment can be used in conjunction with PBPK modelling to simulate the effect of ARAs on the plasma profile of a BCS class II weak basic drug, dipyrindamole. For drugs lacking or showing little precipitation *in vivo*, one-stage dissolution is an appropriate *in vitro* set-up to describe the dissolution behavior. While two-stage experiments help to determine if precipitation can occur upon gastric emptying into the small intestines, this is a worst-case-scenario for precipitation. The transfer test, with its slower simulation of gastric emptying, captured the potential for dipyrindamole precipitation better, however, it lacks an absorptive compartment to provide the sink conditions that are expected *in vivo* for this highly permeable compound. As all three tests lack an absorptive compartment, it is recommended that the results be used in combination with PBPK modeling to predict changes in the pharmacokinetics. Alternatively, an *in vitro* set-up with evolved hydrodynamics and simulation of passive absorption, TIM-1, proved useful for forecasting ARA effects on the fraction of dipyrindamole that is available for absorption for an average subject, provided that the physiological parameters of the set-up are adjusted to reflect the impact of ARA therapy on gastric pH.

Summarizing, our results show that several approaches can be used to study DDIs of weakly basic drugs with ARAs and that this enables a cross-check among methods as well as against *in vivo* data, thus building confidence in their use.

Credit author statement

| | |
|----------------------------|---|
| Conceptualization | Domagoj Segregur, Jennifer Dressman, James Mann |
| Methodology | Jennifer Dressman, Domagoj Segregur, Richard Barker, David B. Turner |
| Validation | Domagoj Segregur |
| Investigation | Domagoj Segregur |
| Resources | James Mann, Andrea Moir, David B. Turner |
| Writing - Original Draft | Domagoj Segregur |
| Writing - Review & Editing | Jennifer Dressman, James Mann, Andrea Moir, Eva M. Karlsson, Richard Barker, David B. Turner, Sumit Arora |
| Visualization | Domagoj Segregur |
| Supervision | Jennifer Dressman |
| Project administration | Jennifer Dressman, James Mann |

Acknowledgment

Certara UK (Simcyp Division) granted free access to the Simcyp Simulators through an academic licence (subject to conditions).

Supplementary materials

Supplementary material associated with this article can be found, in the online version, at doi:10.1016/j.ejps.2021.105750.

References

- Barker, Richard, Abrahamsson, Bertil, Kruusmägi, Martin, 2014. Application and validation of an advanced gastrointestinal in vitro model for the evaluation of drug product performance in pharmaceutical development. *J. Pharmaceut. Sci.* 103 (11), 3794–3712. <https://doi.org/10.1002/jps.24177>. S.
- Brown, Deanna G., Wilkerson, Eric C., Love, W.H.Iot, 2015. A review of traditional and novel oral anticoagulant and antiplatelet therapy for dermatologists and dermatologic surgeons. *J. Am. Acad. Dermatol.* 72 (3), 524–534. <https://doi.org/10.1016/j.jaad.2014.10.027>. S.
- Derendorf, Hartmut, VanderMaeden, Cam P., Briedl, Rolf-Stefan, MacGregor, Tom R., Eisert, Wolfgang, 2005. Dipyridamole bioavailability in subjects with reduced gastric acidity. *J. Clin. Pharmacol.* 45 (7), 845–850. <https://doi.org/10.1177/0091270005276738>. S.
- 4 Food and Drug Administration (FDA): Persantine® (dipyridamole USP) Label. https://www.accessdata.fda.gov/drugsatfda_docs/label/2019/012836s0611bl.pdf, Accessed August 2, 2020.
- Food and Drug Administration (FDA) (2018): Framework for Assessing pH-Dependent Drug-Drug Interactions; Establishment of a Public Docket, Request for Comments <https://www.regulations.gov/document?D=FDA-2018-H-1820-0001>, Accessed July 27, 2020.
- Food and Drug Administration (FDA), 2020. Evaluation of Gastric pH-Dependent Drug Interactions With Acid-Reducing Agents: Study Design, Data Analysis, and Clinical Implications Guidance for Industry. a. <https://www.fda.gov/regulatory-information/search-fda-guidance-documents/evaluation-gastric-ph-dependent-drug-interaction-s-acid-reducing-agents-study-design-data-analysis>. Accessed December 4, 2020.
- Food and Drug Administration (FDA), 2020. The Use of Physiologically Based Pharmacokinetic Analyses — Biopharmaceutics Applications for Oral Drug Product Development, Manufacturing Changes, and Controls. b. <https://www.fda.gov/regulatory-information/search-fda-guidance-documents/use-physiologically-based-pharmacokinetic-analyses-biopharmaceutics-applications-oral-drug-product>. Accessed January 16, 2021.
- Glonne, A., März, J., Dressman, J.B., 2005. Comparison of a miniaturized shake-flask solubility method with automated potentiometric acid/base titrations and calculated solubilities. *J. Pharmaceut. Sci.* 94 (1), 1–16. <https://doi.org/10.1002/jps.20212>. S.
- Hopgood, Matthew, Reynolds, Gavin, Barker, Richard, 2018. Using Computational Fluid Dynamics to Compare Shear Rate and Turbulence in the TBM-Automated Gastric Compartment With USP Apparatus II. *J. Pharmaceut. Sci.* 107 (7), 1911–1919. <https://doi.org/10.1016/j.xphs.2018.03.019>. S.
- Klumpp, Lukas, Dressman, Jennifer, 2020. Physiologically based pharmacokinetic model outputs depend on dissolution data and their input: Case examples glibenclamide and dipyridamole. *European J. Pharmaceut. Sci.* 151, 105380 <https://doi.org/10.1016/j.ejps.2020.105380>. S.
- Kourentas, Alexandros, Vertzoni, Maria, Stavrinoudakis, Nick, Symillidis, Alexandros, Brouwers, Joachim, Augustijns, Patrick, et al., 2016. An in vitro biorelevant gastrointestinal transfer (BioGIT) system for forecasting concentrations in the fasted upper small intestine: Design, implementation, and evaluation. *European J. Pharmaceut. Sci.* 82, 106–114. <https://doi.org/10.1016/j.ejps.2015.11.012>. S.
- Koziolek, M., Schneider, F., Grimm, M., Modeß, Chr, Seekamp, A., Rouston, T., et al., 2015a. Intragastric pH and pressure profiles after intake of the high-caloric, high-fat meal as used for food effect studies. *J. Control. Release* 220 (Pt A), 71–78. <https://doi.org/10.1016/j.jconrel.2015.10.022>. S.
- Koziolek, Mirko, Grimm, Michael, Becker, Dieter, Iordanov, Ventseslav, Zou, Hans, Shimizu, Jeff, et al., 2015b. Investigation of pH and Temperature Profiles in the GI Tract of Fasted Human Subjects Using the Intelliga® System. *J. Pharmaceut. Sci.* 104 (9), 2855–2863. <https://doi.org/10.1002/jps.24274>. S.
- Leppo, J.A., 1994. Dipyridamole myocardial perfusion imaging. *J. Nucl. Med.* 35 (4), 730–733. S.
- Mann, James, Dressman, Jennifer, Rosenblatt, Karin, Ashworth, Lee, Muenster, Uwe, Frank, Kerstin, et al., 2017. Validation of Dissolution Testing with Biorelevant Media: An OrBiTo Study. *Md. Pharmaceut.* 14 (12), 4192–4201. <https://doi.org/10.1021/acs.molpharmaceut.7b00198>. S.
- Makropoulos, Constantinos, Andreas, Cord J., Vertzoni, Maria, Dressman, Jennifer, Reppas, Christos, 2015. In-vitro simulation of luminal conditions for evaluation of performance of oral drug products: Choosing the appropriate test media. *European J. Pharmaceut. Biopharmaceut.* 93, 173–182. <https://doi.org/10.1016/j.ejpb.2015.03.009>. S.
- Obach, R.S., Baxter, J.G., Liston, T.E., Silber, B.M., Jones, B.C., MacIntyre, F., et al., 1997. The prediction of human pharmacokinetic parameters from preclinical and in vitro metabolism data. *J. Pharmacol. Exp. Therapeut.* 283 (1), 46–58. S.
- O'Dwyer, Patrick J., Imanidis, Georgios, Box, Karl J., Reppas, Christos, 2020. On the Usefulness of Two Small-Scale In Vitro Setups in the Evaluation of Luminal Precipitation of Lipophilic Weak Bases in Early Formulation Development. *Pharmaceutics* 12 (3). <https://doi.org/10.3390/pharmaceutics12030272>.
- Pathak, Shritam M., Schaefer, Kerstin Julia, Jamei, Masoud, Turner, David B., 2019. Biopharmaceutic IVIVE-Mechanistic Modeling of Single- and Two-Phase In Vitro Experiments to Obtain Drug-Specific Parameters for Incorporation into PBPK Models. *J. Pharmaceut. Sci.* 108 (4), 1604–1618. <https://doi.org/10.1016/j.xphs.2018.11.034>. S.
- Pepin, Xavier J.H., Parrott, Neil, Dressman, Jennifer, Delvadia, Poonam, Mitra, Amitava, Zhang, Xinyuan, et al., 2020. Current State and Future Expectations of Translational Modeling Strategies to Support Drug Product Development, Manufacturing Changes and Controls: A Workshop Summary Report. *J. Pharmaceut. Sci.* <https://doi.org/10.1016/j.xphs.2020.04.021>.
- Psachoulas, Dimitrios, Vertzoni, Maria, Goumas, Konstantinos, Kalioras, Vasilios, Beato, Stefania, Butler, James, Reppas, Christos, 2011. Precipitation in and supersaturation of contents of the upper small intestine after administration of two weak bases to fasted adults. *Pharmaceut. Res.* 28 (12), 3145–3158. <https://doi.org/10.1007/s11095-011-0506-6>. S.
- Ricevuti, G., Mazzone, A., Pasotti, D., Uccelli, E., Pasquali, F., Gazzani, G., Fregnan, G.B., 1991. Pharmacokinetics of dipyridamole-beta-cyclodextrin complex in healthy volunteers after single and multiple doses. *European J. Drug Metabol. Pharmacokinet.* 16 (3), 197–201. <https://doi.org/10.1007/BF03189959>. S.
- Ruff, Aaron, Fiolka, Tom, Kostewicz, Edmund S., 2017. Prediction of Ketoconazole absorption using an updated in vitro transfer model coupled to physiologically based pharmacokinetic modelling. *European J. Pharmaceut. Sci.* 100, 42–55. <https://doi.org/10.1016/j.ejps.2016.12.017>. S.
- Russell, T.L., Berardi, R.R., Barnett, J.L., O'Sullivan, T.L., Wagner, J.G., Dressman, J.B., 1994. pH-related changes in the absorption of dipyridamole in the elderly. *Pharmaceut. Res.* 11 (1), 136–143. <https://doi.org/10.1023/a:1018918316253>. S.
- Segregur, Domagoj, Hanagan, Talia, Mann, James, Moir, Andrea, Karlsson, Eva M., Hoch, Matthias, et al., 2019. Impact of Acid-Reducing Agents on Gastrointestinal Physiology and Design of Biorelevant Dissolution Tests to Reflect These Changes. *Journal of pharmaceutical sciences* 108 (11), 3461–3472. <https://doi.org/10.1016/j.xphs.2019.06.021>. S.
- Segregur, Domagoj, Mann, James, Moir, Andrea, Karlsson, Eva M., Dressman, Jennifer, 2020. Prediction of plasma profiles of a weakly basic drug after administration of omeprazole using PBPK modeling. *European journal of pharmaceutical sciences: official journal of the European Federation for Pharmaceutical Sciences*, 105656. <https://doi.org/10.1016/j.ejps.2020.105656>. S.

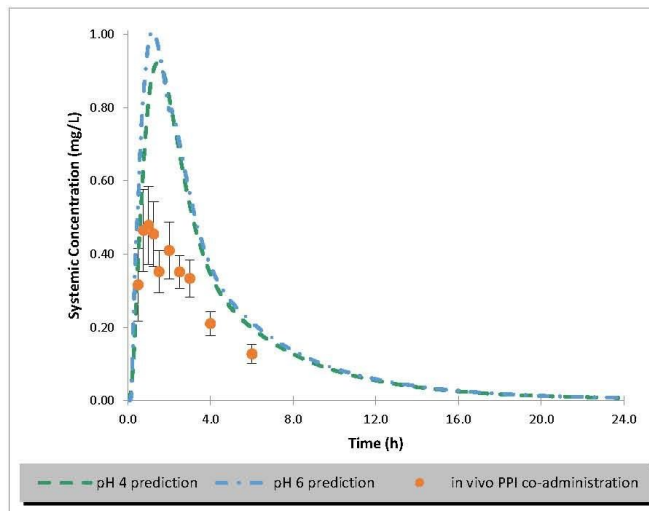


Figure A. Simulation of the plasma concentration profile for a representative healthy population subject showing a gastric pH 4 model (dashed line) and a gastric pH 6 model (dash dot line), using the default dynamic intestinal pH model, compared to the observed average values in volunteers after ARA pre-treatment (full circles), dipyridamole dose 100 mg

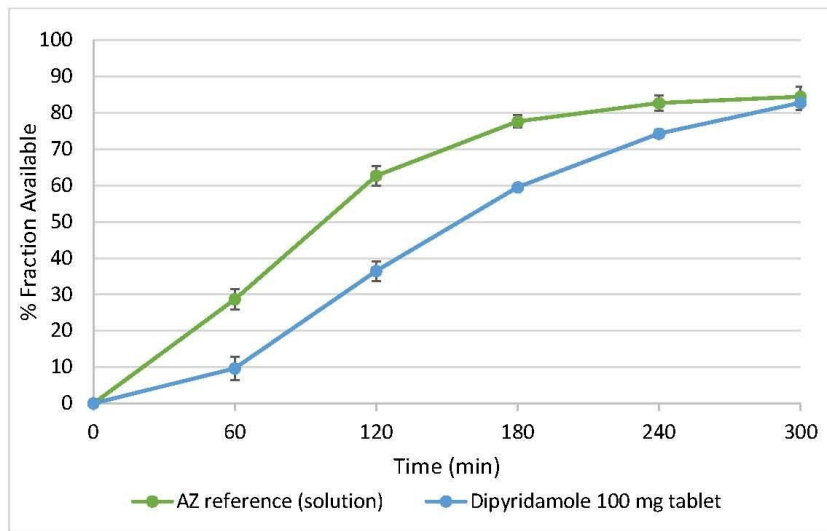


Figure B. Fraction available for absorption with time according to TIM-1 experiments using the standard set-up (gastric pH 2) and an AstraZeneca reference (solution) or a 100 mg dipyridamole tablet

Table A. A summary of pH, buffer species and buffer capacity for biorelevant media used in the dissolution one-stage, two-stage and transfer experiments

| | Biorelevant medium | pH | Buffer species | Buffer capacity (mEq/L/ Δ pH) | Ref. |
|------------------------|--------------------|--------|-------------------|--------------------------------------|-------------------------|
| Gastric compartment | FaSSGF | 1.6* | HCl | n.a. | Markopoulos et al. 2015 |
| | ARA pH 4 acetate | 4 | acetate | 7.5 | Segregur et al. 2019 |
| | ARA pH 4 citrate | 4 | citrate | 7.5 | |
| | ARA pH 4 Mcilvaine | 4 | citrate/phosphate | 7.5 | |
| | ARA pH 6 maleate | 6 | maleate | 1 | |
| | ARA pH 6 citrate | 6 | citrate | 1 | |
| | ARA pH 6 Mcilvaine | 6 | citrate/phosphate | 1 | |
| Intestinal compartment | FaSSIF V1 | 6.5 | phosphate | 12 | Markopoulos et al. 2015 |
| | FaSSIF V2 | 6.5 | maleate | 10 | |
| Double concentrates | FaSSIF V1 2xc | 7.5 | phosphate | n.a.*** | Mann et al. 2017 |
| | FaSSIF V2 2xc | 10.8** | maleate | n.a.*** | n.a. |

n.a. - not applicable

* for two-stage and transfer experiments with FaSSIF V2 2xc, the pH is adjusted to pH 2

** if the gastric medium is ARA pH 4 the pH is adjusted to pH 12.13, and if the gastric medium is ARA pH 6 it is adjusted to pH 6.46

*** comparable to buffer capacity of the corresponding FaSSIF version after 1:1 dilution with FaSSGF



Contents lists available at ScienceDirect

Journal of Pharmaceutical Sciences

journal homepage: www.jpharmsci.org

Pharmacokinetics, Pharmacodynamics Drug Transport Metabolism

Biorelevant *in vitro* Tools and *in silico* Modeling to Assess pH-Dependent Drug-drug Interactions for Salts of Weak Acids: Case Example Potassium Raltegravir

Domagoj Segregur^a, James Mann^b, Andrea Moir^b, Eva M. Karlsson^c, Jennifer Dressman^{a,d,*}

^a Institute of Pharmaceutical Technology, J. W. Goethe University, 9 Max von Laue St., 60438 Frankfurt am Main, Germany (now employed at Product Design and Performance, UCB Pharma, Braine-l'Alleud, Belgium)

^b Oral Product Development, Pharmaceutical Technology & Development, Operations, AstraZeneca, Macclesfield, United Kingdom

^c Oral Product Development, Pharmaceutical Technology & Development, Operations, AstraZeneca, Gothenburg, Sweden

^d Fraunhofer Institute of Translational Medicine and Pharmacology, Theodor-Stern-Kai 7, 60596 Frankfurt am Main, Germany

ARTICLE INFO

Article history:

Received 18 May 2021

Revised 9 September 2021

Accepted 9 September 2021

Available online xxx

Keywords:

Bioavailability

Biopharmaceutics classification system (BCS)

Dissolution

Gastrointestinal tract

HIV/AIDS

In silico modeling

In vitro model(s)

pH

Physiologically based pharmacokinetic (PBPK)

modeling

Salts

ABSTRACT

Background: Early assessment of pH-dependent drug-drug-interactions (DDIs) for salts of poorly soluble weakly acidic compounds offers various advantages for patient safety, the pharmaceutical industry, and regulatory bodies. Biorelevant media and tests reflecting physiological changes during acid-reducing agent (ARA) co-administration can be used to explore and predict the extent of the pH effect during therapy with ARAs.

Methods: Solubility, one-stage and two-stage dissolution of tablets containing potassium raltegravir, the marketed salt form of this poorly soluble, weakly acidic drug, was investigated using biorelevant media specially designed to reflect administration without and during ARA co-therapy. The dissolution data were then converted into parameters suitable for input into an *in silico* model (Simcyp™) and the simulated plasma profiles were compared with available pharmacokinetic (PK) data from the literature.

Results: Dissolution of the potassium raltegravir formulation in media reflecting ARA co-administration, and thus elevated gastric pH, was faster and more complete than in experiments reflecting the low gastric pH observed in the absence of ARA co-administration. Simulations using data from dissolution experiments with ARA media appropriately bracketed the *in vivo* data for ARA co-administration in healthy volunteers.

Conclusion: Dissolution data from *in vitro* experiments in biorelevant media reflecting physiological changes due to ARA co-administration provide valuable information about potassium raltegravir's behavior during concomitant ARA therapy. The approach may also be suitable for salts forms of other poorly soluble, weakly acidic drugs.

© 2021 Published by Elsevier Inc. on behalf of American Pharmacists Association.

Introduction

Next to metabolism-dependent drug-drug interactions (DDIs), assessing pH-dependent DDIs affecting drug absorption has become an important element of pharmaceutical drug development. In a recent draft guidance, the FDA highlighted the importance of evaluating pH-dependent DDIs with acid-reducing agents (ARAs) and gave insight into the approach to assessment and characterization, as well as clinical study design, regarding such DDIs.¹ The focus of both the industry and regulatory bodies on developing best practices in this field arises from the fact that the main groups of ARAs, i.e. proton

pump inhibitors (PPIs), H₂-receptor antagonists (H₂RAs) and anti-acids, are readily available and frequently co-administered with a broad range of drugs, many of which have pH-dependent solubility. Elevated gastric pH during therapy with these drugs may thus potentially have a negative impact on gastrointestinal dissolution and thus efficacy (in the case of poorly soluble, weakly basic compounds) or a positive impact on gastrointestinal dissolution and thus an increase in incidence of side-effects and toxicity (in the case of poorly soluble, weakly acidic compounds).¹

Biorelevant media mimicking the gastric fluids after administration of PPIs and H₂RAs were recently developed as a risk assessment tool to predict the potential range of pharmacokinetic (PK) response to administration of ARAs.² Dissolution of drug products in these media demonstrated an effect of PPIs and H₂RAs on drug dissolution,

* Corresponding author.

E-mail address: dressman@em.uni-frankfurt.de (J. Dressman).<https://doi.org/10.1016/j.xphs.2021.09.037>

0022-3549/© 2021 Published by Elsevier Inc. on behalf of American Pharmacists Association.

and the results were subsequently used as input into *in silico* physiologically based pharmacokinetic (PBPK) models to explore *in vivo* plasma profiles for two poorly soluble basic drugs.^{3,4} In both cases the simulated PK profiles bracketed the DDI observed in clinical studies. These publications showcased the suitability of the ARA biorelevant media in a range of *in vitro* setups, including solubility measurements, one-stage and two-stage dissolution, as well as transfer experiments, for poorly soluble, weakly basic drugs. However, the question remains as to whether pH-dependent DDIs for poorly soluble, weakly acidic drugs can also be forecast using these media.

In this study, pH-dependent DDIs were assessed using ARA biorelevant media for the potassium salt of a poorly soluble, weakly acidic compound, raltegravir. Raltegravir was chosen as a model drug due to its pH-dependent solubility and the availability of clinical pharmacokinetic data for administration without and during ARA co-administration.^{5–8} As a human immunodeficiency virus (HIV) integrase inhibitor, raltegravir is used in Highly Active AntiRetroviral Therapy (HAART) for treatment of HIV infection and acquired immunodeficiency syndrome (AIDS), as well as for postexposure prophylaxis (PEP) against HIV.^{9,10} Raltegravir is available on the market as the potassium salt in Isentress® film-coated tablets (400 mg), Isentress HD® (600 mg) film-coated tablets and Isentress® chewable tablets (25 and 100 mg), as well as in granules for the preparation of an oral suspension (100 mg).¹¹ The film-coated tablets, which have been recently reported to dissolve slowly both in gastric (acidic)¹² and intestinal conditions,¹³ were used to explore the application of the ARA media to raltegravir.

Materials

Raltegravir (Isentress®) 400 mg film-coated tablets (MSD Sharp & Dohme GmbH, Haar, Germany) were ordered through Phoenix Pharma SE (Mannheim, Germany) and potassium raltegravir powder was purchased from Acros Organics B.V.B.A. (Geel, Belgium). FaSSIF/FaSSIF/FaSSGF and FaSSIF-V2 powders were kindly donated by biorelevant.com (London, UK). Acetonitrile, sodium chloride, hydrochloric acid 1 M and sodium hydroxide 1 M were purchased from VWR chemicals ProLabo (Leuven, Belgium). Trifluoroacetic acid, sodium hydroxide pellets, sodium dihydrogen phosphate dihydrate and sodium acetate were purchased from Merck KGaA (Darmstadt, Germany), while maleic acid and pepsin from porcine gastric mucosa were purchased from Sigma-Aldrich (Steinheim, Germany).

Methods

Solubility Measurements

Raltegravir solubility was determined in Fasted State Simulated Gastric Fluid (FaSSGF),¹⁴ ARA pH 4 acetate and pH 6 maleate media,² as well as in Fasted State Simulated Intestinal Fluid (FaSSIF) V1,¹⁴ using a UniPrep™-based method.¹⁵ In this method, 3 ml of the respective medium and an excess of raltegravir salt were added to UniPrep™ vials (GE Healthcare, Whatman Inc., New Jersey, USA) and shaken for 24 hours at 37°C using a platform shaker (Heidolph Polymax 1040, Heidolph Instruments GmbH & CO., Schwabach, Germany) in a Heraeus Function Line heating oven (Thermo Fisher Scientific Inc., Waltham, USA). After 24 hours, the vial was removed from the oven, the incorporated 0.45 µm PTFE filter was plunged through the vial contents and the supernatant was sampled and diluted immediately with mobile phase. Thereafter, the pH of the supernatant remaining in the vial was measured using a pHenomena™ (model pH 1000 H) pH meter. The diluted samples were quantified for raltegravir using HPLC (see section *Quantitative analysis of solubility and dissolution samples*).

The pH measurement at the end of the experiment proved to be essential to interpretation of the results, as in most cases the salt excess overcame the buffer capacity in the small media volume and shifted the pH to a higher value. In the solubility experiments section of the new FDA Guidance draft “Evaluation of Gastric pH Dependent Drug Interactions With Acid-Reducing Agents”, it is suggested that the final pH be adjusted back to the original value before taking the sample.¹ Although this approach in the Guidance is directed toward the standard shake-flask method, it was also possible to make a pH adjustment in the UniPrep™ method as follows: an excess of raltegravir salt was added to UniPrep™ vials and shaken for 24 hours at 37°C. This time, after taking the vial out of the oven, the pH of the suspension within the vial was measured, a small amount of 1 M HCl was added to lower the pH to the target value, the vial was shaken to equilibrate the pH and the pH adjusted again if necessary. Upon achieving the target pH value, the medium was filtered using the incorporated filter. Thereafter, the samples were diluted and analyzed as described above. The final pH of the solution was also measured and this was the value assigned to the sample.

Due to the variations in pH caused by the API excess and/or pH adjustment, the results were plotted individually, even though the solubility measurements in all media were conducted in triplicate (n = 3).

One-Stage Dissolution Experiments

One-stage dissolution experiments were performed in USP 2 (Paddle) apparatus Erweka DT 80 (Erweka GmbH, Langen, Germany). The setup and dissolution parameters were the same as those reported by Komasa et al.¹³: 1-liter peak vessels (Pharma Test Apparatebau, Hainburg, Germany), a paddle rotation speed of 75 rpm and a temperature of 37°C. The volume of the gastric media (FaSSGF, ARA pH 4 and pH 6 media) was set to 250 ml, whereas for the intestinal media (FaSSIF V1 and FaSSIF V2 pH 6.5) the volume was set to 500 ml.

Dissolution of tablets in one-stage experiments was performed in FaSSGF pH 1.6, ARA pH 4 acetate medium, ARA pH 6 maleate medium, as well as in FaSSIF V1 and FaSSIF V2¹⁴ (pH 6.5) media. For the experiments with Isentress® tablets (400 mg raltegravir), sampling time points were 10, 20, 30, 60, 90, 120, 150, 180, 210, 240, 300, 360 and 420 min.

For the one-stage dissolution experiments with the pure API, 434.29 mg of pure potassium raltegravir was weighed (equivalent to the amount of salt in one Isentress® tablet), added to the medium and the sampling scheduled adjusted to the medium: to capture supersaturation and precipitation in FaSSGF accurately, very frequent sampling (every 2.5 min) was conducted from 0 to 20 min, with further sampling timepoints at 25, 30, 40, 50, 60, 90, 120, 150 and 180 min, whereas for ARA pH 4 acetate medium, frequent sampling (every 5 min) was conducted from 0 to 50 min, with further timepoints at 60, 90, 120, 150 and 180 min. For the ARA pH 6 maleate medium, samples were taken at 5, 10, 15, 20, 30, 45, 60, 90 and 120 min.

All samples were filtered using 0.45 µm PTFE filters (ReZist™ filter unit, GE Healthcare, Whatman Inc., New Jersey, USA), diluted immediately with mobile phase and quantified for raltegravir using HPLC UV-Vis analysis.

During one-stage experiments with the tablet formulation, the pH of the medium was measured at 1 h for gastric, and at 3 h for intestinal media, as well as at the end of the experiment in all cases. For experiments with the pure API, the pH was measured 5 minutes after starting the experiment and at the end of the experiment. The pH measurement was made by withdrawing a 3 ml sample from the vessel, filtering the sample into a vial and measuring the pH using the pHenomena™ (model pH 1000 H) pH meter.

Table 1
Sampling timepoints for two-stage dissolution experiments.

| pH shift time | Sampling timepoints (min) | | | | | | | | | | | | | | | |
|---------------|---------------------------|----|----|----|----|-----|-----|-----|-----|-----|-----|-----|-----|-----|-----|-----|
| 30 min | 10 | 20 | 30 | 35 | 40 | 50 | 60 | 90 | 120 | 150 | 180 | 210 | 240 | 300 | 360 | 420 |
| 60 min | 10 | 20 | 30 | 60 | 65 | 70 | 80 | 90 | 120 | 150 | 180 | 210 | 240 | 300 | 360 | 420 |
| 120 min | 10 | 20 | 30 | 60 | 90 | 120 | 125 | 130 | 140 | 150 | 180 | 210 | 240 | 300 | 360 | 420 |

The boldface line shows the time at which the FaSSIF V1 double concentrate was added.

All one-stage dissolution experiments were run in triplicate ($n = 3$).

Two-Stage Dissolution Experiments

Komasaka et al. focused on simulating the pH shift from a low gastric pH medium to an intestinal medium,¹³ and this research developed an analogous approach for the ARA pH 4 and pH 6 gastric media.

To acquire comparable dissolution profiles, the dissolution set-up and parameters for the two-stage experiments were the same as in the one-stage experiments; 1-liter apex (peak) vessels (Pharma Test Apparatebau, Hainburg, Germany) were used, the paddle rotation speed was set to 75 rpm and the temperature to 37°C.

The two-stage experiments with ARA pH 4 and pH 6 media reflected the methods used in the OrBiTo study,¹⁶ but using 250 ml of ARA pH 4 or ARA pH 6 media to represent the gastric conditions. The pH of FaSSIF V1 double concentrate (250 ml) was adjusted to pH 7.4 for experiments with ARA pH 4 acetate medium and to pH 6.43 for experiments with ARA pH 6 maleate medium, to achieve a final pH of 6.5.

Similar to Komasaka et al.,¹³ dissolution data for the Isentress® tablets corresponding to three different gastric residence times were generated for simulation input. The sets differed in the time of the pH shift: with the transition made after the 30 min, 60 min, or 120 min sample was taken from the gastric medium. After the bolus addition of the FaSSIF double concentrate, the composition and pH of the intestinal medium (500 ml) was comparable to that of the FaSSIF V1 medium. Sampling protocols are shown in Table 1.

As with the one-stage experiments, the samples were filtered, immediately diluted with mobile phase and analyzed for raltegravir using HPLC UV-Vis analysis. The pH of the sample was also measured. All experiments were run in triplicate ($n = 3$).

Quantitative Analysis of Solubility and Dissolution Samples

All samples were analyzed using an HPLC Hitachi LaChrom system, consisting of an L-2200 autosampler, L-2130 pump, L-2300 oven and L-2400 UV-Vis detector (VWR Hitachi, Darmstadt, Germany), and a C18, 10 cm, 4.6 mm Ultracarb™ 5 μm ODS (30) column (Phenomenex LTD, Aschaffenburg, Germany). The samples were eluted using the gradient method described in Table 2. The flow rate was set to 1 ml/min, the detection wavelength to 300 nm and the column temperature to 40°C. The limit of quantification (LOQ) of the method was 2.8 μg/ml and the explored linearity range was 2.8 to 282.3 μg/ml.

Mathematical Parametrization of Dissolution Results

Analogous to the approach¹³ described in Komasaka et al., it was necessary to parameterize the two-stage dissolution results in media simulating ARA co-administration at specific pH shift times in order

Table 2
Gradient method used in quantitative analysis of raltegravir samples.

| Time (min) | 0 | 4 | 5 | 10 | 11 | 12 |
|-----------------------------|----|----|----|----|----|----|
| Acetonitrile (%) | 25 | 25 | 60 | 60 | 25 | 25 |
| 0.05 % trifluoroacetic acid | 75 | 75 | 40 | 40 | 75 | 75 |

to acquire data suitable for input into the *in silico* model (see section *In silico modelling*).

This was achieved following several steps (Fig. 1, upper left side): In the first step, the one-stage dissolution profiles were parametrized according to Weibull and exponential equations in Excel. In the second step, the formulae describing one-stage dissolution in gastric and intestinal media were combined to generate profiles representing behavior in the two-stage experiments. To adequately describe the concentration profiles observed in the two-stage tests with a long (two-hour) exposure to gastric conditions, in which either precipitation or extended dissolution in the gastric compartment occurred, a third step had to be added.

The formulae developed to describe the observed two-stage dissolution results were then applied in Excel to generate theoretical dissolution profiles for two-stage dissolution experiments with pH-shift times between 0 and 2 hours, at 0.1 h intervals. These theoretical dissolution profiles were used as the input into the *in silico* model.

In Silico Modelling

Since Isentress® (film-coated) tablets do not readily disintegrate,^{12,13} the approach reported by Komasaka et al. for this tablet formulation¹³ was applied. In this approach, Komasaka et al. introduced the input of theoretical two-stage dissolution profiles corresponding to various pH shift times into a model describing the tablet as a monolithic system which is emptied from the gastric compartment at the time corresponding to the pH shift time in the dissolution profile. The individual plasma profile simulations were then used to generate a mean plasma profile for a population group, taking the statistical distribution of gastric emptying times into account.

To predict the effect of ARA co-administration an analogous approach was taken, as depicted in Fig. 1.

First, the workspace reported by Komasaka et al. was reconstructed (Table 3) in Simcyp Simulator V17 (which was also used in the current simulation studies) and several reported¹³ simulations were repeated to verify the ability of the model to predict *in vivo* data with no ARA co-administration. The workspace generated profiles identical to those reported in the original publication (Supplementary material, Figure A) and predicted the *in vivo* data^{6,7} successfully; average fold error (AFE) = 0.80, absolute average fold error (AAFE) = 1.39 for the Rhee et al. 2014 data (study used as the *in vivo* comparison in the publication by Komasaka et al.) and AFE = 0.85, AAFE = 1.45 for the Iwamoto et al. 2009 data (Supplementary material, Figure B).

Second, the theoretical two-stage dissolution profiles for low gastric pH were replaced by the theoretical profiles generated from the formulae describing the results of two-stage dissolution testing in ARA pH 4 acetate or ARA pH 6 maleate medium to represent the gastric compartment. The simulations were generated for every pH shift/GET from 0 to 2 h, at 0.1 h intervals.

Third, the first 10 gastric emptying time distributions described in the publication by Komasaka et al. were used to generate 10 virtual populations with 12 subjects each. Mean plasma profiles representing data acquired from experiments with ARA pH 4 and pH 6 medium

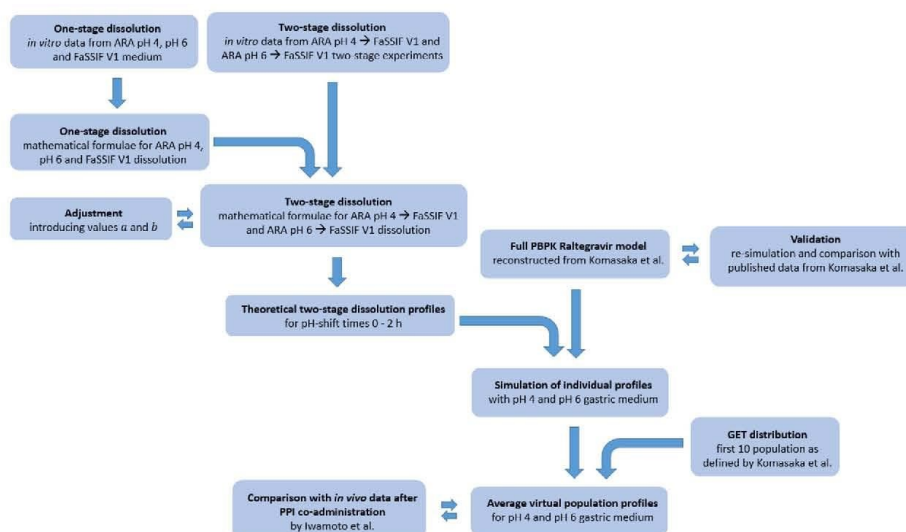


Figure 1. Schematic representation of the development of mathematical formulae and *in silico* model describing ARA co-administration with Isentress® tablets.

Table 3
Summary of the Simcyp V17 raltegravir workspace input parameters and their values.

| Category | Parameter | Value |
|--|--|---|
| Phys. Chem. Properties | M (g/mol) | 444.42 |
| | Log P _{ow} | 1.06 |
| | pKa (Monoprotic Acid) | 6.3 |
| Blood Binding | B/P | 0.62 |
| | f _u | 0.17 |
| Absorption | ADAM | |
| | P _{en, man} | Predicted by MechPeff model |
| | MechPeff model | Total Conc. (bound + unbound) |
| | Absorption Rate Scalars | |
| | Small Intestine Global Colon | 0.71 0.1 |
| Formulation | Solid Formulation (IR) | CR/MR (Dissolution Profile*) Discrete input |
| | Segregated Transit Times Model (Monolithic CR and EC Tablets) | Stomach - (Values 0.01 to 2*) Small Intestine - 3.4 Whole colon (male / female) - 12 |
| Distribution | Full PBPK Model | |
| | V _{ss} Kp Scalar | Predicted by Method 2 0.012 |
| Elimination | Enzyme Kinetics | |
| | UGT1A1 UGT1A9 | V _{max} : 890, K _m : 99 V _{max} : 530, K _m : 296 |
| | CL _r Typical renal (20-30 yr healthy) | 3.6 |
| | Population | |
| Segregated Transit Model MRT (Fluid and Dissolved Drug) | Stomach - 0.176 Small intestine - 3.4 Whole colon (male / female) - 12 | |
| | Trial design | |
| PopRep | Oral dose | 400 mg |

* Values selected according to the pH shift time of the respective theoretical dissolution profile.

for these populations were then calculated and compared with the *in vivo* data for a healthy population after co-administration of omeprazole 20 mg.⁷

Statistics and Data Presentation

Dissolution values are presented as the arithmetic mean with the standard deviation, whereas solubility values are presented individually. To assess the accuracy of the *in silico* predictions to fit the data observed *in vivo*, AFE and AAFE¹⁷ were calculated.

Results

Solubility

Measurement of potassium raltegravir solubility using the Uni-Prep™-based method indicated that the raltegravir salt shifts the pH of the medium to more basic values, thus enhancing the amount dissolved in this small media volume (3 ml). As the API excess shifted the pH of individual vials to a variable degree, individual solubility values are accompanied by the starting medium pH and the pH measured at the end of the experiment in Table 4.

With regard to raltegravir solubility, the pH of the medium plays a significantly greater role than the concentration of bile components in the solution. All solubility values (from gastric and intestinal media) were plotted in Fig. 2 to generate a pH/solubility profile for raltegravir. The individual values are in accordance with the values reported in buffered media by the manufacturer.¹⁸

One-Stage Dissolution

One-stage dissolution in standard biorelevant media

One-stage dissolution of raltegravir from Isentress™ tablets in standard gastric biorelevant medium (FaSSGF pH 1.6) was slow and incomplete, reaching only 13 % dissolved after two hours. After 3.5 h of dissolution in FaSSGF, raltegravir started to precipitate and this continued over the remaining 3 hours. The experimental dissolution

Table 4

Summary of the solubility values from experiments with potassium raltegravir in gastric and intestinal biorelevant media. Each individual experiment is reported in this table, e.g. solubility in FaSSGF was performed with $n=3$ and results are presented individually as FaSSGF (1), (2) and (3).

| Solubility experiments without pH adjustment | Starting pH | pH at the end of the experiment | Raltegravir concentration ($\mu\text{g/ml}$) |
|--|-------------|---------------------------------|--|
| FaSSGF (1) | 1.60 | 2.25 | 23.80 |
| FaSSGF (2) | 1.60 | 1.65 | 26.40 |
| FaSSGF (3) | 1.60 | 1.71 | 28.17 |
| ARA pH 4 acetate (1) | 4.00 | 8.17 | 128.4 |
| ARA pH 4 acetate (2) | 4.00 | 8.34 | 299.9 |
| ARA pH 4 acetate (3) | 4.00 | 8.26 | 232.3 |
| ARA pH 6 maleate (1) | 6.00 | 8.83 | 911.7 |
| ARA pH 6 maleate (2) | 6.00 | 9.10 | 2730 |
| ARA pH 6 maleate (3) | 6.00 | 8.86 | 928.6 |
| FaSSIF V1 (1) | 6.50 | 8.68 | 1264 |
| FaSSIF V1 (2) | 6.50 | 8.54 | 853.7 |
| FaSSIF V1 (3) | 6.50 | 8.65 | 1148 |

| Solubility experiments with pH adjustment | Starting pH | Adjusted pH at the end of the experiment | Concentration ($\mu\text{g/ml}$) |
|---|-------------|--|------------------------------------|
| FaSSGF (1) | 1.60 | 1.34 | 32.16 |
| FaSSGF (2) | 1.60 | 1.67 | 18.60 |
| FaSSGF (3) | 1.60 | 1.61 | 24.74 |
| ARA pH 4 acetate (1) | 4.00 | 3.79 | 21.51 |
| ARA pH 4 acetate (2) | 4.00 | 4.23 | 25.52 |
| ARA pH 4 acetate (3) | 4.00 | 4.15 | 21.91 |
| ARA pH 6 maleate (1) | 6.00 | 6.00 | 61.92 |
| ARA pH 6 maleate (2) | 6.00 | 6.07 | 61.64 |
| ARA pH 6 maleate (3) | 6.00 | 6.06 | 70.35 |
| FaSSIF V1 (1) | 6.50 | 6.49 | 71.76 |
| FaSSIF V1 (2) | 6.50 | 6.45 | 65.49 |
| FaSSIF V1 (3) | 6.50 | 6.42 | 105.2 |

profile in FaSSGF pH 1.6 up to 2 hours of dissolution (the same time-span investigated by Komasa et al.) and the dissolution profile in FaSSIF V2 were in accordance with the data reported by Komasa et al.¹³ Despite its high solubility at the intestinal pH, the dissolution of raltegravir in standard intestinal biorelevant media was slow as well (Fig. 3), suggesting an important role of the formulation in the

dissolution behavior of the drug product. Furthermore, a difference in dissolution between the two intestinal biorelevant media FaSSIF V1 and FaSSIF V2 was observed. In FaSSIF V2, 85 % dissolution was reached at 2 hours of dissolution, whereas for FaSSIF V1, 85 % dissolution was reached only after 4 hours. The pH during experiments with FaSSIF V2 shifted from a starting pH of 6.5 to a value of pH 6.82 at 3 h and pH 6.97 at the end of the experiment, whereas the pH in FaSSIF V1 shifted only slightly, from a starting value of pH 6.5 to pH 6.52 at the end of the experiment.

One-Stage Dissolution in ARA Media

Dissolution experiments in ARA media showed marked differences in the rate and extent of dissolution from Isentress[®] tablets between pH 4 and pH 6.

While dissolution in the ARA pH 6 maleate medium was complete, reaching 85 % dissolved after one hour, dissolution in the ARA pH 4 acetate medium was slower and limited, reaching 37 % dissolved at 90 minutes before precipitating over the following 2.5 hours to a value of approx. 7 % dissolved (Fig. 4). The pH of the ARA pH 6 maleate medium was shifted from the starting value of 6 to pH 7.2 at 1 h and then further to a value of pH 7.69 at the end of the experiment. These results suggest that, at the dose administered, the formulation is able to alter the pH in the stomach when the subject is also receiving high dose/potent ARA therapy. By contrast, the pH of the ARA pH 4 acetate medium, representing low dose/less potent ARA therapy, shifted only slightly from pH 4 at the start to pH 4.32 at the end of the experiment.

Dissolution of Pure Potassium Raltegravir

To investigate the dissolution of the raltegravir salt independent of the formulation effects, one-stage dissolution of 434.29 mg raltegravir potassium was conducted in gastric biorelevant media representing low gastric pH (FaSSGF, pH 1.6) and elevated pH (ARA pH 4 acetate and ARA pH 6 maleate media).

Dissolution of the raltegravir salt was significantly faster in the pure powder form than as a part of the tablet formulation (compare Figs. 3, 4 and 5).

In FaSSGF, potassium raltegravir pure drug powder dissolved rapidly to a much greater extent (over 30% dissolved) than during experiments with the tablet formulation, producing supersaturation

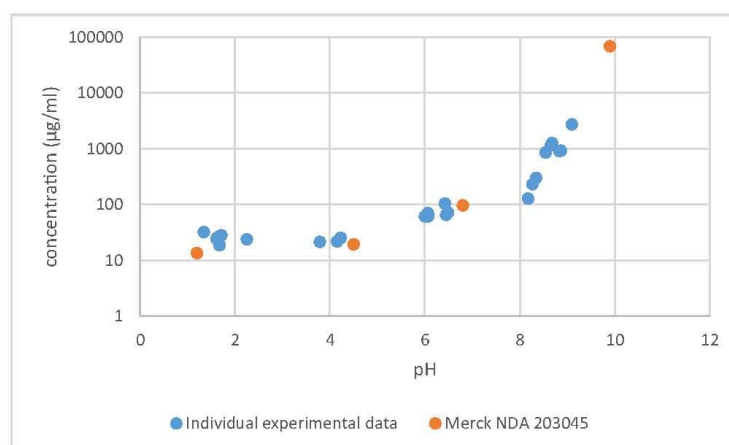


Figure 2. Raltegravir pH/solubility distribution comparing experimental data and data reported by the manufacturer.

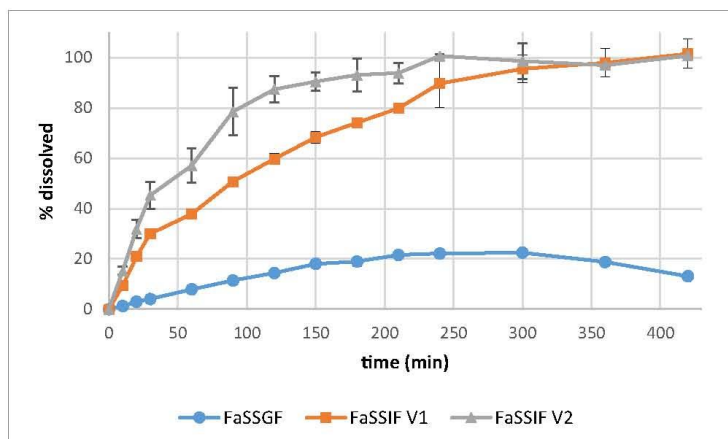


Figure 3. Dissolution of raltegravir from 400 mg Isentress® tablets in standard biorelevant media.

at a low pH with subsequent rapid precipitation, presumably as the free acid. The pure drug also dissolved rapidly and to a greater extent than the tablet in acetate pH 4 medium (30 - 60 % dissolved), again triggering precipitation.

The final pH after the dissolution of the pure drug in FaSSGF and ARA pH 4 acetate media (1.6 and 4.34) was comparable to the final pH after the dissolution of the tablet in the same media (1.6 and 4.32). The pH in ARA pH 6 maleate medium was shifted to pH 7.5 within the first 5 minutes of the experiment, which facilitated fast and complete dissolution.

The final % dissolved in the experiments with pure drug powder achieved values higher than the theoretical % dissolved values calculated from the solubility values (see Fig. 2) for the corresponding pH, which indicates that the salt form is capable of producing a pronounced supersaturation in biorelevant media. The final and maximum raltegravir concentration reached in the experiment with the pH 6 medium was 1600 µg/ml (compared to the 100 - 200 µg/ml

solubility value estimated from Fig. 2 for a pH 7.5 medium), whereas the maximum concentration reached in the experiment with the pH 4 medium averaged 707 µg/ml (compared to a solubility value of approximately 25 µg/ml). Although the supersaturation is followed by precipitation in the pH 4 ARA media, it is clearly sustained in the case of the pH 6 medium over the two-hour dissolution experiment.

Two-Stage Dissolution

Two-Stage Dissolution in ARA pH 4 Acetate Medium

Dissolution of raltegravir from Isentress® tablets during the first stage (dissolution in the gastric medium) of the two-stage dissolution experiments was comparable to its dissolution in the one-stage experiments in the same ARA pH 4 medium (Fig. 6b). After the pH shift to the intestinal medium, no dissolution lag was observed, in contrast to the lag described by Komasa et al. in two-stage experiments with FaSSGF¹³ as the gastric medium (Fig. 6a). In the ARA pH 4

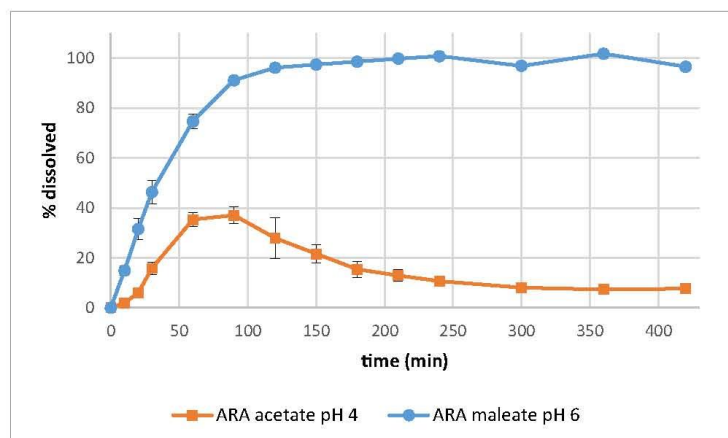


Figure 4. Dissolution of raltegravir from 400 mg Isentress® tablets in ARA pH 4 acetate and pH 6 maleate media.

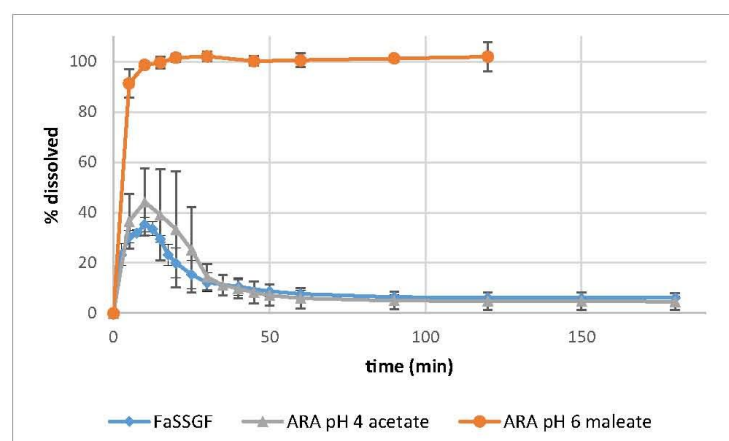


Figure 5. Dissolution of 434.29 mg of pure raltegravir potassium (equivalent to 400 mg raltegravir) in gastric biorelevant media.

media experiments with a pH shift at 0.5 h or 1 h, the dissolution of raltegravir in the intestinal medium was similar to the behavior of the tablets in 500 ml of FaSSIF V1 medium in one-stage experiments. During experiments with the pH shift at 2 h, however, dissolution in the second stage was highly variable and reached a lower % dissolved than in two-stage experiments with a shorter “gastric exposure” time. Interestingly, the precipitation observed in the “gastric” phase of the two-stage test at long exposure times (around 10 %) was on the same order of magnitude as the amount that remained undissolved at the end of the experiment (around 20 %), suggesting that the precipitate was not able to dissolve well in the intestinal medium.

Two-Stage Dissolution in ARA pH 6 Maleate Medium

The dissolution profiles in two-stage experiments using ARA pH 6 medium as the gastric medium are shown in Fig. 6c. As for the two-stage experiments with the ARA pH 4 acetate medium, no dissolution lag in the intestinal medium was observed when ARA pH 6 maleate medium was used as the gastric medium.

In experiments with the pH shift at 0.5 hour, the dissolution profile in the second stage followed the same dissolution profiles as in one-stage dissolution experiments in FaSSIF V1. When the pH shift was performed at 1 or 2 h, the dissolution in ARA pH 6 medium (first stage) was faster than in FaSSIF V1 in a one-stage experiment, leading to a higher % dissolved at all sampling times up to 300 minutes.

Mathematical Formulae to Describe Two-Stage Dissolution Results

In order to simulate a virtual population, two-stage dissolution data for every pH shift timepoint within the first 2 hours of dissolution with 0.1 h intervals had to be generated. This was done in an analogous manner to the approach used by Komasa et al.¹³

As shown in Fig. 1, the first step to generating virtual dissolution profiles was to describe the one-stage dissolution behavior using mathematical formulae.

For the dissolution of the tablets in FaSSIF V1, a Weibull function was fitted to the *in vitro* data, resulting in the following formula:

$$F_{diss \text{ FaSSIF V1}} = 100 * \left(1 - e^{-\left(\frac{t}{x_{50}}\right)^{0.95}} \right)$$

where

$$F_{diss} = \% \text{ dissolved}$$

$$t = \text{time in hours}$$

As the dissolution behavior during one-stage ARA pH 4 acetate dissolution experiments could not be described using just one Weibull function, the profile was divided into two functions.

The first function defined the profile until 1.5 h of dissolution. Here a Weibull function was fitted to the corresponding data to obtain the following formula:

$$F_{diss I} = 36.99 * \left(1 - e^{-\left(\frac{t}{0.75}\right)^{2.52}} \right)$$

The second function defined the profile during precipitation and was represented by an exponential function:

$$F_{diss II} = 57.32 * t^{-1.141}$$

In Excel, one-stage pH 4 acetate dissolution profile was generated using an *if* function, where the first segment within the parentheses defines a condition of the logical test for the variable *t*, the second segment defines the function output if the condition is met (if true), and the third segment defines the output if the condition is not met (if false):

$$F_{diss \text{ pH 4}} = \text{if} (t < 1.5, F_{diss I}, F_{diss II})$$

The ARA pH 6 maleate one-stage dissolution was described by the following Weibull function:

$$F_{diss \text{ pH 6}} = 100 * \left(1 - e^{-\left(\frac{t}{0.75}\right)^{1.20}} \right)$$

The next steps were to incorporate the formulae for one-stage dissolution in the gastric and intestinal compartment, as well as the identified patterns of behavior specific to the two-stage dissolution experiments, into the formulae reflecting two-stage dissolution. The fit of the generated theoretical dissolution profiles to the *in vitro* dissolution data can be seen in Figure C (Supplementary material).

For the two-stage experiments with pH 4 acetate medium as a gastric medium, $F_{diss \text{ pH 4}}$ was used until the pH shift timepoint. After the pH shift timepoint, $F_{diss \text{ FaSSIF V1}}$ was used. If the time point of the pH shift was more than 1.5 h (start of visible precipitation), $F_{diss \text{ FaSSIF V1}}$ was scaled down by the value *a*. Value *a* represented

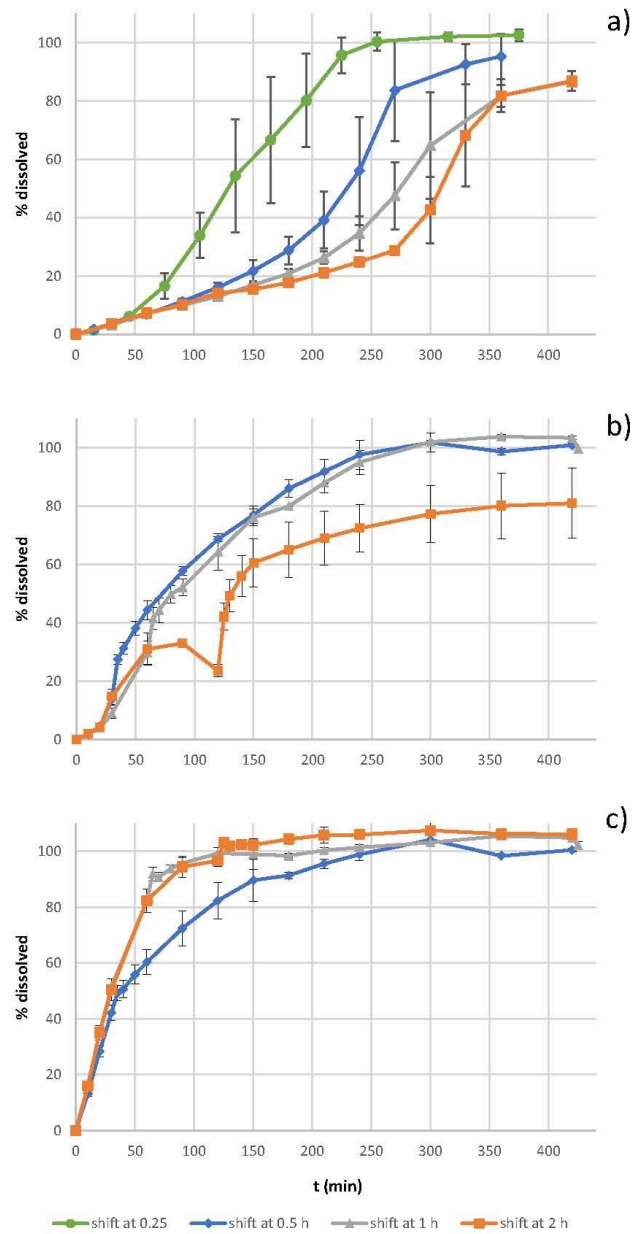


Figure 6. Dissolution of raltegravir from 400 mg Isentress® tablets in two-stage experiments with FaSSGF pH 1.6 as the gastric medium (literature data by Komasa et al.) (a), ARA pH 4 acetate medium as the gastric medium (b) and ARA pH 6 maleate medium as the gastric medium (c), with the shift to the intestinal medium at 0.25, 0.5 h, 1 h, or 2 h.

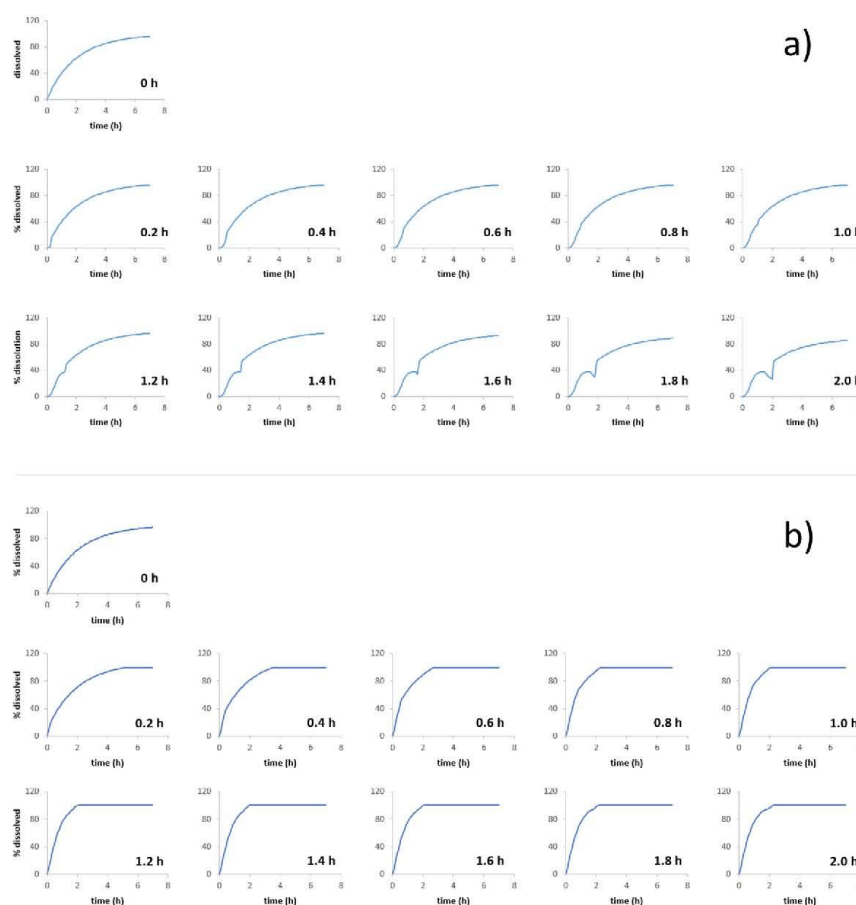


Figure 7. Theoretical dissolution profiles for two-stage dissolution with a) ARA pH 4 acetate medium as the gastric medium or b) ARA pH 6 maleate medium as the gastric medium, and pH-shift times between 0 and 2 hours.

the % of dose precipitated in the first stage and was used to limit the final % dissolved, as observed in the *in vitro* data.

$$F_{diss\ pH\ 4\ two\ stage} = \text{if } (t > t_{pH\ shift}, (F_{diss\ FaSSIF} - a), F_{diss\ pH\ 4})$$

where a is defined as 0 if $t_{pH\ shift} \leq 1.5$ h and as $F_{diss\ pH\ 4}$ at $t = 1.5$ h minus $F_{diss\ pH\ 4}$ at $t_{pH\ shift}$ if $t_{pH\ shift} > 1.5$ h.

For the two-stage experiments with pH 6 maleate medium as a gastric medium, $F_{diss\ pH\ 6}$ was used until the pH shift timepoint. To account for a greater % dissolved resulting from the first stage, after the pH shift timepoint, $F_{diss\ FaSSIF\ V1}$ was adjusted by value b . Value b represents the difference between % dissolved in the formula for dissolution in one-stage ARA pH 6 maleate and % dissolved in the one-stage FaSSIF V1 profile at the $t_{pH\ shift}$. Furthermore, to avoid values above 100 %, 100 was set as the highest value.

$$F_{diss\ pH\ 6\ two\ stage} = \text{if } (t > t_{pH\ shift}, (F_{diss\ FaSSIF} + b), F_{diss\ pH\ 6})$$

where

b is defined as $F_{diss\ pH\ 6}$ at $t_{pH\ shift}$ minus $F_{diss\ FaSSIF\ V1}$ at $t_{pH\ shift}$ and

$$F_{diss\ pH\ 6\ two\ stage\ maximum} = 100$$

In the next step, these formulae were used to simulate two-stage dissolution data for pH shift timepoints ranging from 0 to two hours. For each 0.1 hour pH shift timepoint within the first 2 hours of dissolution a separate two-stage dissolution profile was calculated, once when ARA pH 4 acetate was used as the gastric medium, and again for when ARA pH 6 maleate was used as the gastric medium.

A selection of these profiles can be seen in Fig. 7.

In Silico Predictions

As a first step in predicting the data of the Iwamoto et al. study reflecting healthy volunteer administration of Isentress® during PPI co-administration,⁷ selected simulations from the study by Komasa et al. were repeated to confirm the ability of the approach used in this study to reproduce the results.

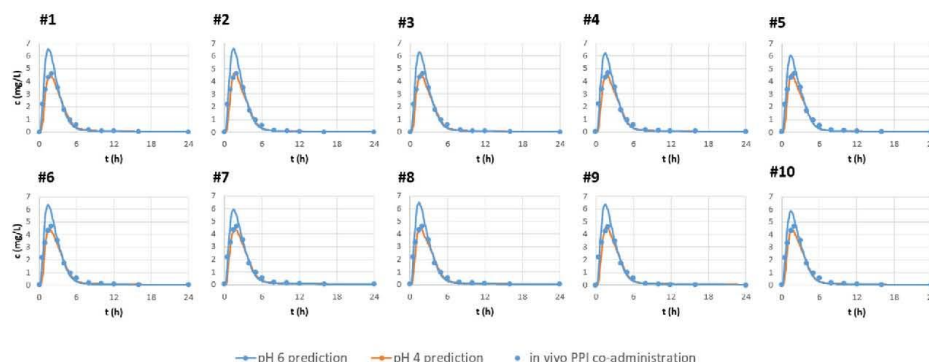


Figure 8. Average profiles of 10 virtual population simulations for the administration of 400 mg raltegravir using simulated dissolution profiles with ARA pH 6 maleate and pH 4 acetate media as gastric media, in comparison to the *in vivo* data reflecting the effect of a PPI by Iwamoto et al.

Using the simulation set-up described in Table 3, the PopRep simulation of raltegravir tablet administration using the first virtual population set for the healthy state (using two-stage dissolution data with FaSSGF and FaSSIF V2), as described by Komasa et al., was identical to the results reported in their publication¹³ (Supplementary material, Figure A).

Next, the virtual dissolution profiles for tablet administration at low gastric pH were exchanged for the virtual two-stage dissolution profiles at gastric pH 4 and pH 6 for every pH shift / gastric emptying time ranging from 0 to 2 h at 0.1 h intervals. In V17, the input of a monolithic formulation dissolution profile does not allow for values lower than the one of the previous time points, which would be necessary to describe the dissolution profiles in ARA pH 4 medium where precipitation occurred. To partially overcome this, when the highest % dissolved was reached in the first stage, this value was held constant until the pH shift/gastric emptying occurred. Furthermore, the % dissolved in the second stage was adjusted by the value α , to maintain the overall lower % dissolved in the simulation.

Finally, the first 10 reported sets of gastric emptying time distributions in Komasa et al. were used to generate virtual population average profiles with gastric pH 4 and pH 6. The sets of predictions were compared with the *in vivo* data after co-administration of 20 mg omeprazole⁷ and are shown in Fig. 8.

The simulations acquired from dissolution experiments with ARA media bracket the *in vivo* data of the tablet administration during PPI co-administration, with the gastric pH 4 prediction closely resembling the *in vivo* data.

Discussion

In vitro Experiments

Solubility

Solubility experiments indicate that media pH plays an important role in the solubility of potassium raltegravir, as expected for the salt of a poorly soluble, weakly acidic drug. Studying the ability of the salt form to alter the medium's pH in the solubility experiments proved beneficial to understanding differences in the impact of the salt form on the dissolution of raltegravir in the various media used. Indeed, the pH appears to be the main factor in the solubility of potassium raltegravir, since addition of bile components had little impact on solubility. The lack of bile component effects can be traced back to the low logP of raltegravir.

One-Stage Dissolution Testing

One-stage dissolution of raltegravir from Isentress[®] tablets in standard biorelevant media were conducted under the conditions described by Komasa et al. The results in FaSSGF as well as those in FaSSIF V2 were identical to the results that had been published previously.¹³

In addition to repeating these experiments, dissolution in FaSSIF V1 was explored and a difference in the dissolution between the two intestinal biorelevant media was observed. Faster dissolution in FaSSIF V2 cannot be explained by a different bile salt composition of the dissolution media, as the logP, as well as the solubility results, suggest a minor role of surface active compounds on the solubility of raltegravir. pH measurements of the media provided insight into the reason for the observed difference in dissolution behavior of the two FaSSIF versions. The raltegravir salt shifted the pH of the V2 medium to higher values during the dissolution test. The lower buffer capacity of the FaSSIF V2 was not sufficient to counteract the pH shift caused by the salt at its standard dose and the increase in pH to 6.97 resulted in faster dissolution. By contrast, FaSSIF V1 has a somewhat higher buffer capacity and was able to hold the pH constant during the dissolution experiment.

Dissolution of the tablets in the ARA pH 6 maleate medium was faster than in FaSSIF V1. Similar to the dissolution in FaSSIF V2, this was likely a result of this medium's low buffer capacity (1 mEq/l/pH) and the subsequent pH shift to the final pH 7.69.

The relatively higher buffer capacity of the ARA pH 4 acetate medium appeared to play an important role in precipitation of raltegravir during the dissolution experiment. In this case the buffer system withstands the tendency of the potassium salt of raltegravir to change the pH.

Comparing the final pH values in one-stage media after the dissolution of a tablet or the pure drug suggests that the raltegravir salt is the main - and most likely only - cause for the increase in pH during the dissolution experiments.

Interestingly, the rapid dissolution of pure potassium raltegravir as well as the dissolution of raltegravir from Isentress[®] tablets in ARA pH 4 acetate medium results in a temporary supersaturation of raltegravir in this medium, as was also observed in FaSSGF. We also compared the final concentration of raltegravir in ARA pH 6 maleate medium to its solubility at the final pH in the dissolution medium. The comparison shows that 100% dissolution corresponds to a concentration of 1.6 mg/ml, far higher than the solubility at the final pH of 7.5, which is around 100–200 $\mu\text{g/ml}$. The comparison suggests that the potassium salt of raltegravir is not only effective in creating a

supersaturated solution in media with a low buffer capacity, but also in sustaining the supersaturation over several hours. To our knowledge, this is the first report of a salt form of a poorly soluble weak acid creating a sustained supersaturation in a biorelevant medium.

While the dissolution of the pure raltegravir salt in ARA media shows similarities to the dissolution of the tablets, the dissolution profiles in FaSSGF are not comparable. Raltegravir slowly dissolves from the Isentress® tablet formulation and starts to precipitate slowly only after several hours of dissolution, whereas raltegravir precipitates quickly from the pure API due to the strong supersaturation in low pH media. According to the manufacturer, the Isentress® film-coated tablet, which is erodible rather than disintegrating, was developed to prevent high peak plasma concentrations¹⁹ which would result from an immediate release of the drug.

Two-Stage Dissolution Testing – Choice of Intestinal Medium

As discussed in a previous publication,⁴ changes in the pH due to an ionizable drug or excipient may also occur *in vivo*. Due to its lower buffer capacity, one-stage dissolution in FaSSIF V2 is theoretically preferable to detect such effects. Despite this advantage, FaSSIF V1 was chosen as the experimental intestinal medium for the two-stage testing due to its better compatibility with the ARA media: whereas the value of the FaSSIF V1 double concentrate pH does not need to deviate far from the original intestinal biorelevant medium (double concentrate pH is 7.4, final pH is 6.5 in experiments with ARA pH 4 acetate medium), the value of the FaSSIF V2 double concentrate pH (for experiments with ARA pH 4 acetate gastric medium) has to be elevated to a much higher⁴ pH, pH 12.13, in order to generate the target final pH of 6.5 after mixing with the ARA medium. Although the addition of such a high pH double concentrate does result in a medium with the same final composition as FaSSIF V2, the bolus addition of the double concentrate could result in temporary loci of unphysiological pH values.

In Silico Modelling

Newer versions of Simcyp Simulator (starting with V19) include a default workspace with pre-assigned parameters for raltegravir. This workspace provides a reasonable fit of the *in vivo* data for the administration of 400 mg raltegravir without ARA co-administration⁷ without a need to input any data on the formulation. This may be because several parameters under the absorption, distribution and elimination categories were “optimized” and indeed are marked as such. If any data on (slow) dissolution behavior of the tablet were to be added to this workspace, the plasma concentration predictions would substantially underestimate the *in vivo* data. As the dissolution behavior of Isentress® tablets changes depending on both gastric emptying time and the gastric pH, the V19 default workspace was not an optimal choice for *in silico* modelling to study effects of formulation on raltegravir pharmacokinetics. By contrast, the workspace in V17 developed by Komasa et al. incorporated the dissolution data from *in vitro* experiments,¹³ rendering this workspace more appropriate for simulation of the ARA effect.

The potential impact of ARA co-administration on the average gastric emptying time (GET) was discussed in a previous publication,² in which a literature review revealed no definite trend for a change in GET after co-administration of PPIs or H2RAs, with at most a slight trend towards slower gastric emptying. Thus, the GET distribution of the “healthy” virtual populations was not changed from one used by Komasa et al.

Plasma concentration predictions generated from dissolution experiments with ARA media bracket *in vivo* data for PPI co-administration within a narrow range of values. Furthermore, the plasma concentration prediction based on a gastric pH of pH 4 closely resembles the *in vivo* data.

It should be noted that in the publication of the pharmacokinetic data, Iwamoto et al. did not report either standard deviations in the plasma concentrations, or the gastric pH of the volunteers under PPI-therapy. However, Iwamoto et al. did report the dose of omeprazole (20 mg) administered, which is lower than the dose of 40 mg usually prescribed. Thus, the dose used corresponds to a lower dose/less potent PPI therapy, in accord with the simulations using ARA pH 4 acetate medium, which was designed to reflect pH-dependent DDIs in precisely this scenario.

With regard to the literature on increases in plasma levels of other weak acids due to co-administration with ARAs, there have been only a few reports to date, two examples being diclofenac sodium and evacetrapih.^{20,21}

Other Literature Data on ARA-Raltegravir Interactions

An additional set of raltegravir *in vivo* plasma concentrations without and during ARA co-administration is available in a publication by Rhame et al.⁹ However, these authors reported higher average plasma concentrations after raltegravir tablet administration alone, compared to data by Iwamoto et al.⁷ This difference can be explained by the fact that the two studies were conducted using quite different populations – while Iwamoto et al. conducted their study in healthy volunteers, Rhame et al. reported plasma profile values in HIV-positive patients. A higher average gastric pH is not uncommon in HIV patients,^{22,23} which would improve raltegravir dissolution in the gastric compartment and its consequent absorption even in the absence of ARAs, thus at least partly explaining the difference between the two data sets.

Regarding co-administration of ARAs, Rhame et al. reported lower raltegravir plasma values, on average, in HIV-positive patients co-administering a PPI or an H2RA than the data that Iwamoto et al. reported for PPI co-administration in healthy volunteers. Moreover, the *in silico* predictions (ARA pH 4 and pH 6) reported in Fig. 8 would overpredict the ARA effect reported by Rhame et al. This suggests that there may be differences in the gastrointestinal physiology of the two populations which should be taken into consideration when estimating the ARA effect in HIV-positive patients. Besides the gastric pH, the most impactful factor for simulations reported in this study was the pH-shift time in *in vitro* experiments, corresponding to the GET values used in the simulations. Individual simulations using *in vitro* dissolution data with late pH-shift times in ARA pH 4 acetate media show lower plasma profiles than the individual simulations using data with early pH-shift times. The simulation using a pH shift time of 2 hours comes closest to the *in vivo* data from Rhame et al. Although there are some indications in the literature that gastric emptying in this patient population is slower,^{24,25} no specific values for GET in this population have been reported to date. To appropriately define the HIV population, a GET distribution tailored to this specific population would be necessary.

Conclusions

The ability to assess the effect of ARA co-administration on therapy with different drugs offers multiple advantages during drug development and planning of clinical studies. Thus, early assessment of such DDIs, *in vitro*, is viewed as best practice by pharmaceutical companies and encouraged by regulatory authorities. In this research, biorelevant media and dissolution experiments reflecting ARA co-administration were investigated using a model poorly soluble weakly acidic drug, potassium raltegravir, in a formulation that disintegrates slowly in biorelevant media. By combining the drug dissolution from these *in vitro* experiments with a PBPK model workspace under consideration of formulation effects, it was possible to bracket the PPI effect reported *in vivo*. Moreover, a simulation reflecting a lesser PPI effect closely resembled the *in vivo* data from a study in

which a low dose of omeprazole was administered. This research showed the suitability of the biorelevant ARA media for evaluation of the ARA pH effect for a poorly soluble, weakly acidic drug, thus complementing previous research on the implementation of ARA media in dissolution testing of poorly soluble, weakly basic drugs.

Overall, it was shown that the ARA media and associated *in vitro* experiments are an essential part of the *in silico* model input when simulating the pH effect during ARA therapy. This work also displays the importance of taking formulation effects, as well as key population parameters, into account when modelling drug behavior *in silico*.

Acknowledgment

Certara UK (Simcyp Division) is gratefully acknowledged for granting free access to the Simcyp Simulator through an academic license (subject to conditions).

Supplementary Materials

Supplementary material associated with this article can be found in the online version at doi:10.1016/j.xphs.2021.09.037.

References

- Food and Drug Administration. Evaluation of Gastric pH Dependent Drug Interactions With Acid-Reducing Agents: Study Design, Data Analysis, and Clinical Implications: Guidance for Industry (Draft Guidance). Available at: <https://www.fda.gov/media/144026/download>. Accessed January 6, 2021.
- Segregur D, Flanagan T, Mann J, Moir A, Karlsson EM, Hoch M, et al. Impact of acid-reducing agents on gastrointestinal physiology and design of biorelevant dissolution tests to reflect these changes. *J Pharm Sci*. 2019;108(11):3461–3477. <https://doi.org/10.1016/j.xphs.2019.06.021>.
- Segregur D, Mann J, Moir A, Karlsson EM, Dressman J. Prediction of plasma profiles of a weakly basic drug after administration of omeprazole using PBPK modeling. *Eu J Pharm Sci*. 2020;158. <https://doi.org/10.1016/j.ejps.2020.105656>.
- Segregur D, Barker R, Mann J, Moir A, Karlsson EM, Tuner DB, et al. Evaluating the impact of acid-reducing agents on drug absorption using biorelevant *in vitro* tools and PBPK modeling - case example dipyridamole. *Eu J Pharm Sci*. 2021;160:105750. <https://doi.org/10.1016/j.ejps.2021.105750>.
- Iwamoto M, Wenning LA, Petry AS, Laethem M, Smet MD, Kost JT, et al. Safety, tolerability, and pharmacokinetics of raltegravir after single and multiple doses in healthy subjects. *Clin Pharmacol Ther*. 2008;83(2):293–299. <https://doi.org/10.1038/sj.cpt.6100281>.
- Rhee EG, Rizk ML, Brainard DM, Gendrano 3rd IN, Jin B, Wenning LA, et al. A pharmacokinetic comparison of adult and paediatric formulations of raltegravir in healthy adults. *Antivir Ther*. 2014;19(6):619–624. <https://doi.org/10.3851/IMP2765>.
- Iwamoto M, Wenning LA, Nguyen B-Y, Teppler H, Moreau AR, Rhodes RR, et al. Hedy Teppler, Allison R Moreau, Rand R Rhodes. Effects of omeprazole on plasma levels of raltegravir. *Clin Infect Dis*. 2009;48(4):489–492. <https://doi.org/10.1086/596503>.
- Rhame F, Matson M, Wood D, Comisar W, Petry A, Liu C, et al. Abstracts of the 12th European AIDS Conference/EACS, Poster Exhibition Abstracts: Pharmacology and Drug Interactions. Effects of Famotidine and Omeprazole on Raltegravir Pharmacokinetics in HIV-Infected Persons. 2019;76:10.
- Wisher D. Martindale: the complete drug reference. 37th ed. *J Med Libr Assoc*. 2012;100(1):75–76. <https://doi.org/10.3163/1536-5050.100.1.018>.
- Drugs.com. Raltegravir. Available at: <https://www.drugs.com/monograph/raltegravir.html>. Accessed March 12, 2021.
- merck.com. Highlights of prescribing information. Available at: https://www.merck.com/product/usa/pi_circulars/i/isentress/isentress_pi.pdf. Accessed March 12, 2021.
- Cattaneo D, Baldelli S, Cerea M, Landonio S, Meraviglia P, Simioni E, et al. Comparison of the *in vivo* pharmacokinetics and *in vitro* dissolution of raltegravir in HIV patients receiving the drug by swallowing or by chewing. *Antimicrob Agents Chemother*. 2012;56(12):6132–6136. <https://doi.org/10.1128/AAC.00942-12>.
- Komasaka T, Dressman J. Simulation of oral absorption from non-bioequivalent dosage forms of the salt of raltegravir, a poorly soluble acidic drug, using a physiologically based biopharmaceutical modeling (PBPM) approach. *Eu J Pharm Sci*. 2021;157:105630. <https://doi.org/10.1016/j.ejps.2020.105630>.
- Markopoulos C, Andreas CJ, Vertzoni M, Dressman J, Reppas C. In-vitro simulation of luminal conditions for evaluation of performance of oral drug products: Choosing the appropriate test media. *Eur J Pharm Biopharm*. 2015;93:173–182. <https://doi.org/10.1016/j.ejpb.2015.03.009>.
- Glomme A, März J, Dressman JB. Comparison of a miniaturized shake-flask solubility method with automated potentiometric acid/base titrations and calculated solubilities. *J Pharm Sci*. 2005;94(1):1–16. <https://doi.org/10.1002/jps.20212>.
- Mann J, Dressman J, Rosenblatt K, Ashworth L, Muenster U, Frank K, et al. Validation of dissolution testing with biorelevant media: an OrBITo study. *Mol Pharm*. 2017;14(12):4192–4201. <https://doi.org/10.1021/acs.molpharmaceut.7b00198>.
- Obach KS, Baxter JG, Liston TE, Silber BM, Jones BC, MacIntyre F, et al. The prediction of human pharmacokinetic parameters from preclinical and *in vitro* metabolism data. *J Pharmacol Exp Ther*. 1997;283(1):46–58.
- FDA. CLINICAL PHARMACOLOGY AND BIOPHARMACEUTICS REVIEW(S): Application Number: 203045Orig1s000. Available at: https://www.accessdata.fda.gov/drugsatfda_docs/nda/2011/203045Orig1s000ClinPharmR.pdf. Accessed March 15, 2021.
- FDA. Chemistry Review(s): Application Number: 22-145. Available at: https://www.accessdata.fda.gov/drugsatfda_docs/nda/2007/022145_ChemR.pdf. Accessed March 15, 2021.
- Small DS, Royalty J, Cannady EA, Hale C, Wang M-D, Downs D, et al. Impact of increased gastric pH on the pharmacokinetics of evacetrapib in healthy subjects. *Pharmacotherapy*. 2016;36(7):749–756. <https://doi.org/10.1002/phar.1778>.
- Kataoka M, Fukahori M, Ikemura A, Kubota A, Higashino H, Sakuma S, et al. Effects of gastric pH on oral drug absorption: In vitro assessment using a dissolution/permeation system reflecting the gastric dissolution process. *Eur J Pharm Biopharm*. 2016;101:103–111. <https://doi.org/10.1016/j.ejpb.2016.02.002>.
- Lake-Bakaar G, Quadros E, Beidas S, Elsakr M, Tom W, Wilson DE, et al. Gastric secretory failure in patients with the acquired immunodeficiency syndrome (AIDS). *Ann Intern Med*. 1988;109(6):502–504. <https://doi.org/10.7326/0003-4819-109-6-502>.
- Herzlich BC, Schiano TD, Moussa Z, Zimbalist E, Panagopoulos G, Ast A, et al. Decreased intrinsic factor secretion in AIDS: relation to parietal cell acid secretory capacity and vitamin B12 malabsorption. *Am J Gastroenterol*. 1992;87(12):1781–1788.
- Konturek JW, Fischer H, van der Voort IR, Domschke W. Disturbed gastric motor activity in patients with human immunodeficiency virus infection. *Scand J Gastroenterol*. 1997;32(3):221–225. <https://doi.org/10.3109/00365529709000198>.
- Neild PJ, Nijran KS, Yazaki E, Evans DF, Wingate DL, Jewkes R, et al. Delayed gastric emptying in human immunodeficiency virus infection: correlation with symptoms, autonomic function, and intestinal motility. *Dig Dis Sci*. 2000;45(8):1491–1499. <https://doi.org/10.1023/a:1005587922517>.

Supplementary material

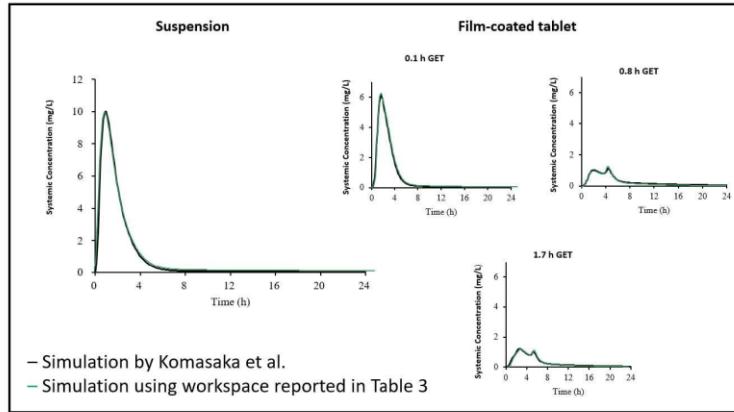


Figure A. Comparison between individual (PopRep) simulations conducted by Komasaka et al. and this study (lines overlap and are thus indistinguishable)

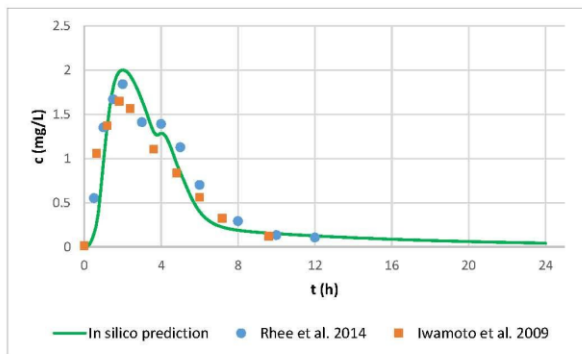


Figure B. Comparison of the fit between the *in silico* prediction of the average raltegravir plasma profile for a virtual population without ARA co-administration and the literature *in vivo* data

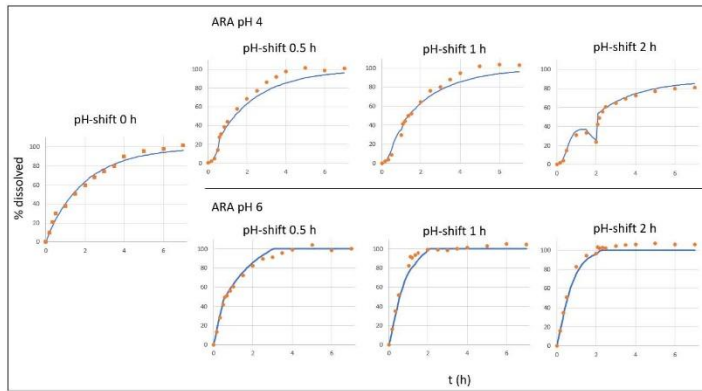



Figure C. Fit of the theoretical dissolution profiles to the *in vitro* dissolution data from two-stage experiments with ARA pH 4 and pH 6 media as the gastric media and pH-shift times 0, 0.5, 1 or 2 hours

7.2 Curriculum vitae

| | | |
|--|---|---|
| Personal Data: | |  |
| Name: | DOMAGOJ ŠEGREGUR | |
| Date of birth: | 3. August 1993 | |
| Place of birth: | Virovitica, Croatia | |
| Nationality: | Croatia | |
| Education and academic background: | | |
| 5/2021 - ongoing | Biopharmaceutics Project Lead at UCB Pharma, Braine-l'Alleud, Belgium | |
| 1/2018 – 4/2021 | Ph.D. studies under the supervision of Prof. Dr. Jennifer Dressman, Institute of Pharm. Tech., Goethe-University, Frankfurt am Main <ul style="list-style-type: none">AstraZeneca collaborative project “Development of biorelevant media and dissolution tests for gastrointestinal disease states” | |
| 11/2016 – 10/2017 | Practical year Sanofi Aventis, Frankfurt am Main <ul style="list-style-type: none">Project on particle characterisation using micro-flow imaging | |
| 10/2012 – 10/2016 | Pharmacy studies Goethe-University, Frankfurt am Main <ul style="list-style-type: none">Elective courses in Analytical Sciences (MALDI) and Pharm.Tech. and Biopharm. (WHO Biowaiver monographs) | |
| 6/2012 | Secondary school graduation VII. Grammar school, Zagreb, Croatia | |
| Language skills: | | |
| | Croatian – mother tongue | |
| | English – high level of written and spoken language | |
| | German – high level of written and spoken language | |
| Additional relevant skills: | | |
| | PBPK modelling - Simecyp simulator, SIVA - 3 years of experience | |
| | Mentoring of (under)graduate and Master’s students - 3 years of exp. | |
| Distinctions and awards: | | |
| 2012 – 2016 | DAAD full study scholarship | |
| 2012 | International conference of young scientists, Nijmegen, The Netherlands – Gold medal | |
| 2009 – 2012 | City of Zagreb excellence scholarship | |
| Teaching activity (2018-2021): | | |
| 7 th semester - Pharmacy studies | Supervision of students in seminars and practical course on capsules, rectalia, vaginalia and inhalanda | |
| 2 nd semester - Pharmacy studies | Supervision of students in the practical course “Drug formulation studies I” | |
| Elective courses - Pharmacy studies and Master’s of Pharmacy | Supervision and introduction to <i>in vitro</i> dissolution, HPLC analytics and <i>in silico</i> modelling for Pharmacy and Master’s students | |

Academic Teachers:

Prof. Dr. Theodor Dingermann, Prof. Dr. Jennifer Dressman, Prof. Dr. Gunter Eckert, Prof. Dr. Eberhard Ehlers, Prof. Dr. Robert Fürst, Prof. Dr. Axel Helmstädter, Prof. Dr. Michael Karas, Prof. Dr. Jochen Klein, Prof. Dr. Hanns-Christian Mahler, Prof. Dr. Rolf Marschalek, Prof. Dr. Eugen Proschak, Prof. Dr. Dr. Achim Schmidtko, Prof. Dr. Manfred Schubert-Zsilavec, Prof. Dr. Dieter Steinhilber, Prof. Dr. Mona Tawab

7.3 Eidesstattliche Erklärung (Statutory declaration)

ERKLÄRUNG

Ich erkläre hiermit, dass ich mich bisher keiner Doktorprüfung im Mathematisch-Naturwissenschaftlichen Bereich unterzogen habe.

Frankfurt am Main, den 01.11.2021


Unterschrift

Versicherung

Ich erkläre hiermit, dass ich die vorgelegte Dissertation über

Development of biorelevant media and dissolution tests

for gastrointestinal disease states

.....

selbständig angefertigt und mich anderer Hilfsmittel als der in ihr angegebenen nicht bedient habe, insbesondere, dass alle Entlehnungen aus anderen Schriften mit Angabe der betreffenden Schrift gekennzeichnet sind.

Ich versichere, die Grundsätze der guten wissenschaftlichen Praxis beachtet, und nicht die Hilfe einer kommerziellen Promotionsvermittlung in Anspruch genommen zu haben.

Frankfurt am Main, den

01.11.2021


(Unterschrift)